bulletin 40

technical report

fib
CEB-FIP

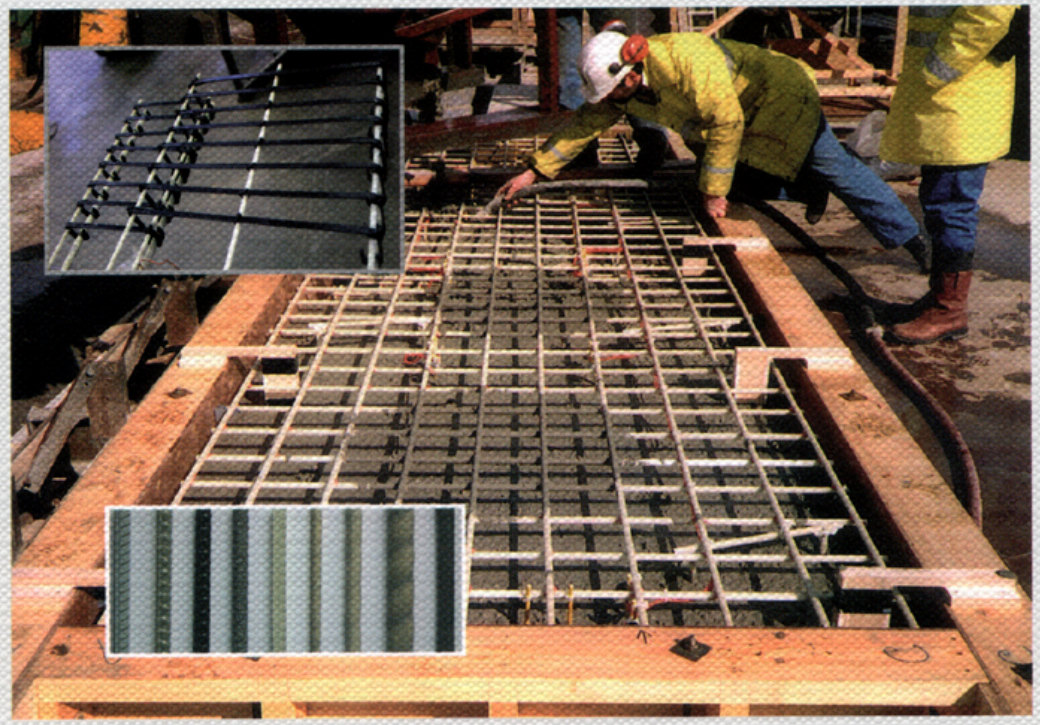

FRP reinforcement in RC structures

FRP reinforcement in RC structures

Technical report prepared by a working party of Task Group 9.3,
FRP (Fibre Reinforced Polymer) reinforcement for concrete structures

September 2007

Subject to priorities defined by the Technical Council and the Presidium, the results of ***fib***'s work in Commissions and Task Groups are published in a continuously numbered series of technical publications called 'Bulletins'. The following categories are used:

category	minimum approval procedure required prior to publication
Technical Report	approved by a Task Group and the Chairpersons of the Commission
State-of-Art Report	approved by a Commission
Manual, Guide (to good practice) or Recommendation	approved by the Technical Council of ***fib***
Model Code	approved by the General Assembly of ***fib***

Any publication not having met the above requirements will be clearly identified as preliminary draft.
This Bulletin N° 40 was approved as an ***fib*** Technical Report by Task Group 9.3 in July 2007.

This report was drafted by a working party of Task Group 9.3, *FRP (Fibre Reinforced Polymer) reinforcement for concrete structures*, in Commission 9, *Reinforcing and prestressing materials and systems*. The following authors were:

- chapter co-ordinators:

Chris J. Burgoyne [2] (Cambridge Univ., United Kingdom), Ewan Byars ✞ [3] (Univ. of Sheffield, United Kingdom;), Maurizio Guadagnini [6] (Univ. of Sheffield, United Kingdom), Gaetano Manfredi [A] (Univ. of Naples, Italy), Kyriacos Neocleous [4, 8, B] (Univ. of Sheffield, United Kingdom), Kypros Pilakoutas [1, 4, 5, 6, 7, 8, A, B] (Univ. of Sheffield, United Kingdom), Luc Taerwe [1] (Ghent Univ., Belgium), Nicolae Taranu [2] (TU Iasi, Romania), Ralejs Tepfers [7] (Ralejs Tepfers Consulting, Sweden), André Weber [3] (Schöck Bauteile GmbH, Germany)

- and/or significant contributors:

Raed Al-Sunna [5] (Univ. of Sheffield, United Kingdom), Chris J. Burgoyne [3] (Cambridge Univ., United Kingdom), Sotiris Demis [3] (Univ. of Sheffield, United Kingdom), Douglas Gremel [4] (Hughes Brothers, USA), Maurizio Guadagnini [1, 4, 5, 7, 8, B] (Univ. of Sheffield, United Kingdom), Gaetano Manfredi [5, 7, 8] (Univ. of Naples, Italy), Kyriacos Neocleous [1] (Univ. of Sheffield, United Kingdom), Carlos E. Ospina [5, 6] (Berger/Abam Engineers Inc.), Marisa Pecce [5] (Univ. of Sannio, Italy), Kypros Pilakoutas [2,3] (Univ. of Sheffield, United Kingdom), Andrea Prota [5] (Univ. of Naples, Italy), Andreea Serbescu [2] (Univ. of Sheffield, United Kingdom), Peter Sheard [3] (Eurocrete Ltd., United Kingdom), Harsha Sooriyaarachchi [4, 7, A] (Univ. of Sheffield, United Kingdom), Luc Taerwe [4, 5, 8] (Ghent Univ., Belgium), Vitauts Tamuzs [2, 3] (Riga Technical Univ., Latvia), Ralejs Tepfers [3,7] (Ralejs Tepfers Consulting, Sweden), André Weber [2] (Schöck Bauteile GmbH, Germany)

[1, 2, ...] chapters in which the author was involved as coordinator or contributor.

Other contributors:

Peter Bischoff (Univ. of New Brunswick, Canada), Valter Dejke (IFP Research AB, Sweden), Stijn Matthys (Ghent Univ., Belgium), Marco Pisani (Univ. of Milan, Italy), Lluis Torres (Univ. of Girona, Spain)

Full address details of Task Group members may be found in the ***fib*** Directory or through the online services on ***fib's*** website, www.fib-international.org.

Cover photo: Casting of a FRP reinforced bridge deck. Top left insert: close-up of FRP reinforcing cage of a guideway for an urban light transport system. Bottom left insert: samples of FRP reinforcing bars.

First published in 2007 by the International Federation for Structural Concrete (*fib*)
Postal address: Case Postale 88, CH-1015 Lausanne, Switzerland
Street address: Federal Institute of Technology Lausanne - EPFL, Section Génie Civil
Tel +41 21 693 2747 • Fax +41 21 693 6245
fib@epfl.ch • www.fib-international.org

ISSN 1562-3610
ISBN 978-2-88394-080-2

Printed by Sprint-Digital-Druck, Stuttgart

Preface

In December 1996, CEB set up a Task Group on non-metallic reinforcement with the main objective of elaborating design guidelines for the use of FRP (Fibre Reinforced Polymers) reinforcement in concrete structures, in accordance with the design format of the CEB-FIP Model Code. As a result of the merger of CEB and FIP into *fib* in 1998, this Task Group continued as *fib* TG 9.3 "FRP reinforcement for concrete structures" and is linked to Commission 9 "Reinforcing and prestressing materials and systems". The Task Group has a fairly high number of active members from universities, research institutes and companies working in the field of advanced composites. Also many young researchers participated in the meetings and contributed to this bulletin. This is mainly due to the fact that there were close working links between TG 9.3 and the EU TMR (European Union Training and Mobility of Researchers) Network "ConFibreCrete", coordinated by Prof. Kypros Pilakoutas from Sheffield University and, more recently, to the EN-CORE Research Training Network.

The Task Group typically met twice a year and the work was carried out by several working parties. The first output of the working party on externally bonded reinforcement (EBR) was published in 2001 as *fib* Bulletin 14 "Externally bonded FRP reinforcement for concrete structures".

The working party on reinforced concrete, under the convenorship of Kypros Pilakoutas, elaborated the present bulletin, which deals mainly with the use of FRP bars as internal reinforcement for concrete structures. Although FRP also has been used in tendons for pre-tensioning and post-tensioning applications in the last two decades, this mostly concerned specific applications and products for which the design approach was adapted to meet specific performance requirements related to the project in question. Consequently, it was decided not to include design approaches for prestressed concrete members.

The fact that in FRP reinforcement different types of fibres can be combined with different types of polymers in various volume fractions to obtain bars in various shapes and surface treatments, results in the fact that rather generic designations such as AFRP (aramid fibres), GFRP (glass fibres) or CFRP (carbon fibres) are not related to a unique product but rather to a range of products with varying properties, in contrast to steel reinforcing bars, of which the main physical and mechanical properties vary within narrow limits. It follows that it is rather difficult to elaborate generally valid design rules from the abundance of test results obtained under a wide variety of product characteristics.

In this bulletin the background of the main physical and mechanical properties of FRP reinforcing bars is presented with special emphasis on durability aspects. For each of the typical ultimate and serviceability limit states, the basic mechanical model is given, followed by different design models according to existing codes or design guidelines. As all FRP materials exhibit an almost linear elastic behaviour followed by brittle failure, the design formulae for steel reinforcement, which in contrast has a marked plastic behaviour, have to be adapted in one way or another. Perhaps even the complete design philosophy of RC members needs to be reconsidered, as proposed in the last chapter.

In this bulletin, no final set of design formulae and approaches is proposed. However, future activities of the Task Group will deal with the elaboration of design formulae in a code type format.

I hope that the present bulletin will be useful and instructive to readers not familiar with the subject and that it will stimulate the use of FRP, not just as replacement of steel reinforcement but as a fascinating class of materials with its own specific properties and field of application.

Finally I would like to thank all the members of Task Group 9.3 and in particular the members of the working party on RC for their contributions throughout the years and their stimulating discussions during many meetings. Special thanks go to Kypros Pilakoutas and Maurizio Guadagnini of Sheffield University (UK) for the coordinating activities in the later stages of the bulletin preparation and to Stijn Matthys of Ghent University (Belgium) who serves as secretary and webmaster of Task Group 9.3.

Ghent, 28 September 2007

Luc Taerwe
Convenor of *fib* Task Group 9.3

Contents

Symbols

Roman upper case letters

A	effective tension area of concrete surrounding the tension reinforcement divided by the number of rebars
A_c	area of concrete
A_f	area of longitudinal FRP reinforcement
A_s	area of longitudinal steel reinforcement
A_t	cross-sectional area of transverse reinforcement normal to assumed splitting plane
E_o	basic value for elastic modulus (200 kN/mm^2)
E_c	elastic modulus for concrete
E_f	elastic modulus for FRP
E_{fk}	characteristic value of elastic modulus of FRP
E_s	modulus of elasticity for steel
E_t	modulus of transverse reinforcement
F_f	force developed in an FRP bar
F_s	force developed in a steel bar
I_{cr}	moment of inertia for cracked concrete section
I_e	effective moment of inertia
I_g	moment of inertia for gross concrete section
I_m	modified effective moment of inertia
I_t	moment of inertia of uncracked section transformed to concrete
K_l	boundary condition factor
L	span
MAT	mean annual temperature
M_{cr}	applied moment causing the occurrence of the first crack
M_f	factored moment
M_{max}	maximum bending moment under service loads
NDP	nationally determined parameter
P_{ft}	target probability of failure
R_{10}	standard reduction of tensile strength in percent per decade
TBD	to be determined
V_{cf}	concrete shear resistance of an FRP RC member
V_{sf}	shear resistance of FRP shear reinforcement

Roman lower case letters

b	width of beam
b_o	perimeter of critical section for slabs and footings
b_w	width of web (T-section)
c	concrete cover to the centre of the tension reinforcement (Ch. 5)
c	the lesser between concrete cover for tension reinforcement and one half of the bar spacing (Ch 7)
c_f	center-to-center distance between rebars
d	effective depth (Ch. 4, Ch. 6)
d	bar diameter
d_b	diameter of an FRP bar in the bent portion
f_c, f'_c	concrete cylinder compressive strength
f_{cu}	concrete cube compressive strength
f_{cd}	design value of concrete compressive strength
f_{ck}	characteristic value of concrete compressive strength
f_{ct}	concrete tensile strength
f_{ctm}	mean value of concrete tensile strength
f_f, f_{fu}	ultimate tensile strength of longitudinal FRP reinforcement
f_{fb}	strength of FRP bent bars
f_{bod}	design bond strength
f_{fd}	design value of tensile strength for FRP
f_{fkd}	design strength of FRP (long term)
$f_{fk\ res}$	characteristic value of residual tensile strength
f_{fk}	characteristic value of tensile strength of FRP reinforcement
f_{fk0}	characteristic value of tensile strength (short term test)
$f_{fk1000h}$	characteristic value of tensile strength (1000h test)
f_{Test}	sustained stress during ageing test
f_y	yield strength of steel reinforcement
f_{yk}	characteristic yield strength of steel reinforcement
h	depth (thickness) of the member
k	ratio of the depth of compressive concrete zone to the effective depth under cracked elastic conditions
k	coefficient which allows the effect of FRP on contribution of concrete to shear capacity (Ch. 6)
k_b	FRP-concrete bond quality coefficient, evaluated to 1.0~1.3; 1.2 for deformed bars
l	crack spacing

m	coefficient accounting for the tension stiffening effect
n	modular ratio
n_{mo}	exponent for moisture influence
n_T	exponent for temperature influence
n_{SL}	exponent for service life influence
n_d	exponent for diameter influence
r_b	bending radius of FRP bar
s	slip
s	bar spacing (Ch. 5)
s	spacing of shear links (Ch. 6, Ch. 7)
v_{cf}	concrete shear strength of an FRP RC member
v_{sf}	hear strength of FRP shear reinforcement
w	maximum probable crack width at the bottom surface
w_{cr}	design crack width
x	neutral axis depth
z	lever arm (Ch. 6)

Greek lower case letters

α	angle of reaction force
α_b	bond-dependent coefficient, taken equal to 0.5 for all FRP bar types (until further research data become available)
α_{cc}	coefficient taking into account the long term effects on the compressive strength and of unfavourable effects resulting from the way the load is applied
α_d	dimensionless exponent equal to 0.5 for rectangular sections (Ch. 5)
β	ratio of distance between neutral axis and tension face to distance between neutral axis and reinforcement steel
β	coefficient accounting for the duration of load and bond (Ch. 5)
β_d	bond reduction factor
β_1	concrete strength factor
γ_c	partial safety factor for concrete
γ_s	partial safety factor for steel
γ_f	partial safety factor for FRP
ε_c	concrete compressive strain
ε'_{csd}	compressive strain due to the effects of creep and shrinkage
ε_{cu}	ultimate concrete compressive strain
ε_f	tensile strain in longitudinal FRP reinforcement
ε_{fu}	ultimate strain of longitudinal FRP reinforcement

ε_s	steel reinforcement strain
ϕ	strength reduction factor
η	factor defining effective strength of concrete
η_{env}	environmental strength reduction factor
$\eta_{env,t}$	environmental strength reduction factor - tension
$\eta_{env,b}$	environmental strength reduction factor – bond
λ	factor defining effective height of compression zone (Ch. 4)
λ	factor accounting for concrete density (Ch. 6)
λ	multiplier for additional long-term deflection (Ch. 5)
ξ	coefficient accounting for tension-stiffnening
ξ	time-dependent factor for sustained load, equal to 2.0 for 5 years or more (Ch. 5)
ξ	ratio of the neutral axis depth to the effective depth (Ch. 4)
ρ'	reinforcement ratio of the compressive reinforcement
ρ_f	reinforcement ratio for FRP
ρ_{fb}	balanced reinforcement ratio
ρ_{min}	minimum ratio of longitudinal FRP reinforcement
ρ_r	reinforcement ratio within the effective tension area
ρ_s	longitudinal steel reinforcement ratio
δ	deflection
δ_r	coefficient to limit deflection of RC elements at SLS (e.g $\delta_r = 250$)
σ_f	tensile stress developed in longitudinal FRP reinforcement
σ_{fe}	stress increase in the reinforcement
σ_s	stress in the tension reinforcement in a cracked section
σ_c	stress in concrete
σ_{sr}	stress in tension reinforcement under first crack load
τ	bond stress
τ_{max}	maximum bond stress
τ_{Rd}	design value of resisting shear strength of concrete

1 Introduction

Fibre reinforced polymer (FRP) bars became commercially available as reinforcement for concrete over the last 15 years and by now over 10 million m are used in construction every year. There are several reasons why civil and structural engineers may need to use resin-matrix continuous fibre (fibre reinforced polymer – FRP) reinforcement in concrete. The primary reason is durability, but other reasons include electromagnetic neutrality, high strength and lightweight [Pilakoutas (2000)]. Each of these is briefly examined in the first section of this introductory chapter and likely applications are identified.

Composite FRP materials are still new in construction and most engineers are unfamiliar with their properties and characteristics. The second chapter of this bulletin aims to provide practising engineers with the necessary background knowledge in this field. This chapter also shows the typical products currently in the international market. It is important that engineers get an appreciation of the factors that influence the mechanical properties of composites, but also to realize that FRP is a family of materials with quite diverse properties that can be changed by suitable design at the manufacturing stage.

The chemical durability of FRP materials is often taken for granted, since after all composites have been used in aggressive environments for more than fifty years. However, until recently there was no experience of composites in the highly alkaline and chemically complex concrete environment. The third chapter deals with the issue of durability and identifies the parameters that can lead to deterioration. The information from this chapter is necessary when addressing the design issues. A series of parameters is used to identify the allowable stress in the FRP after exposure for a specified period of time in a specific environment.

The remainder of the bulletin is dedicated to design issues. By now there are several design guidelines that have been produced from around the world. A chronological chart of the developments in this field is presented in Table 1-1.

The first to introduce design guidelines for FRP reinforced concrete (RC) were the Japanese in 1996 [ref, 1996]. These guidelines provided the blueprint for most subsequent guidelines and codes. The modifications made to the existing code equations for concrete are in general still valid to date. However, neither that nor any of the subsequent guidelines address the fundamental issue of Design Philosophy. Hence, in this bulletin it was decided to present the various design aspects first before entering this fundamental issue.

The bulletin covers in four chapters the issues of Ultimate Limit States (primarily dealing with flexural design), Serviceability Limit States (dealing with deflections and cracking), Shear and Punching Shear and Bond and Tension Stiffening. It provides both the state-of – the-art but also in many cases the ideas for the next generation of design guidelines which hopefully will follow soon after this bulletin.

The final chapter deals with the fundamental issue of Design Philosophy. The use of these new materials as concrete reinforcement has forced researchers in the field to re-think many of the fundamental principles used until now in RC design. On a number of fronts there is the realisation that our simplified approaches are prohibiting the introduction of new materials and a fundamental rethink is required. Central points to this debate are whether brittle modes of failure should be accepted, what are the levels of safety that are required and if our current partial material safety factor approach can lead us to the desired results. The bulletin finishes by proposing a new framework for developing partial safety factors to ensure specific safety levels that will be flexible enough to cope with new materials.

Table 1-1: Chronological developments in the field

1818	1849	1887	1904
The Institution of Civil Engineers was founded (UK)	Reinforced concrete was invented	the Canadian Society for Civil Engineering (CSCE) was founded (Canada)	The American Concrete Institute (ACI) was founded (USA)
1910	**1941**	**1953**	**1964**
The first ACI building code was published	The first edition of ACI 318 was published	The Comité Euro-International du Béton CEB (European Committee for Concrete) was founded	The First CEB International recommendations were published
1970s	**1987**	**1991**	**1992**
Use of fibre reinforcement in concrete	The Japan Society of Civil Engineers (JSCE) established a committee on continuous fibre reinforced materials CSCE technical committee on FRP's was established	CSCE published a report on FRP's ACI founded Committee 440 on fiber reinforced polymer for internal and external reinforcement of concrete BRITE-EURAM Project started	The JSCE published a state-of-the-art report on continuous fiber reinforcing materials
1993	**1996**	**1997**	**1998**
The 4-year European funded project EUROCRETE started	TG9.3 of the International Federetion for Structural Concrete (*fib*) was founded JSCE published a set of design recommendations for FRP RC EUROCRETE published a set of design recommendations for FRP RC	The 4-year European funded TMR Network ConFibreCrete started	The CSCE published a set of design recommendations for FRP RC in bridges
1999	**2000**	**2001**	**2002**
The Institution of Structural Engineers published a set of design recommendations for FRP RC The Swedish National code for FRP RC was published	The Concrete Society published technical report TR55 for externally bonded FRP reinforcement *fib* published bulletin 10 on bond of reinforcement (one chapter addressed bond of FRP bars)	*fib* published bulletin 14 on externally bonded FRP reinforcement ISIS Canada published a series of manuals on the use of internal, external and prestressed FRP reinforcement ACI Committe 440 published the first version of their design recommendation for internal FRP reinforcement (440.1R)	ACI Committe 440 published the first version of their design recommendation for external FRP reinforcement (440.2R) CUR Building & Infrastructure published a set of recommendations for FRP RC (The Netherlands)
2003	**2004**	**2005**	**2006**
ACI Committe 440 published the second version of their design recommendation for internal FRP reinforcement (440.1R)	ACI Committe 440 published ACI 440.3R (Guide to test methods) and ACI 440.4R (Prestressing Concrete Structures with FRP Tendons) The National Research Council (CNR) published the Italian design recommendations for externally bonded FRP reinforcement (CNR-DT 200/2004)	The 4-year European funded RTN Marie Curie Network En-Core started	The National Research Council (CNR) published the Italian design recommendations for internal FRP reinforcement (CNR-DT 203/2006) ACI Committe 440 published the third version of their design recommendation for internal FRP reinforcement (440.1R)

1.1 Reasons for using FRP and possible applications

1.1.1 Durability of reinforced concrete

It is estimated that the current worldwide infrastructure repair and maintenance bill exceeds 100 Billion Euros. A large proportion of this expense is spent trying to address durability problems in concrete structures.

The alkaline environment of concrete normally provides the necessary protection to conventional steel reinforcement from the environment. Nonetheless, when exposed or when the alkaline environment is neutralised, conventional steel corrodes and leads to spalling of the concrete cover. Codes of practice prescribe thick concrete covers to the steel reinforcement together with other measures to control concrete crack widths and reduce permeability, whilst the alkalinity of the cement has increased on purpose over the years. However, the environmental attack is relentless and sooner or later the alkaline properties of the concrete cover are reduced leading to corrosion and concrete spalling [Holland (1997)].

Different solutions to the reduction of the risk of corrosion in highly aggressive environments include concrete surface protective coatings to stop the ingress of CO_2 and water soluble chemicals, corrosion inhibitor admixtures at the wet stage, epoxy coating of reinforcement and galvanizing of reinforcement. A more innovative approach adopted in recent decades is cathodic protection. This technique, which was initially developed as a rehabilitation measure, utilizes an electric current or a sacrificial anode to protect the main reinforcement [Allen and Edwards (1987)]. In some cases, stainless steel reinforcement offers the most robust anti-corrosion solution. However, most such solutions have either had failures or are expensive.

FRP reinforcement appeared in the market in the early 1990's as another solution to the corrosion problem [Clarke (1993), Bakis (1993)], even though the ability of such composites to resist the alkaline environment of concrete was not thoroughly investigated. However, by now, durable FRP reinforcement that has been designed to resist the alkaline concrete environment is available in the market.

The use of FRP in concrete for anti-corrosion purposes is expected to find applications in structures in or near marine environments, in or near the ground, in chemical and other industrial plants, in places where good quality concrete can not be achieved and in thin structural elements. Most initial applications of FRP reinforcement in concrete were built in Japan, where many demonstration projects were developed in the early 90's. Research and development is now actively taking place in many countries, most prominently in North America and Europe. Aramid prestressing bars were used, for example, in the late 80's in the Netherlands to reinforce some of the posts of a noise barrier along a highway. The choice of the reinforcing material for this application was made mainly because of the aggressive environment these posts would be subjected to during their life due to exposure to deicing salts and exhaust gasses of cars [Taerwe (1993)]. In the United Kingdom, the EUROCRETE project, installed the first completely FRP reinforced footbridge in 1996 (Fig. 1.1).

This was followed by a number of other demonstration projects including another bridge in a golf course in Norway and a fender in Qatar. In thin structural elements, FRP reinforcement offers the possibility of reducing the concrete cover needed to protect the reinforcement and, hence, this can lead to reducing sections and new designs. Examples of such elements include cladding panels, parapets and manhole covers.

Figure 1-1: The first concrete footbridge in Europe with only FRP reinforcement (EUROCRETE project)

1.1.2 Electromagnetic neutrality

Steel reinforcement can interfere with magnetic fields and, hence, it is usually avoided in applications where magnetic neutrality is required, such as bases of large motors, magnetic scanning equipment and magnetic railway levitation systems. In Japan, much of the initial work on the use of composites in concrete was driven by the research on the railway magnetic levitation system, MAGLEV (Fig. 1.2).

Figure 1-2: Magnetic Levitation Railway System in Japan

Figure 1-3: Soft eye FRP reinforcement

Electromagnetic interference is progressively a nuisance especially to the mobile telecommunications industry and to the defence industry. Applications in these industries are increasing with time, both in the vicinity of transmitting stations and receiving devices. The magnetic neutrality of FRPs makes them also an ideal reinforcing solution for rooms in hospital buildings where magnetic resonance imaging (MRI) equipment is used.

1.1.3 High strength and light weight

The high strength of FRP reinforcement can be utilized to reduce congestion of reinforcement in certain applications. However, since the strength is developed at a high strain this has other structural implications. Hence, it is not anticipated that the high strength of FRP will be a major advantage in many RC applications. However, if FRP is prestressed, not only is the high strength utilized, but also the lower elastic modulus will imply lower losses in the longer term. However, the problem of stress corrosion of FRP, particularly of Glass FRP, should not be overlooked, which means that Carbon and Aramid FRP are likely to dominate most such applications. Some of the earliest uses of prestressed FRPs took place in Japan. The first application of Carbon FRP cable strands as tensioning materials dates back to 1988 for the construction of a prestressed concrete bridge over a highway [Zia et al. (1997)]. Aramid FRP prestressing tendons were used in the deck of a stressed ribbon pedestrian bridge erected in 1991 near Tokyo [Taerwe (1993)].

The favourable weight of FRP may have some practical advantages in construction, but again it is not anticipated to be the driving force behind its application as reinforcement in concrete. Normally, the weight of the concrete is high, and hence, small savings in reinforcement weight will not be significant. However, in some exceptional circumstances, the use of lightweight reinforcement may speed up construction, especially in inaccessible or confined spaces, where it is difficult to have many workers side by side. The light weight of FRP becomes a real advantage when dealing with externally bonded reinforcement for repair purposes [fib (2001)].

1.1.4 High cuttability in temporary applications

High cuttability of FRP reinforcement, particularly Glass fibre, make it the ideal material to temporary reinforce concrete structures such as diaphragm walls, which have to be partially destroyed by TBM machines.

Commonly RC diaphragm walls are reinforced with steel cages that are split in different sections and than assembled and lowered to the bottom of the excavation trench. Steel cages prevent TBMs from being used, as the machines would not be able to break the wall without damaging both its cutting tools and shield.

A solution to this problem is to use a “soft-eye” in the area that will be bored. The “soft eye” consists of a reinforcing cage using Glass fibre reinforced polymers (GFRP) bars and stirrups, which can be easily cut by the Tunnel Boring Machine (TBM), thanks to their low shear strength [Arduini et al. (2005)]. In addition the low weight of the FRP cages enables easy assembly and handling on site. The use of soft-eye technique reduces significantly the time needed to build and reinforce diaphragm walls as well as to excavate shaft and station diaphragm walls along the TBM route. An example of a soft-eye is shown in Fig.1.3.

2 Material characteristics

2.1 Types of material

2.1.1 General

Fibre Reinforced Polymer bars are made of continuous fibres impregnated with polymeric resins. In fibrous polymeric composites, continuous fibres with high strength and high stiffness are embedded in and bonded together by the low modulus polymeric matrix. In the case of FRP composites the reinforcing fibres constitute the backbone of the material and they determine its strength and stiffness in the direction of the fibres.

The polymeric matrix is required to fulfil the following main functions: to bind together the fibres and protect their surface from damage during handling, fabrication and service life of the composite; to disperse the fibres and separate them; to transfer stresses to the fibres. The matrix should be chemically and thermally compatible with the fibres and plays an important role in controlling the overall stress-strain behaviour of the composite and its resistance to corrosive environments. The type of polymeric matrix also affects the failure mechanism and fracture toughness of the resulting composite.

The most common manufacturing process is the pultrusion process in which the fibres are pulled and impregnated before curing takes place in a heated die. Special fibre arrangements or a combination of two or more types of reinforcing fibres can be used to impart to the composite unique mechanical properties. Furthermore, in order to enhance the bond characteristics of FRP reinforcing bars in concrete, several techniques can be used including surface deformations, sand coating, over-moulding a new surface on the bar or a combination of the techniques.

FRP concrete reinforcement does not need to have the same shape as steel reinforcement. It could take the form of bars, rods, profiles and even permanent formwork. Owing to its good corrosion resistance, FRP does not need as much cover protection as steel reinforcement and can be exposed to more severe environments. However, the polymeric matrix may limit its fire resistance. The main characteristics of the various fibres and polymeric resins used to make FRP are introduced in the following subsections. The values quoted here should be regarded as typical - most manufacturers produce different grades of fibre for different applications, and improved manufacturing techniques may improve composites properties.

2.1.2 Fibres

Fibres are used in polymeric composites because they are strong, stiff and lightweight. Fibres are stronger than the bulk material that constitutes the fibres due to their preferential orientation of molecules along the fibre direction and because of the reduced number of defects present in fibre compared to the bulk material. The desirable structural and functional requirements of the fibres in composites are: high elastic modulus for an efficient use of reinforcement; high ultimate strength and convenient elongation at tensile fracture; low variation of strength between individual fibres; stability of properties during handling and fabrication; uniformity of fibre diameter and surface; high toughness; durability; availability in suitable forms and acceptable cost. The most common fibres used to make FRP reinforcing bars are glass, carbon and aramid [Wallenberger et al. (2001), Walsh (2001), Chang (2001)]. Recently, basalt fibres are also commercially available. All these fibres exhibit a linear elastic behaviour under tensile loading up to failure [Hollaway (1993)] without showing any yield

(Figure 2-1). Carbon and aramid fibres are anisotropic with different values of mechanical and thermal properties in the main directions whereas glass fibres are isotropic [Gay et al. (2003), Gibson (1994)] as well as basalt fibres.

Typical properties of various types of reinforcing fibres are summarized in Table 2-1.

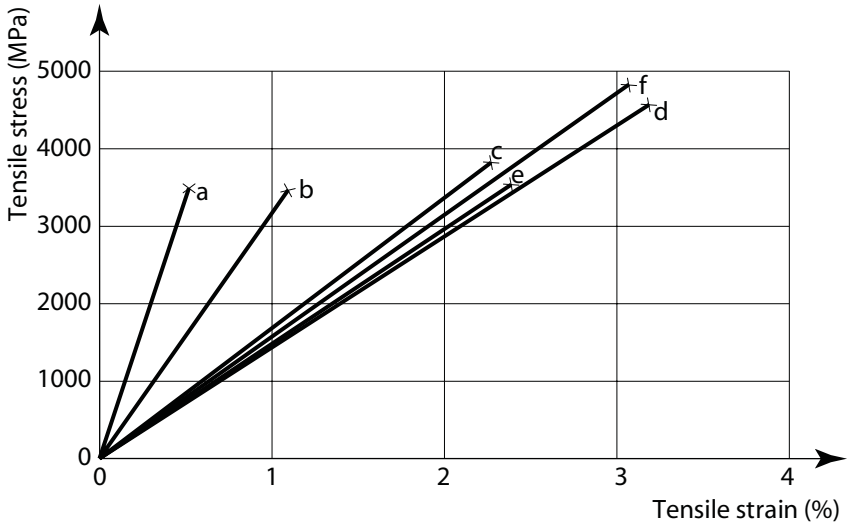

Figure 2-1: Stress-strain curves of typical reinforcing fibres: a) carbon (high modulus); b) carbon (high strength); c) aramid (Kevlar 49); d) S-glass; e) E-glass; f) Basalt

Table 2-1: Typical properties of fibres for FRP composites

Fibre Type	**Density**	**Tensile strength**	**Young modulus**	**Ultimate tensile strain**	**Thermal expansion coefficient**	**Poisson's coefficient**
	(kg/m^3)	(MPa)	(GPa)	(%)	($10^{-6}/^oC$)	
E-glass	2500	3450	72.4	2.4	5	0.22
S-glass	2500	4580	85.5	3.3	2.9	0.22
Alkali resistant glass	2270	1800-3500	70-76	2.0-3.0	-	-
ECR	2620	3500	80.5	4.6	6	0.22
Carbon (high modulus)	1950	2500-4000	350-650	0.5	-1.2...-0.1	0.20
Carbon (high strength)	1750	3500	240	1.1	-0.6...-0.2	0.20
Aramid (Kevlar 29)	1440	2760	62	4.4	-2.0 longitudinal 59 radial	0.35
Aramid (Kevlar 49)	1440	3620	124	2.2	-2.0 longitudinal 59 radial	0.35
Aramid (Kevlar 149)	1440	3450	175	1.4	-2.0 longitudinal 59 radial	0.35
Aramid (Technora H)	1390	3000	70	4.4	-6.0 longitudinal 59 radial	0.35
Aramid (SVM)	1430	3800-4200	130	3.5	-	-
Basalt (Albarrie)	2800	4840	89	3.1	8	-

2.1.2.1 Glass fibres

Glass fibres are the most commonly used reinforcing fibres for polymeric matrix composites. Molten glass can be drawn into continuous filaments that are bundled into rovings. During fabrication, fibre surfaces are coated with a "sizing" to improve wetting by the matrix and provide better adhesion between the composite constituents. Coating the glass fibres with a coupling agent provides a flexible layer at the interface, improves the strength of the bond and reduces the number of voids in the material. The most common glass fibres are made of E-glass, S-glass and Alkali-resistant glass. E-glass is the least expensive of all glass types and it has a wide application in fibre reinforced plastic industry. S-glass has higher tensile strength and higher modulus than E-glass. However, the higher cost of S-glass fibres makes them less popular than E-glass. Alkali-resistant (AR) glass fibres, which help prevent corrosion by alkali attack in cement matrices, are produced by adding zirconium. AR-glass fibres with fibre sizings that are compatible with commonly utilized thermoset resins, however, are not currently available.

The tensile strength of glass fibres reduces at elevated temperatures but can be considered constant for the range of temperatures at which polymer matrices can be exposed. The tensile strength also reduces with chemical corrosion and with time under sustained loads.

2.1.2.2 Carbon fibres

Carbon and graphite fibres are used interchangeably, but there are some significant differences between these two as far as their modular structure is concerned. Most of the carbon fibres are produced by thermal decomposition of polyacrylonitrile (PAN). The carbon atoms are arranged in crystallographic parallel planes of regular hexagons to form graphite, while in carbon, the bonding between layers is weak, so that it has a two-dimensional ordering. The manufacturing process for this type of fibre consists of oxidation at 200-300°C, different stages of carbonization at 1000-1500°C and 1500-2000°C and finally graphitization at 2500-3000°C. Graphite has a higher tensile modulus than carbon, therefore high-modulus fibres are produced by graphitization. Carbon fibres are commercially available in long and continuous tows, which are bundles of 1,000 to 160,000 parallel filaments. These fibres exhibit high specific strength and stiffness; in general, as the elastic modulus increases, ultimate tensile strength and failure elongation decrease (Fig. 2-1). The tensile modulus and strength of carbon fibres are stable as temperature rises; they are also highly resistant to aggressive environmental factors. The carbon fibres behave elastically to failure and fail in a brittle manner (Fig. 2-1). The most important disadvantage of carbon fibres is their high cost. They are 10 to 30 times more expensive than E-glass. The high cost of these fibres is caused by the high price of raw materials and the long process of carbonization and graphitization. Moreover, graphite fibres cannot be easily wetted by the matrix, therefore sizing is necessary before embedding them in a matrix.

2.1.2.3 Aramid fibres

Polymeric fibres, using a suitable processing method, can exhibit high strength and stiffness. This happens as a result of the alignment of the polymer chains along the axis of the fibre. Aramid is a generic term for a group of organic fibres having the lowest specific gravity and the highest tensile strength-to-weight ratio among the current reinforcing fibres. Aramid fibres are currently produced by DuPont (Kevlar), Teijin (Technora) and Akzo Nobel (Twaron). SVM aramid fibres are also produced in Russia. Kevlar fibres are produced by extruding liquid crystalline solution of the polymer with partially oriented molecules. Kevlar

is an aromatic polyamide with rigid aromatic rings. There are several types of Kevlar fibres: Kevlar 29 (for composites with maximum impact and damage tolerance), Kevlar 49 (used in reinforced plastics) and Kevlar 149 (with the highest tensile modulus among all available aramid fibres). The compressive strength of Kevlar fibres is less than 20% of its tensile strength. Kevlar 49 has brittle behaviour in tension, but under compressive load it is ductile and absorbs a large amount of energy. It also shows a large degree of plasticity in compression when subjected to bending. This type of behaviour, not observed in glass or carbon fibres, gives Kevlar composites better impact resistance. Kevlar has very good tension fatigue resistance, low creep and it can withstand relatively high temperatures. The strength and modulus of Kevlar fibres decrease linearly when the temperature rises, but they retain more than 80% of their original strength at 180°C. Kevlar fibres absorb some water, the amount of absorbed water depends on the type of the fibre. They are sensitive to UV light. At high moisture content, Kevlar fibres tend to crack internally at pre-existing micro-voids and produce longitudinal splitting. Kevlar fibres are resistant to many chemicals but they can be degraded by some acids and alkalis.

2.1.2.4 Basalt fibres

Basalt fibres (Albarrie, Sudaglass, Kammeny Vek and Technobasalt) are single-component materials obtained by melting crushed volcanic lava deposits, having better physicomechanical properties than glass fibres, but being significantly cheaper than carbon fibres. The main advantages of basalt fibres are: fire resistance, significant capability of acoustic insulation and vibration isolation capacity and resistance to chemically active environments. The working temperature of 982ºC and the melting point of 1450ºC are making basalt useful in applications that demand fire resistance. Investigation of basalt fibres, as structural reinforcement for concrete structures, is still at the development stage.

2.1.3 Polymeric matrices

2.1.3.1 General

Matrix in a polymeric composite can be regarded as both a structural and a protection component. Resin is a generic term used to designate the polymer, polymer precursor material, and/or mixture or formulation thereof with various additives or chemically reactive components. In general, a polymer is called resin system during processing and matrix after the polymer has cured. Composite material fabrication and properties are fundamentally affected by resin, its chemical composition and physical properties. The matrix materials generally account for 30-60% by volume of a polymeric composite. The main functional and structural requirements of a matrix are to bind the reinforcing fibres together, transfer and distribute the load to the fibres and protect the fibres from environmental attack and mechanical abrasion. Hence, the choice of matrix is of paramount importance when designing a composite system and will affect both the mechanical and physical properties of the final product.

There are two basic classes of polymeric matrices used in FRP composites: thermosetting and thermoplastic resins. Thermosetting resins [Boyle at al. (2001), Pepper (2001), Mil. Handbook (1999)] are polymers which are irreversibly formed from low molecular weight precursors of low viscosity. These polymers have strong bonds both with the molecules and in-between the molecules. They develop a network structure that sets them in shape. If they are heated after they have been cured, they do not melt and will retain their shape until they begin to thermally decompose at high temperature.

Thermoplastics are polymers that do not develop cross-links. They are capable of being reshaped and repeatedly softened and hardened by subjecting them to temperature cycles reaching values above their forming temperature.

2.1.3.2 Thermosetting resins

Thermosetting resins have initial low viscosity allowing for high fibre volume fractions to be incorporated while still retaining good fibre wet-out. Thermosets are easy to process and low in cost. The three-dimensional network of thermosets results in less flow under stress, better dimensional stability, lower coefficient of thermal expansion and greater resistance to solvents. Thermosetting polymers, however, have a limited storage life; long fabrication time and low failure strain which results in low impact resistance. Shelf life is the time the unmixed resin system can be stored without degradation. Pot life or gel time is the time the mixed resin can be handled before the viscosity grows to a point where processing is no longer possible. The cure cycles can take place at room temperature or at high temperature and can vary from minutes to hours depending on the choice of catalyst and the reactivity of the resin. The reactions are exothermic and gelation is usually rapid. Once cured, the mixture thickens, releases heat, solidifies, and shrinks. The volumetric shrinkage upon curing varies between 4% for epoxy to 8% for polyester. Since the fibrous reinforcement does not shrink internal stresses can be induced causing cracking, fibre misalignment and dimensional inaccuracy. In civil engineering applications the most common thermosetting resins are epoxy, polyesters and vinyl ester. Typical properties of thermosetting matrices are shown in Table 2.2.

Table 2-2: Typical properties of thermosetting matrices

Property	***Matrix***		
	Polyester	Epoxy	Vinyl ester
Density (kg/m^3)	1200 - 1400	1200 - 1400	1150 - 1350
Tensile strength (MPa)	34.5 - 104	55 - 130	73 – 81
Longitudinal modulus (GPa)	2.1 – 3.45	2.75 – 4.10	3.0 – 3.5
Poisson's coefficient	0.35 – 0.39	0.38 – 0.40	0.36 – 0.39
Thermal expansion coefficient (10^{-6}/^{o}C)	55 - 100	45 - 65	50 - 75
Moisture content (%)	0.15 – 0.60	0.08 – 0.15	0.14 – 0.30

Table 2-3: Typical properties for some thermoplastic matrices

Property	***Matrix***		
	PEEK	PPS	PSUL
Density (kg/m^3)	1320	1360	1240
Tensile strength (MPa)	100	82.7	70.3
Tensile modulus (GPa)	3.24	3.30	2.48
Tensile elongation (%)	50	5	75
Poisson's coefficient	0.40	0.37	0.37
Thermal expansion coefficient (10^{-6}/ ^{o}C)	47	49	56

2.1.3.2.1 Epoxy resins

The term epoxy resin defines a class of thermosetting resins prepared by the ring-opening polymerization of compounds containing an average of more than one epoxy group per molecule. Prior to adding fibres, small amounts of reactive curing agents are added to liquid resin to initiate polymerization. Cross links are formed and epoxy liquid resin changes to a

solid material. The density of cross-links depends on the chemical structure of the starting resin, curing agent and reaction conditions. The cross links formed during the curing process have a major role in establishing the final properties of the solid epoxy. Tensile modulus and tensile strength, thermal stability and chemical resistance are improved as the density of the cross links increases. On the other hand, fracture toughness and strain-to-failure are reduced. High-performance epoxies have been prepared with a variety of phenolics and aromatic amines. Epoxy resins can be partially cured; thus the reinforcement can be pre-impregnated with liquid resin and partially cured to give a prepreg.

The main advantages of epoxy resins are high mechanical properties, easy processing, low shrinkage during cure (leading to good bond characteristics when used as adhesives) and good adhesion to a wide variety of fibres. Epoxies have high corrosion resistance and are less affected by water and heat than other polymeric matrices. Curing of such resins can be achieved at temperatures ranging between 5°C and 150°C. Epoxy resins can be formulated to have a wide range of stiffness [Schwartz (1992)] and other mechanical properties (Fig. 2-2)

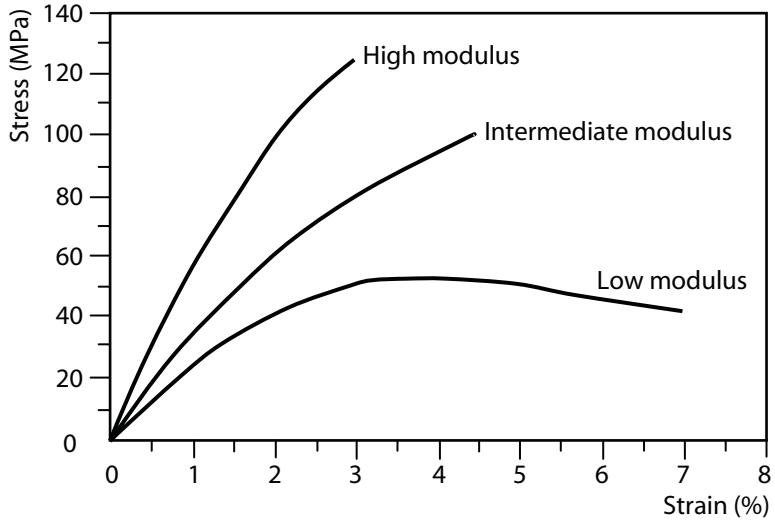

Figure 2-2: Stress-strain curves of epoxy matrix resins of different modulus

The main disadvantage of epoxy resins are their relatively high cost and long curing period. The cost of epoxies is proportional to their performance, and varies over a broad range, but epoxies are generally more expensive than polyesters and vinyl esters. The toughness of the resin and the composite can be controlled by adding additives, including thermoplastics.

2.1.3.2.2 Polyester matrix

The so-called general purpose polyester unsaturated resins are made by using ethylene glycol, either orthophthalic or isophtalic acid as the saturated diacid, and fumaric as the unsaturated diacid. A wide variety of polyesters is available, based on the choice of the diacid. The flexibility of polyesters may be controlled by the choice of diacids and diols. Relatively flexible polyesters are produced from highly aliphatic precursors; high-modulus (stiff) polyesters, brittle, with increasing glass-transition temperatures may be obtained from combinations with large amounts of aromatic diacids and/or aromatic diols.

Polyester resins are low viscosity liquids based on unsaturated polyesters, which are dissolved in a reactive monomer, such as styrene. The addition of heat and a free radical

initiator, such as organic peroxide, results in a cross-linking reaction, converting the low viscosity solution into a three dimensional thermosetting matrix. Cross linking can also be accomplished at room temperature using peroxides and suitable activators. Polyester resins can be formulated to have good UV resistance and to be used in outdoor applications. There are many glass fibre reinforced polyester structures that have been in use for more than 30 years, only affected by some discolouration and small loss in strength. Superior durability and resistance to fibre erosion can be obtained when styrene is supplemented with methyl methacrilate (MMA). The resistance to burning of polyester resins can be achieved by using either fillers or a specially formulated flame-retardant polyester resin, depending on the degree of resistance required. Incorporating halogens into a polyester resin has been found to be an effective way of improving fire retardancy. Polyester resins are used in applications requiring corrosion resistance.

The use of glass fibre does not improve and may even reduce the corrosion resistance of polyester resins. This is especially true in strong caustic and hydrofluoric environments because these chemicals can attack and dissolve glass fibres. Other chemical agents are added to extend pot life, modify the chemical structures between cross-links and reduce resin viscosity. Some representative material data for polyester resin are given in Table 2-2. They correspond to unreinforced cast samples of resin. Using any fibrous reinforcement dramatically improves the mechanical properties of the resin. The main disadvantage of polyester resins is their high volumetric shrinkage. This volumetric shrinkage can be reduced by adding a thermoplastic component. Cross link can affect the properties of polyester resins in the same manner as for epoxy resins. Fig. 2-3 gives typical stress-strain curves for general purpose polyester matrices tested in tension and compression. The graph shows a non-linear relationship and this is a function of the viscoelastic nature of the material.

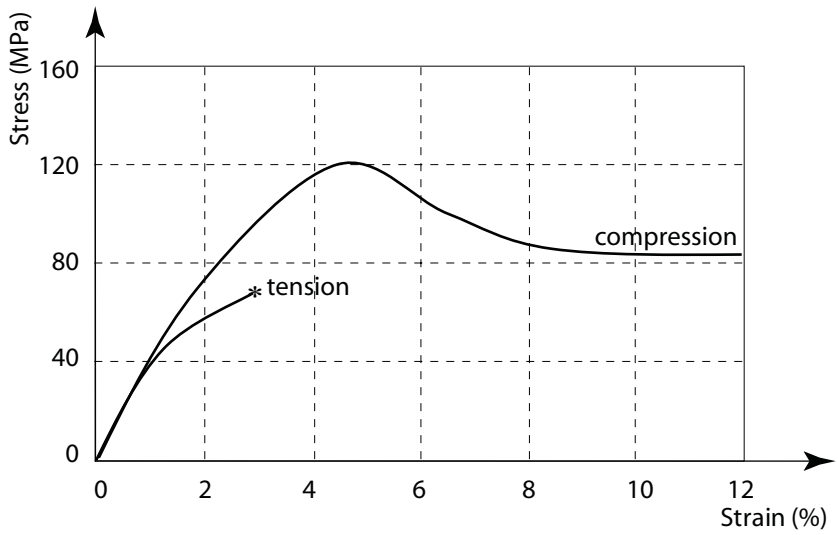

Figure 2-3: Stress-strain curves for general purpose polyester resin

2.1.3.2.3 Vinyl ester matrix

Vinyl esters are resins based on methacrylate and acrylate. Some variations contain urethane and ester bridging groups. Due to their chemical structure these resins have fewer cross links and they are more flexible and have higher fracture toughness than polyesters. They also have very good wet-out and good adhesion when reinforced with glass fibres. Their properties are a good combination of those of epoxy resins and polyesters and make them the preferred choice for the manufacturing of glass fibre reinforced composites. They exhibit

some of the beneficial characteristics of epoxies such as chemical resistance and tensile strength, as well as those of polyesters such as viscosity and fast curing. However, their volumetric shrinkage is higher than that of epoxy and they have only moderate adhesive strength compared to epoxy resins. There is a great variety of vinyl ester resins available for applications up to 170°C. Vinyl ester resins are highly resistant to acids, alkalis, solvents and peroxides. Brominated versions have high flame retardancy. Typical properties are given in Table 2-2.

2.1.3.3 Thermoplastic matrices

Thermoplastic resins [Barbero (1999), McKague (2001)] are softened from solid state to be processed hot and they return to this state after processing is completed and they cool down. They do not undergo any chemical transformation during processing. Thermoplastics have high viscosity at processing temperature, and, therefore, they are difficult to process. Since impregnation is impaired by high viscosity, special care must be taken to ensure contact between the fibres and the polymeric resin.

Composites with thermoplastic matrices can be repaired because the transition to the softened state can be achieved any number of times by application of heat. Polyether ether ketone (PEEK) is the most common thermoplastic resin for high performance applications. It has high fracture toughness, which is important for damage tolerance of composites. PEEK has very low water absorption (about 0.5% by weight) at room temperature. Polyphenylene sulphide (PPS) is a thermoplastic with very good chemical resistance. Polysulfone (PSUL) is a thermoplastic with very high elongation to failure and excellent stability under hot and wet conditions. Some properties of these thermoplastic matrices are given in Table 2-3.

2.2 Typical available FRP products

The use of FRP products in civil engineering field starts around the 1950s when GFRP rebars have been firstly investigated. Nowadays commercially available FRP products (Fig. 2-4) used as internal or external reinforcement for concrete members are: grids (Fig. 2-5), rebars (Fig 2-6 and Fig. 2-7), fabrics (Fig. 2-8) and plates or strips (Fig. 2-9).

2.3 FRP characteristics

2.3.1 General

The use of FRP reinforcing bars in concrete structures is strongly influenced by their physical and mechanical properties. FRP bars can be designed and manufactured to meet specific requirements of a particular application. Available design variables include the choice of constituents (fibre and polymeric matrix), the volume fractions of fibre and matrix, fibre orientation and the manufacturing process. Other factors such as dimensional effects and quality control during fabrication play an important role in determining the characteristics of FRP bars. The properties of FRP materials are also influenced by loading history, duration of loading, temperature and humidity.

Figure 2-4: FRP products

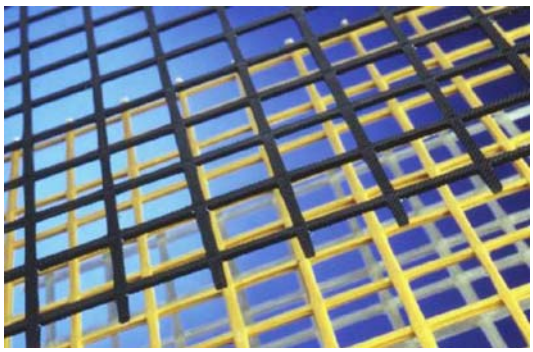

Figure 2-5: FRP grids (Nefcom Ltd.)

Figure 2-6: FRP rebars (Schöck Bauteile GmbH)

Figure 2-7: FRP rebars

Figure 2-8: FRP fabrics

Figure 2-9: FRP plate and strips

A key element in evaluation of FRP properties is the characterization of the relative volume and/or mass content of the various constituent materials. The mass fractions are easier to obtain during fabrication or using one of the experimental methods after fabrication. The volume fractions are used in the micromechanics of composites. Consider a volume v_c of a composite material which consists of volume v_f of fibres and volume v_m of the matrix material. The subscripts c, f and m represent the composite material, fibres, and the matrix material respectively. Also consider m_c, m_f and m_m the corresponding mass of the composite, fibres and the matrix material respectively. The volume fraction and the mass fraction are denoted by V and M respectively. Assuming that no voids are present in the composite the volume fractions and the mass fractions are defined as follows:

$$v_c = v_f + v_m \tag{2-1}$$

$$V_f = \frac{v_f}{v_c} \quad \text{and} \quad V_m = \frac{v_m}{v_c} \tag{2-2}$$

$$V_f + V_m = 1 \tag{2-3}$$

$$m_c = m_f + m_m \tag{2-4}$$

$$M_f = \frac{m_f}{m_c} \quad \text{and} \quad M_m = \frac{m_m}{m_c} \tag{2-5}$$

2.3.2 Physical properties

2.3.2.1 Density

The density ρ_c of the composite can be obtained in terms of the densities of the constituents (ρ_f and ρ_m) and their volume fractions using the "rule of mixtures" for densities:

$$\rho_c = \rho_f V_f + \rho_m V_m \tag{2-6}$$

Using the values for the densities of constituents, Table 2-1 and Table 2-2, the densities of FRP composite reinforcements, based on thermosetting resins, for usual values of fibre volume fractions (V_f = *0.5 to 0.75*) are given in Table 2-4. As can be seen from this table, FRP elements have a density ranging from 0.165 to 0.275 that of steel, which leads to easier handling on the construction site and lower transportation costs.

Table 2-4: Typical densities of reinforcing bars for V_f = 0.5 to 0.75 (kg/m^3)

FRP / Matrix	CFRP	AFRP	GFRP	Steel
Polyester	1430-1650	1310-1430	1750-2170	7850
Epoxy	1440-1670	1320-1450	1760-2180	
Vinyl ester	1440-1630	1300-1410	1730-2150	

2.3.2.2 Coefficient of thermal expansion

The coefficients of thermal expansion (CTE) of FRP bars depend on the types of fibre, resin and volume fraction of the constituents. The polymeric matrices and the glass fibres can be considered isotropic, while carbon and aramid fibres are orthotropic. The longitudinal CTE, (α_L), is dominated by the properties of the fibres, while the transverse CTE, (α_T), is mainly determined by the polymeric matrix. Fig. 2-10 indicates the main directions of a unidirectional FRP rod.

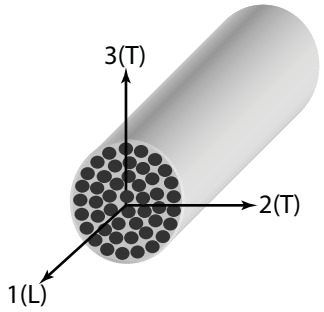

Figure 2-10: Unidirectionally reinforced composite FRP bar with main material axes: 1(L) - longitudinal direction; 2(T), 3(T) - transverse directions

For the case of isotropic constituents the following expressions [Schapery (1968)] have been developed to determine CTEs:

$$\alpha_L = \frac{E_f V_f \alpha_f + E_m V_m \alpha_m}{E_f V_f + E_m V_m} \tag{2-7}$$

$$\alpha_T = (1+\nu_m) V_m \alpha_m + (1+\nu_f) V_f \alpha_f - \alpha_L \nu_{LT} \tag{2-8}$$

where α_f is the CTE of fibre, α_m is the CTE of matrix, E_f is the Young's modulus of fibres, E_m is the Young's modulus of matrix and ν_{LT} is the the major Poisson's ratio of composite determined with Eq. (2-9):

$$\nu_{LT} = \nu_f V_f + \nu_m V_m \tag{2-9}$$

in which ν_f is the Poisson's ratio of fibre and ν_m is the Poisson's ratio of matrix.

For the case of orthotropic fibres (such as aramid and carbon/graphite) the longitudinal fibre modulus, E_{fL}, is different from the transverse modulus, E_{fT}, and so are α_{fL} and α_{fT}, the CTEs in the main directions. Since the matrix is assumed to be isotropic the matrix modulus does not need a second subscript and the thermal expansion coefficients [Kollar and Springer (2003)] can be determined with:

$$\alpha_L = \frac{E_{fL} V_f \alpha_{fL} + E_m V_m \alpha_m}{E_{fL} V_f + E_m V_m} \tag{2-10}$$

$$\alpha_T = V_f \alpha_{fT} + V_m \alpha_m + V_f \nu_{fLT} (\alpha_{fL} - \alpha_L) + V_m \nu_m (\alpha_m - \alpha_L) \tag{2-11}$$

in which α_{fL} is the the fibre longitudinal CTE, α_{fT} is the the fibre transverse CTE and ν_{fLT} is the Poisson's ratio of the reinforcing fibre in the plane LT (Fig. 2-10). Coefficients of thermal expansion for some FRP reinforcing bars with fibre volume fractions V_f = 0.5 to 0.75 are given in Table 2-5 [Rizkalla and Mufti (2001), ACI (2006)].

Table 2-5: Typical coefficients of thermal expansion for steel and FRP materials (V_f = 0.5 to 0.75)

Direction	**Coefficient of Thermal Expansion (x 10^{-6}/°C)**				
	Steel	Stainless Steel	GFRP	CFRP	AFRP
Longitudinal, α_L	11	10 to 16.5	6 to 10	-9 to 0	-2 to -6
Transverse, α_T	11	10 to 16.5	21 to 23	74 to 104	60 to 80

The negative values of CTEs indicate that the material contracts when temperature increases and expands when temperature decreases. Plain concrete is considered isotropic and has a coefficient of thermal expansion that varies from 7×10^{-6} to 13×10^{-6}/°C [Neville (1996)]. Long-term effects of differences in coefficients of thermal expansion and elastic properties of bonded materials (FRP bars and concrete) need to be considered. Test methods to determine the coefficients of thermal expansion for FRP bars have been developed by JSCE [JSCE E-536 (1995)] and ACI 440K [Benmokrane et al. (2001)].

2.3.2.3 Thermal effects on FRP reinforcing bars

It is now accepted that, in case of FRP composites, not all thermal exposure has a damaging effect, since in some cases, it can actually be beneficial to the post cure of FRP composites. At high temperatures polymeric resins will soften due to increased molecular mobility causing an increase in the viscoelastic response accompanied by a reduction in mechanical properties and, in some cases, an increased susceptibility to moisture absorption [Karbhari et al. (2003)]. FRP composites should not be used at temperatures above their glass transition temperature, T_g (T_g is the temperature at which increased molecular mobility results in significant changes in the properties of a cured resin system). At T_g the transition between the soft rubbery state of the polymeric resin and its stiffer or glassy state occurs. The value of T_g depends on the type of resin and it is normally in the range of 70 to 175°C: 70 to 100°C for polyester, 70 to 163°C for vinyl ester and 95 to 175°C for epoxy resin [Bootle et al. (2001)]. For purposes of design it is recommended that materials have T_g at least 30°C above the maximum expected temperature [Karbhari et al. (2003)]. Although above T_g fibres continue to support some load in their direction, the tensile properties of FRPs decrease due to the reduction of the matrix/fibre bond. Experiments carried out at temperatures well beyond T_g, have proven the reduction of other FRPs mechanical properties such as shear and bending strength [Kumahara et al. (1993), Wang and Evans (1995)].

The bond between FRP bars and concrete is mainly dependent on the properties of polymeric resin at the surface of the bar [*fib* (2000)]. At temperatures close to T_g the mechanical properties of matrix are sharply reduced and the matrix is not able to transfer stresses from concrete to the fibres. Reductions in bond strength have been reported in tests carried out by Katz et al. (1999) at temperatures above T_g: 20-40% reduction in strength when reinforcing bars with T_g = 60-124°C were tested at 100°C and 80-90% reduction at a temperature of 200°C [ACI (2006)]. Experimental work has also been performed on FRP reinforced beams subjected to elevated temperatures under sustained load [Okamoto et al. (1993)]. Failure of these beams occurred when the temperature of reinforcement reached values of 250 to 350°C [Sakashita et al. (1997)].

Localised effects, such as increased width of cracks and increased deflections, can also occur in FRP reinforced beams. To avoid structural collapse high temperatures should not reach the end regions of FRP bars allowing anchorage to be maintained. Structural collapse can occur if anchorage is lost due to softening of the polymer and also when temperature rises above the temperature threshold of fibres: 880°C for glass fibres, 180°C for aramid fibres and 1600°C for carbon fibres [Wallenberger et al. (2001), Walsh (2001), Chang (2001)].

Low (negative) temperatures acting on FRP composites can result in matrix hardening, matrix microcracking, and fibre-matrix bond degradation. Freeze–thaw cycles associated with salt can result in degradation evident in swelling and drying as well as expansion of salt deposits. Fire may ignite composite materials with organic matrices and the results of this ignition are the spread of flame on the composite surface, release of heat and generation of smoke (potentially toxic). When the polymeric resin in the outermost layer of FRP bar burns, heat-induced gasification occurs. This has an insulating effect, slowing the heat penetration in the depth of composite. The first effect of fire is to heat up the composite surface. At temperatures beyond T_g the elastic modulus of composite decreases. This loss in modulus is reversible below the temperature of chemical degradation. Further increase in temperature results in the degradation of the chemical structure of the resin and irreversible loss in load carrying characteristics of the material. In FRP reinforced concrete elements the reinforcing bars are embedded in concrete and the reinforcement cannot burn due to the lack of oxygen but the resin will soften due to the excessive heat with the effects described above. When operating at elevated temperatures, other issues may also affect the performance of FRP

reinforcement. The high transverse coefficient of thermal expansion of FRP may induce additional tensile stresses in the surrounding concrete. This phenomenon can be particularly significant in prestressed elements as these additional stresses, in combination with those resulting from the Hoyer-effect, may cause severe longitudinal cracks. FRPs, however, can be engineered to improve their performance in such applications and, for instance, the Arapree bars were developed with a compressible coating that serves as outer layer [Taerwe (1993)].

Fire related issues associated with polymeric composites are more severe in closed spaces (such as buildings and tunnels) than in open spaces (such as bridges). Based on the existing state of knowledge, the use of FRP reinforcing bars is not recommended for structures in which fire resistance is vital to maintain structural integrity [ACI (2003)].

2.3.3 Short term mechanical properties of FRP

The properties of composite materials can be determined by experimental measurements (see for example ACI 2004), but one set of experimental measurements determines the properties of a fibre-matrix system produced by a single fabrication process. When any change in the system variable occurs, additional measurements are required. These experiments, however, may become time consuming and cost prohibitive and a micromechanical approach may be used to estimate properties of composite materials in terms of the properties of their constituent materials [Agarwal and Broutman (1990), Daniel and Ishai (1994)].

2.3.3.1 Tensile properties

The main factors influencing the tensile properties (strength and elastic modulus) of FRP reinforcing bars are: the properties of the constituents (fibres and matrix) and their volume fractions, distribution of the constituents, physical and chemical interactions, fabrication procedure and the manufacturing quality control. The composite literature [Agarwal and Broutman (1990)] gives the following analytical models to determine the longitudinal modulus, E_L, and the longitudinal tensile strength f_{Lt}:

$$E_L = E_{fL}V_f + E_m(1-V_f) \tag{2-12}$$

where E_{fL} is the elastic modulus of the fibre in the longitudinal direction and E_m is the elastic modulus of matrix material considered isotropic. Carbon and aramid fibres are orthotropic and they have different values of longitudinal modulus and transverse modulus, E_{fT}. The ratio E_{fL}/E_{fT} is 24.0 for Kevlar, 15.3 for high strength carbon and 65.0 for high modulus carbon [Gay et al. (2003)]. In case of a hybrid FRP, which includes two or more types of fibres embedded in polymeric matrix, the longitudinal modulus is expressed as:

$$E_L = E_{1fL}V_{1f} + E_{2fL}V_{2f} + E_m(1-V_{1f}-V_{2f}) \tag{2-13}$$

where indexes $_{1f}$, $_{2f}$ denote the first type of fibres and the second type of fibres, respectively. FRP bars do not exhibit any yielding before tension failure and their behaviour shows a linearly elastic stress-strain relation until tensile rupture (Fig. 2-11). Usually in FRP composites the ultimate tensile strain of the fibre is lower than that of the matrix and the following expression can be used to determine the longitudinal tensile strength:

$$f_{Lt} = f_{ft}\left[V_f + \frac{E_m}{E_{fL}}(1 - V_f)\right] \tag{2-14}$$

where f_{ft} is the longitudinal fibre tensile strength. The tensile properties of typical FRP composite bars are given in Table 2-6. The tensile strength of FRP bars varies with cross sectional area. Reductions in strength of GFRP up to 40% as the diameter increases from 9.5 to 22.2mm have been reported in the literature [Faza et al. (1993)] comparing results from different manufacturers. However a 7% strength reduction in pultruded AFRP bars has been identified when the bar diameter increased from 3 to 8mm [ACI (2006)]. Therefore the bar manufacturers should provide the strength values of all different bar sizes.

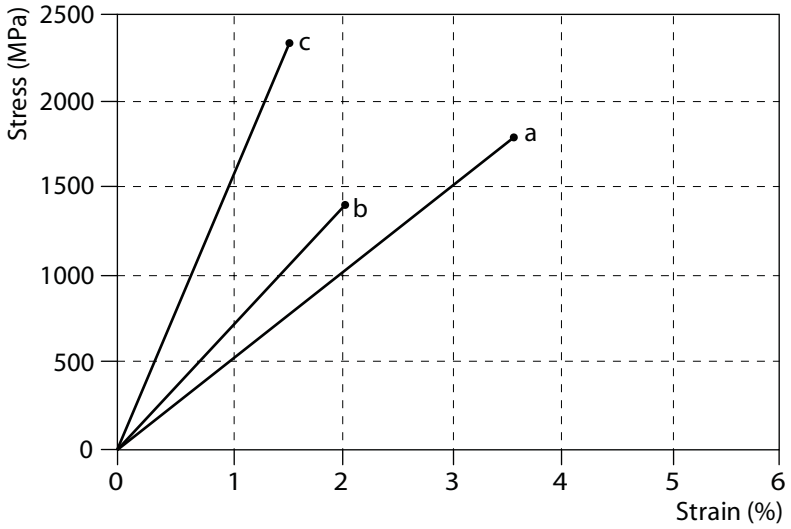

Figure 2-11: Stress-strain diagrams of unidirectional epoxy composites in fibre direction: a) glass/epoxy; b) aramid/epoxy; c) carbon/ epoxy.

Table 2-6: Typical tensile properties of FRP (V_f = 0.5 to 0.75) and steel reinforcing bars

Property	**Material**			
	Steel	GFRP	CFRP	AFRP
Longitudinal modulus (GPa)	200	35 to 60	100 to 580	40 to 125
Longitudinal tensile strength (MPa)	450 to 700	450 to 1600	600 to 3500	1000 to 2500
Ultimate tensile strain (%)	5 to 20	1.2 to 3.7	0.5 to 1.7	1.9 to 4.4

A test method for tensile strength and modulus of FRP bars has been developed and published by ACI Committee 440 [ACI (2004)], and has been submitted to ASTM for approval and standardization. Also a test method for evaluation of tensile properties of continuous fibre reinforced materials used in place of steel reinforcement [JSCE-E 531 (1995)] was adopted by the Japan Society of Civil Engineering [Machida (1997)]. The bar manufacturer should provide the tensile properties of a particular FRP bar and a description of the method used to determine these properties. The FRP bars made of thermosetting resins cannot be bent once they have been manufactured. FRP bars can be fabricated with bends, but in this case a strength reduction of 40% to 50% compared to the tensile strength of the straight bar can occur in the bent regions (see Chapter 6). This reduction is caused by fibre buckling and stress concentration [ACI (2003)].

2.3.3.2 Compressive properties

Although it is not recommended to rely on FRP bars to resist compressive stresses a brief description of their behaviour under compression is useful and it is given in the following. When FRP components are loaded in longitudinal compression the theoretical models for tensile longitudinal strength cannot be used since the failure of the composites is, in many cases, associated with microbuckling or kinking of the fibre within the restraint of matrix material. Accurate experimental values for the compressive strength are difficult to obtain and they are highly dependent on specimen geometry and the testing method. The mode of failure depends on the properties of constituents (fibres and resin) and the fibre volume fraction. The main longitudinal compression failure modes are microbuckling of fibres, transverse tensile fracture due to Poisson strain and shear failure of fibres without buckling. Analytical models have been developed for each failure model to determine the longitudinal compressive strength, f_{Lc}, and they are given below.

a) microbuckling of fibres in the shear mode [Jones (1999)] when $V_f \geq 0.4$:

$$f_{Lc} = \frac{G_m}{1 - V_f} \tag{2-15}$$

where G_m is the shear modulus of matrix:

$$G_m = \frac{E_m}{2(1 + \nu_m)} \tag{2-16}$$

b) transverse tensile fracture due to Poisson strain [Agarwal and Broutman (1990)]:

$$f_{Lc} = \frac{\left[E_f V_f + E_m (1 - V_f)\right](1 - V_f^{1/3})\varepsilon_{mu}}{\nu_f V_f + \nu_m (1 - V_f)} \tag{2-17}$$

where ε_{mu} is the the ultimate tensile strain of the matrix.

c) failure of fibres in direct shear [Daniel and Ishai (1994)] when V_f is very high:

$$f_{Lc} = 2 f_{fs} \left[V_f + (1 - V_f) \frac{E_m}{E_f} \right] \tag{2-18}$$

where f_{fs} is the shear strength of the fibres.

Experimental work [Mallick (1988)] has proved that compressive strength of FRPs are lower than the tensile strengths. Compressive strength is higher for bars with higher tensile strengths, except for AFRP bars where fibres have a nonlinear behaviour in compression even at low levels of stress. The compressive modulus of elasticity of FRP reinforcing bars is also smaller than its tensile modulus of elasticity, being above 80% for GFRP and 85% for CFRP and 100% of the same products [ACI (2006)]. Premature failures in the test resulting from end brooming and internal fibre microbuckling seem to be the cause for the lower values of the compressive modulus. Standard test methods existing in composite literature are not suitable for FRP bars. Specific standard methods to characterise the compressive behaviour of FRP

bars have not yet been developed. The compressive properties for a particular bar should be given by the manufacturer who should also provide a description of the test method used to determine the properties.

2.3.3.3 Shear properties

The behaviour of FRP composites under shear loading is dominated by the matrix properties and local stress distributions. The specialised composite literature is particularly dedicated to the in-plane shear of lamina and laminated structures, but FRP reinforcing bars are mainly subjected to transverse shear. Therefore shear properties should be evaluated with respect to this type of loading (Fig. 2-12).

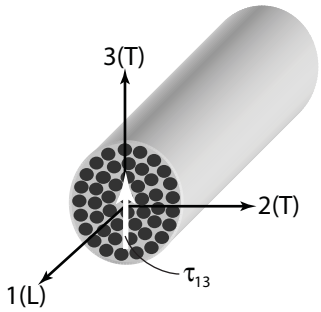

Figure 2-12: FRP bar subjected to transverse shear

The interlaminar shear modulus can be determined with the semiempirical stress-partitioning parameter [Tsai and Hahn (1980)]:

$$G_{13} = G_m \frac{V_f + \eta_{13}(1-V_f)}{\eta_{13}(1-V_f) + V_f G_m / G_f} \tag{2-19}$$

where

$$\eta_{13} = \frac{3 - 4\nu_m + G_m / G_f}{4(1-\nu_m)} \tag{2-20}$$

in which G_f is the fibre shear modulus. The transverse shear may cause matrix splitting without shearing off any fibres. The interlaminar (transverse) shear strength is a matrix dominated property, because the shear force acts on a plane perpendicular to the fibre direction. In this case, fibres do not resist shear and, even worst, the cross sections of the fibres can be considered circular inclusions causing stress concentrations in the matrix. There are no predictive theoretical models for the transverse shear strength; therefore it can be taken in preliminary design as the value of the shear strength of bulk matrix [Barbero (1999)]. Placement of fibres in off-axis directions across the layers of longitudinal fibres increases the shear resistance of unidirectional FRP composites. In case of FRP bars a significant increase in shear resistance can be achieved by winding or braiding fibres transverse to the main reinforcing fibres. Pultruded bars can be strengthened in shear by using continuous strand mat in addition to longitudinal fibres [ACI (2006)]. Test methods for the characterization of the shear behaviour of FRP bars, in terms of both dowel action and interlaminar shear, have been developed by various committees and are now available in the literature [JSCE-E 540 (1995), ACI (2004), ASTM (2002)]. The properties needed for a particular application should be obtained from the bar manufacturer who should also provide information on the test method used to determine the reported shear values.

2.3.3.4 Effects of loading direction on mechanical properties

FRP bars are orthotropic and their best properties are in the fibre direction. When FRP reinforcement is utilised in stirrups the strength in an inclined direction *x* with an angle θ to the fibre direction (so called off-axis strength) is required. Formulas have been developed for both stiffness and strength in off-axis direction (Fig. 2-13).

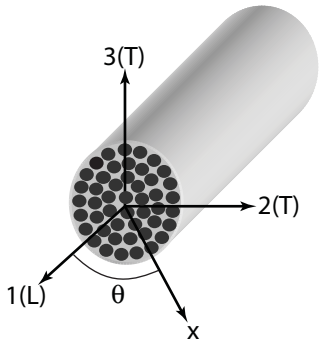

Figure 2-13: Axis x rotated with respect to L

The elastic modulus along a certain direction *x* rotated with an angle θ with respect to axis L, (Fig. 2-13) is given in the expression below [Taranu and Isopescu (1996)], where c = cosθ and s = sinθ. This modulus decreases rapidly as θ increases.

$$E_{x(\theta)} = \frac{1}{\frac{c^4}{E_L} + \frac{s^4}{E_T} + 2c^2 s^2 \left(\frac{1}{2G_{LT}} - \frac{\nu_{LT}}{E_L} \right)} \tag{2-21}$$

where E_T and G_{LT} are the transverse modulus and the in-plane shear modulus respectively:

$$E_T = \frac{E_m E_{fT}}{E_m V_f + E_{fT}(1 - V_f)} \tag{2-22}$$

$$G_{LT} = \frac{G_m G_f}{G_m V_f + G_f (1 - V_f)} \tag{2-23}$$

The ultimate tensile strength along any direction θ [Gay et al. (2003)] is given by the following relation:

$$f_{x(\theta)t} = \frac{1}{\sqrt{\frac{c^4}{f_{Lt}^2} + \frac{s^4}{f_{Tt}^2} + c^2 s^2 \left(\frac{1}{f_{LTs}^2} - \frac{1}{f_{Lt}^2} \right)}} \tag{2-24}$$

where f_{Tt} and f_{LTs} are the transverse tensile strength and the in-plane (Fig. 2-14) shear strength respectively. The ultimate tensile strength transverse to the fibre direction can be determined [Nielsen (1974)] using the following formula:

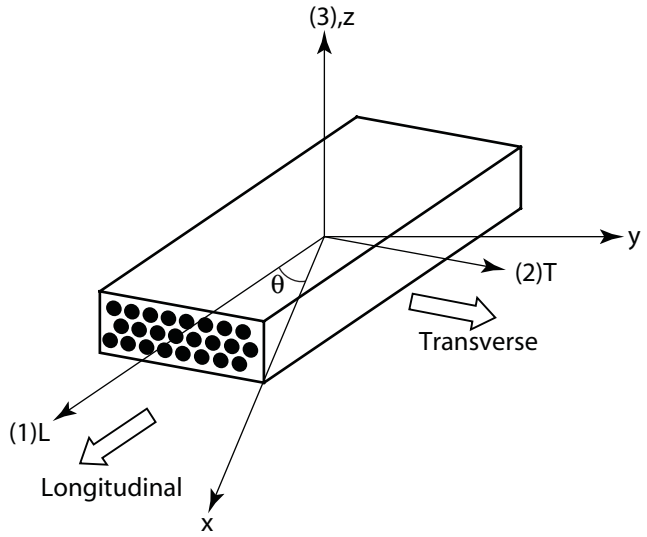

Figure 2-14: Principal and rotated axes of rectangular FRP bar

$$f_{Tt} = \frac{E_T f_{mt}}{E_m}(1 - V_f^{1/3}) \tag{2-25}$$

where f_{mt} is the tensile strength of the matrix. The in-plane shear strength of the composite can be determined [Barbero (1999)] by:

$$f_{LTs} = \left[1 + (V_f - V_f^{1/2})\left(1 - \frac{G_m}{G_f}\right)\right] f_{ms} C_v \tag{2-26}$$

where f_{ms} is the shear strength of matrix material, C_v is a reduction coefficient to account for voids (Eq. 2-27) and V_v is the void volume fracture which usually can be neglected; a good FRP material should have less than 1% voids.

$$C_v = 1 - \sqrt{\frac{4V_v}{\pi(1 - V_f)}} \tag{2-27}$$

When θ exceeds 15^o the tensile strength decreases dramatically since the influence of the transverse properties, matrix dominated, prevail. FRP reinforcing bars are essentially unidirectional anisotropic composites with very different stiffness and strength characteristics in the fibre and transverse directions. A comparative presentation of the main typical short-term mechanical properties in the principal material directions is given in Table 2-7 [Daniel and Ishai (1994), Gibson (1994), Taranu and Isopescu (1996)].

Table 2-7: Typical short-term mechanical properties of GFRP, CFRP and AFRP

Property	**E-glass/epoxy**	**Kevlar 49/epoxy**	**Carbon/epoxy**
Fibre volume fraction	0.55	0.60	0.65
Density (kg/m^3)	2100	1380	1600
Longitudinal modulus (GPa)	39	87	177
Transverse modulus (GPa)	8.6	5.5	10.8
In-plane shear modulus (GPa)	3.8	2.2	7.6
Major Poisson ratio	0.28	0.34	0.27
Minor Poisson ratio	0.06	0.02	0.02
Longitudinal tensile strength (MPa)	1080	1280	2860
Transverse tensile strength (MPa)	39	30	49
In-plane shear strength (MPa)	89	49	83
Ultimate longitudinal tensile strain (%)	2.8	1.5	1.6
Ultimate transverse tensile strain (%)	0.5	0.5	0.5
Longitudinal compressive strength (MPa)	620	335	1875
Transverse compressive strength (MPa)	128	158	246

2.3.4 Long term properties of FRP

FRP composites differ significantly from steel with respect to their long-term properties and it is important to understand their behaviour and apply the corresponding rationale in the design of reinforced concrete elements. This section deals with the most important issues regarding the long term behaviour of FRP composites and their consequences on the design process.

2.3.4.1 Creep and creep rupture

Creep is the term used to describe the progressive deformation of a material with time under constant load. Polymeric resins are viscoelastic and their behaviour is characterized by creep, stress relaxation and load rate effects [Ferry (1980)] (see also Chapter 3).

Two main issues need to be distinguished in relation to creep: the creep strain under long-term load and the long-term tensile strength under sustained load [Balazs and Borosnyoi (2001)]. Most materials start to exhibit significant creep when significant loads are imposed at temperatures exceeding 40% of their melting temperatures [Hull and Clyne (1996)]. Thermosetting resins do not have well defined melting temperatures, but they tend to degrade when subjected to temperature increases of about 100°C above ambient. They are fairly resistant to creep at room temperature. A typical creep curve is shown in Figure 2-15.

After an instantaneous initial elastic strain the curve shows a primary creep region where strains grow fast over a short period of time. The secondary creep stage is characterized by a constant slope and it extends over a long period of time. This is the region that includes the period of time in which the structure will be in operation [Barbero (1999)].The tertiary stage occurs usually for high level of stress. It is characterized by simultaneous accumulation of creep strain and material damage. In many situations with composites it can be assumed that fibres experience no creep, but the creep behaviour of the composite as a whole depends on the load partitioning and constraint [Hull and Clyne (1996)].

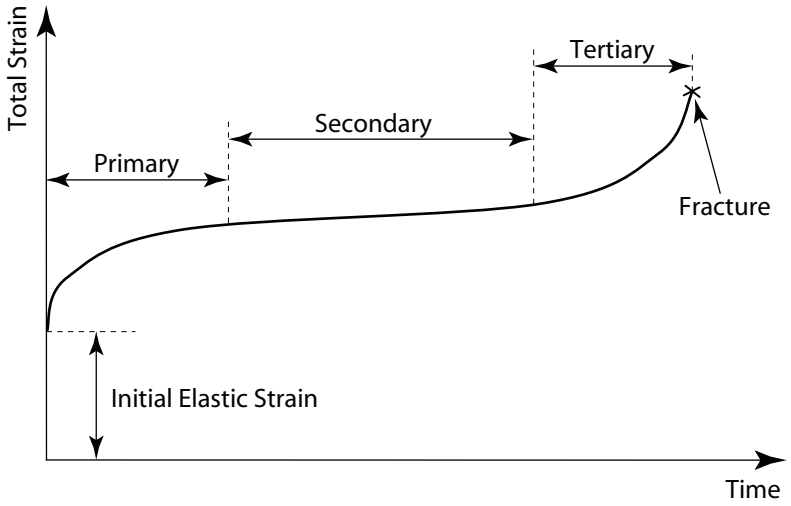

Figure 2-15: Typical strain history curve during creep deformation

The treatment of axial creep of unidirectional FRP composites is straightforward. The initial strain in composite can be determined by dividing the applied stress (σ) by the longitudinal modulus:

$$\varepsilon_0 = \frac{\sigma}{E_{fL}V_f + E_m(1-V_f)} \tag{2-28}$$

As creep occurs in matrix the entire applied stress is transferred progressively to the fibres and the stress increases until the fibres carry the total applied load. At this point the strain of the fibres (ε_∞) and hence of the composite can be determined with:

$$\varepsilon_\infty = \frac{\sigma}{E_{fL}} \tag{2-29}$$

The strain approaches this value asymptotically, since the rate of matrix creep decreases as the stress it carries decreases, and a steady state is never reached [Hull and Clyne (1996)]. Creep coefficients can be determined by linearizing the isostress-creep curve into strain versus log time axes. When plotted in such a manner most polymeric materials approximate to a linear relationship [Hollaway (1993)]. The equation for the total strain of the material can be written as:

$$\varepsilon(t) = \beta \log t + \varepsilon_0 \tag{2-30}$$

where $\varepsilon(t)$ is the total strain in the material after time period t, ε_∞ is the initial strain value and β is the creep rate parameter is equal to $d\varepsilon(t)/dt$.

FRP composites subjected to sustained loads for a long period of time may suddenly fail after a period of time called “endurance limit”. This phenomenon, known as creep rupture, applies to all structural materials. This type of failure is dependent on the fibre type. Carbon and glass fibres have excellent resistance to creep while most polymeric resins are susceptible to creep. Therefore the fibre orientation and the fibre volume fractions have a significant influence on the creep performance of FRP reinforcing bars. The endurance limit decreases as the ratio of the sustained tensile stress to the short term strength increases. Other factors such as high temperature, exposure to UV radiation, high alkalinity, wet and dry cycles and freeze-

thaw cycles may also irreversibly decrease the creep rupture endurance time. Creep failure strength can be defined as the stress causing failure after a specified period of time following the start of a sustained load. Some experimental work [Budelman and Rostasy (1993)] indicates that creep rupture does not occur if sustained stress is limited to 60% of the short term strength. There are an important number of papers published on this subject, from fundamental to practical aspects, but few data are currently available for endurance times beyond 100 hours [ACI (2006)]. Until more research is done on this subject design conservatism is recommended.

Results from a comprehensive experimental programme [Yamaguchi et al. (1997)], carried out on 6mm FRP bars made of GFRP, AFRP and CFRP, indicated that a linear relationship exists between creep rupture strength and the logarithm of time, for intervals up to 100h. By extrapolating the results to 500,000h (57 years) the ratios of stress level at creep rupture to the short-term strength of the GFRP, AFPR and CFRP reinforcing bars were linearly extrapolated to be 0.29, 0.47 and 0.93 respectively. Commercial twisted CFRP bars and AFRP bars with an epoxy matrix were tested at room temperature to determine the endurance time [Ando et al. (1997)].The estimated retained percentage of short term strength after 50 years was found to be 79% for CFRP and 66% for AFRP. Creep rupture strength in GFRP bars with vinyl ester matrix has been investigated at room temperature [Seki et al. (1997)]. A percentage of 55% of the short-term strength has been determined at an extrapolated 50 year endurance time.

Test results of a comprehensive experimental programme on long-term properties of AFRP and CFRP bars carried out in various environments at an applied stress equal to 40% of the initial strength have been reported [Saadatmanesh and Tannous (1999a), (1999b)]. Creep strains recorded were higher in the AFRP bars than in CFRP bars. The results also indicated a slight trend towards higher creep strain in larger diameter bars and in bars immersed in acidic solutions.

A test method to characterize creep rupture of FRP bars was proposed by Japan Society of Civil Engineers [JSCE-E533 (1995)] and ACI 440K proposed "Test Method for Creep of FRP Bars" [ACI (2004)]. These test methods are intended to determine the load-induced tensile strain at imposed ages for FRP bars under a selected set of controlled environmental conditions and the corresponding load rate. To avoid creep rupture Canadian Highway and Bridge Design Code [CAN/CSA (2000)] recommends the use of adjusting factors for material resistance. Values for safe sustained stresses are also recommended [ACI (2006)], (see Chapter 3).

2.3.4.2 Relaxation

Stress relaxation is the decay in stress with time when the material is kept under a constant strain condition [Hollaway (1993)]. The relaxation phenomenon is characterized by the time dependent decrease in load in a FRP bar held at a given constant temperature with prescribed initial load applied and held at a given constant strain [Machida (1997)]. A relaxation rate can be determined by dividing the load measured in the relaxation test by the initial load. It represents the percentage reduction of load versus its initial value after a specified period of time, when its initial load is applied and the strain specified. The most common is the relaxation value after 1 million hours, which is referred to as the million hours relaxation rate. A test method for long-term relaxation of FRP bars has been adopted by JSCE [JSCE-E534 (1995)] and a ACI sub-committee 440K proposed a similar test method [ACI (2004)].

Experimental work has been carried out on different FRP products and on different load durations [Ando et al. (1997)]. The FRP tendons used were 12.5mm-diameter CFRP and

15mm-diameter AFRP. Tests were performed at 20°C, 40°C and 60°C for periods of time exceeding 3000 hours. Estimated relaxation rates by setting the service life of the structures to 50 years have been calculated: 2.0 to 3.1% for CFRP bars and 18.4 to 23.4% for AFRP bars. Test results indicate that the higher the temperature, the greater the relaxation rate and this tendency is stronger with AFRP bars. Relaxation after 1000 hours can be estimated as 1.8 to 2.0% for GFRP tendons, 0.5 to 1.0% for CFRP tendons and 5.0 to 8.0% for AFRP tendons, while relaxation of GFRP, CFRP and AFRP tendons after 50 years of loading can be estimated as 4.0 to 14.0%, 2.0 to 10.0% and 11.0 to 25.0%, respectively, depending on the initial tensile stress [Balazs and Borosnyoi (2001)].

2.3.4.3 Fatigue

Fatigue is defined as the degradation of the integrity of a material as a result of repeated applications of a large number of loading cycles. The integrity of the material is commonly measured in terms of mechanical properties such as strength and stiffness. The loss of strength is directly associated with the failure of the component. Such a failure can occur at a small fraction of the static strength of material. Advanced polymeric composites exhibit superior fatigue performance due to their high fatigue limit and resistance to corrosion. Fatigue damage in FRP composites is complex due to several damage mechanisms occurring at many locations throughout an element: matrix cracking, fibre breaking, crack coupling, delamination initiation and delamination growth [Schaff (2001)]. As a result FRP composite components fail due to a series of interdependent damage events. The fatigue behaviour of unidirectional FRP composites depends on the constituent behaviour and on the fibre/interface properties. They have very good fatigue resistance and are essentially linear to failure. If the composite contains angle-plies damage mechanisms can occur under load and the stress-strain response becomes non-linear. A unidirectional FRP composite exhibits little damage until immediately before failure whereas a multidirectional composite shows a gradual reduction in strength and stiffness values [Hollaway (1993)].

A large amount of data for fatigue behaviour of FRP composites has been generated so far, mainly relating to aerospace applications. Some general observations on FRP materials used in construction can be made despite the differences in quality and consistency between aerospace and commercial-grade FRPs [ACI (2002)]. Special research programmes have also been carried out in the last two decades to evaluate the fatigue behaviour of FRP bars and tendons as reinforced and prestressed concrete reinforcement. Individual glass fibres are not prone to fatigue failure but are susceptible to delayed rupture caused by the stress corrosion induced by the growth of surface flaws in the presence of moisture [ACI (2006)]. GFRP bars subjected to cyclic tensile loading may loose approximately 10% in the initial static strength per decade of logarithmic lifetime [Mandell (1982)]. No clear fatigue limit (the stress level below which a material can be stressed cyclically for an infinite number of times without failure) can usually be defined. Models for fatigue behaviour prediction of GFRP composites under various stress ratios and test frequencies have been recently developed [Epaarachi and Clausen (2003)]. Environmental factors significantly influence the fatigue behaviour of GFRP composites due to vulnerability of glass fibres to moisture, alkaline and acidic solutions. CFRP composites are thought to be the least vulnerable to fatigue failure. The average downward slope of CFRP data on a plot (S-N) is about 5 to 8% of initial static strength per decade of logarithmic life. At one million cycles the fatigue strength (residual strength after being subjected to fatigue) is usually between 50 and 70% of the initial static strength. These values seem to be relatively unaffected by normal moisture and temperature exposures of concrete structures unless the fibre/matrix interface is significantly degraded by the environment. Reports of data to 10 million cycles [Curtis (1989)] indicated a continuous

downward slope of 5 to 8% in the S-N curve. In the case of CFRP bars encased in concrete the fatigue strength decreased when the temperature increased from 20°C to 40°C [ACI (2006)]. In the same report endurance limit was found to be inversely proportional to loading frequency. It has also been found out that the endurance limit decreases due to the higher mean stress or a lower stress ratio (minimum stress/maximum stress), [Saadatmanesh and Tannous (1999a)]. The fatigue behaviour of AFRP composites subjected to cyclic tensile loading appears to be similar to GFRP and CFRP materials. Strength degradation per decade of logarithmic lifetime is about 5 to 6%. No distinct endurance limit is known for AFRP but for 2 million cycles the fatigue strength reported is 54 to 73% of the initial ultimate strength [Odagiri et al. (1997)]. The addition of any type of deformations, ribs or wraps induces local stress concentrations that affect the performance of FRP bars under repeated loading. The stress concentrations generate multiaxial stresses and increase matrix-dominated damage mechanisms. Depending on the construction of the FRP bar, additional fibre-dominated damage mechanisms can also be activated near deformations [ACI (2006)]. A test method to determine the fatigue characteristics of FRP rods under tensile cyclic loading has been adopted by JSCE [JSCE-E 535 (1995)] and a similar method has been proposed by ACI 440K [Benmokrane (2001)].

3 Durability: performance and design

3.1 Scope

This chapter examines the long-term durability of FRP composites used as internal reinforcement and prestressing tendons. It is important to note that the durability issues for post-tensioned structures are different, since the tendons are, in principle, not directly exposed to concrete alkalinity. As the FRP technology is constantly developing, the guidance given here may need to be periodically reviewed and updated to keep pace with new developments in fibres, resins, advances in manufacturing techniques and composite chemical and physical properties.

3.2 Introduction

This section discusses the concrete environment and its effect on fibre-reinforced polymers (FRP) in terms of internal and external aggressive conditions that may affect its durability. The specific conditions considered are the effects of moisture, chlorides, alkali, stress, temperature, UV actions, carbonation and acid.

The differences in performance between glass, aramid and carbon fibres and the binding polymers are identified where possible. However, variability may also arise from bar manufacturing techniques and differences within generic material performance.

Notwithstanding the above, the potential degradation mechanisms are discussed with reference to internationally published research and some very general recommendations are given at the end of each section in an attempt to give some guidance to engineers when selecting FRP for construction.

Existing international Design Guidelines are also discussed and summarised in this section. A new method of addressing FRP durability issues, based on more specific identification of the environments within which FRP would be used [Byars *et al.* (2003)] is also introduced and adjusted to consider the material properties and the chemical cinetics.

3.3 State of the art

FRP durability in concrete has predominantly been measured by accelerated test methods that expose specimens to environments harsher than they would normally encounter in service. These data are then used to extrapolate estimates of the likely long-term performance.

Mechanical changes in tensile strength, interlaminar shear and bond strength and elastic modulus, are the best indirect indicators of durability of FRP composite reinforcement. These may be complemented by studies of physical and microstructural properties using techniques including TGA (Thermogravimetric Analysis), Light and SE (Scanning Electron) Microscopy, DMA (Dynamic Mechanical Analysis), DSC (Differential Scanning Calorimetry), Potentiodynamic Polarisation Scans, Galvanic Coupling test and FTIR (Fourier Transform Infrared Spectroscopy).

Although considerable progress has been made towards understanding the deterioration mechanism of FRP reinforcement in concrete, limited design data is available that can be easily used by design engineers. The lack of international agreement on FRP durability test methods, variability in FRP production methods, various fibre/polymer types, research approaches and lack of real-time performance data further complicates the issue. In order to develop a sound and practical design guideline, a scientific link between research test data and FRP design properties is proposed in this document.

There is, therefore, a need to identify and ratify standard test methods, by the international research community, that could be confidently recommended to civil engineers for use as a basis upon which to select FRP materials for use as concrete reinforcement and pretensioning tendons. This document presents substantial work that has been done to date by researchers as well as the most important design guidelines that can be used as basis for specifying FRP as reinforcement for concrete structures.

3.3.1 The concrete environment

Concrete contains calcium, sodium and potassium hydroxides creating pore water solutions with a pH value of about 13. This high alkalinity causes the formation of a passivating oxide layer on the surface of the steel reinforcement, preventing it from direct contact with water and oxygen, and consequently, inhibiting corrosion. The most common depassivating schemes are: carbonation of concrete, penetration of chloride ions and sulphuric acids leading to corrosion of steel. Steel corrosion leads to a significant increase in the volume of the bar, causing further concrete and steel deterioration.

Carbonation is the most common durability problem. It occurs at a rate depending on the concrete W/C ratio, cement type, curing process, humidity and CO_2 concentration. Chloride attack is observed at reinforced concrete structures with a supply of chlorides, such as sea structures (marine environment), swimming pools, and concrete bridges in cold regions. Sources of chloride can be wind-borne or direct contact of saltwater or de-icing salts. Sulphuric acids are mostly of biogenic nature. Concrete structures may also experience heating/cooling, freezing/thawing, and wet/dry cycles that likewise promote concrete decay and subsequent steel corrosion.

The factors affecting FRP durability are different from those affecting steel reinforcement. For instance, FRP does not appear to be significantly affected by chlorides or the process of carbonation. The following discussion gives guidance on the use of FRPs in structural elements subjected to a variety of environmental exposure conditions.

3.4 Durability of FRP as internal reinforcement

There are three components within a composite material that influence its long term properties, as follows:

- the matrix
- the fibres
- the fibre/matrix interface

Each of these elements can be susceptible to attack by various aggressive environments, yet all three should continue to function fully throughout the design life of the composite. The matrix is inherently resistant to the aggressive medium (in this instance - strong alkalis), therefore, it prevents deterioration of the fibres and the interface region by providing a barrier against the concrete and the external environment. External factors which may influence the effectiveness of this protection include:

- nature of the environment (pH and presence of aggressive ionic species),
- stress in the composite,
- temperature,
- condition of composite (cut ends, damage etc.), and
- quality of composite (surface finish, voids, resin homogeneity).

The effectiveness of the resin will depend upon the continuity of its surface. This is why cut ends of short FRP reinforcement bars and exposed fibres can be problematic from a durability point of view. Such regions generally provide a transport network throughout the composite by a wicking mechanism. Here the media can attack the fibre/matrix bond and continue to progress along the fibre length very rapidly, which then exposes both fibres, matrix and the resin/fibre interface to direct attack by the surrounding environment. Cut surfaces of short bars, may need to be sealed to avoid penetration of chemical agents.

The quality of a composite in terms of its durability performance can be expressed by a number of factors.

- resin wet out (how well the fibres are covered by resin).
- absence of cracks (either surface or through out the cross section).
- absence of voids (generally smaller and well distributed is better).
- degree of cure of resin (if the production process is not well controlled the resin may be insufficiently cross-linked to provide the designed protection).
- strong fibre/matrix interface (incorrect selection of fibre or matrix type or incorrect processing can lead to a poor interface prone to environmental attack).

All the above factors need to be addressed to ensure optimum durability of the composite system. The key area where durability advantages may be achieved by the matrix, is the selection of a suitable resin which should be:

- inherently able to resist alkali and chloride attack,
- sufficiently tough to resist micro cracking,
- sufficiently impermeable to resist environment penetration to the interior,
- easily processable to minimise quality variations,
- very compatible with fibres to ensure a strong fibre/matrix bond.

3.4.1 Effect of water

The effect of water on the properties of FRP composites has been studied in air at different relative humidities (% RH) and different temperatures, as well as immersed in water at different temperatures and stresses [Bank and Gentry (1995), Saadatmanesh and Tannous (1997), Hayes *et al*. (1998), Steckel *et al.* (1998), Verghese *et al.* (1998) and Dejke (2001)]. Common indicators for evaluating long-term durability performance of FRP under these conditions are changes in tensile strength and elastic modulus.

Studies indicate that deterioration of polymer resins may occur when water molecules act as resin plasticizers and disrupt Van-der-Waals bonds in polymer chains [Bank and Gentry (1995)]. This causes changes in modulus, strength, failure strain, toughness and swelling stresses leading to polymer matrix cracking and, hydrolysis and fibre-matrix de-bonding [Hayes *et al.* (1998)]. The literature indirectly suggests that the last of these is fibre-dependent, it appears to be more serious at elevated temperatures (>60^{o}C), in line with increased moisture absorption content at saturation, particularly for polyesters with higher water diffusivity. However Hayes *et al.* (1998) found improved mechanical properties with some FRPs in water.

Summary

With the above mixed findings in mind, in moist conditions above 40^{o}C, the use of FRP as reinforcement bar in more aggressive conditions than the proposed exposure environment should be backed by laboratory data on the performance of the specific fibre/polymer combination. Tables 3.6 and 3.7 in section 3.5.3.5 and 3.5.3.6 also give some additional conservative guidance for generic FRP materials.

3.4.2 Effects of chlorides

A potential application of FRP is in saline environments where steel is likely to corrode without additional protection. Researchers [Saadatmanesh and Tannous (1997), Sasaki *et al.* (1997), Sen *et al.* (1997), Gangarao and Vijay (1997), Chin *et al.* (1997), Steckel *et al.* (1998), Rahman *et al.* (1998), Toutanji and El-Korchi (1998)] have investigated glass, aramid and carbon fibre reinforced polymer (GFRP, AFRP and CFRP) products with different surface veil systems in chloride concentrations up to 4%. Stressed and unstressed bars at ambient temperatures of up to 70^{o}C and varying RH have been investigated, and in some cases effective weathering periods of >50 years have been claimed.

As results vary widely, differentiation between chloride attack and degradation due to moisture diffusion and/or alkali attack of the fibres is difficult. In broad terms, CFRP bars exposed to combined chloride/moisture attack in concrete show very little degradation with time, exposure or temperature. AFRP and GFRP elements may show up to 50% loss of strength and stiffness and stress relaxation of up to 30% .

It needs to be emphasised here that deterioration of FRP may not occur due to chloride attack but instead due to alkali attack or resin plasticization by water uptake. However, there are some indications that saline solutions are a slightly more severe environment than fresh water.

Summary

The data on chloride attack are insufficient to draw definite conclusions. The use of FRP as reinforcement should be based on knowledge of the performance of a specific bar in a chloride environment in combination with the effects of moisture and alkali attack on the selected system.

3.4.3 Effects of alkali

Although concrete traditionally protects steel reinforcement, concrete alkalinity may affect glass fibres unless suitable polymer resins [Steckel *et al.* (1998)] are used to protect them. Resistance is generally thought to be best with carbon, followed by aramid and then glass fibres [Machida (1993)].

Alkali attack is widely studied, however, the absence of an internationally accepted durability test method, and the use of various types/combinations of commercially available fibre/polymer materials and production methods in the FRP market resulted in widely diverse test data. These test results are rather divergent, resulting in variable implications. In some investigations, FRP has been embedded in concrete to study changes in the bond properties [Scheibe and Rostasy (1998)], while the majority of research projects has used simulated concrete pore solutions containing $NaOH_2$, KOH and saturated $Ca(OH)_2$ with pH of 12-13.5. Temperature ranges used have been 20-80°C [Conrad *et al.* (1998)].

It is important to note here that there is significant evidence that simulated pore solutions are much more aggressive than the concrete environment due to increased OH- ion mobility. Consequently, data of this type should not be interpreted as having a linear relationship with FRP resistance in the concrete environment and more work needs to be done to develop robust real-time models from this type of accelerated exposure data.

Mechanical testing

Residual changes in tensile strength, Young's Modulus and ultimate strain; physical analysis (TGA, DMTA, DSC, FTIR) [Bank *et al*. (1998), Chin *et al.* (1998)] and diffusion tests [Alsayed and Alhozaimy (1998), Scheibe and Rostasy (1998)] have also been used to

correlate physical properties with mechanical behaviour. For concrete members, changes in moment capacity [(Scheibe and Rostasy (1998), Gangarao and Vijay (1997)] and pullout tests [Sheard *et al*. (1997), Sen *et al*. (1999)] have been assessed. Stress rupture life tests (time to failure tests under different loads) in different environments have been performed by different investigators [Greenwood (2001), Renaud (2005), Alwis and Burgoyne (2006), Weber (2005)]. The following factors affecting the rate of alkali attack of FRP have been identified.

- the susceptibility of plain fibres to alkali attack.
- the alkali-diffusivity of the resin, and therefore the level of protection available to the fibre.
- the quality of the fibre-resin bond, through which alkali may permeate and attack the fibre.
- the temperature, which affects reaction rates and rates of diffusion.
- the concentration of alkali (affected by cement type and concrete mix).
- alkali ion mobility (affected by degree of saturation and the pore volume).

Due to commercial sensitivities, some researchers tend not to reveal technical details on fibres and polymers properties, and this makes interpretation of test data and robust conclusion difficult. In addition, no sound models yet exist for the conversion of accelerated results into reliable real-time data. The following discussion of alkali attack should be read with these factors in mind. In general two different approaches are adopted by researchers.

According to the first approach the durability test should cover the whole service life. Residual properties are, in general, determined after conditioning the composite at elevated temperatures to accelerate ageing.

According to the second approach stress rupture life tests are performed in concrete or simulated concrete pore solutions under different stress levels. Long term strength is then extrapolated from these results.

Exposure to alkaline solution – fibres

A study by Bank *et al.* (1998) showed that immersed E-glass/vinyl ester rods in ammonium hydroxide (NH_4OH) solution (30%) at 23°C (224 days) exhibited 12% tensile strength loss, while TGA analysis showed deterioration at the matrix-fibre interface. Steckel *et al.* (1998) immersed CFRP and GFRP systems in $CaCO_3$ solution (pH 9.5) at 23°C (125 days). The systems were unaffected except for a 10% reduction in elastic modulus for one GFRP system and a 30% reduction in short beam shear strength.

Combined freeze-thaw/alkali-exposure testing by Gangarao and Vijay (1997) generated 7-49% tensile strength loss and 3-31% drop in elastic modulus for E-glass GFRP systems (with vinyl ester or polyester resins). Saadatmanesh and Tannous (1997) immersed CFRP, AFRP and GFRP specimens in saturated $Ca(OH)_2$ solution at 25°C and 60°C and showed that Fick's Law could predict FRP tensile strength losses.

A summary of strength loss results for stressed and unstressed bars in alkaline environment is given in Table 3.1.

Exposure to alkaline solution – resins

Chin et al (1998) immersed polymeric resins in alkali at ambient and elevated temperatures and tested the specimens for tensile strength and using DMTA, DSC, TGA and FTIR. The results showed that vinyl ester polymers had a higher resistance than iso-polyester (80% and 40% tensile strength remaining respectively). Bakis *et al*. (1998) tested three different GFRP rods by 28-days immersion in a saturated solution of $Ca(OH)_2$ at 80°C. The 100% vinyl ester rods were less affected than vinyl ester/polyester blended matrixes.

Table 3-1: Strength loss for stressed and unstressed bars in alkaline environment.

Author	Material	Resin	pH	Env.	Temp.	Duration	Stress while ageing	Strength loss	Claim
Tannous et al. (1998)	AFRP AFRP CFRP CFRP CFRP CFRP		12 12 12 12 12 12	sat. $Ca(OH)_2$	60°C 25°C 60°C 25°C 60°C 25°C	1a 1a 1a 1a 1a 1a		6,4% 4,3% 0% 0% 0% 0%	
Porter (1997)	GFRP GFRP CFRP		12,5-13		60°C 60°C 60°C	3m 3m 3m		55% 73% 0%	50a
Uomoto (1997)	GFRP AFRP AGFRP			NaOH	40°C 40°C 40°C	4m 4m 4m			
Allmusallam Al-Salloum (2005)	GFRP	VE	>13	Cement paste 1%Na_2O in sea water	40°C 40°C 40°C 40°C 40°C 40°C	4m 8m 16m 4m 8m 16m	0 0 0 20-25% 20-25% 20-25%	2.1% 15.6% 19.7% 29.4% 39% 47.9%	
Alsayed Alhozaimy (1998)	GFRP GFRP GFRP GFRP	VE+UP VE+UP		cement paste 20g/l NaOH	Out-door	4m 4m 4m 4m		20% 0% 30% 0%	
Micelli, Myers, Nanni (2001)	GFRP GFRP GFRP GFRP CFRP CFRP CFRP CFRP		12,6	0,16% $Ca(OH)_2$ +1% NaOH + 1,4% KOH	60°C 60°C 60°C 60°C 60°C 60°C 60°C 60°C	21d 42d 21d 42d 21d 42d 21d 42d		0% 0% 30% 41% 1% 8% 0% 0%	14a 28a 14a 28a 14a 28a 14a 28a
Benmokrane et al. (2005)	GFRP GFRP GFRP GFRP GFRP	VE: d= 9,5mm 9,5mm 12,7mm 16mm 16mm	12,8	ACI	64°C 20°C 57°C 55°C 61°C	2m 14m 4m 1m 2m	19-29% 19-29% 19-29% 19-29% 19-29%	12% 15% 17% 2% 16%	
Rahman (1998)	GFRP CFRP	VE VE		58g/l NaOH	70°C	45d 370d	30% 50%	70%	
Arockiasamy *et al*. (1998)	CFRP		13-14			9m	65%	0%	
Scheibe Rostasy	AFRP AFRP			Air 0,4m KOH	20°C 20°C	3308h 714h	75% 75%	25% 25%	
Weber (2004)	GFRP GFRP GFRP	VE VE VE	13,7	sat. $Ca(OH)_2$ NaOH KOH	60°C 60°C 60°C	2000h 2000h 2000h	20% 25% 30%	<5% <5% <5%	87 years

Alkali exposure under accelerated conditions (stressed and or elevated temperature)

In real concrete structures, most reinforcement is stressed due to both sustained and live load actions. The influence of stress and alkali has been studied by several researchers. Gangarao and Vijay (1997) found strength reductions (1-76%) for stressed GFRP bars in alkaline solution of pH 13 for 201 days. Vinyl ester resin showed the best resistance. Sheard *et al.* (1997) reported reduced interlaminar shear strength for some GFRP and CFRP systems in pH 11.5-13.5 solutions, but others were almost unaffected. In a related study, Clarke and Sheard (1998) showed that CFRP specimens performed less well than GFRP after 6 months exposure in accelerated conditions (pH 12.5, 5% ultimate bending stress at 38^{o}C). Benmokrane *et al*. (1998) also found reduced strengths in stressed alkali exposure when evaluating the influence of resin type and manufacturing processes and concluded that vinyl ester is the most suitable polymer for GFRP bars.

Porter *et al.* (1997) immersed embedded E-glass/vinyl ester rods in 60^{o}C water and 60^{o}C alkali (pH 12). In pullout tests the rods were unaffected, possibly because thick concrete cover protected the bars from full exposure. Pantuso *et al*. (1998) embedded GFRP bars in concrete and subjected them to wetting/drying cycles in water for 60 days. Tensile strength decreased by up to 21% compared to 7% for naked rods immersed in a water bath. To simulate a tidal zone, CFRP specimens in concrete were subjected to wetting/drying cycles for 18 months at 20-60^{o}C by Sen *et al*. (1998). The bond strength increased due to swelling of the FRP bars, but flexural tests on reinforced beam specimens did not show similar improvement. Sheard *et al*. (1997) also reported no mechanical or physical deterioration in GFRP or CFRP after 12 months in various alkaline solutions at 20-38^{o}C. Porter *et al*. (1997) studied prestressed beams (0.4 ultimate tensile strength) immersed in highly alkali solutions and reported that GFRP/polyester resin tendons lost their pre-stressing force whilst CFRP, also made with polyester resin, appeared unaffected. Adimi *et al.* (1998) studied tension-tension fatigue of GFRP and CFRP reinforcement in varying alkalinity and reported only negligible effects.

An AFRP durability study by Scheibe and Rostasy (1998) tested prestressed (to 0.7-0.85 of ultimate tensile strength) slabs, pre-cracked and stored for 2 years. The moment capacity was unchanged. In other study, Gangarao and Vijay (1997) immersed GFRP-reinforced concrete beams in salt water for 240 days and showed a reduced moment capacity of 18%, attributed to alkali-induced bond deterioration. Tomosawa and Nakatsuji (1997) exposed reinforced beams on the Japanese coast for two years and found no flexural strength reduction for AFRP, CFRP or GFRP bars but a small reduction for prestressed beams with AFRP and CFRP tendons. Field exposure tests using GFRP and CFRP pullout specimens by Sheard *et al*. (1997) showed a slight increase in pullout strength after 12 months, which was attributed to increased concrete strength. Similar results were found by Sen *et al*. (1999) for CFRP epoxy rod specimens in an outdoor environment for 18 months. In this case the increase was ascribed to swelling of the CFRP material.

Table 3.2 gives a summary of results from Chalmers University for tensile strength reductions obtained for GFRP bars in alkaline solutions, concrete and water at 60^{o}C and 20^{o}C [Dejke (2001)].

Table 3-2: Effect of Temperature on GFRP exposed to alkali, concrete and water

Exposure Condition	Temp (^{o}C)	% of original tensile strength				
		Age at Test (days)				
		28	90	180	365	545
Alkali	60	82	55	37	32	31
Concrete	60	91	80	57	51	45
Water	60	93	84	75	73	72
All (average)	20	95	92	90	88	80

The results presented in Table 3.2 show that the most aggressive environments in descending order are alkali 60°C, concrete 60°C, and then water 60°C. The results obtained for the alkali, concrete and water at 20°C were similar and an average of these conditions is shown in the table (around 20% deterioration after 18 months). The hotter environments demonstrate the significant effects of temperature on GFRP degradation and show that extra, carefully evaluated safety factors should be used when bars are subjected to elevated temperatures. From these results Dejke (2001) determined a model for the strength retention as a function of time for different corrosion intensities (see Fig. 3-1).

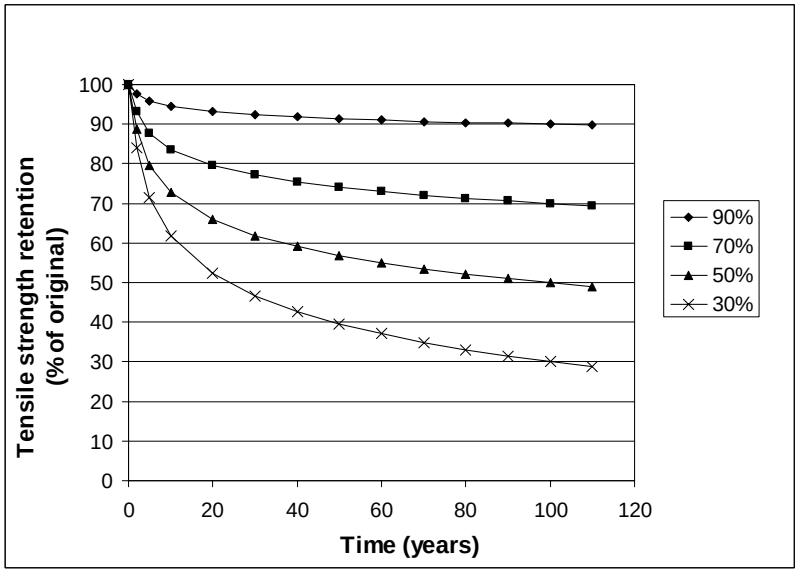

Figure 3-1: Shape of theoretical strength retention curves. Examples shown relate to retained strengths of 90%, 70%, 50% and 30% after 100 years [Dejke (2001)]

A durability study conducted in Canada under the umbrella of the ISIS Network [Mufti et al. (2005), Mufti et al. (2007)] has shown that GFRPs have excellent performance in concrete structures. As part of this study, five bridge decks across Canada, from British Columbia to Nova Scotia, were closely monitored for eight years under service conditions. Test results of core samples taken from these five structures revealed that the alkaline environment developed in these concrete bridge decks did not have any detrimental effect on the GFRP reinforcement. The extremely positive results obtained from this study led to the publication of an updated version of the Canadian Highway Bridge Design code that permits the use of FRPs for strengthening and reinforcement on both new and rehabilitated bridges and concrete structures.

A new approach to FRP durability specifications [Byars *et al.* (2001), Weber (2006a)], which takes temperature, moisture and time effects into account, and therefore allows environment-specific durability design of FRP to be applied to the structural design process, is discussed later in this section.

Summary

Performance of FRP reinforcement and pretensioning tendons in alkali environment varies with the materials (fibres and resins) used and with the manufacturing processes. Literature suggests that FRP deteriorates much faster in alkaline solution than in concrete, which is probably due to the higher mobility of the OH^- ions. Specific observations are given below.

- extensive degradation has been evidenced in GFRP rods after exposure to alkaline solutions at high temperature. Bars embedded in concrete at various temperatures and with

good fibre-resin combinations show only limited degradation, but this increases with temperature and stress level.
- alkalis affect AFRP bars and tendons less than GFRP, but a combination of alkali solution and high tensile stress (in the order of 0.75 ultimate tensile strength) may damage AFRP bars significantly.
- there is no significant alkali attack problem for CFRP with a proper fibre-resin system.
- vinyl esters have much better alkali resistance than polyester resins.

3.4.4 Effect of sustained stress (stress rupture)

FRP subjected to sustained tensile stresses lower than ultimate short-term stress may fail by stress rupture, also referred to as creep rupture or static fatigue. For GFRP and AFRP, stress-rupture can take place at relatively low stress, while CFRP has a better resistance. A straight line describes the relationship between the logarithm of the sustained load and the logarithm of time to failure. Thus, data obtained for high stresses may be extrapolated to determine the theoretical stress levels that correspond to the required service-life (say 100 years).

The stress-rupture mechanism is not, however, exclusively stress-related. Researchers have reported that the surrounding environmental conditions affect the time to failure. A dry glass fibre can resist 70% of its ultimate strength for 100 years, a fibre in water can resist only 50% of its ultimate strength for the same time, while the contact to acids or alkalis can lead to a sudden failure at even lower stress values (Maxwell et al. 2005). Some researchers have made predictions of the time to stress-rupture for fibres and fibre composites. For E-glass fibre strands the maximum sustained stress levels corresponding to 120 years were reported to be 30% and 25% of the original short-term strength for stress-rupture tests in air and water respectively (Proctor et al. 1967). Scheibe and Rostasy (1997) reported that the theoretical stress-rupture strength for a GFRP bar (Polystal) in dry air (20°C, 65% RH) was approximately 70% of the original ultimate short-term strength after 10^6 hours (114 years). Greenwood (2001) extrapolated to 45% of the original short term strength for pultruded profiles in air. For saltwater and cement extract, he extrapolated lower values.

According to Yamaguchi *et al.* (1997) the critical stresses due to stress-rupture are 0.3, 0.47 and 0.91 for GFRP, AFRP and CFRP, respectively, after 50 years. For the same period of time, Ando et al (1997) found the critical stresses to be 0.66 (AFRP) and 0.79 (CFRP), Alwis and Burgoyne (2006) found a stress limit of 0.45 for AFRP.

Table 3-3: Extrapolated Load (% ultimate) from Stress-Rupture Regression Analysis at 50 years according to Greenwood (2001)

Environment	Traditional E-glass	Boron-free E-glass
Air at 23° C	44.6	45.8
Salt Water at 23° C	27.1	36.8
Cement Extract at 23° C	14.8	24.8
Acid at 23° C	0.9	12.1
Cement Extract at 60° C	8.2	18.8
Acid at 60° C		9.5

Summary

Using the most conservative results reported in the literature, stress-limits for a service-life of 50 years are suggested (Table 3-3), which should be applied to the design value f_{fd}. It should be noted that where engineers are confident that a particular selected FRP will perform better in long-term loading than the worst-case values suggested. A decision to use less

conservative values, based on test results, can be made. This is the case for some existing GFRP and AFRP materials and, as quality of fibres, polymers and production techniques improves, this approach is likely to become more common in the future. This confirms the need for internationally agreed test methods to determine stress-rupture characteristics, which can be used to characterise the performance of the material. In recognition of potential material variation, the philosophy of stress-rupture classes for GFRP and AFRP bars and tendons has also been introduced. The stress limits for these have not been defined at this time, but it is envisaged that as FRP bar classification methods develop, the choice of appropriate values for these will become clear.

3.4.5 Ultraviolet radiation

Ultraviolet rays (UV) affect polymeric materials [Bank and Gentry (1995)]. Although FRP reinforcing bars embedded in concrete are not exposed to UV while in service, the UV rays may cause degradation during storage or if FRP is used as external reinforcement. Exposure tests have been performed in the laboratory [Kato *et al.* (1997)] and under field conditions [Tomosawa and Nakatsuji (1997)]. The tensile strength of aged and virgin samples was measured and compared to evaluate degradation. Kato *et al*. (1997) examined the effect of the UV rays on AFRP, CFRP and GFRP rods exposed to a high-UV intensity laboratory environment for 250, 750 and 1250 wetting/drying cycles, with UV-intensity of 0.2MJ/m^2/hour and temperature of 26°C. In addition, fibres were also tested after UV exposure of up to 1,000 hours. AFRP rods showed around 13% reduction in tensile strength after 2500 hours exposure, GFRP rods 8% after 500 hours (no reduction thereafter) and CFRP rods showed no reduction. The pattern was almost identical for the fibre testing.

Summary

For embedded FRP reinforcement, UV-attack poses no problems, but rods and tendons should be protected against direct sunlight whilst in storage. All external FRP reinforcements, e.g. bonded strip/sheets, bars, and tendons should be protected from sunlight using proprietary protection systems.

3.4.6 Thermal actions

Deterioration by thermal action may occur in FRP when constituents have different coefficients of longitudinal and transverse thermal expansion, which is particularly important for good bond. Sen and Shahawy (1999) studied the effects of diurnal/seasonal temperature change on the durability of 12 pre-cracked piles pretensioned with CFRP, designed to fail by rupture of the prestressing tendons. These were stored in tanks and subjected to wetting/drying and temperature cycles (20-60°C). The durability was assessed over three years by periodic flexural tests. The results of these tests indicated that the performance of the piles was largely unaffected, but both bond degradation and reductions in ultimate load capacity were observed for some specimens in which the pre-exposure pre-cracking damage was greatest. Bank, Puterman et al. (1998) showed ageing of bond specimen at 80°C in water leads to degradation of the material and a decrease in residual bond strength. Vinyl esters showed less degradation than polyester. Katz, Berman et al. 1999 performed bond tests at elevated temperatures. All FRP rebars showed a clear decrease of bond strength depending on T_G of the used resin. Around 90% of the bond strength is lost at 250°C for all tested rebars.

Summary

The literature suggests that temperatures over 60°C may present significant problems for FRP, but further research is needed to make robust conclusions and recommendations.

3.4.7 Carbonation

A limited amount of research work on the effect of carbonated concrete on FRP was carried out as part of the EUROCRETE project [Sheard *et al.* (1997)], which studied a wide range of FRP durability aspects. The data obtained was more variable than that for other accelerated conditions; however no deterioration due to carbonation was observed.

Summary

It is unlikely that carbonation promotes deterioration of FRP bars in concrete. On the contrary, the associated reduction in pH is likely to increase the service life and improve the durability of FRP reinforced concrete since it reduces the concrete pore-water alkali that attacks some fibres and polymers.

3.4.8 Acid attack

There is little published data on the effects of acid attack on FRP. Indeed, it is likely that in acid conditions, deterioration of concrete would be of greater concern. There is clearly a need to investigate this issue and produce some guidance for circumstances when acid resistant cement, such as high-alumina cement, is used in conjunction with FRP reinforcement.

3.4.9 Concluding remarks

The previous sections discussed durability-related aspects of FRP embedded in concrete and the approaches taken by various researchers. It is clear that whilst broad conclusions can be drawn about the relative performances of FRP materials, these cannot be applied strictly in all cases, due to variations in the materials and manufacturing processes used to produce FRP.

It is also clear that a unified design approach to FRP durability issues has to be developed to enable the international construction community to have more confidence in predictions of FRP service life in aggressive environments. The biggest problem is the perception that glass is sensitive to alkali attack and that the concrete environment is therefore intrinsically aggressive. Research has shown that the concrete environment is, however, not as aggressive as alkaline solutions and that alkali resistance can be significantly improved by the selection of appropriately treated glass fibres, suitable resins and better production techniques.

3.5 Designing for durability

In the first part of this section, the existing design codes and guidelines in Japan, Canada, USA, GB and Norway are summarized.

In section 3.5.2 a simplified durability approach based on accelerated ageing under load and residual strength testing is presented. In this form, the approach conforms to the international semiprobabilistic safety concept.

In section 3.5.3 a new integral approach to durability specification for FRP in concrete, emerging from the work of the fib Task Group 9.3 [Byars *et al*. (2000), (2001), (2003), Weber (2006a)] is presented. This approach has been elaborated to take specific aggressive

environments into account in a similar way to that used by engineers for steel-reinforced concrete design. The philosophy identifies the main aggressive situations and introduces a series of stress reduction factors to account for potential deterioration of FRP in these environments. The factors allow for the relative resistance of generic FRP types to aggressive environments and the desired design life of the structure. This approach is therefore considerably more flexible and less conservative than existing methodologies contained in international design codes.

3.5.1 Existing codes and guidelines

Currently, design guides exist in Japan, Canada, the USA and the UK. In Norway, provisional design recommendations have been developed. Table 3-4 summarises the durability-related strength reductions or stress limiting factors assumed for non pre-stressed FRP reinforcement in the various guidelines.

The main point to note here is that these guidelines have a single "environmental effect" factor for each FRP material depending on its fibre type, only. However, the main environmental effects identified in the literature are moisture, alkali, temperature and time. Provided that the in service exposure conditions are known, it should be possible to refine the environmental effect factors to produce a more economic and conservative results. This is the approach that has been taken in the following section, which presents a new methodology for FRP durability specification, by utilising the best parts of existing codes and introducing new classes of exposure, appropriate to common exposure environments.

Table 3-4: Reduction factors used in existing guidelines to take account of tensile strength reduction due to environmental actions and sustained stress

Factor	ACI 440.1R-06	NS3473	CSA-S806-02 CHBDC-2006	JSCE	IStructE
Reduction for environmental deterioration (ULS)	C_E "environmental reduction factor" wet/dry GFRP: 0.70-0.80 AFRP: 0.80-0.90 CFRP: 0.90-1.00	η_{env} "conversion factor" GFRP: 0.50 AFRP: 0.90 CFRP: 1.00	Φ_{FRP} "resistance factor" GFRP: 0.50 AFRP: 0.60 CFRP: 0.75	$1/\gamma_{fm}$ "material factor" GFRP: 0.77 AFRP: 0.87 CFRP: 0.87	$1/\gamma_m$ "material factor"
Reduction for sustained stress (ULS)	Pending	η_{lt} "conversion factor" GFRP: 0.8-1.0 AFRP: 0.7-1.0 CFRP: 0.9-1.0			GFRP: 0.30 AFRP: 0.50 CFRP: 0.60
Total strength reduction for environmental actions (SLS)	Including Φ (0,55...0,65) GFRP: 0.39-0.52 AFRP: 0.44-0.59 CFRP: 0.50-0,65	GFRP: 0.40-0.50 AFRP: 0.63-0.90 CFRP: 0.90-1.00	F_{SLS}: Max Stress at service load GFRP: 0.25 AFRP: 0.35 CFRP: 0.65	GFRP: 0.77 AFRP: 0.87 CFRP: 0.87	GFRP: 0.30 AFRP: 0.50 CFRP: 0.60
Stress limits for permanent load (SLS)	GFRP: 0.14-0.16 AFRP: 0.24-0.27 CFRP: 0.44-0.50	Reduction for modulus Stress limits not specified	Pre/Post tension: GFRP: 0.25-0.30 AFRP: 0.35-0.40 CFRP: 0.65-0.70	0.8 × "creep failure strength" not more than 0.7 GFRP: ≤ 0.7 AFRP: ≤ 0.7 CFRP: ≤ 0.7	Stress limits not specified

3.5.2 Design value of tensile strength based on residual strength tests: simplified approach

Researchers around the world have tested an extensive amount of rebars primarily under accelerated environmental conditions and determined their residual properties. This kind of testing is specified in a variety of defined test setups in test guidelines (ACI 2004) and the drafts of international testing standards (ISO 2003). But the design engineers still have to decide what conditions to choose and how to use the residual strength, since no threshold is specified in these guidelines. A kind of threshold is specified in the informative annex of the Canadian Standard CAN/CSA 806. In Annex O of the CSA 806 it is defined that specimens should be loaded to a level equal to 1.1 times the "design allowable strength" while ageing in an artificial concrete pore solution of pH 12.7, or in concrete.

To meet the international safety concept in this proposal, the test load is specified as the design load, meaning the specimen is stressed during the testing time under factored loads. The testing time is specified to be 2000h at a temperature of 60°C, to represent the life cycle of the structures. For the concrete a high alkaline cement (Na_2O content = 1%) is used with a water cement ratio higher than 0,45 leading to the highest possible pH value. During testing the concrete is water saturated and cracked leading to additional realistic bond stresses. As an alternative an artificial pore solution with the same pH value can be used as test medium.

After conditioning in the above environment, the rebar is tested for residual strength. The design value of tensile strength should be taken as the minimum of the sustained stress during testing and the characteristic value of the residual tensile strength divided by the material factor, γ_f:

$$f_{fd} = \min (f_{Test} , f_{fk\,res} / \gamma_f) \quad (3\text{-}1)$$

This simple approach leads to conservative results under "normal" conditions. This means normal indoor climate or outdoor climate with mean annual temperatures around 10°C. For higher temperatures or a climate with more extreme temperature variations, longer conditioning times are recommended.

If a more economic design is desired, or conditions are different from these normal conditions, a new approach which is adapted to the special conditions for each particular application, which takes all the environmental influences into account, has to be chosen.

3.5.3 Refined approach for durability specification for FRP

The existing approaches for durability specification are very general in nature and do not take into account all the parameters that literature has identified as being significant to FRP durability in concrete. The new approach addresses these issues and conservatively quantifies the impact of various aggressive environments on FRP design life.

3.5.3.1 The FRP design strength equation

It is proposed that FRP is designed for durability on the basis of a simple design strength equation that multiples the characteristic tensile strength by a factor which is linked to various environmental parameters that increase or decrease the factored tensile strength depending on the severity of the exposure environment, as follows:

$$f_{fd} = f_{fk0} / (\eta_{env,t} \ \gamma_f) \quad (3\text{-}2)$$

3.5.3.2 The environmental strength reduction factor ($\eta_{env,t}$)

The environmental tensile strength reduction factor $\eta_{env,t}$, is the ratio between the characteristic short term strength and the characteristic long term strength, i.e. the creep rupture stress limit. It can be determined accurately if the 1000h strength $f_{fk1000h}$ and the standard reduction per logarithmic decade R_{10} is known, (see also Fig. 3-2). There is a shift of about three log decades from 1000h to 880,000h. The following power equation can be used [DIN 1990].

$$\eta_{env,t} = f_{fk1000h}/f_{fk0} / ((100 - R_{10})/100)^{n} \quad (3\text{-}3)$$

For normal conditions n equals 3. If $f_{fk1000h}$ is not known, an estimation using the above approach can be used. Therefore the 1000h value is determined from short term data, creep rupture limits [ACI (2006)] and literature data on strength retention. The following equation is recommended [Weber (2006a)] (see also §3.5.3.4).

$$\eta_{env,t} = 1 / ((100 - R_{10})/100)^{n+2} \quad (3\text{-}4)$$

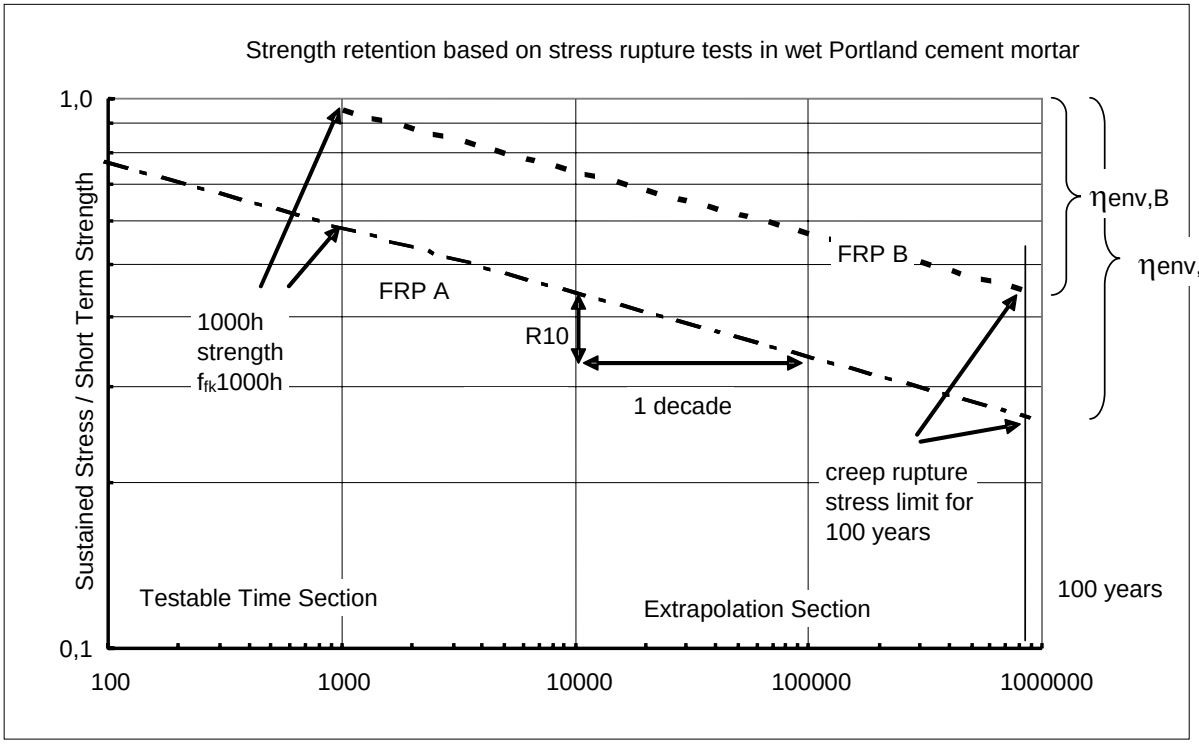

Figure 3-2: Environmental strength reduction factor and 1000h strength for two different GFRP materials with different durability

Where R_{10} is the standard reduction of tensile strength in percent per decade (logarithmic decade) due to environmental influence. The exponent n (Eq. 3.5) is the sum of three influence terms: n_{mo} is the term for moisture condition (Table 3-6), n_T is the term for temperature (Table 3-7), n_{SL} is the term for desired service-life (Table 3-8) [DIN 53768 (1990), Weber (2006a)] and n_d is the term for diameter correction (Table 3.9).

$$n = n_{mo} + n_T + n_{SL} + n_d \quad (3\text{-}5)$$

The four influence terms for moisture, temperature, service life and diameter are defined in the following sections.

Table 3-5 shows standard reduction factors for tensile strength expected after 100 years in concrete under "standard exposure conditions", which are defined as an "outdoor" climate (not constantly in contact with water) with an annual average temperature of 5 to 15°C. Suggested values of $\eta_{env,t}$ for GFRP, AFRP and CFRP are also shown inverse to represent fractions of the original tensile strength. For example, the expected tensile load where 5% of all CFRP rebars fail after 100 years in standard conditions is around 77% of the original tensile strength, while the limit values for AFRP and GFRP are 44% and 24%.

Table 3-5 also shows that ACI 440.1 creep rupture limits recalculated to characteristic values according to the international safety concept, lead to the same values for sustained loads for standard materials as for the new approach. The table also allows for different classes of products to be specified for each material, if enough long term data is available.

Table 3-5: Standard environmental strength reductions for 100 years, moist environment and 10°C MAT, ACI values(left) are compared to the new approach (right)

Environmental standard reduction of tensile strength $\eta_{env,t}$						
	ACI creep rupture limit (SLS)	stress under factored loads (g=v) γ_M=1,425 for this limit (ULS)	char. strength 100a γ_M=1,25 (ULS)	R_{10} from literature (%)	$\eta_{env,t}$	$1/\eta_{env,t}$
GFRP class 3	0,14	0,20	0,25	25	**4,16**	0,24
GFRP class 2	-	-	-	TBD	TBD	TBD
GFRP class 1	-	-	-	TBD	TBD	TBD
AFRP class 2	0,24	0,34	0,43	15	**2,25**	0,44
AFRP class 1	-	-	-	TBD	TBD	TBD
CFRP class 2	0,44	0,63	0,78	5	**1,29**	0,77
CFRP class 1	-	-	-	TBD	TBD	TBD

3.5.3.3 Standard reduction of tensile strength per decade due to environmental influence (R_{10})

The environmental influence parameter, $R_{10,}$ is the slope of the load vs. time to failure line in double logarithmic scale. A constant slope means the same percentage of strength loss for the same ratio of time. Several tests at room temperature and elevated temperatures show the linear behaviour in a double logarithmic scale [Alwis and Burgoyne (2006), Kato, Uomoto et al. (1997), Greenwood (2001), Weber (2006, 2006a)]. In this case the reduction per decade (tenfold time (log(10) =1)) is chosen to get a concise value. This kind of representation is well known for dynamic fatigue. As the other name "static fatigue" for creep rupture failure indicates, these are related processes. For every group of materials under similar conditions this value is nearly constant, [Renaud 2001, Weber 2006]. Figure 3.3 shows two different materials with different durability but similar slope. For materials with known R_{10} value an extrapolation from long term values to service life is simple [DIN 53769]. For materials with unknown R_{10} value, an estimate can be performed based on literature data for this material group.

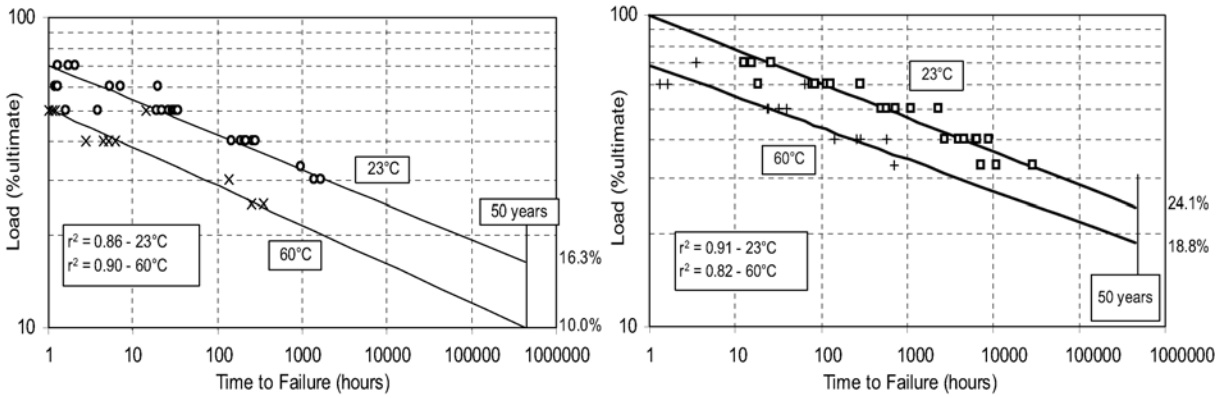

Figure 3-3: Experimental strength retention curves in log/log scale (left E-glass, right ECR-glass)

3.5.3.4 1000h endurance strength ($f_{fk1000h}$)

The endurance strength is the characteristic value of the load which the composite rebar can resist after exposure to a practical test environment for 1000h. This value can be expressed as a percentage of the tensile strength or as absolute value. As can be seen in fig.3-3, different materials of the same group show similar short term values as well as similar slopes of the strength retention curves. Hence, durability can only be determined with some confidence if some long term test data are determined. The longer the duration of the test the more precision can be given to the extrapolation. 1000h is a good compromise for these materials. During this period the diffusion processes are stabilized and on the other hand, the proposed tests can be completed within a few months. From this point a straight line for three decades to 1 million hours is extrapolated.

If no value exists for the 1000h endurance strength, an estimation can be made for this value by the same approach as for equation 3-4:

$$f_{fk1000h} = f_{fk} [(100 - R_{10})/100]^{2} \quad (3\text{-}6)$$

This means that a standard GFRP bar should be able to sustain 56% of its tensile strength for 1000h in wet concrete at room temperature. The corresponding values for AFRP and CFRP are 72% and 90% (see Table 3.5). Higher values can be shown through testing. The long term design strength can be determined by using equation 3-7.

$$f_{fkd} = f_{fk1000h} [(100 - R_{10})/100]^{n}/\gamma_f \quad (3\text{-}7)$$

3.5.3.5 Term for moisture condition (n_{mo})

It is known that the rate of deterioration of FRP depends to a large extent on the moisture condition of the environment. For example, faster deterioration in tensile strength occurs for FRP bars immersed directly in simulated concrete pore solution and similar observations have been made when comparing deterioration of bars embedded in wet concrete with that in dry concrete [Scheibe and Rostasy (1998)].

In the ACI design guidelines [American Concrete Institute (2006)] two climate classes are suggested: “Enclosed Conditioned Space” (roughly “Dry” conditions) and “Unenclosed or

Unconditioned Space" (roughly, "Moist" conditions), with strength reductions of 20% and 30% for "dry" - and "moist" respectively for GFRP. However, there is probably a more significant difference between moisture-saturated concrete and normal outdoor concrete in regions with temperate climate that have a relative humidity of approximately 80%. In line with this, 3 exposition (moisture) classes are proposed [Byars (2001)]:

1) *Dry*: Indoor conditions, protected from rain with an average relative humidity of approximately 50%. (XC1 dry)
2) *Moist*: Outdoor conditions, subjected to rain but not constantly in contact with water with an average relative humidity of approximately 80%. (XC3, XD1, XD3, XS1, XS3)
3*) Saturated*: Constantly in contact with water with average relative humidity close to 100%. (XC2, XC4, XD2, XS2)

A correction term n_{mo} with relative values of -1 for "Indoor climate", 0 for "Outdoor climate", and 1 for "Moisture saturated concrete", is suggested, as seen in Table 3.6.

Table 3-6: Correction term for moisture condition in concrete members

Correction term for moisture in concrete, n_{mo}		
Dry (RH app. 50%)	Moist (concrete not constantly in contact with water, RH app. 80%)	Moisture saturated (concrete constantly in contact with water, RH app. 100%)
-1	0	1

3.5.3.6 Term for temperature (n_T)

As a rule of thumb, increasing the temperature by 10°C doubles the rate of a chemical reaction [Perez-Bendito and Silva (1988)], so if a linear relationship between the strength reduction and the logarithm of time is assumed (see Figure 3.4), a change in strength reduction can be expected for a temperature increase or decrease by 10°C, similar to twice the time or half the time, respectively. In stress corrosion tests, the reduction factor for 10°C was observed to be slightly higher, with values between 2,25 and 2,85 [Renaud (2002), Weber (2005)]. With this background, to be on the safe side a logarithm of 0,5 instead of 0,3 is proposed. In line with this, 4 temperature classes are suggested with ranges of approximately 10°C, (see Table 3.7). If seasonal temperature variations are high (continental climate) the higher value is recommended.

Table 3-7: Term for mean annual temperature (MAT)

Term for mean annual temperature, n_T			
MAT < 5°C	5°C < MAT < 15°C	15°C < MAT < 25°C	25°C < MAT < 35°C
-0,5	0	0,5	1

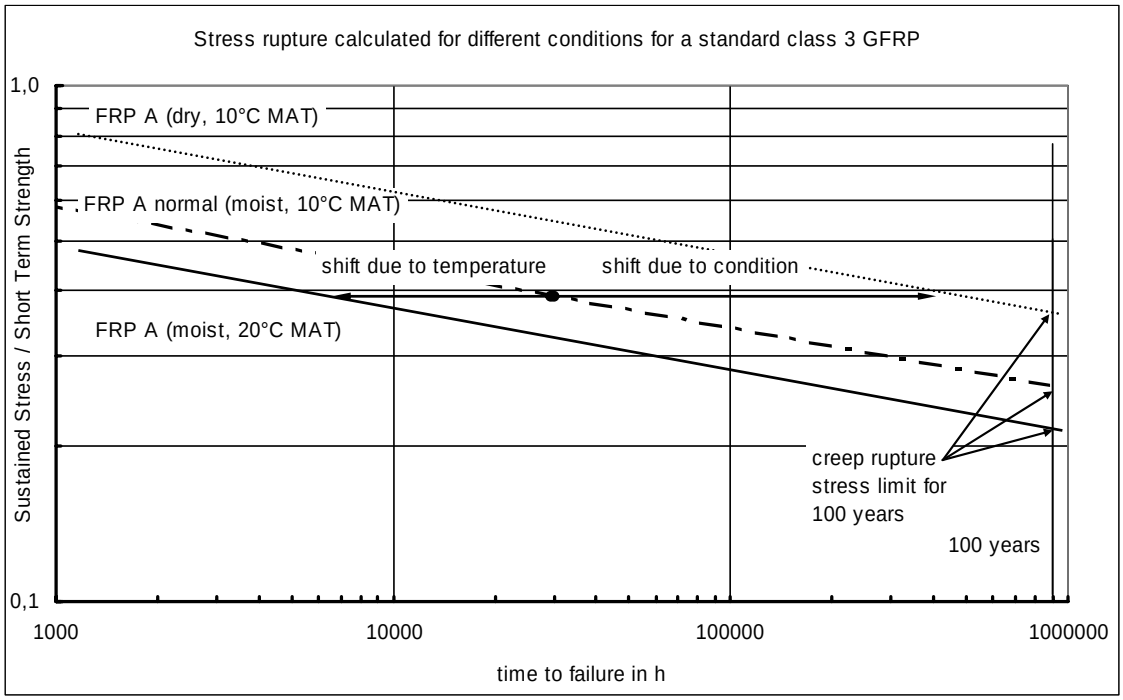

Figure 3-4: Effect of the parameter humidity and temperature on stress rupture curves. (Weber 2006a)

3.5.3.7 Term for service-life, n_{SL}

As the standard reduction for tensile strength, $\eta_{env,t}$ is intended for a service-life of 100 years, a lower strength reduction may be used if the required service-life is, for example, only 10 years. If again, a linear relationship between strength reduction and the logarithm of time is assumed, the strength reduction $\eta_{env,t}$ may be recalculated by the term n_{SL} (Table 3.8).

Table 3-8: Term for Desired Service-Life, n_{SL}

Term for specified service life, n_{SL}			
Servicelife =1 year	Service-life = 10 years	Service-life = 50 years	Service-life = 100 years
1	2	2,7	3

3.5.3.8 Correction term for tested diameter n_d

As all the deterioration processes are a function of temperature, time and humidity the Fickian diffusion law can be applied. With this law the diameter has an influence on the time to failure. Under constant conditions, a fourth of the time to failure is observed for half the diameter. If a diameter smaller than the one tested is used, a correction term has to be used. For larger diameter no compensation is recommended, because of the size effect of strength. The values in brackets are calculated on the basis of the diffusion law.

Table 3-9: Diameter correction

Diameter correction factor, n_d			
Bigger than tested	Same as tested	75% of tested	50% of tested
0	0	0,5 (0,3)	1(0,6)

3.5.3.9 Material factor γ_f

As the environmental factor is dependent on the material and exterior conditions, the material factor takes into account the scattering of the strength values and the failure mode. In some european design guides [CUR (2003), BÜV(2002), EN 13706(2002)], pultruded profiles material factors for FRP are proposed to be in the range between the value used for steel and that used for concrete. Because there is no big difference between the FRP materials in production, as well as in failure modes the material factor is proposed to be 1,25 (Table 3-10).

Table 3-10: Material Factor without environmental influence

MATERIAL FACTOR, γ_f		
GFRP	AFRP	CFRP
1,25	1,25	1,25

See Chapter 8 for further information in partial material safety factors and design philosophy issues.

3.5.3.10 Environmental design examples

To see the effects of the different terms for the environmental influence, some practical examples are given. In each row of Table 3.11 the strength (f_{fk0} and if known $f_{fk1000h}$), the standard strength reduction per decade R_{10} and the different influence terms (n_{mo}, n_T and n_{SL}) are stated. From these values $\eta_{env,t}$ and $1/\eta_{env,t}$ are calculated. By using a material factor in the last column the design value is determined.

In the first four rows 4 different prestressing materials are compared for a post-tensioning application in a dry cold environment (dry, 10°C, 100 years). The design value is highest for the material with the slowest deterioration (smallest R_{10}). Despite of the high short term strength of the class 2 GFRP tendons only a low and probably uneconomical design strength of 30% of the ultimate strength is possible for this material.

In row 5, 6 and 7 environmental design examples for a standard class 3 GFRP are given. In row 5, for this GFRP the conditions of a long-term harbour application (wet, 20°C, 50 years) is calculated, while in row 6 a typical softeye short term application (wet, 10°C, 1 years) and in row 7 the ceiling of a hospital (dry, 20°C, 100 years) is taken as an example.

Rows 8-10 show examples for a certified tested class 1 rebar system, which shows a reduction of 18% per decade and a 1000h strength $f_{fk1000h}$ of 1000 N/mm². The main difference between a normal rebar and a rebar system designed for durability from the same material class is not the slope but the starting point of the line.

Without certified long term tests the rebar system has to be classified into the lowest class for the particular kind of rebar (CFRP, AFRP, GFRP).

Table 3-11: Examples for environmental design

Material	f_{tk0}	f_{tk1000}	R_{10}	Moist.	n_{mo}	MAT	n_T	Serv Life	n_{SL}	n	$\eta_{env,t}$	$1/\eta_{env,t}$	γ_f	f_f
	MPa	MPa		cond.		°C		years						N/mm²
CFRP class 1	2000	2000	3%	Dry	-1	10	0	100	3	2,0	1,1	94%	1,25	1505
CFRP class 2	2000	2000	5%	Dry	-1	10	0	100	3	2,0	1,2	90%	1,25	1444
AFRP class 1	2000	1800	15%	Dry	-1	10	0	100	3	2,0	1,6	65%	1,25	1040
GFRP class 2	1400	1000	20%	Dry	-1	10	0	100	3	2,0	1,9	46%	1,25	512
GFRP class 3	650	366	25%	Wet	1	20	0,5	50	2,7	4,2	5,9	17%	1,25	87
GFRP class 3	650	366	25%	Wet	1	10	0	1	1	2,0	3,2	32%	1,25	165
GFRP class 3	650	366	25%	Dry	-1	20	0,5	100	3	2,5	3,6	27%	2,25	143
GFRP class 1	1100	1000	18%	Wet	0	10	0	100	3	3,0	1,8	55%	1,25	441
GFRP class 1	1100	1000	18%	Wet	1	10	0	1	1	2,0	1,5	67%	1,25	538
GFRP class 1	1100	1000	18%	outdoor	0	30	1	100	3	4,0	2,2	45%	1,25	362

3.6 Safety factor for bond strength

A safety factor for bond strength, which takes into account bond deterioration with time, also needs to be used in the design of FRP-reinforced concrete structures. In the IStructE recommendations [IStructE (1999)], a material safety factor of 1.4 was suggested for all FRPs, to account for "long-term effects". This is equal to a reduction of the original strength by approximately 30% (1-1/1.4=28%).

In this proposed methodology, a similar bond strength reduction is suggested by default, but this reduction can be adjusted to account for ambient conditions, as per the tensile strength durability specification. It is suggested that the bond strength be reduced by $\eta_{env,b}$ determined according to the equation below, where n_{mo} , n_T, n_d and n_{SL} are obtained from the tables in paragraph 3.5.

$$\eta_{env,b} = 1 / [(100 - R_{10})/100]^{n} \qquad (3\text{-}8)$$

Where: R_{10} is the % standard reduction of bond strength due to environmental influence.

For durability of bond like for durability of the rebar itself, the sustained (bond) stress as well as the environmental parameters have a dominant influence. It has to be taken into account that concrete strength (as well as phenomena such as shear off and spalling) can limit the bond stress for the rebar. Furthermore bond stress is not constant for the whole embedment or lap splice length.

To determine the maximum bond strength of the rebar, short centric pullout tests with different concrete strengths are recommended. For the durability of bond this kind of test should be performed with different sustained bond stresses.

See Chapter 7 for further information on bond behaviour.

3.7 Conclusions

This section has discussed how the durability-related aspects of FRP used as an internal concrete reinforcement are treated in existing design guidelines and has proposed a new, less conservative approach to match the environmental conditions.

Based on the literature review presented above, the following points can be summarized from the existing guidelines.

- The widely used ACI 440 design guideline divides between only two environmental conditions: wet and dry environment. Additionally, there exists a big difference between loads at the ultimate limit state and loads after creep rupture limit check, leading to a two step design.
- The JSCE design guideline uses a single factor that incorporates several uncertainty aspects including environmental durability. Stress limits for sustained stress are used.
- The UK IStructE design guideline deals with environmental degradation of FRP by using one factor that takes into account the influence of environment, sustained stress and a few other uncertainties.
- The Norwegian design guideline has a single factor to account for environmental deterioration.
- The Canadian design guideline uses a slightly different approach than the others. Liberal stress limits/design strengths are adopted, complemented by design examples. Restrictions in the use of certain FRP types are widely withdrawn in the 2006 version, but now three different classes of quality (class 1-3) are defined for each material group: aramid, carbon and glass reinforcement.

It is clear that these differences in design approach to FRP durability makes it difficult for the international construction community to have confidence in predictions of FRP service life in aggressive environments. The biggest problem is the perception that GFRP is sensitive to alkali attack and that the concrete environment is therefore intrinsically highly aggressive. Research has shown that the concrete environment is not as aggressive as the alkaline solutions that most researchers use and that alkali resistance can be significantly improved by the selection of appropriately treated glass fibres, suitable resins and better production techniques [Mufti et al. (2005), Mufti et al. (2007), Demis et al. (2007)].

Consequently, a more rigorous and less conservative approach to durability specification is presented. This has been developed from an in-depth study of the parameters that affect FRP durability in concrete and allows engineers to increase or decrease margins of safety depending on environmental and stress conditions, generic FRP type and required design life. This approach can become less conservative as more data, particularly from real life structures, are acquired.

4 Ultimate limit states for bending, compression and tension

4.1 General

The majority of research work undertaken in this field to date relates to the bending (flexural) characteristics/behaviour, whilst little information exists on the tension and compression of FRP RC elements. Hence, this chapter addresses primarily the flexural behaviour.

4.2 Bending

4.2.1 Section properties

Section analysis of steel RC sections is normally based on two basic assumptions: a) plane sections remain plane at any stage of loading and b) a perfect bond exists between concrete and reinforcement, ensuring strain compatibility along the section. The validity of adopting these assumptions for RC sections reinforced with FRP reinforcement has been verified by Duranovic et al. (1997a, 1997b). As result, normal section analysis techniques can be used for the determination of the flexural characteristics of FRP RC sections. However, significant bond deterioration can lead to violation of these assumptions; hence the following apply to FRP bars with adequate bond characteristics.

4.2.2 Bending characteristics of FRP RC elements

In RC design, when the strength of reinforcement is fully utilized, the section is considered to be "under-reinforced". The effectiveness of flexural reinforcement is reduced when the cross-section becomes "over-reinforced". A RC section becomes over-reinforced when the reinforcement does not reach its full potential and concrete crushes in compression. In a balanced section, the reinforcement's tensile strength and concrete compressive strength are attained simultaneously. In conventional RC design with steel reinforcement, balanced conditions are often assumed. However, the use of safety factors means that the sections achieved are in general under-reinforced, enabling yielding of the reinforcement to be achieved before concrete crushing.

For conventional steel reinforcement, the strength to stiffness ratio is similar to that of normal concrete and, hence, the neutral axis depth for a balanced rectangular section is around the middle of the overall effective depth. For FRP reinforcement, the strength to stiffness ratio is an order of magnitude greater than that of concrete and, hence, the neutral axis depth for the balanced section is very close to the compressive end, as shown in Figure 4-1.

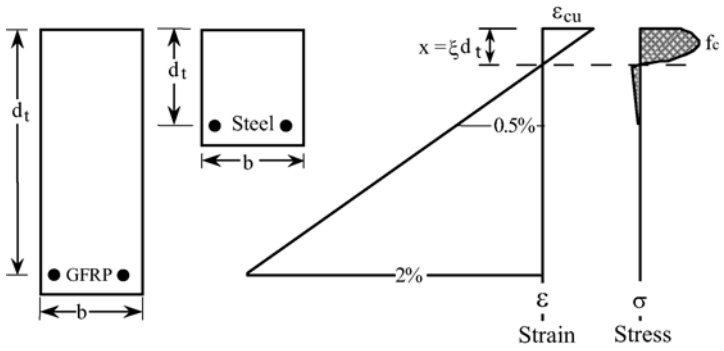

Figure 4-1: Strain distribution for a GFRP and steel RC balanced section [Pilakoutas (2000)]

The above implies that, for balanced FRP RC elements, which utilise the full strength of FRP, a large proportion of the cross-section would be subjected to tensile strains. As a result, much larger flexural deflections would be expected, and a greater strain gradient would exist in the compressive zone than in a similar steel RC section. Prestressing or post-tensioning the FRP reinforcement will eliminate most of the above problems. However, it makes the construction process much more difficult and expensive.

If all other modes of failure are avoided, flexural failure in FRP RC sections will be reached either by crushing of the concrete in compression or rupturing the FRP reinforcement in tension. The tensile rupture of FRP reinforcement depends on its type, but also on its bond characteristics. By its nature, RC cracks in tension and the FRP reinforcement is there to prevent or control the opening crack. However, due to the very large difference in stiffness between the cracked and un-cracked section, the stress in the reinforcement is expected to vary substantially from the cracked to the uncracked section. This will result in high surface shear stresses which put a very high demand on bond capacity and can lead to excessive slip around a crack.

In order to predict the mode of failure of RC sections, it is necessary to examine the stress developed in the reinforcement and concrete. Figure 4-2 exemplifies the variation of the stress level in the reinforcement as a function of the amount of reinforcement.

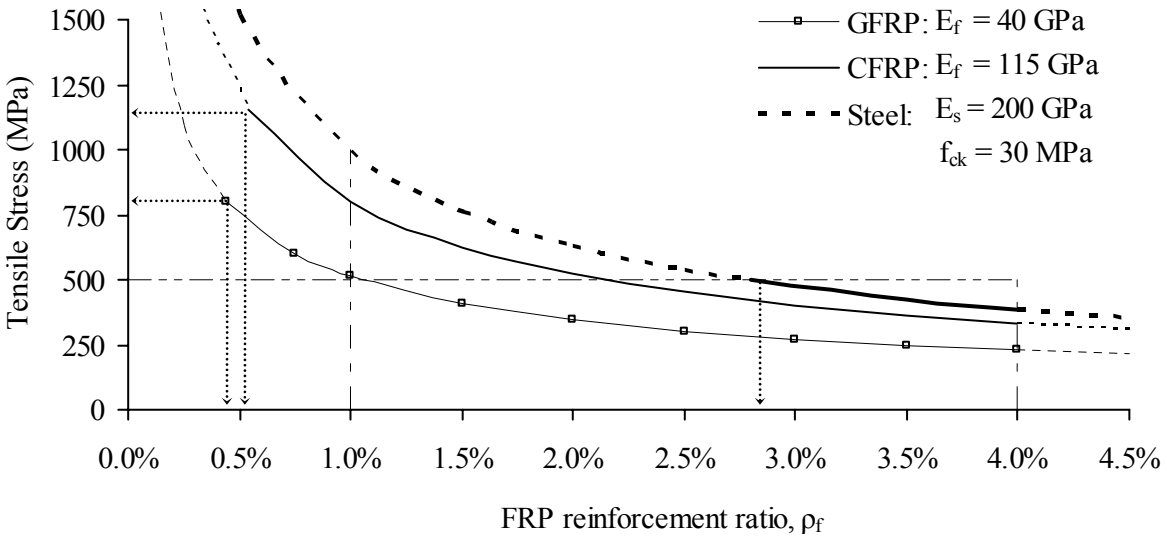

Figure 4-2: Example of stress in reinforcement at concrete failure versus percentage amount of reinforcement

For the particular section analysed to produce the results of Figure 4-2, it is shown that the steel RC section becomes over-reinforced at values of ρ_f around 3%. Below that ρ_f, the section is under-reinforced and the steel is yielding. In the case of the GFRP and CFRP reinforced sections, they both remain over-reinforced for ρ_f above 0.5%. For ratios below 0.5%, rupture of the re-bar occurs, depending on the strength of the FRP.

It is obvious from Figure 4-2 that as the reinforcement ratio increases, the stress developed in the FRP bar decreases. When this stress reduces below the strength of steel, larger areas of reinforcement are required to achieve the same applied moment. The ratio of reinforcement has several implications:

- Cost. Higher ratios of reinforcement, lead to less economic elements.
- Design philosophy. FRP material partial safety factors become irrelevant if their design strength is not utilised.
- Short-term deformations. They will be larger, if high strains are needed from the FRP.
- Long-term deformations. If the concrete stress under sustained loading exceeds 0.45 f_c, (recommended in EC2, NDP) then much larger creep deformations will take place.

It is by now universally accepted that FRP over-reinforced concrete sections will be inevitable in most structural applications. Naturally, this has implications on the ductility of RC elements since unconfined concrete fails in an abrupt manner. Other sources of ductility may be utilized if it is necessary to overcome this problem [Pilakoutas (2000)]. Possible solutions include confinement of the concrete compression zone to provide concrete ductility, use of hybrid FRP rebars or combination of FRP rebars with different characteristics, failing at different strains, to provide pseudo-ductility. FRP rebars with plastic bond failure may also be used to develop pseudo-plastic behaviour, or enhanced structural redundancy may be provided through the addition of sacrificial rebars, which do not lead to collapse once they fail. Finally, a combination of FRP and steel reinforcement may be used, in particular when the FRP is placed near the surface of the concrete and steel deep inside.

4.2.2.1 Amount of longitudinal reinforcement for "balanced" sections

Existing design guidelines for FRP, such as ACI-440.1R (2006) and CAN/CSA (2006), distinguish between the two types of flexural failure (i.e. concrete crushing and FRP rupture) through the reinforcement ratio for "balanced" sections, ρ_{fb}. This ratio is influenced by the mechanical properties of FRP and concrete and is calculated from expressions derived by considering internal-force equilibrium. For instance, ACI-440.1R-06 adopted equation 4-1, and a similar expression was adopted by the CAN/CSA (2006). Similarly, Pilakoutas et al. (2002) proposed equation 4-2 derived from EC2 for FRP RC beams, which also accounts for the material variability of concrete; while El-Ghandour (1999) proposed a semi-empirical expression for FRP RC slabs (equation 4-3).

$$\rho_{fb} = 0.85\beta_1 \frac{f_c'}{f_f} \quad \frac{E_f \varepsilon_{cu}}{E_f\, \varepsilon_{tu} + f_f} \tag{4-1}$$

$$\rho_{fb} \;=\; \frac{0.81\,(f_{ck} + 8)\,\varepsilon_{cu}}{f_{fk}\left(\dfrac{f_{fk}}{E_{fk}} + \varepsilon_{cu}\right)} \tag{4-2}$$

$$\rho_{fb} = 2.1\left(\frac{f_{cu}}{40}\right)\left(\frac{E_f}{110*10^3}\right)^{0.7}\left(\frac{500}{f_f}\right)^{1.6} \tag{4-3}$$

The effect of concrete compressive strength and tensile characteristics of FRP on the value of ρ_{fb} is depicted in Figure 4-3. The value of ρ_{fb} increases with concrete compressive strength, whilst it reduces as the tensile strength of FRP increases. The values calculated by the expressions proposed by El-Ghandour (1999) and Pilakoutas et al. (2002) are higher than those predicted by the ACI-440.1R-06, in an attempt to ensure that if the balanced reinforcement ratio is provided the concrete will not fail prematurely due to its natural variability.

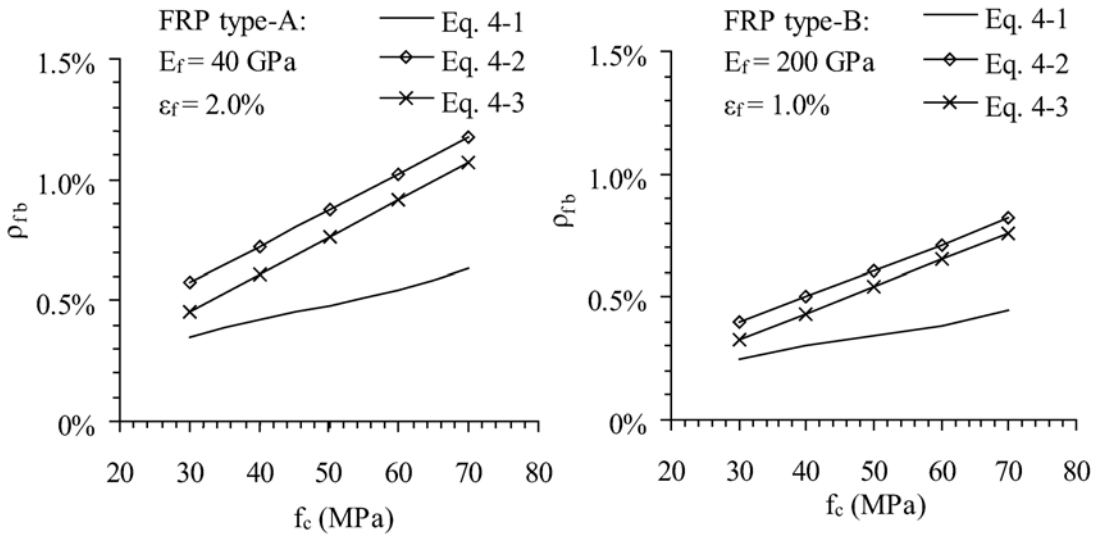

Figure 4-3: Effect of concrete cylinder strength and FRP properties on ρ_{fb}

4.2.3 Moment resistance of FRP RC elements

The ultimate moment resistance of FRP RC sections can be evaluated by adopting the framework of Eurocode-2 (CEN 2004, Figure 4-4). The compression strength of any FRP reinforcement can be ignored due to the anisotropic nature of the reinforcement and its low contribution to the resistance-capacity.

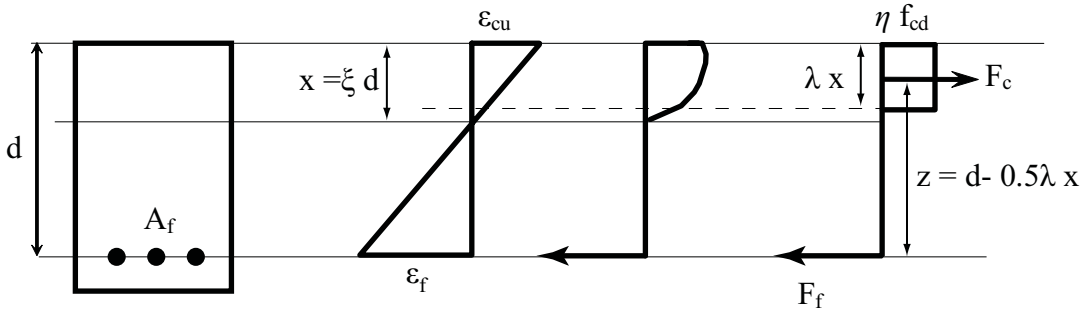

Figure 4-4: Simplified stress block proposed for FRP RC elements

When the amount of longitudinal FRP reinforcement, ρ_f, is higher than ρ_{fb}, flexural failure is expected to occur due to concrete crushing, and the ultimate moment resistance (M_u) can be calculated by equation 4-4.

$$M_u = \eta f_{cd}\, bd^2\, (\lambda\, \xi) \left(1 - \frac{\lambda\, \xi}{2}\right) \quad \text{(Nmm)} \qquad (4\text{-}4)$$

where:

$$f_{cd} = \frac{\alpha_{cc} f_{ck}}{\gamma_c} \quad \text{(MPa)} \tag{4-5}$$

α_{cc} = nationally determined parameter, the recommended value in EC2 is 1

$$\left.\begin{array}{l}\lambda = 0.8 \\ \eta = 1\end{array}\right\} \text{ for } f_{ck} \le 50 \text{ MPa}$$

$$\left.\begin{array}{l}\lambda = 0.8 - \left(\dfrac{f_{ck} - 50}{400}\right) \\ \eta = 1.0 - \left(\dfrac{f_{ck} - 50}{200}\right)\end{array}\right\} \text{ for } 50 < f_{ck} \le 90 \text{ MPa} \tag{4-5}$$

$$\xi = \frac{x}{d} = \frac{\varepsilon_{cu}}{\varepsilon_f + \varepsilon_{cu}} \tag{4-6}$$

$$\varepsilon_f = \frac{-\varepsilon_{cu} + \sqrt{\varepsilon_{cu}^2 + \dfrac{4\ \eta\ \alpha_{cc} f_{ck}\ \lambda\ \varepsilon_{cu}}{\gamma_c\ \rho_f\ _f}}}{2} \tag{4-7}$$

Equation 4-10 can be used to calculate the stress developed in the FRP reinforcement and, hence, verify that failure due to FRP rupture is avoided.

$$\sigma_f = \varepsilon_f\ E_f\ < \frac{f_{fk}}{\gamma_f} \tag{4-8}$$

Alternatively, charts such as Figure 4-5 for constant-width FRP RC elements can be used to determine the required reinforcement ratios given the applied moment. The dimensionless parameter μ is determined by dividing M by $bd^2 f_{cd}$. Once the required ρ_f is determined, a check must be made on the reinforcement stress, σ_f, by using charts such as Figure 4-6.

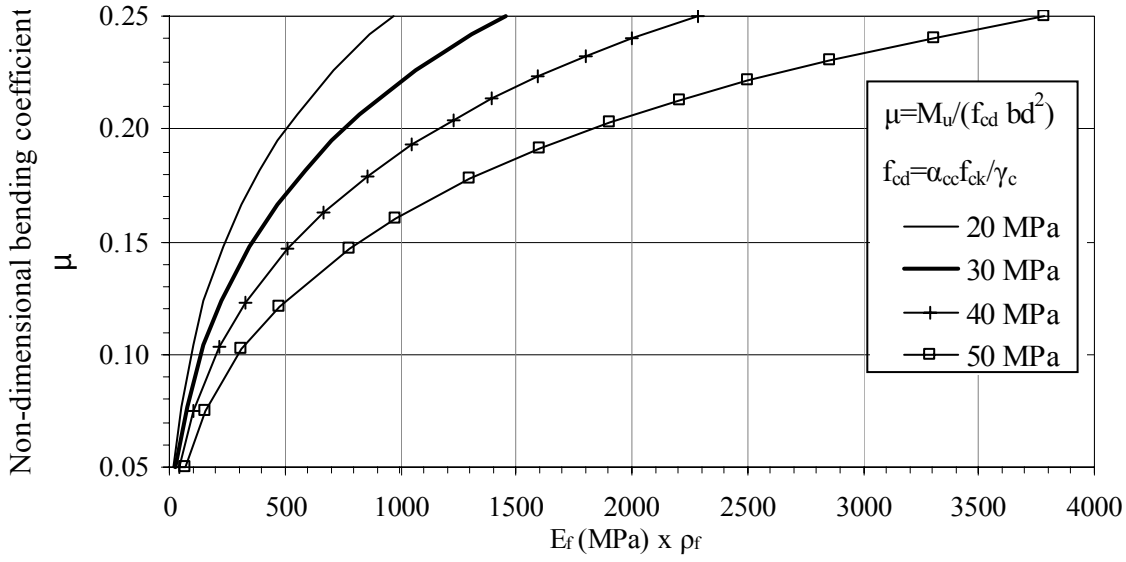

Figure 4-5: Design chart for flexural capacity of constant width FRP RC elements

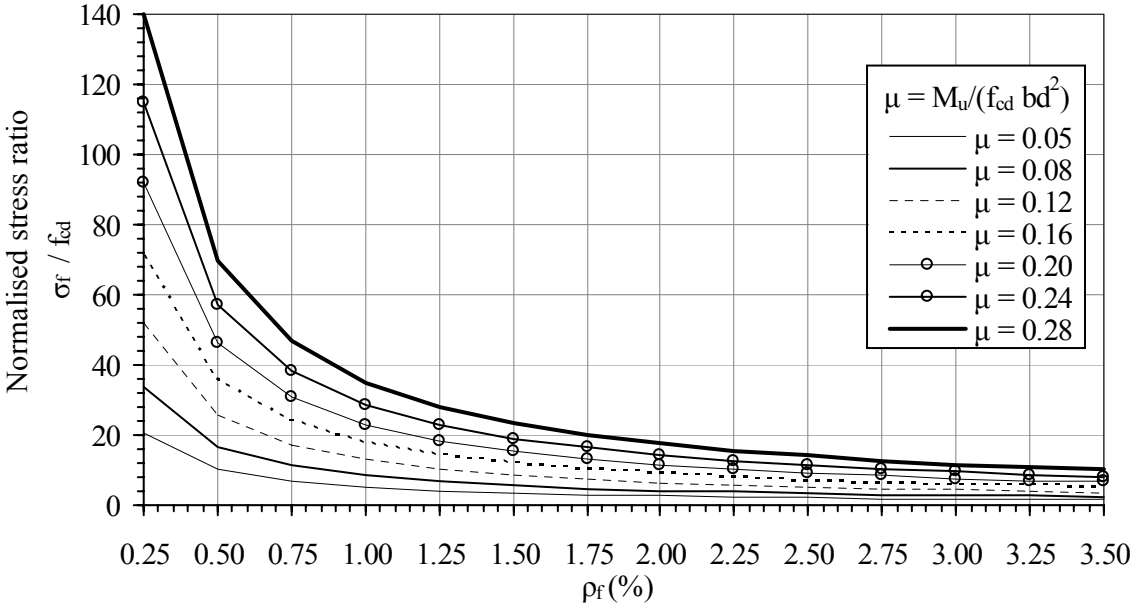

Figure 4-6: Design chart for tensile stress developed in FRP longitudinal reinforcement

Figure 4-7 shows the M_u obtained for an FRP RC section (250 mm wide and 350 mm deep) by utilising the design charts. As expected, M_u increases with the amount of FRP reinforcement and the concrete compressive strength as well as with the tensile strength of FRP reinforcement.

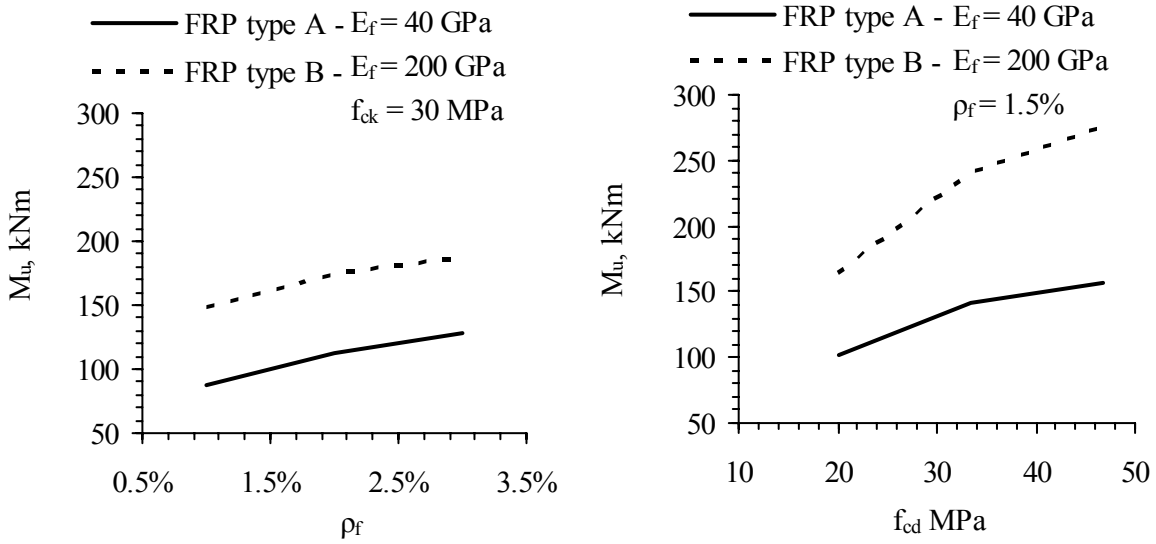

Figure 4-7: Effect of ρ_f, f_{cd} and elastic modulus of FRP reinforcement on M_u (flexural concrete crushing)

If the amount of reinforcement in an FRP RC section is below ρ_{fb}, the expected type of flexural failure is FRP rupture and, to calculate the ultimate moment of resistance (equation 4-11), it is necessary to determine the concrete compressive strain (ε_c) at which FRP rupture occurs. This can be achieved through an iterative procedure by solving equations 4-12 and 4-13.

$$M_u = \frac{A_f f_{fk}}{\gamma_f}\left(1 - \frac{\xi}{2}\right) \quad \text{(N mm)} \qquad (4\text{-}11)$$

$$\xi = \frac{x}{d} = \frac{\varepsilon_c}{\varepsilon_{fu} + \varepsilon_c} \tag{4- 12}$$

$$F_C = F_T \rightarrow b\ d\ \xi \frac{\int_0^{\varepsilon_c} f_c d\varepsilon_c}{\varepsilon_c} = \frac{A_f f_{fk}}{\gamma_f} \quad \text{(N)} \tag{4-13}$$

where f_c is calculated from equation 4-14. The values proposed by Eurocode 2 [CEN (2004)] are used for concrete strains ε_{c2} and ε_{cu}, with the factor "n" depending on the characteristic strength of concrete.

$$f_c = f_{cd}\left[1 - \left(1 - \frac{\varepsilon_c}{\varepsilon_{c2}}\right)^n\right] \quad for \quad 0 \le \varepsilon_c \le \varepsilon_{c2}$$

or (MPa) (4-14)

$$f_c = f_{cd} \quad for \quad \varepsilon_{c2} \le \varepsilon_c \le \varepsilon_{cu2}$$

To ensure that the ultimate moment resistance is higher than the cracking moment of the RC section, a minimum limit may be applied on the amount of longitudinal reinforcement. For instance, ACI440.1R-06 has adopted equation 4-15 for this limit.

$$A_{f,\min} = \frac{0.41\sqrt{f_c'}}{f_{fu}} b_w d \ge \frac{2.26}{f_{fu}} b_w\, d \tag{4-15}$$

An alternative equation 4-16 can be derived by using EC2 (NDP).

$$A_{f,\min} = 0.26\frac{f_{ctm}}{f_{fk}} bd \ge 0.0013bd \tag{4-16}$$

It should be pointed out that these equations do not necessarily control cracking.

4.2.4 Compression

The contribution of the compressive strength of FRP (or just GFRP) to the load-carrying capacity of an FRP RC element is less than the contribution of steel reinforcement. Hence, the contribution of such bars in carrying compression loads can be ignored. However, more experimental research is required to verify this conclusion.

4.2.5 Tension

Tensile behaviour of FRP RC elements is influenced by the tension stiffening effect, i.e. the ability of concrete to carry tension between the cracks. Experimental investigations [e.g. Sooriyaarachchi et al. (2005)], suggest that concrete strength and reinforcement ratio have direct influence on the tension stiffening behaviour (see Chapter 7). Accounting for tension stiffening behaviour correctly is always important for predicting the overall tensile behaviour of FRP RC elements.

5 Serviceability Limit States

5.1 Introduction

Serviceability Limit States (SLS) are applied to RC structures to ensure their functionality and structural integrity under service conditions. The design approach for conventional RC requires SLS of the structure to be checked for relevant loading combinations. However, for FRP RC structures, the specific mechanical characteristics of the FRP rebars are expected to result in SLS-governed design. It is therefore important to define the serviceability checks and corresponding limitations that are required for the design of such elements.

There are no fundamental reasons why the principles behind the verification of SLS for FRP RC elements should not be similar to those already established in the codes of practice for steel RC elements, such as Eurocode 2 [CEN (2004)] and CEB-FIP Model Code 1990 [CEB (1993)]. However, the actual limits could be different to account for differences in both short and long-term properties between the steel and FRP reinforcement. The following SLS for FRP RC members need to be considered:

- Stresses in materials.
- Deflections (short and long-term).
- Crack width and spacing.

5.2 Current code limits for SLS

5.2.1 Code limits for stresses in materials

Determination of stresses developed within an FRP RC member depends on many parameters such as: short and long-term behaviour and properties of concrete and FRP materials, creep and shrinkage, loading history, crack distribution and environmental conditions. Nonetheless, it has been already acknowledged that the same methodology used for prediction of short-term behaviour of steel RC can be applied to FRP RC members [Benmokrane et al. (1996), Masmoudi et al. (1998), Toutanji et al. (2000), Pecce et al. (2000)]. This approach is also recommended by the various modifications to other existing steel RC codes of practice. Within the service range, the stress levels in the materials should remain below their elastic limit, and are therefore evaluated by elastic sectional analysis.

Codes of practice for steel RC members tend to limit the concrete compressive stresses under service conditions. At higher stress levels, the concrete starts to behave non-linearly, and the creep effect on the long-term behaviour of the element becomes more pronounced. Eurocode 2, for instance, imposes limits on the maximum compressive concrete stresses depending on the environmental conditions and the load combinations as shown in Table 5-1.

Table 5-1: Eurocode 2 serviceability stress limitation ratio σ_c/f_{ck}.

Environment	Load combination	
	Rare	Quasi-permanent
High corrosive	0.5	0.4
Low corrosive	0.6	0.45

To avoid the formation of large and permanent cracks that could affect the durability of steel RC elements, some codes of practice tend to limit also the stress in the steel reinforcement. Eurocode 2, for instance, recommends that steel stress, σ_s, should be limited to $0.8 \cdot f_{yk}$ for the rare load combination.

When dealing with the stress limitation in FRP rebars, other factors also come into play. FRP rebars under constant load can creep to failure after a certain "endurance" time in what is referred to as creep rupture or stress corrosion. This is a particularly severe problem for GFRP as discussed in Chapter 2.

FRP composite materials generally have good durability, with the fibres being protected by the resin. However, at high stress levels, micro-cracks can develop in the resin. This situation may be critical for fibres, in particular glass, because they can be damaged by moisture and the alkaline concrete environment.

The ACI 440.1R design guideline [ACI (2006)] provides different limits for each type of FRP reinforcement, which should not be exceeded under sustained and cyclic loading (Table 5-2). The Japanese recommendations limit the tensile stresses to the value of 80% of the characteristic creep-failure strength of the FRP reinforcement, and it is noted that the stress limitation should not be greater than 70% of the characteristic tensile strength of the FRP reinforcement [JSCE (1997)]. The IStructE (1999) imposes even more severe limitations through the use of the material partial safety factors "γ_m" in BS8110 as shown in Table 5-3. Similarly, ISIS Canada (2001) applies a reduction factor, F, to the material resistance factors. Values of the factor F account for the ratio of sustained to live load as well as the type of FRP reinforcement (Table 5-4).

Table 5-2: Allowable stresses for FRP rebars according to ACI 440.1R

Fibre type	Glass FRP	Aramid FRP	Carbon FRP
Allowable stress	$0.20f_{fu}$	$0.30f_{fu}$	$0.55f_{fu}$

Table 5-3: Material partial safety factors according to IStructE (1999)

Material	Material partial safety factor "γ_m"
E-glass reinforcement	3.6
Aramid reinforcement	2.2
Carbon reinforcement	1.8

Table 5-4: FRP material reduction factor "F" [(ISIS Canada 2001)]

FRP Type	Resistance Factors (ϕ_{frp})	Reduction Factor "F"		
		Ratio of sustained to live load stresses		
		0.5	1.0	2.0
CFRP	0.8	1.0	0.9	0.9
AFRP	0.6	1.0	0.6	0.5
GFRP	0.4	1.0	0.9	0.8

5.2.2 Code limits for deflections

FRP RC members are expected to undergo larger deformations than steel RC members. The allowable overall deflection depends on the importance of a given structural member, the type of action (static or dynamic, permanent or 'live' loads) and the type of structure being considered (building, frame, bridge).

To satisfy the SLS of deflection, codes of practice for steel RC specify a minimum thickness by limiting the ratio of the element's effective span to its effective depth. Alternatively, deflections can be calculated and checked to be less than predefined limits that are normally taken as a certain percentage of the effective span of the member. Eurocode 2, for instance, typically limits the design deflections to either span/250 or span/500. Table 5-5 shows some common limitations for the maximum deflections.

Table 5-5: Maximum deflection limitation for RC members

Code	Type of structures	Limit
Eurocode 2	Aesthetic and functionality conditions (quasi permanent loads)	L/250
	Damage limitation of non-structural elements sustained or attached (quasi permanent loads)	L/500
ACI 318-05	Roofs and floors supporting or attached to non-structural elements (Sum of long term deflection due to all sustained loads and immediate deflection due to any additional live load):	
	Not likely to be damaged by large deflections	L/240
	Likely to be damaged by large deflections	L/480
	Elements not supporting or attached to non-structural elements likely to be damaged by large deflections (immediate deflection due to live loads):	
	Floors	L/360
	Flat roofs	L/180

The limits on deflections for steel RC elements are equally applicable to FRP RC. However, the ratios of effective span to depth are not. ACI 440.1R-06 [ACI (2006)] considers that these ratios are not conservative for FRP RC and recommends further studies.

5.2.3 Code limits for cracking

Control of cracking in steel RC members is important for aesthetic purposes or specialized performance like water tightness and, arguably, for mitigating the risk of corrosion of steel rebars. When FRP reinforcement is used, corrosion is not the main issue because the rebars are designed to be highly durable. However, crack widths have to be controlled to satisfy the requirements of appearance and specialized performance.

Codes of practice tend to satisfy the SLS of cracking by simplified, deemed-to-satisfy rules that control the detailing of the reinforcement. Alternatively, the maximum crack width can be calculated and checked not to exceed predefined limits. Maximum values for design crack width in FRP and steel reinforced concrete members, taken from several codes of practice, are given in Table 5-6. It can be seen that the crack width limits have been relaxed for FRP RC. However, these limits may not be adequate for structures exposed to extreme and aggressive environmental conditions, or for those designed to be water-tight. In the absence of more information, limitations suggested for steel RC structures could also be

adopted for FRP RC structures. For temporary structures and those not requiring the limitation of crack width for aesthetic reasons, the limitation on crack widths can be omitted. ISIS Canada (2001) does not give much weight to crack width calculations, but emphasizes that for crack control under normal conditions, the strain in the FRP reinforcement must not exceed 2000 micro-strains. Likewise, CAN/CSA-S806-02 requires a quantity "*z*" not to exceed 45000 N/mm for interior exposure or 38000 N/mm for exterior exposure, where "*z*" is the same quantity used in ACI 318-05 for steel RC, but with modification factors for FRP, as follows.

$$z = k_b \frac{E_s}{E_f} f_f \sqrt[3]{cA} \tag{5-1}$$

It is worthwhile to mention that, in ACI 318 (2002) and ACI 318 (2005), control of cracking under normal exposure conditions is only provided by limiting the spacing of steel rebars, without calculating the quantity "*z*". ACI Committee 318 (2002) emphasizes that crack widths in structures are highly variable, which makes crack width prediction equations unreliable as a basis for crack control. It is further explained that the role of cracks in corrosion of reinforcement is controversial, which does not warrant the former distinction between normal interior and exterior exposure conditions.

Table 5-6: Crack width limitations for FRP and steel RC elements

Code	Material	Exposure	w_{max}
Eurocode 2	Steel	Normal	0.3 mm
Model Code 1990	Steel	Normal	0.3 mm
JSCE (1997)	FRP		0.5 mm
ACI 440.1R-06 CSA (2002)	FRP	Interior	0.7 mm
ACI 440.1R-06 CSA (2002)	FRP	Exterior	0.5 mm
IStuctE (1999)	FRP	Close to observer Away from observer	0.3 mm >0.3 mm

5.3 Deflection: code models and approaches for FRP RC

Under similar conditions, in terms of concrete, loading, member dimensions and area of reinforcement, FRP RC members would develop larger deformations than steel reinforced members. This is mainly due to the lower modulus of elasticity of the FRP rebars, but is also influenced to a certain extent by the differences in bond characteristics.

FRP rebars have high tensile strengths and stress-strain behaviour that is linear up to failure. This leads, under pure bending and beyond the crack formation phase, to almost linear moment-curvature and load-deflection relationships up to failure. Despite this brittle behaviour, FRP elements are capable of achieving large deformations that are comparable to those of steel RC elements [Pilakoutas (2000)].

Several simplified models are used for the prediction of both short and long-term deflections of steel RC members. Some of these models were modified to become applicable for FRP RC, and are discussed in this section.

5.3.1 Deflections in accordance with Eurocode 2 and CEB-FIP Model Code 1990

Eurocode 2 and Model Code 1990 adopt the following approach for the calculation of short and long-term deflection "δ" for steel RC.

$$\delta = \delta_2 \cdot \xi + \delta_1 \cdot (1 - \xi) \tag{5-2}$$

where, the ratio between the cracking and maximum bending moment under service loading is taken into account using the following equation.

$$\xi = 1 - \beta \cdot \left(\frac{M_{cr}}{M_{\max}} \right)^m \tag{5-3}$$

In the above expressions δ_1 and δ_2 are calculated assuming constant uncracked and cracked sectional moments of inertia along the element.

Values recommended for these coefficients in Model Code 1990 and Eurocode 2 are shown in table 5-7.

Table 5-7: Values for coefficients β and m

	β	m
Eurocode 2	1	2
Model Code 1990	0.8	1

For FRP rebars the coefficients β and m should be evaluated experimentally. Zhao (1999) concluded that both the Eurocode 2 and Model Code 1990 prediction equations for the instantaneous deflection of steel RC elements could be adopted directly for GFRP RC members in bending. Pecce et al. (2000) pointed out that the model proposed for steel reinforcement by Eurocode 2 is reliable and could be used for GFRP RC beams if the bond performance is comparable.

Pecce et al. (2001) carried out a statistical analysis to assess the reliability of the ACI and Eurocode equations adopted to predict deflections. The study pointed out that the evaluation of the cracking moment could play a crucial role in the effectiveness of model predictions, since the serviceability load is not far from the cracking load when FRP rebars are used. The statistical analysis based on experiments conducted on GFRP RC elements indicated a large scatter of results.

5.3.2 Deflections in accordance with ACI 440.1R-06

The short-term deflection of a steel RC cracked beam can be simply obtained by applying the standard linear-elastic approach and using a constant effective moment of inertia [Branson (1966), (1977)], as in equation 5.4.

$$I_e = I_g \cdot \left(\frac{M_{cr}}{M_{\max}} \right)^3 + I_{cr} \cdot \left[1 - \left(\frac{M_{cr}}{M_{\max}} \right)^3 \right] \leq I_g \tag{5-4}$$

This equation, however, has been found to yield a beam response that is too stiff for FRP RC members, thus underestimating deflections [Yost et al. (2003)]. Several approaches to modify this equation have been proposed by researchers in the field and are discussed in the following.

ACI 440.1R-03 modifies the model for the evaluation of the effective moment of inertia of FRP RC elements, as follows:

$$I_e = \beta_d I_g \cdot \left(\frac{M_{cr}}{M_{max}} \right)^3 + I_{cr} \cdot \left[1 - \left(\frac{M_{cr}}{M_{max}} \right)^3 \right] \leq I_g \tag{5-5}$$

$$\beta_d = \alpha_b \left(\frac{E_f}{E_s} + 1 \right) \tag{5-6}$$

Experimental analyses carried out by Pecce et al. (2000) and Toutanji and Deng (2003) pointed out that the deflections in GFRP RC beams could be accurately predicted by the approach of ACI 440.1R and assuming a value of α_b, a bond dependent coefficient, equal to 0.5. Stone et al. (2002) found that the above approach could be very conservative in predicting the experimental deflection of CFRP RC elements.

Conversely, Zhao, Pilakoutas and Waldron (1997) reported that the deflections of FRP RC elements are predictable in the same way as for steel RC elements and went on to demonstrate that through their experimental work (using Eurocrete rebars). Hence, they concluded that the original ACI equations, without any modification, could adequately predict the deflections of FRP RC elements.

ACI 440.1R-06 abandons the reliance of β_d on bond and takes β_d as proportional to the ratio of reinforcement ratio to the balanced reinforcement ratio:

$$\beta_d = \frac{1}{5} \left(\frac{\rho_f}{\rho_{fb}} \right) \tag{5-7}$$

The above expression for β_d, however, is based on a statistical fit of experimental data and does not build upon the underlying principles of tension stiffening. As such, the above equation has been subject of debate by various researchers and alternative expressions have already been proposed (see Equation 5-14) [Bishoff (2007)].

ACI 318-05 (2005) calculates long-term deflections of steel RC by simply multiplying the short-term deflection due to sustained load by the following factor.

$$\lambda = \frac{\xi}{1 + 50\rho'} \tag{5-8}$$

For FRP RC, ACI 440.1R adopts the same approach to evaluate long-term deflections, but considers ρ' equal to zero because the FRP reinforcement is not effective in compression. Also, the factor ξ is reduced by 40% to allow for the larger initial deflection of FRP RC and the compressive stress level in the concrete. Hence, λ is evaluated as follows.

$$\lambda = 0.6\xi \tag{5-9}$$

5.3.3 Deflections in accordance with ISIS Canada (2001)

To calculate deflections, ISIS Canada (2001) adopts the same modified Branson equation for the effective moment of inertia as in ACI 440.1R, shown earlier. It is emphasized, however, that the correction factor, β_d, was based on limited test data, with doubtful applicability to other loading and boundary conditions.

Another equation for the effective moment of inertia, described as derived from CEB-FIP Model Code (1990), is proposed as follows.

$$I_e = \frac{I_t I_{cr}}{I_{cr} + \left[1 - 0.5\left(\frac{M_{cr}}{M_{\max}}\right)^2\right]\left(I_t - I_{cr}\right)} \tag{5-10}$$

This equation was reported to work well with different types of FRP reinforcement.

5.3.4 Deflections in accordance with CAN/CSA-S806 (2002)

CAN/CSA-S806 (2002) evaluates short-term deflections of FRP RC members by integration of curvatures at sections along the span. A tri-linear moment-curvature relation is assumed with the flexural stiffness being E_cI_g for the first segment, zero for the second, and E_cI_{cr} for the third. Alternatively, simple deflection equations, clearly derived from the assumed moment-curvature relation, are provided. The long-term deflections after 5 years are obtained by multiplying the short-term sustained deflection by a factor of "2".

5.3.5 Deflections in accordance with the Japanese JSCE (1997)

The Japanese [JSCE (1997)] uses the same methods as those for steel RC. However, where the FRP Young's modulus is low compared to steel, and where the reinforcement ratio is low, the increased deformations are expected to be associated with shear cracking, which in turn is expected to affect the deformation of the whole structure. In such cases, it is required that shear cracking be properly allowed for in calculating deformation levels.

5.3.6 Other approaches for evaluation of deflection in FRP RC members

Faza and GangaRao (1992) proposed a model for the evaluation of the average second moment of area I_m for the entire beam, which is only valid for the four-point loading pattern, with the loads applied at third points. I_m was derived assuming I_{cr} between the point loads and I_e at the end sections, as follows.

$$I_m = \frac{23 I_e I_{cr}}{8 I_{cr} + 15 I_e} \tag{5-11}$$

where: I_e is the original Branson effective moment of inertia.

Brown and Bartholomew (1996) used the same original Branson equation for the effective moment of inertia, but with increased exponent of "5" instead of "3", to soften the member response and take into account a lower tension stiffening effect when FRP bars are used

[Bishoff (2006)]. Prediction of results according to this modified equation, however, has shown to underestimate deflection at lower load levels [Bishoff (2005)].

Toutanji and Saafi (1999) concluded, based on their work and work of others, that Branson's equation underestimated FRP deflections, but only for low reinforcement ratios (less than 1%). A modified exponent (m), which incorporated the effect of reinforcement ratio (ρ_f in percent) and modulus of elasticity, was proposed to be used in Branson's equation as follows.

$$m = 6 - \frac{10E_f}{E_s}\rho_f \quad \text{for} \quad \frac{E_f}{E_s}\rho_f < 0.3 \tag{5-12}$$

$$m = 3 \text{ for } \frac{E_f}{E_s}\rho_f \geq 0.3 \tag{5-13}$$

Based on statistical evaluation of FRP RC test data, Yost et al. (2003) proposed a modified form for the factor β_d in the effective moment of inertia (I_e) equation in ACI 440.1R-06, as in eq. (5-8).

The use of this equation has been reported to work well for rectangular but not T-beams. Moreover, this equation inappropriately entails that deflection depends on the ultimate tensile stress of the FRP reinforcement.

Bischoff and Scanlon (2007) proposed a totally different form for the effective moment of inertia (I_e). I_e was derived based on tension stiffening of curvatures rather than moments of inertia; similar to the CEB (1993) and Eurocode 2 (CEN 2004) approaches. Bischoff considered his equation to be equally applicable for FRP and steel RC. I_e was given as follows.

$$I_e = \frac{I_{cr}}{1 - \eta\left(\frac{M_{cr}}{M_{\max}}\right)^2} \leq I_g \tag{5-14}$$

$$\eta = 1 - \frac{I_{cr}}{I_g} \tag{5-15}$$

5.3.7 Dimensioning for deflection control

ISIS Canada (2001) proposes an equation for the span to total depth ratio for FRP RC as follows.

$$\left(\frac{L}{h}\right)_f = \left(\frac{L}{h}\right)_s \left(\frac{\varepsilon_s}{\varepsilon_f}\right)^{\alpha_d} \tag{5-16}$$

El-Ghandour (1999) proposed a dimensioning method to achieve deflection control. The equation for determining span to depth ratios (L/h) according to specific SLS for slabs and beams was given as:

$$(L/h) = 24.2\,(250/\delta_r)^{1.9}\,(E_f\,\rho/99000)^{0.1}\,(f_{cu}/40)^{-0.44} \quad (5\text{-}17)$$

Ospina et al. (2001) defined a minimum depth for beams and one-way slabs (h), or equivalently a maximum span to depth ratio (L/h), by the limiting cracked curvature at a target deflection-to-span limit $(\delta/L)_{max}$, as follows.

$$\frac{L}{h} \le \frac{48\eta}{5K_1}\left(\frac{1-k}{\varepsilon_f}\right)\left(\frac{\delta}{L}\right)_{max} \quad (5\text{-}18)$$

where K_1 is 1.0, 0.8, 0.6, and 2.4 for uniformly loaded simply-supported, one-end continuous, both-ends continuous, and cantilevered spans, respectively; $\eta=d/h$ and k is the ratio of the compressive concrete zone to the effective depth under cracked elastic conditions.

Ospina and Gross (2005) modified Equation (5-18) to allow for tension stiffening by using the curvature tension stiffening model of CEB (1993). They also developed a table for minimum member thickness, Table 5-8, by multiplying Equation (5-18) by the ratio I_e/I_g. This equation has also been adopted by ACI (2006).

Table 5-8: Recommended Minimum Thickness of Non-prestressed Beams and One-Way Slabs Reinforced with FRP rebars

	Minimum Thickness, h			
	Simply Supported	**One End Continuous**	**Both Ends Continuous**	**Cantilever**
Solid one-way slabs	*L/13*	*L/17*	*L/22*	*L/5.5*
Beams	*L/10*	*L/12*	*L/16*	*L/4*

5.4 Cracking: code models and approaches for FRP RC

This section is concerned only with the most common structural type of cracks, namely, transverse flexural cracks.

Crack width is primarily a function of the deformation of the reinforcement and concrete between two adjacent cracks. Therefore, crack width is a function of crack spacing. Researchers differ in the method of correlating crack width to crack spacing and concrete cover. In general, the following points are accepted [Zhao (1999)].

- Crack width is a function of reinforcement strain, which sometimes approximates to a linear relationship.
- The concrete cover has an important effect on crack width.
- Crack width is a function of crack spacing up to a certain limit.
- Crack width and crack spacing are variable in magnitude and follow approximately a normal distribution.

Similar to deflections, flexural cracks in FRP RC members tend to be wider than those in steel RC members. Again, this is mainly due to the lower modulus of elasticity of the FRP rebars, and, to some extent, to the difference in bond characteristics. Several simplified models are used for the prediction of crack width and spacing of steel RC members. Some of these models were modified to become applicable for FRP RC, and are discussed in this section.

5.4.1 Crack width in accordance with Eurocode 2

The crack width calculations according to Eurocode 2 for steel RC are as follows.

$$w_{cr} = \beta s_{rm} \varepsilon_{sm} \tag{5-19}$$

$\beta = 1.3$

ε_{sm} is the mean reinforcement strain allowing for tension stiffening;

$\varepsilon_{sm} = \sigma_s [1 - \beta_1 \beta_2 (\sigma_{sr} / \sigma_s)^2] / E_s$

β_1 equals 1.0 for high-bond bars and 0.5 for plain bars;

β_2 equals 1.0 for a single, short-term loading and 0.5 for a sustained or cyclic load;

s_{rm} is the average final crack spacing;

$s_{rm} = 50 + 0.25 k_1 k_2 \frac{d}{\rho_r}$;

k_1 equals to 0.8 for high-bond bars and 1.6 for plain bars;

k_2 equals to 0.5 for bending and 1.0 for pure tension;

The Eurocode 2 crack width equation is strain based and can be adopted directly for the crack width determination of FRP RC elements. The approach adopted is also sophisticated enough to allow both for different bond characteristics, via parameter β_1, and for long-term stress, via parameter β_2. The accuracy of the crack width predictions by the Eurocode 2 approach was demonstrated by Zhao (1999).

5.4.2 Crack width in accordance with ACI 440.1R-06

ACI 224 (2001), which deals with cracking of steel RC, explains that statistical analysis of maximum crack width data by Gergely and Lutz (1968) leads to a formula for the maximum probable crack width. This formula has been simplified as follows.

$$w = 2.2 \beta \varepsilon_s \sqrt[3]{cA} \tag{5-20}$$

Based on Frosch (1999) equation, ACI 440.1R modifies the model for the evaluation of crack width in FRP RC, as follows:

$$w = 2 \frac{f_f}{E_f} \beta k_b \sqrt{c^2 + \left(\frac{s}{2}\right)^2} \tag{5-21}$$

in which, $\frac{f_f}{E_f} = \varepsilon_f$ is the FRP reinforcement strain. If the bond is similar to steel, then k_b is equal to one. If the bond is weaker than steel then k_b is larger than one, and vice versa. If k_b is not provided from experimental data, the value of 1.2 may be adopted. Zhao (1999) confirmed that the above ACI (2001) expression was valid for the Eurocrete rebars. ISIS Canada (2001) adopts an expression similar to ACI (2001) where crack width calculations are needed. CAN/CSA-S806 (2002) also adopts the ACI approach, but modifies the quantity "*z*" instead of the crack width (Equation 5-1).

5.4.3 Crack width in accordance with the Japanese JSCE (1997)

For the evaluation of crack widths, JSCE (1997) uses the following equation to obtain the maximum crack width.

$$w_{\max} = k_b \cdot \left[4c + 0.7\left(c_f - d\right) \right] \cdot \left[\frac{\sigma_{fe}}{E_f} + \varepsilon'_{csd} \right] \tag{5-22}$$

This approach is the same as that used for calculation of crack widths of steel RC members. The bond coefficient "k_b" is to be determined for each type of FRP rebar. However, when the FRP and steel rebars have similar bond characteristics, "k_b" may be taken as 1.0.

5.4.4 Other approaches for evaluation of crack width in FRP RC members

Faza and GangaRao (1991) proposed calculations for crack widths that incorporated the actual bond strength of the FRP rebars, as follows, but this procedure did not compare well to experiments involving sand-coated GFRP rebars, characterized by high bond strength.

$$w_{max} = l\varepsilon_f \tag{5-23}$$

$$l = \frac{(2 f_{ct} A)}{\tau_{\max} \pi d} \tag{5-24}$$

where:

ε_f is the maximum strain in FRP reinforcement at service load level with $0.5(0.8f_{fu})$ to be used if no computations were available

f_{fu} is the experimental rupture stress

Bakis et al. (2006) recommend a value of 1.4 for rebars that are not smooth.

5.4.5 Dimensioning for crack width control

Newhook et al. (2002) proposed a procedure aiming at dimensioning the cross-sectional area of FRP rebars required for a section subjected to flexure. By following this approach, crack width in service is controlled and adequate curvature before failure is ensured. The procedure is based on limiting the allowable FRP strain in service to 2000 micro-strains, and on a ductility factor of 4, taken as the ratio of the products of moment and curvature at ultimate and service loads. This procedure appears to be unduly conservative and more research is required to establish more economic limits.

6 Shear and punching shear

6.1 General

Shear behaviour of reinforced concrete (RC) members is a complex phenomenon that relies on the development of internal carrying mechanisms, the magnitude and combination of which is still a subject of debate. Nevertheless, it has been recognised that the shear resistance of RC elements is determined mainly by the contribution offered by the un-cracked compression zone, aggregate interlock, dowel action and, when provided, shear reinforcement. The development of all of these basic mechanisms, however, depends not only on the characteristics of the concrete itself, but also on the mechanical properties of the reinforcing material and the nature of the interaction between concrete and reinforcement.

This chapter examines how the use of FRP reinforcement will affect the various shear resisting mechanisms and how the overall behaviour can be accounted for in the development of design recommendations that can accommodate effectively the use of this type of reinforcement.

6.2 Effect of FRPs' mechanical properties on local shear carrying mechanisms

The distinctive mechanical properties of FRPs are paramount to the way in which the various mechanisms contributing to the total shear resistance develop and interact. The larger strains that are induced in the reinforcement of FRP RC elements in general result in larger deflections and wider cracks, and the absence of plastic behaviour in the reinforcement always leads to a brittle failure and renders more problematic the redistribution of stresses within the structure. Furthermore, the anisotropic nature of composite reinforcement needs to be taken into account when determining its performance under a combination of axial and transversal forces. This is especially important for shear links. All of these aspects, and their effect on local shear carrying mechanisms, are discussed in turn in the following.

6.2.1 Shear transfer in the compression zone

In reinforced concrete elements, the depth of the compression zone substantially determines shear strength, but it is highly dependant on the properties of the longitudinal reinforcement. The shear capacity of FRP RC sections is therefore expected to be somewhat different than that of conventional steel RC sections. While steel reinforced elements s eem to deteriorate in shear very quickly once the yield strain of the flexural reinforcement is reached, similar behaviour is not observed in those reinforced with FRP. This can be attributed to the fact that the neutral axis depth of the former reduces rapidly after yielding (Figure 6-1), hence reducing the area of concrete in compression [Zhao et al. (1997a; 1997b)]. As a consequence, the shear resistance offered by the concrete in compression also reduces after yielding. In FRP reinforced elements, after cracking, the area of concrete under compression is considerably smaller than that developed in similar steel RC sections already at relatively low load levels. As strain in the bars increases, however, the compression area does not decrease further as is the case for steel (Figure 6-1). In fact, due to non-linearity in the mechanical characteristics of concrete in compression, the area of concrete under compression increases and the shear resistance is influenced in a less profound way. Although a smaller shear resistance is

expected from FRP RC elements straight after cracking, a less rapid degradation will occur with increasing the strain in the reinforcing bars.

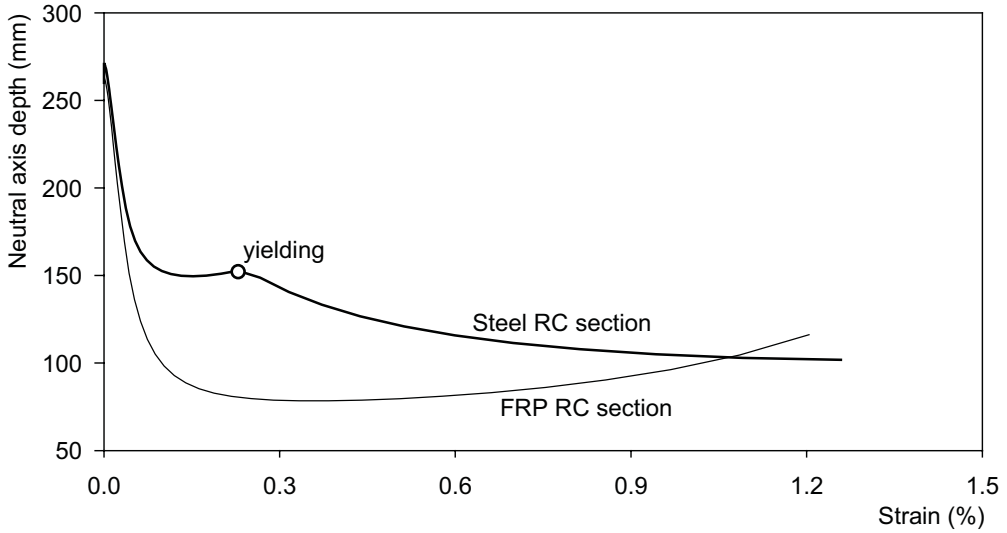

Figure 6-1: Behaviour of steel and FRP RC sections with same geometry and amount of longitudinal reinforcement

6.2.2 Aggregate interlock

In the tensile zone, shear transfer across a crack by mechanical interlock is developed when a shear displacement parallel to the direction of the crack occurs (Figure 6-2). Many experimental programmes were conducted over the years to investigate aggregate interlock and to determine its contribution to the total shear capacity of a concrete structure. The results of such investigations have shown that, for beams without web reinforcement, the relative magnitude of shear force carried by aggregate interlock can be estimated to be between 33% and 50% of the shear capacity of uncracked concrete [Taylor (1970)]. This percentage, however, reduces with increasing crack width [Walraven (1981)].

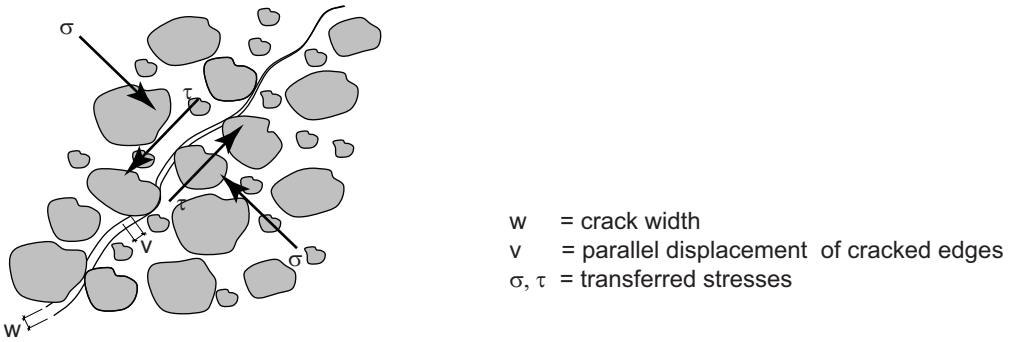

Figure 6-2: Transfer of forces across cracks due to aggregate interlock

When FRP bars are used in a RC element, higher deflections and wider cracks are expected to develop. For example, Mikani *et al.* (1989) observed crack widths in GFRP RC beams about three times wider than those in equivalent steel RC beams for the same sustained load. A smaller amount of shear force is therefore expected to be carried by aggregate interlock in FRP reinforced structures.

6.2.3 Dowel action of reinforcement

The term dowel action refers to the combination of the tensile resistance of the concrete surrounding the flexural reinforcement and the bending and transverse shear resistance of the reinforcing bars (Figure 6-3). Studies have shown that for lightly reinforced elements [for example Kotsovos and Pavlovic (1999)], dowel action is a shear carrying action that is of a relatively minor importance in comparison to other shear transfer mechanisms.

When FRP reinforcement is used as flexural reinforcement, the resistance to the shear capacity offered by its dowel action can be considered negligible, mainly because of the very low transverse stiffness typical of FRP materials [Kanakubo and Shindo (1997), Tottori and Wakui (1993)].

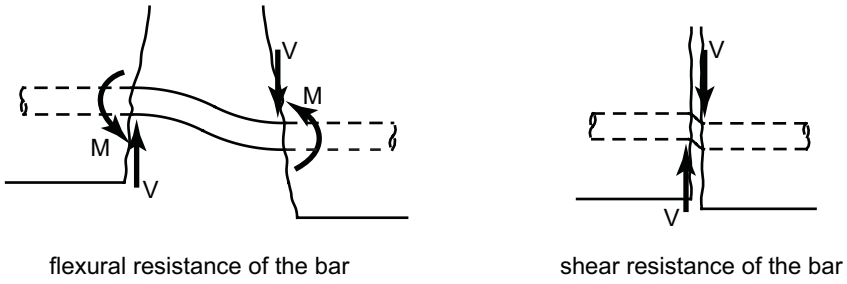

Figure 6-3: Mechanisms of dowel action for flexural bars crossing a crack

6.2.4 Shear reinforcement

When shear demand exceeds the inherent shear capacity of concrete, transverse reinforcement needs to be provided. The provision of transverse reinforcement, most commonly in the form of vertical links, enables the transfer of tensile forces across inclined shear cracks (Figure 6-4).

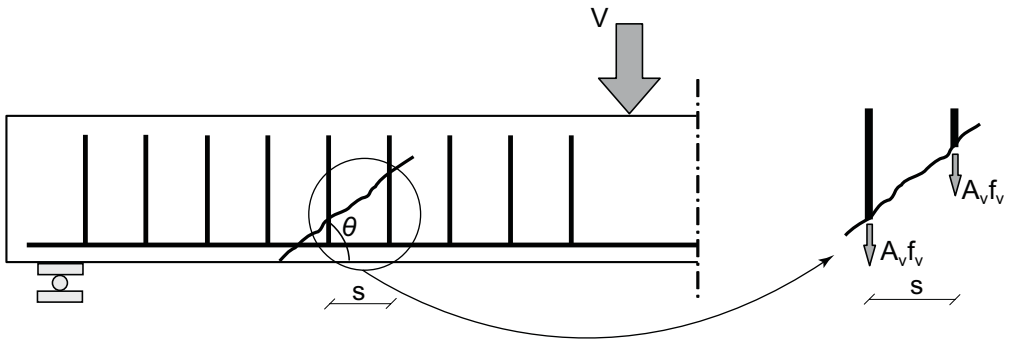

Figure 6-4: Shear reinforcement contribution to total shear capacity

Shear reinforcement is mobilised only in the tension zone of a beam and its contribution to shear resistance depends upon the maximum stress that the reinforcement can support. In the case of conventional steel reinforcement, this is equal to the yield stress while with FRP reinforcement, which is linear elastic up to failure, other governing phenomena such as slip and elongation become more relevant. Furthermore, as reported in various studies [Eshani *et al.* (1995); Maruyama *et al.* (1989); Mochizuki *et al.* (1989); Nagasaka *et al.* (1989)], the tensile strength of FRP rods is largely reduced under a combination of tensile and shear stresses (Figure 6-5). Consequently, if high stresses are developed in the links, failure is

expected at the corner anchorages. The reduction in strength that occurs at the corners of a FRP bar depends on the embedment length to diameter ratio, type of composite, bond properties and type of anchorage provided. Researchers working in this area recommend using, as a design parameter, a maximum strength equal to 40%-50% of the guaranteed uniaxial strength of the composite [Morphy *et al.* (1997); Shehata *et al.* (2000)].

The Japan Society of Civil Engineering [JSCE (1997)] imposes a limit on the maximum strength that can be developed in bent bars (Eq. (6-1)) and the same limit is adopted in the design recommendations proposed by the American Concrete Institute [ACI (2006)] and the ISIS Network [ISIS (2001)].

$$f_{fb} = \left(0.05 \frac{r_b}{d_b} + 0.3 \right) f_{fu} \leq f_{fu} \tag{6-1}$$

The strain limit recommended by the various committees, together with the limit imposed by Eq. (6-1), protects against shear failure due to fracture of the shear reinforcement.

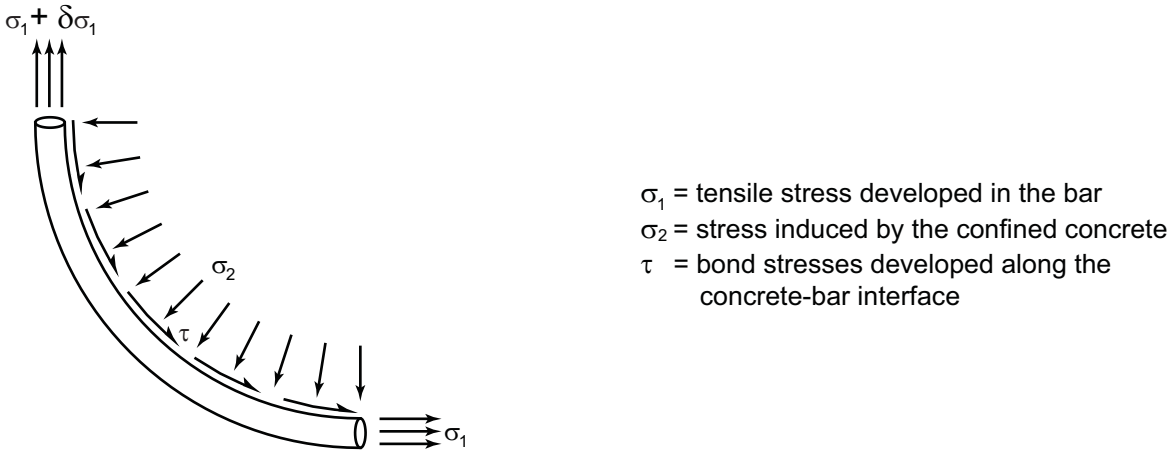

Figure 6-5: Schematization of forces acting on the bent portion of a bar embedded in concrete

6.3 Shear modes of failure in FRP RC elements

Failure of RC elements due to shear is always preceded by the formation of cracks inclined to the main axis of the element. The formation of shear cracks changes the internal behaviour of the element and failure can subsequently take place either simultaneously with the formation of new or extending shear cracks or after an increase in the applied load.

In addition to the typical shear modes of failure that can occur in a conventionally reinforced concrete element, most commonly diagonal tension failure and shear compression failure, FRP RC elements can fail in shear due to fracture of the shear reinforcement (*cf.* §6.2.4).

Shear failure for crushing of the concrete struts is a failure mechanism that depends only on the concrete characteristics and therefore recommendations as for current design codes for steel RC remain valid and are adopted for FRP RC elements as well.

6.4 Shear design approach for FRP RC elements

Over the past decades, several explanatory theories have been proposed, and contrasting assumptions regarding how shear forces are resisted and transferred within a concrete element still divide the scientific community [Mitchell and Collins (1974), Nielsen (1984), Vecchio and Collins (1986), Hsu *et al.* (1987), Kotsovos (1988)]. Although a greatly improved understanding of the shear behaviour of reinforced concrete has been achieved since the truss analogy theory (Morsh 1909), the complexity of the various predictive models makes them difficult to incorporate directly into design equations. Consequently, the majority of existing national and international design codes (e.g. ACI 2005, BSI 1990) are based upon a semi empirical approach and rely on the underlying assumption that the various mechanisms that develop are plastic and redistribution of stresses can occur following yielding of the reinforcement. According to this approach, the shear capacity can be expressed in terms of a concrete contribution and, when provided, an additional contribution offered by the shear reinforcement.

Redistribution of stresses, however, is more problematic when adopting elastic-brittle materials such as FRP. Researchers in the field have argued that the design approach used for steel RC members, which relies heavily on stress redistribution and on the underlying principles of plasticity theory, may not be safely applied to FRP RC members [Stratford and Burgoyne (2003)]. Nevertheless, evidence shows that, provided shear cracks are effectively controlled and the individual shear resistances of the concrete and shear reinforcement are effectively mobilised, the assumption that the contribution of the two mechanisms can be simply added together yields analytical predictions that are in good agreement with the experimental evidence [Guadagnini *et al.* (2003, 2006)]. Experimental tests carried out by various researchers on both beams [for example Maruyama and Zhao (1994, 1996), Nagasaka *et al.* (1995), Alsayed *et al.* (1996)] and slabs [for example Matthys and Taerwe (2000), El-Ghandour *et al.* (2003), Ospina *et al.* (2003)] showed that the shear capacity of FRP RC elements can be predicted with an adequate margin of safety by adopting the classic formulation that was derived for steel RC and taking into account the reduced stiffness of the different type of reinforcement to that of steel.

6.4.1 Design principles

The basic principle underlying existing recommendations for the design of FRP RC structures is that, assuming that adequate bond between concrete and reinforcement can be developed, the concrete section experiences forces and strains that are independent of the type of flexural reinforcement utilized. Hence, if a design using FRP maintains the same strain in the longitudinal reinforcement ($\varepsilon_f = \varepsilon_s$), and the same design forces are developed ($F_f = F_s$), then that design, by definition, will lead to the same safe result as when steel reinforcement is used. In the literature this approach is most often referred to as the 'strain approach' [for example Guadagnini *et al.* (2003)]. Based on this assumption (Eq. (6-2)), an equivalent area of flexural reinforcement (A_e) can be determined according to Eq. (6-3).

$$F_f = \varepsilon_f \cdot E_f \cdot A_f = \varepsilon_s \cdot E_s \cdot A_s = F_s \tag{6-2}$$

$$A_e = A_f \cdot \frac{E_f}{E_s} \tag{6-3}$$

Most researchers and code developers working in the field adopt this principle of equivalent area of reinforcement, or apply similar correction terms that take into account the different axial rigidity of the flexural reinforcement, in order to evaluate concrete shear resistance.

As far as shear reinforcement is concerned, the amount of FRP required is determined by controlling the maximum strain (ε_{fw}) that can be developed in the shear reinforcement. The limiting values of strain used in initial design recommendations were based on the yielding strain of steel (between 0.2% - 0.25%) and were imposed primarily to preserve the integrity of the section and guarantee the additive nature of the resisting mechanisms. On the basis of experimental evidence, higher allowable strain values were subsequently proposed by researchers in the field, and are now implemented in less conservative design guidelines, to capture more adequately the true behaviour of FRP RC elements (Figure 6-6). The maximum stress that can be developed in the shear links (f_{fw}) is then simply computed according to Eq. (6-4) and the amount of shear reinforcement is designed according to the well established truss analogy theory.

$$f_{fw} = \varepsilon_{fw} \cdot E_{fw} \tag{6-4}$$

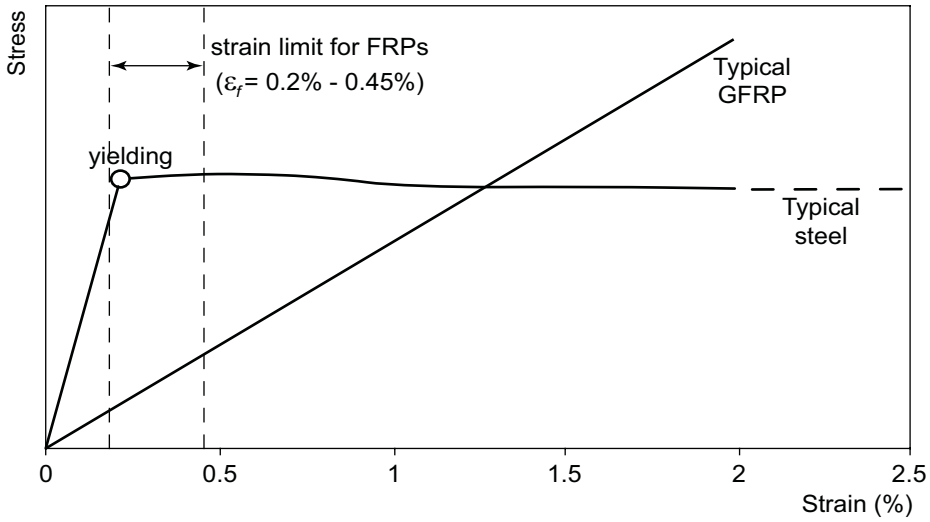

Figure 6-6: Limiting strain for shear reinforcement adopted by current design recommendations for FRP RC

6.5 Modifications to code design equations to allow for the use of FRP reinforcement

On the basis of the considerations above, and to facilitate the rapid adoption of FRP in concrete construction, all of the code developers working in the field have attempted to provide simple design rules using modified versions of existing predictive equations based on the well-established philosophy for steel reinforced structures.

In the following, various shear and punching shear design recommendations to allow for the use of FRP reinforcement are presented and discussed. It should be noted that all of the partial factors for materials as well as load and resistance factors adopted by the different design standards are not included in the equations below in order to allow for easier comparison between the various formulations. For a detailed description of the equations, including limiting values for the various factors, the reader is invited to refer to the original documents.

6.5.1 Shear in FRP RC Beams

6.5.1.1 Modifications to the JSCE standard specifications

The Japan Society of Civil Engineers published the first set of design recommendations for the design of concrete structures reinforced with advanced composites [JSCE (1997)]. According to these recommendations, shear capacity of FRP RC elements can be estimated adopting the same principles as for the design of steel RC. Hence, the shear capacity of the concrete is determined by using an empirical equation that follows the same format as that provided in the Japanese design code for steel RC and includes a modifying term to account for the different stiffness of the reinforcement (Eq. (6-5)). The direct application of the strain approach introduced in §6.4.1 is instantly recognizable (see symbols in bold).

$$V_{cf} = 0.2 \cdot \sqrt[4]{1/d} \cdot \sqrt[3]{100 \frac{\boldsymbol{A}_f}{b_w d} \frac{\boldsymbol{E}_f}{\boldsymbol{E}_s}} \cdot \sqrt[3]{f_c'} \cdot b_w \cdot d \tag{6-5}$$

The design shear capacity offered by the FRP shear reinforcement can be computed according to the classical formulation for steel RC in which the different nature of the shear reinforcement is taken into account by substituting the yield stress of the reinforcement with the product of the Young's modulus of the FRP shear reinforcement, E_{fw} and its strain design value, ε_{fwd} (Eq.(6-6)). The strain design value of FRP shear reinforcement is taken accordingly to Eq. (6-7).

$$V_{sf} = \frac{A_{fw} \cdot E_{fw} \cdot \varepsilon_{fwd}}{s} \cdot z \tag{6-6}$$

$$\varepsilon_{fwd} = \sqrt{\left(\frac{h}{0.3}\right)^{-1/10} f_c' \frac{\rho_f E_f}{\rho_{fw} E_{fw}}} \cdot 10^{-4} \tag{6-7}$$

Where the design stress, $E_{fw}.\varepsilon_{fwd}$, is greater than the strength of the bent portion of FRP calculated according to Eq. (6-1), the latter should be used instead.

6.5.1.2 Modifications to the British standard

The Institution of Structural Engineers published an "Interim guidance on the design of reinforced concrete structures using fibre composite reinforcement" [IStructE (1999)]. This guide is in the form of suggested changes to the British Design Codes BS8110: "Structural use of concrete Part 1" [BSI (1997)] and BS5400: Part 4 "Code of practice for the design of concrete bridges" [BSI (1990)]. The suggested modifications are in line with the strain approach (§6.4.1) and propose the use of the modification factor given in Eq. (6-3). Hence, the modified BS8110 equation for concrete shear strength of sections reinforced with FRP, v_{cf}, is given in Eq. (6-8).

$$v_{cf} = 0.79 \cdot \left(\frac{100}{b_w \cdot d} \cdot A_f \cdot \frac{E_f}{200}\right)^{1/3} \cdot \left(\frac{400}{d}\right)^{1/4} \cdot \left(\frac{f_{cu}}{25}\right)^{1/3} \tag{6-8}$$

As far as the shear strength resisted by the vertical shear reinforcement is concerned, this can be evaluated using the usual formulation derived according to the truss analogy theory as reported for steel, but controlling the maximum strain developed in the vertical bars, according to the strain approach.

Following these recommendations, and limiting the strain to the value of 0.0025, the shear strength offered by the web reinforcement is given in Eq. (6-9).

$$v_{sf} = \frac{0.0025 E_{fw} \cdot A_{fw}}{b_w \cdot s} \tag{6-9}$$

6.5.1.3 Modifications to the ACI design specifications

Committee 440 of the American Concrete Institute made modifications to the existing code for steel RC structures [ACI (2005)] based on an adaptation of the strain approach, since the reinforcement area cannot be modified directly in the simple shear equation (*cf.* ACI 318-05 Eq. 11-3).

The shear design equation for FRP RC beams without stirrups in ACI 440.1R-06 [ACI (2006)] is based on the model of Tureyen and Frosch (2002, 2003) and represents a significant change to the way in which the computation of the concrete shear contribution was dealt with in the previous editions of this document (see for example ACI (2003)). According to this model, the axial stiffness of the longitudinal FRP reinforcement is taken into account through the depth of the concrete in compression, c. The concrete shear resistance, V_{cf}, of flexural members with FRP reinforcement is then evaluated according to Eq (6-10).

$$V_{cf} = 0.4\sqrt{f_c'} b_w c \tag{6-10}$$

For singly reinforced rectangular sections, and assuming elastic-cracked conditions

$$c = k \cdot d \tag{6-11}$$

where

$$k = \sqrt{2\rho_f n_f + (\rho_f n_f)^2} - \rho_f n_f \tag{6-12}$$

and

$$\rho_f = \frac{A_f}{b_w d} \tag{6-13}$$

$$n_f = \frac{E_f}{E_c} \tag{6-14}$$

Eq. (6-10) can also be re-written as

$$V_{cf} = \left(\frac{12}{5} k\right) 0.167 \sqrt{f_c'} b_w d \tag{6-15}$$

which is simply the ACI 318 equation for the concrete shear resistance of steel RC, modified by the factor (*12/5k*) which accounts for the axial stiffness of the FRP reinforcement.

The contribution of FRP stirrups is taken into account using the same method as for steel stirrups, but adopting a value of FRP tensile strength, f_{fw}, that is taken as the smallest of $0.004E_{fw}$ and the strength of the bent portion of FRP stirrups calculated according to Eq. (6-1) .

6.5.1.4 Modifications to the CSA design specifications

The Canadian Standard Association published a set of standards for the design of concrete structures reinforced with FRP reinforcement [CAN/CSA (2004)]. According to the simplified design method considered by the CSA for steel RC elements, the concrete shear resistance is calculated according to the characteristics of the section. For members having an effective depth not exceeding 300 mm or an amount of transverse reinforcement at least equal to the minimum required, the concrete contribution is given by Eq. (6-16). For members with an effective depth greater than 300 mm or with transverse reinforcement less than the required, equation (6-17) is used instead.

$$V_{cf} = 0.035\lambda \left(f_c' \rho_f E_f \frac{V_f}{M_f} d \right)^{1/3} b_w d \tag{6-16}$$

$$V_{cf} = \left(\frac{130}{1000 + d} \right) \lambda \sqrt{f_c'} b_w d \tag{6-17}$$

If FRP shear reinforcement is used in lieu of steel, its contribution is taken into account using the same method as for steel reinforcement but only 40% of the ultimate strength of the stirrups is considered for design purposes (Eq. (6-18)).

$$V_{sf} = \frac{0.4 A_{fw} f_{fw} d}{s} \tag{6-18}$$

6.5.1.5 Modifications to the Italian design specifications

The Italian National Research Council (CNR) proposed modifications to the Italian national design code [CNR (2006)], which is based on the Eurocode 2 design equations as they were formulated prior to the changes implemented in 2004. The design approach suggested in this document implements the standard design method according to which the contributions of concrete and shear reinforcement are added together to obtain the total shear resistance of RC members.

The concrete contribution is modified to account for the axial stiffness of the FRP longitudinal reinforcement according to Eq. (6-19).

$$V_{cf} = 1.3 \left(\frac{E_f}{E_s} \right)^{1/2} \tau_{Rd} k (1.2 + 40 \rho_f) b_w d \tag{6-19}$$

The contribution of FRP stirrups is taken into account using the same method as for steel stirrups. The implementation of a reduced tensile strength for FRP shear reinforcement, however, limits the stress that can be developed in the links to the smallest of 50% of their design strength and the strength that can be developed at the bend (Eq. (6-1)).

6.5.1.6 Design approach of Guadagnini *et al.*

Experimental tests carried out on FRP reinforced concrete beams by various researchers [Duranovic et al. (1997), Tottori and Wakui (1993), Yost *et al.* (2001)], have provided evidence that the restrictions imposed by the current modifications to the value of maximum allowable strain that can be developed in the FRP reinforcement are unnecessarily conservative (recorded values of up to 1% have been reported). Having regard to these results and to the results obtained from an extensive experimental investigation, Guadagnini *et al.* (2003) have proposed a modified approach for the design of FRP reinforced beams in which the limit set by early design recommendations is increased to the higher value of 0.45% for both the shear and flexural reinforcement. This modified approach, has been successfully applied to various code equations [Pilakoutas and Guadagnini (2001), Guadagnini *et al.* (2003)]. Different formulations are required for each code, however, to allow for the fact that not all of the codes take into consideration the effect of flexural reinforcement in a similar fashion when deriving empirically the contribution of the concrete to the total shear resistance. Hence, they cannot be modified directly by simply taking into account the different stiffness of the reinforcement. To compensate for this, the following modifications to the Eurocode 2, BS 8110 and ACI-318-05 code equations are proposed when deriving the concrete shear resistance:

Eurocode 2

$$V_{cf} = 0.12\left(1+\sqrt{\frac{200}{d}}\right)\left(100\cdot\frac{A_f}{b_w d}\cdot\frac{E_f}{E_s}\cdot\phi_\varepsilon\cdot f_{ck}\right)^{1/3} b_w d \qquad (6\text{-}20)$$

BS 8110

$$V_{cf} = 0.79\left(\frac{100}{b_w\cdot d}\cdot A_f\cdot\frac{E_f}{200}\cdot\phi_\varepsilon\right)^{1/3}\cdot\left(\frac{400}{d}\right)^{1/4}\cdot\left(\frac{f_{cu}}{25}\right)^{1/3} b_w d \qquad (6\text{-}21)$$

ACI-318-05

$$V_{cf} = V_c\cdot\left(\frac{E_f}{E_s}\cdot\phi_\varepsilon\right)^{1/3} \qquad (6\text{-}22)$$

where $\phi_\varepsilon = \varepsilon_f / \varepsilon_y$ represents the ratio between the maximum strain allowed in the FRP reinforcement, $\varepsilon_f = 0.0045$ and the yield strain of steel, ε_y.

The contribution of FRP shear reinforcement is taken into account using the same method as for steel RC, but considering a level of stress in the shear links corresponding to the maximum allowable strain of 0.0045.

As for the modifications to Eurocode 2 are concern, these apply to the set of equations adopted in its latest edition [CEN (2004)]. A variable strut angle approach, however, is the only shear design method used in the latest revision of Eurocode 2 for steel RC beams, thus

ignoring the concrete contribution for members with shear reinforcement. Nevertheless, a simplified, fixed strut angle approach (θ=45°) is still recommended by the authors when calculating the shear resistance of RC beams with FRP shear reinforcement, and the additive nature of the shear resistance offered by concrete and shear reinforcement is maintained.

6.5.2 Punching shear in FRP RC slabs

Although experimental tests on FRP RC slabs are still limited, the evaluation of available experimental data has confirmed that existing punching shear design procedures for steel-reinforced concrete slabs need to be modified to account for the different mechanical properties of the reinforcing material. The shear strength of slabs, however, is governed by the same general principles as for beams (see §6.2) and it is expected that the overall punching resistance be affected in a similar fashion when using FRPs instead of steel reinforcement. Models proposed thus far include modifications of current design equations that adhere to the same principles as used for FRP RC beams. Amongst the various design recommendations available in published form to date, only those produced by ACI Committee 440 include a proposal for punching shear design of FRP RC slabs. Models proposed by various researchers and that had a significant input on the knowledge in this field, however, are also reported.

6.5.2.1 Modifications to the ACI design specifications

The punching shear design procedure included in ACI 440.1R-06 [ACI (2006)] is based on the work of Ospina (2005), who extended the beam shear concepts introduced by Tureyen and Frosch (see §6.5.1.3) to two-way shear design. In this model, the punching capacity of FRP RC slabs is evaluated as

$$V_c = 0.8\sqrt{f_c'}\, b_o\, c \tag{6-23}$$

The depth of the neutral axis, c, is calculated based on Eq. (6-11), where ρ_f is the slab reinforcement ratio, calculated as the average of the reinforcement ratios in the two directions. The control perimeter, b_o, is calculated at $0.5d$ away from the column face and is rectangular regardless of the column shape.

Eq. (6-23) can also be written as

$$V_c = \left(\frac{12}{5}k\right) 0.33\sqrt{f_c'}\, b_o d \tag{6-24}$$

which is simply the ACI 318 punching shear equation for steel RC slabs modified by the factor ($12/5k$). This modifying factor accounts for the effect of the axial stiffness of the FRP reinforcement on the contribution of concrete to the total punching shear capacity.

Eq. ((6-23) or (6-24)) was adopted by ACI 440.1R-06 mainly because of its conceptual similarity with the beam shear model of Tureyen and Frosch. It has been shown that this approach renders very conservative punching capacity estimates for FRP RC slabs. The degree of conservativeness, however, is intentional to acknowledge that punching shear tests on FRP RC slabs are still scarce.

6.5.2.2 Other predictive models available in the literature

Design approach of Matthys and Taerwe

Matthys and Taerwe (2000) found that the design equations in CEB/FIP MC90, EC2, and BS 8110 tend to overestimate the shear capacity of slabs reinforced with very flexible FRP bars or grids. Based on previous work reported by Gardner (1990) and the BS 8110-95 formulation, Matthys and Taerwe proposed the following equation to calculate the punching capacity of a two-way FRP-reinforced concrete slab.

$$V_c = 1.36 \frac{\left(100\rho_f \frac{E_f}{E_s} f_{cm}\right)^{1/3}}{d^{1/4}} b_o d \qquad (6\text{-}25)$$

where f_{cm} is the mean compressive strength of concrete. As per BS 8110, the critical perimeter b_o, which is assumed to be rectangular or square regardless of the column cross-sectional shape, is measured at a distance of *1.5d* from the column face.

Design approach of El-Ghandour et al.

El-Ghandour *et al.* (2003) introduced two design procedures for estimating the punching capacity of two-way slabs reinforced with FRP. The first procedure, applicable to design models that account for the reinforcement ratio effect, is to replace ρ_f with the factor $\rho_f \frac{E_f}{E_s} k_\varepsilon$, where k_ε is a constant equal to 1.8. This constant is obtained by dividing a FRP strain of 0.0045 (which the FRP reinforcement can mobilize) by 0.0025 (assumed yield strength of steel).

The second model proposed by El-Ghandour *et al.* (2003) is a modification of the ACI 318 punching equation (Eq. (6-26)).

$$V_c = 0.33 \sqrt{f_c'} \left(\frac{E_f}{E_s}\right)^{1/3} b_o d \qquad (6\text{-}26)$$

Eq. (6-26) leads to conservative predictions yet considerable scatter is observed because the proposed modification does not account for the FRP reinforcement ratio effect.

Design approach of Ospina et al.

Ospina *et al.* (2003) suggested two modifications to Eq. (6-25). The first concerns the effect of reinforcement stiffness and the second addresses the size effect. They found that taking the cube root of $\frac{E_f}{E_s}$ slightly overestimates the effect of reinforcement stiffness whereas the square root produces slightly better results. Notwithstanding the fact that the size effect influences slab punching, its importance for FRP RC slabs is not evident according to the available body of test data. On the basis of these considerations, the authors proposed the following empirical equation:

$$V_c = 2.77\left(\rho_f \ f_c'\right)^{1/3}\sqrt{\frac{E_f}{E_s}}\, b_o d \tag{6-27}$$

where ρ_f is the FRP reinforcement ratio, and b_o is calculated as in BS 8110. The control surface perimeter shape is rectangular regardless of the column shape.

Design approach of El-Gamal et al.
El-Gamal *et al.* (2005) proposed the following modification of the ACI 318 punching shear design equation:

$$V_c = 0.33\sqrt{f_c'}\ \alpha\,(1.2)^N\, b_o d \tag{6-28}$$

where α is an empirical factor defined as

$$\alpha = 0.62\left(\rho_f E_f\right)^{1/3}\left(1+\frac{8d}{b_o}\right) \tag{6-29}$$

where b_o is evaluated as in ACI 318 and N represents the continuity effect of the slab. N shall be zero for one span slab in both directions, 1 for slabs along one direction, and 2 for slabs continuous along their two directions. Eq. (6-28) appears to be the only equation in the literature, to date, that accounts for the effect of edge restraint conditions on the punching shear capacity of FRP RC slabs.

6.6 Comments on current modifications to existing code equations

All of the modifications presented thus far have been based on the design principles outlined in §6.4.1 (cf. §6.5.1.2), or an adaptation of it (cf. §6.5.1.3). Experimental results for a total of about 100 beam specimens, including over 50 specimens without shear reinforcement [Duranovic *et al.* (1997); Maruyama and Zhao (1994, 1996), Zhao *et al.* (1995), Alsayed *et al.* (1997), El-Sayed *et al.* (2005), Guadagnini *et al.* (2006), Razaqpur *et al.* (2004), Wegian and Abdalla (2005), Tureyen and Frosh (2002), Yost *et al.* (2001)], were analysed and their ultimate shear capacity was estimated according to the design recommendations suggested by the Institution of Structural Engineers (IStructE-1999) and the American Concrete Institute (ACI 440.1R-06) to assess the reliability of the adopted design principles. The comparative results are presented in Figure 6-7. It is worth noting that the shear capacity of the beams examined was derived by setting the values of the various safety and load factors to unity. Nevertheless, the comparison shows clearly that the existing recommendations are conservative in general, and hence, provide a suitable starting point for the safe design of FRP RC beams in shear. It can be also seen from the graphs that the two different codes examined here yield quite different ranges of results. In comparison, the IStructE modification to the British Standard seems to yield predictions that are in better agreement with the experimental results, although these predictions still appear to be conservative. The disparity between the predicted values can be attributed to differences both in the original formulation of the empirical equations derived for steel reinforced concrete and the way in which the influence of the change in the stiffness of the reinforcement is accounted for. Figure 6-8 and Figure 6-9, for example, illustrate the main differences between the American and British design equations, for both steel and FRP RC beams, by comparing the variation in the values of

concrete shear strength as a function of the flexural reinforcement ratio and concrete strength, respectively. As can be observed, the ACI 440.1R-06 equation always estimates a much lower concrete shear strength than is predicted by the IStructE-1999 equation. The conservative nature of the equation proposed by ACI 440 Committee to determine the concrete shear resistance becomes more obvious when observing the behaviour of FRP RC beams without shear reinforcement (Figure 6-10). In addition, the equation proposed in the ACI document implies that most of the shear is transferred through the uncracked compression zone. This assumption, however, is questionable, especially when considering concrete elements with shear reinforcement.

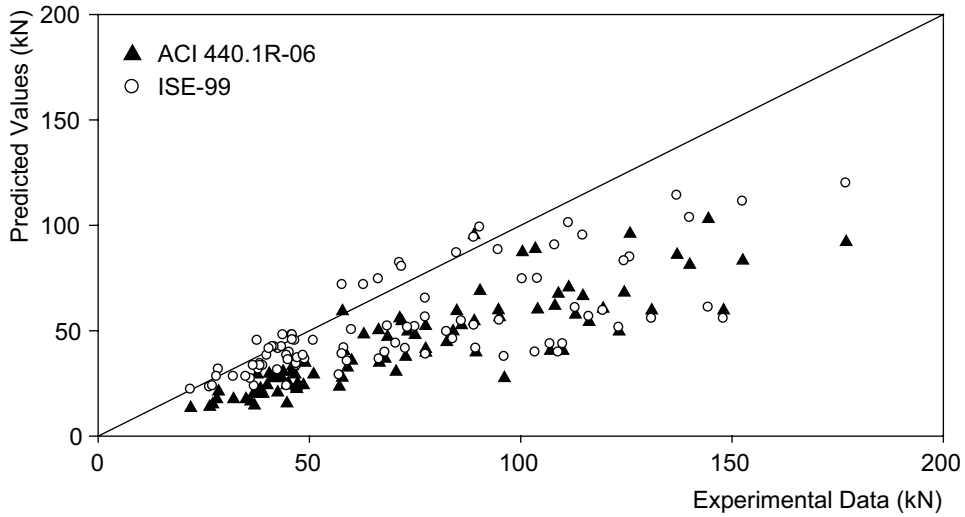

Figure 6-7: Prediction of experimental shear capacities using current modification to incorporate the use of FRP reinforcement

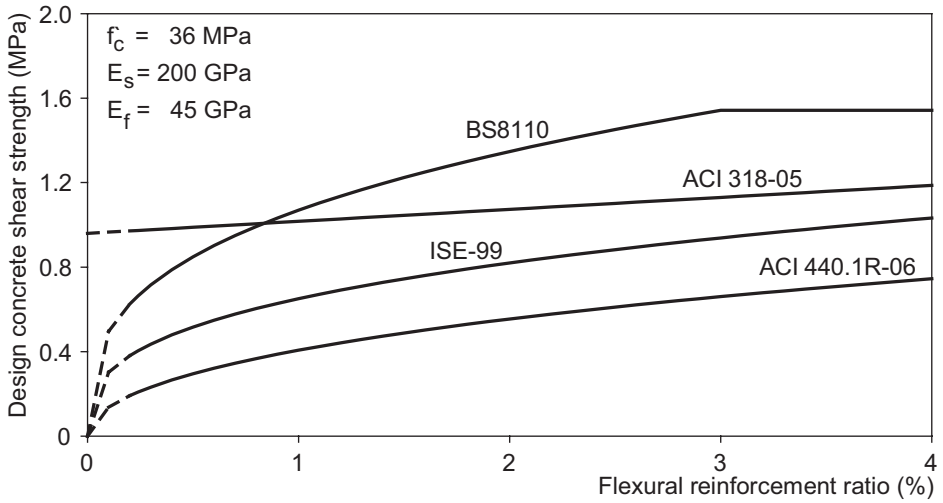

Figure 6-8: Comparison of the effect of flexural reinforcement ratio on concrete shear strength according to the British and American design equations

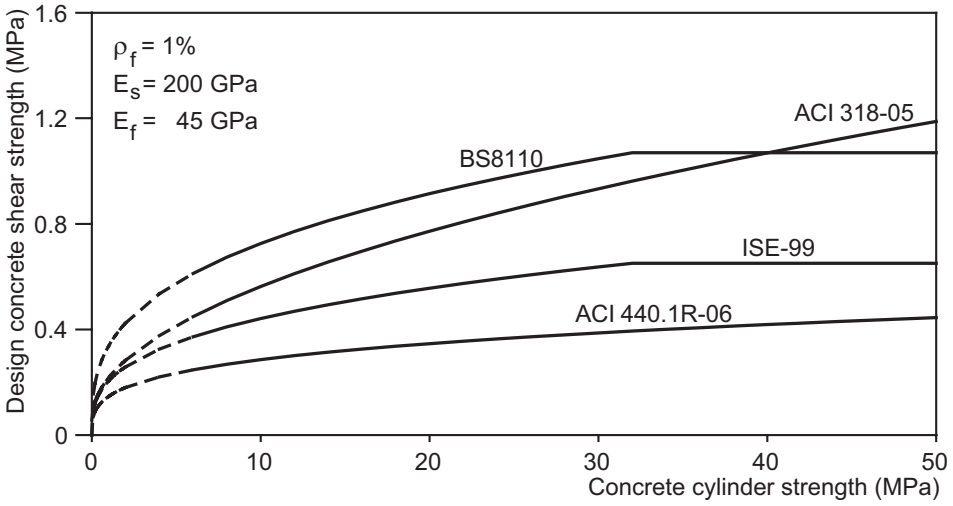

Figure 6-9: Comparison of the effect of concrete compressive strength on concrete shear strength according to the British and American design equations

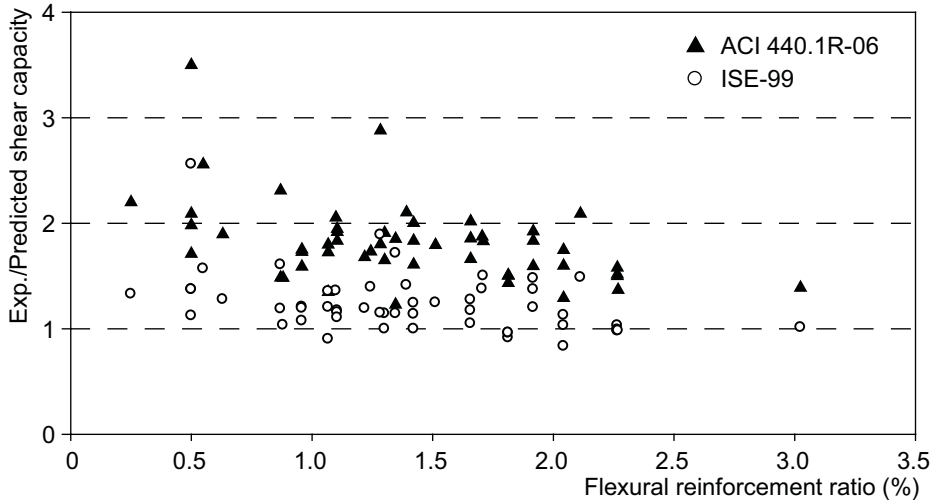

Figure 6-10: Prediction of shear capacity of FRP RC beams without shear reinforcement using current modification to incorporate the use of FRP reinforcement

6.7 Detailing

6.7.1 Minimum amount of shear reinforcement

A minimum area of shear reinforcement is generally required by design codes in beams of structural importance. Table 6.1 gives the minimum required ratio of shear reinforcement, $\rho_{w,min}$, and the corresponding minimum design shear resistance provided by the shear links according to some of the design guidelines reviewed above.

While BS 8110 specifies the minimum reinforcement ratio as a function of the yield strength of the shear reinforcement, the ACI 318-05, the Canadian Standard (CAN/CSA A23.3-94) and the Eurocode 2 (CEN 1992-1) take into account the concrete compressive strength. In each case, the requirement for a minimum amount of shear reinforcement, however, aims to provide an adequate shear reserve capacity by ensuring full shear transfer across cracks and avoiding the development of large crack widths in the shear span. As a result, it is reasonable to assume that this limit should ensure a minimum stiffness and this can

be achieved by using a strain/stress control. The current modifications to the steel RC codes to allow for the use of FRP reinforcement, limit the maximum strain/stress that can be developed in the shear reinforcement and derive the minimum ratio of FRP shear reinforcement, $\rho_{fw,min}$, accordingly (Table 6.1).

Table 6.1: Minimum ratio of shear reinforcement according to different design codes for steel RC and relevant modifications

Steel RC	$\rho_{w,min}$	FRP RC	$\rho_{fw,min}$
ACI 318-05	$0.06\sqrt{f_c'}\frac{1}{f_y} > 0.35\frac{1}{f_y}$	ACI 440.1R-06	$0.35\frac{1}{f_{fw}}$
CSA A23.3-94	$0.06\sqrt{f_c'}\frac{1}{f_y}$	CAN/CSA-S806-02	$0.3\sqrt{f_c'}\frac{1}{f_{fh}}$
BS 8110	$0.4\frac{1}{f_y}$	IStructE-99	$0.4\frac{1}{0.0025\cdot E_f}$
EN 1992-1	$0.08\sqrt{f_c'}\frac{1}{f_y}$	Guadagnini *et al.*	$0.08\sqrt{f_c'}\frac{1}{0.0045\cdot E_f}$

f_{fw} and f_{fh} correspond to the design tensile strength of FRP shear links, or the stress corresponding to $0.004E_f$, or the strength of the bent portion, whichever is least.

6.7.2 Maximum spacing requirements

Observations from tests performed on beams with GFRP shear reinforcement [Duranovic et al. (1997), Guadagnini (2002)] have shown that a limiting situation in terms of spacing emerged when the shear crack developed in such a way that it never crossed more than one link. Figure 6-11 illustrates the geometry for a 45° failure line crossing vertical shear links. By expressing the maximum spacing between the links as a function of the height, h_l, of the link, three different situations can be identified: more than one link is always crossed ($s<0.5h_l$), one or two links are crossed ($0.5h_l<s<h_l$) and one or less links are crossed ($s>h_l$).

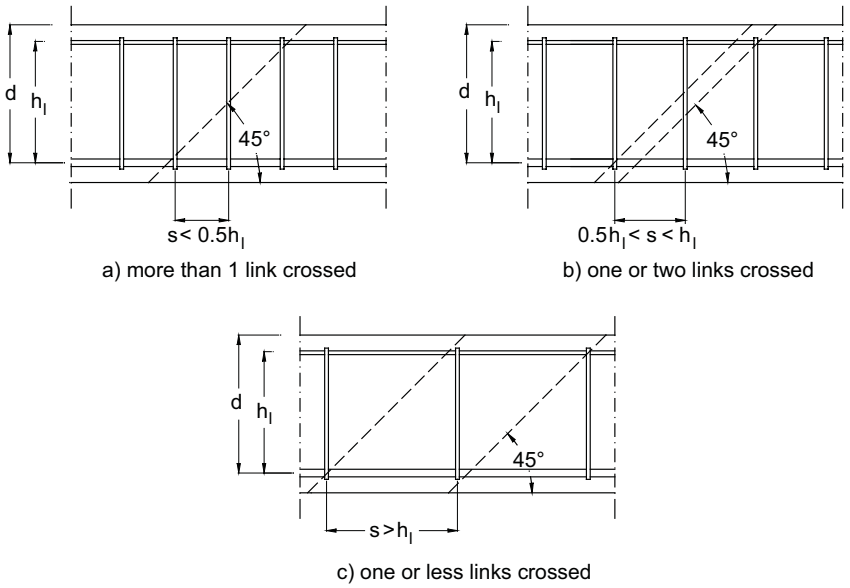

Figure 6-11: Geometrical arrangement for a 45° failure line crossing vertical link

If the relationship between the height of the link and the effective depth, d, of the beam is assumed as follows:

$$h_l = 0.9d \tag{6-30}$$

the provision of having more than one link crossing the 45° failure line will be ensured by limiting the maximum spacing between the stirrups to the following value:

$$s = 0.45d \tag{6-31}$$

The proposed value, which is lower than the recommended in the BS 8110 and Eurocode 2 (0.75*d*) is in line with the requirements of the ACI 318-05 design code (0.5*d*) and allows a better distribution of the shear reinforcement within the shear span.

6.7.3 Effect of corners on the strength of stirrups

As reported in §6.2.4, various studies have shown that a substantial reduction in tensile strength is noticeable at the corners of an FRP bar. This issue can become problematic when very high strains are developed in a bar and premature failure (i.e. failure at a level of stress below the ultimate value) is deemed to occur at the corners. These types of failure are designed for by carrying out a check on the ultimate strain that can be safely transferred through the bent region and by taking this as a limiting lower value (see Eq. (6-1)).

7 Bond, anchorage and tension stiffening behaviour

7.1 Introduction

Bond between concrete and FRP reinforcing bars is the key to developing the composite action of FRP RC. To secure composite action, sufficient bond must be mobilised between reinforcement and concrete for the successful transfer of forces from one to the other. This section will deal with bond, anchorage, tension stiffening behaviour and also behaviour of splices and end anchorages.

Bond interaction of FRP bars is different from that of deformed steel bars in many ways. In the case of the deformed steel bars the interaction arises primarily from the mechanical action of the bar lugs against concrete. Once the tensile stress of the concrete is exceeded this mechanical bond action leads to primary cracking extending to the surface. In addition multiple secondary cracks can develop from the lugs along the length of the bar in between the primary cracks. These secondary cracks normally are inclined and get trapped inside the concrete matrix without surfacing. In the case of FRP bars, with lower elastic modulus and lower surface undulations, bond interaction has more of a frictional character. Bond failure in steel bars is by crushing of concrete in the vicinity of the lugs whereas in FRP it is largely caused by partial failure in the concrete and some surface damage on the FRP.

Constitutive models for bond mechanics can be grouped into three levels: micro levels; meso levels and macro levels. This categorization is mainly done depending on the size of the control volume under investigation (see Fig. 7-1). If the behaviour of different parts of the interface is considered, like the different mechanism by which bar lugs transfer stresses to concrete from the rest of the bar, that is considered microlevel analysis. On the other hand if the member response is considered in a global scale, as in the case of tension stiffening effect, that is considered macro modelling. Results of pull out tests and direct tension tests fall in between these two extremes as the control volume length is not short enough to simulate micro behaviour nor long enough to simulate macro behaviour. Hence, it can be referred to as meso level modelling. Hierarchy of bond modelling schemes is shown below.

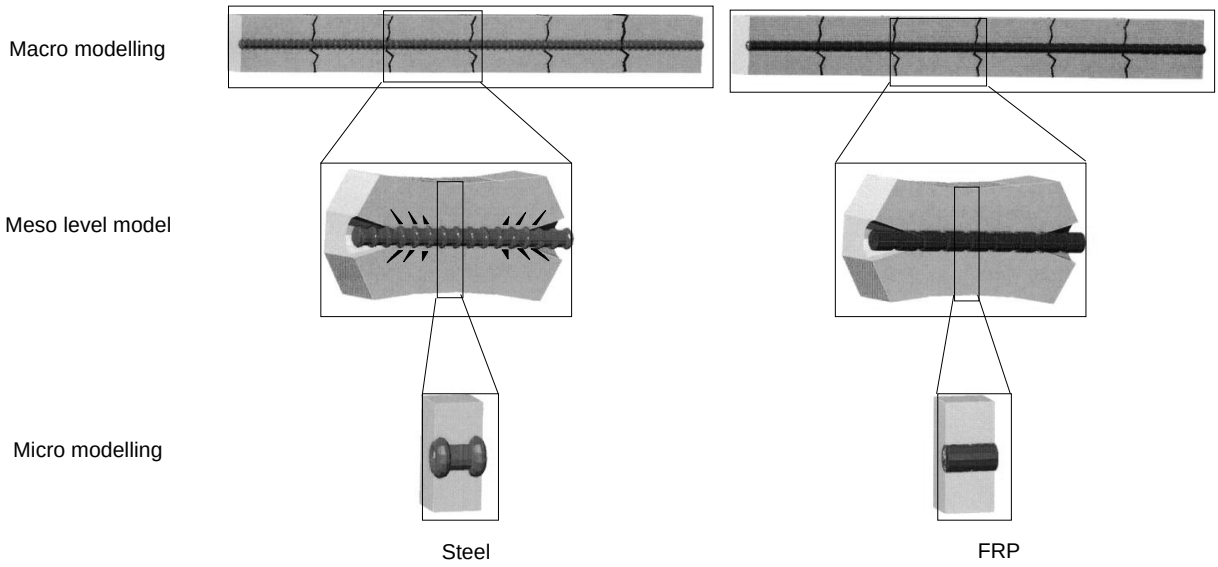

Figure 7-1: Hierarchy of bond modelling for steel and FRP bars

In the first part of this chapter bond is evaluated in terms of different levels according to the hierarchy given above, first taking the macro level bond modelling followed by the meso level modelling. As FRP has a uniform texture micro level bond modelling is not attempted. Splitting resistance of the reinforced concrete is examined next. These sections are introduced generally with sufficient information to allow the reader to grasp the fundamentals and implications of bond modelling. Then the different models for modelling average bond stress slip relationship and the transfer length of FRP are introduced. The chapter ends by presenting different code based approaches to model bond and anchorage of FRP reinforcement.

7.2 Macro level bond modelling: Tension stiffening effect

7.2.1 General

The ability of concrete to carry tension between cracks and provide extra stiffness to RC in tension is defined as the tension stiffening effect of concrete. This phenomenon relies heavily on the bond between concrete and reinforcement to transfer stresses. In other words tension stiffening can be referred to as a global response to a local phenomenon, the bond between concrete and reinforcement. Tension stiffening is very important for determining the structural response especially at service loads. With the increasing use of average stress strain approaches for characterising material properties (MCFT (Vecchio, 1986) & STMT (Hsu, 1988)) in FEM analysis, modelling tension stiffening behaviour has become essential for FEM analysis of FRP-RC elements. A direct tension test is the best way to study the influence of different parameters on tension stiffening. Fig. 7-2 below shows a schematic response of a direct tension test.

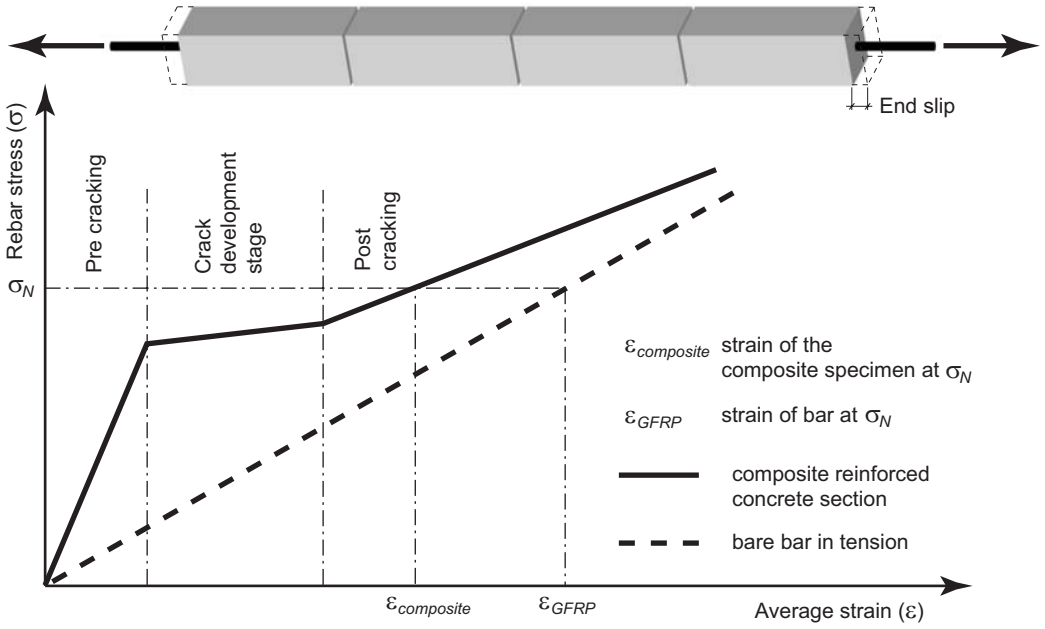

Figure 7-2: Schematic representation of tension stiffening behaviour of FRP reinforced concrete.

As shown in Fig. 7-2 there are three distinct gradients to tension response of reinforced concrete. Fig. 7-3 shows the strain distribution as derived by direct tension tests by Sooriyaarachchi (2005) of a tension member (similar to the one shown in Fig. 7-2) during the various stages of crack propagation. It is clear from the strain measurements that reinforced concrete composite action between cracks is lost after crack propagation. The figure shows the development of three cracks which take place between applied load of 37 and 53 KN. Fig.

7-4 shows the derived bond stress distribution from strain profiles between the first and second cracks. This shows degradation of bond at the crack face fairly early in the loading. Peak bond stresses which are close to the crack faces at the initial loading propagate towards the centre with increasing load confirming early bond deterioration near the crack section. This is contrary to what is expected from steel bars where in general it is assumed that once the bond reaches a certain maximum it maintains that value of strength and the peak value spreads away from the crack in an almost elasto-plastic manner.

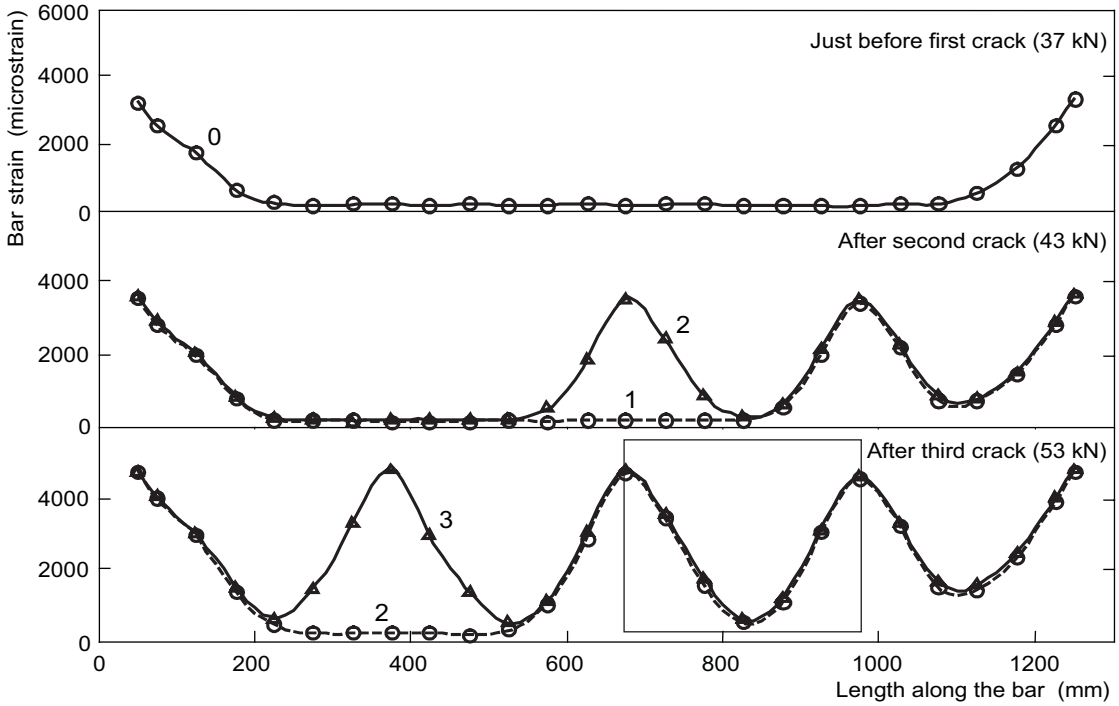

Figure 7-3: Strain patterns (0 – before 1st crack; 1 – after 1st crack; 2 – after 2nd crack; 3 – after 3rd crack)

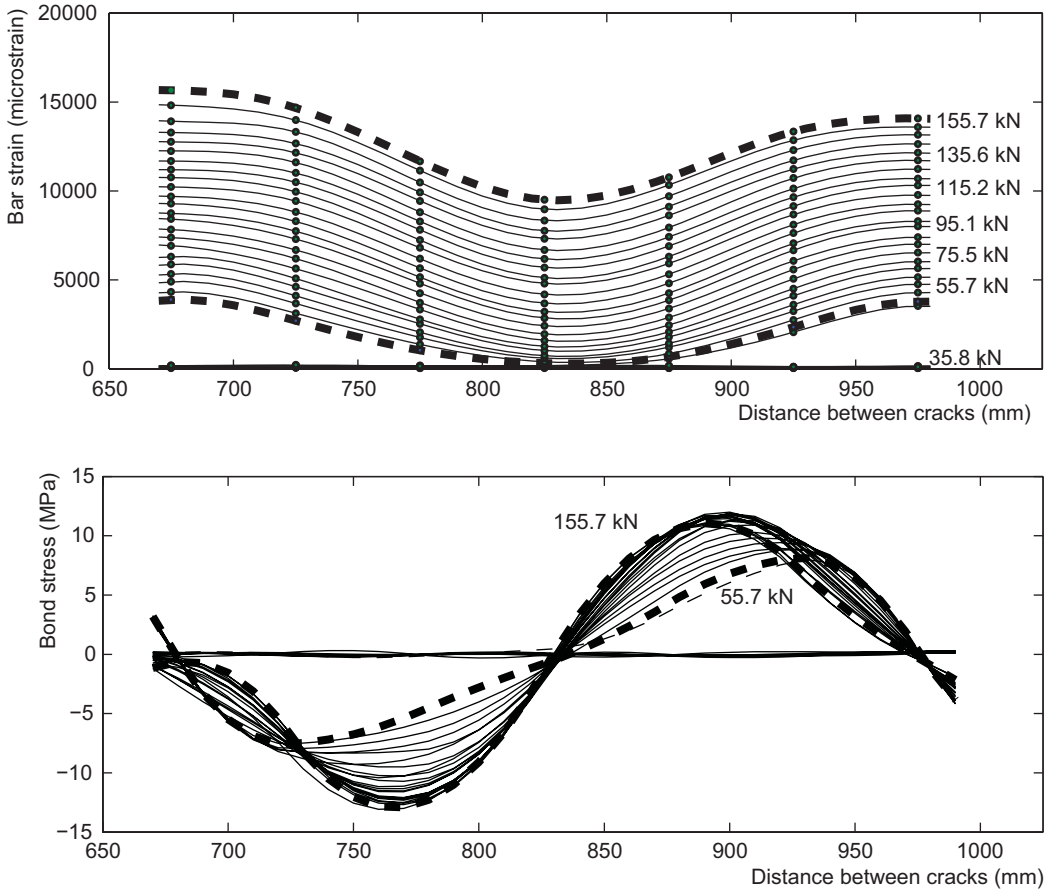

Figure 7-4: Typical strain distribution and bond stress distribution between cracks

7.2.2 Effect of various parameters on tension stiffening effect

Effects of reinforcement ratio, concrete strength and bar diameter were studied by Sooriyaarachchi (2005). The ASLAN 100 bar was used in the study.

7.2.2.1 Influence of reinforcement ratio

It is important to understand how the area of concrete around the bar contributes to the tension stiffening effect. Fig. 7-5 compares the tension stiffening effect of different reinforcement ratios tested. As the experimental work involved testing two grades of concrete, the results are plotted in separate graphs: Fig. 7-5(a) shows normal strength concrete (C50) whilst Fig. 7-5(b) shows high strength concrete (C90). It is clear from the figures that tension stiffening increases with a decrease in reinforcement ratio for the tested reinforcement ratios. For steel reinforcement above a certain reinforcement ratio (1%), the influence of reinforcement ratio on tension stiffening behaviour has been found to be less significant, and it is logical to assume this trend for FRP reinforcement.

7.2.2.2 Influence of concrete strength

Concrete strength can influence the tension stiffening behaviour in two different ways. Firstly, high strength concrete requires higher loads to crack the specimens. In addition, better

bond between concrete and reinforcement allows stresses to be transferred more effectively between the bar and concrete making the average stress contribution of concrete higher. Fig. 7-6 illustrates this effect by comparing different concrete strengths at constant reinforcement ratios.

7.2.2.3 Influence of bar size on tension stiffening behaviour

Bar size is another factor that can influence tension stiffening. However, in this experimental study no significant influence on tension stiffening was recorded for different bar sizes when results of the same reinforcement ratio are compared as shown in Fig. 7-7.

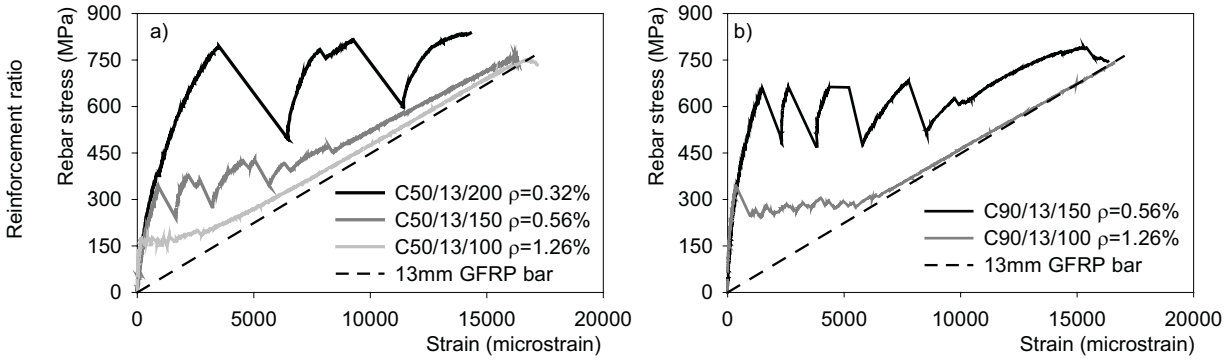

Figure 7-5: Influence of reinforcement ratio on the tension stiffening (a) C 50 (b) C90

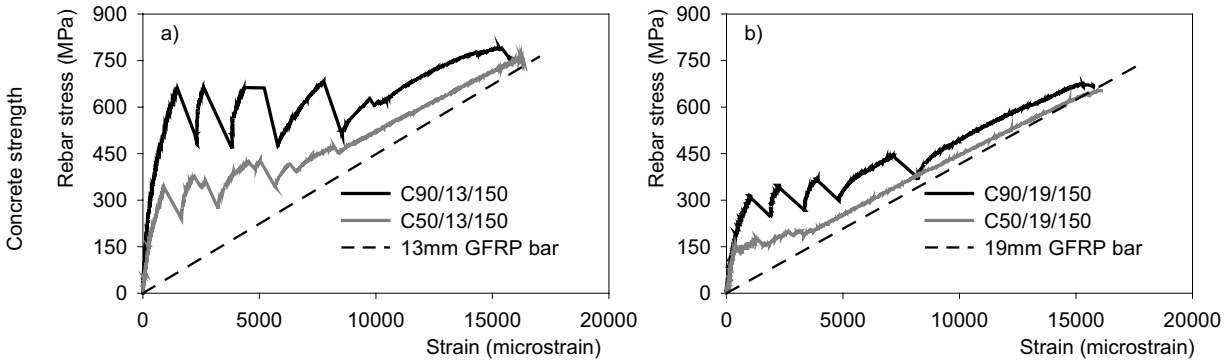

Figure 7-6: Influence of concrete strength on tension stiffening (a) 13 mm (b) 19 mm bar

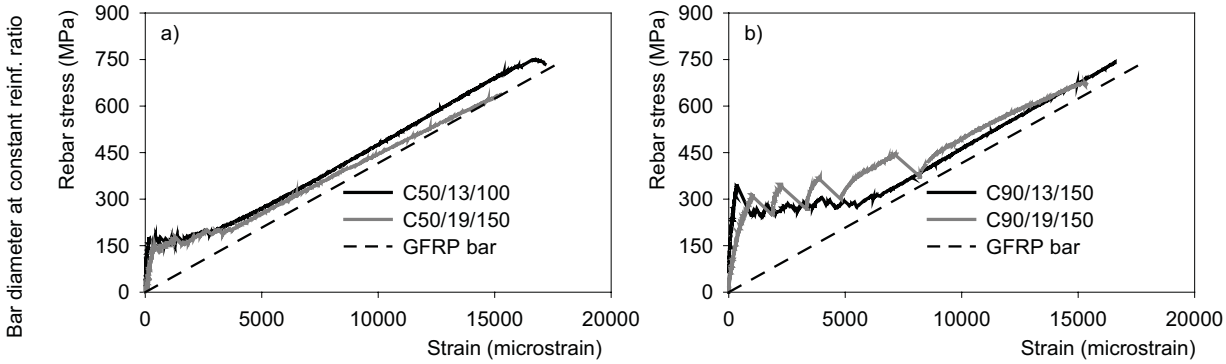

Figure 7-7: Influence of bar diameter on tension stiffening (a) C50 (b) C90 concrete (ρ =1.26%)

7.3 Meso – level modelling of bond

7.3.1 General

Pull out tests, tension tests and hinge beam tests can be considered as examples of experiments on meso-level bond modelling. Each method has its own advantages and disadvantages; however, it is very important to note that all of these tests with external measuring arrangements provide only an average bond stress slip relationship. Fig. 7-8(b) shows bond stress slip relationships determined at various points along the reinforcing bar between cracks recorded during direct tension tests (Sooriyaarachchi (2005)). These results have been derived by strain profiles established during tests conducted on specially manufactured GFRP bars with strain gauges placed at close intervals (50mm apart) near the center of the bar. Measured strain gauge readings were then approximated using cubic splines (series of third order polynomial functions) and were then used to derive the bond stress at various points of the bar. Results shown in Fig. 7-8 represent only half the specimen, from the centre to the crack. These results show clearly that local bond stresses are different from point to point and that there is no unique bond stress slip relationship that can describe the behaviour along the bar.

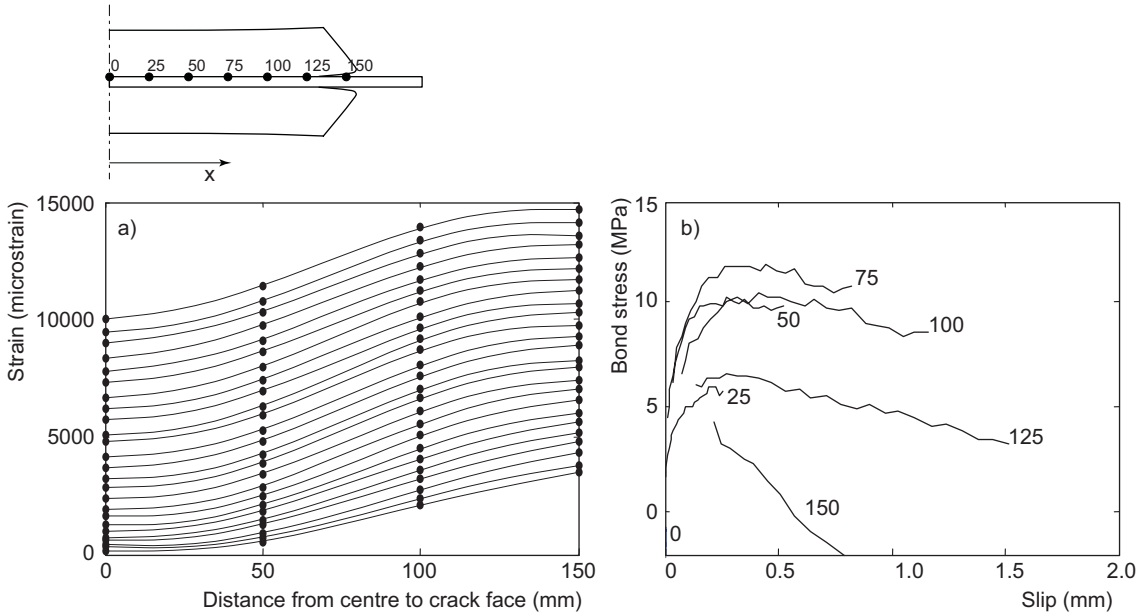

Figure 7-8: Strain profile and derived bond stress slip relationship at various locations along the bar (distances in fig. (b) are distances measured from the centre of a tension specimen)

7.3.2 Pull out test

Despite its inability to represent the concrete stress state in most practical situations, due to simplicity the pull-out test is the most widely used test for establishing meso level models. It is widely used to find average bond slip relationships for FRP with short embedment lengths using a procedure similar to steel reinforcement as reported in (CEB Bulletin, 1982). The pull-out test can also be used to study other important design issues like splitting of concrete. Fig. 7-9 shows a typical test arrangement used in pull out tests along with possible test results with different modes of failure.

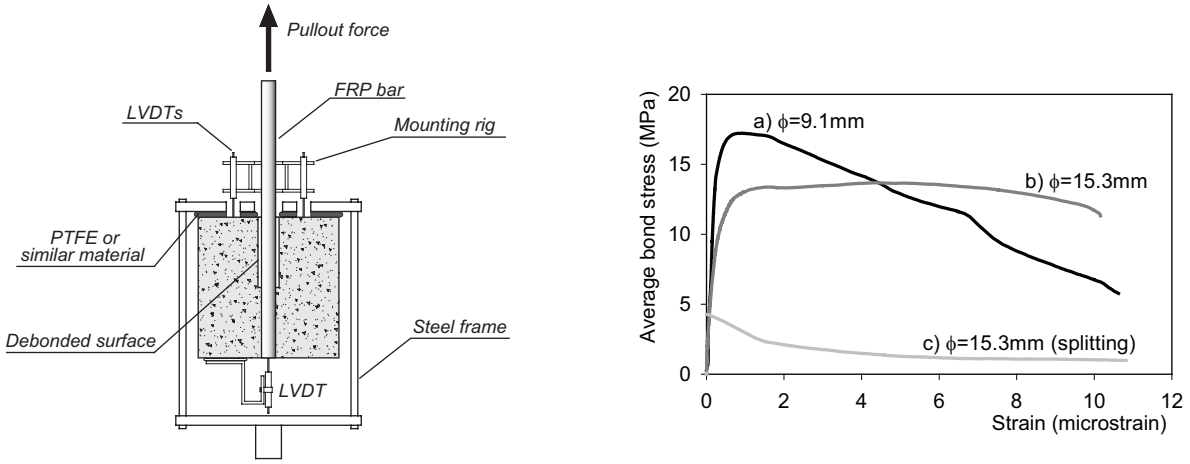

Figure 7-9: Testing arrangement and typical test results of a pull-out

Considering the pull out failure modes of FRP it is possible to categorize them into three different types as shown in fig. 7-9: a) sharp post peak loss without splitting failure, b) relatively mild post peak behavior, c) splitting failure. Splitting can again be divided into two main categories depending on the cover crack induced failure and failure by splitting off surrounding concrete as shown in Fig. 7-10.

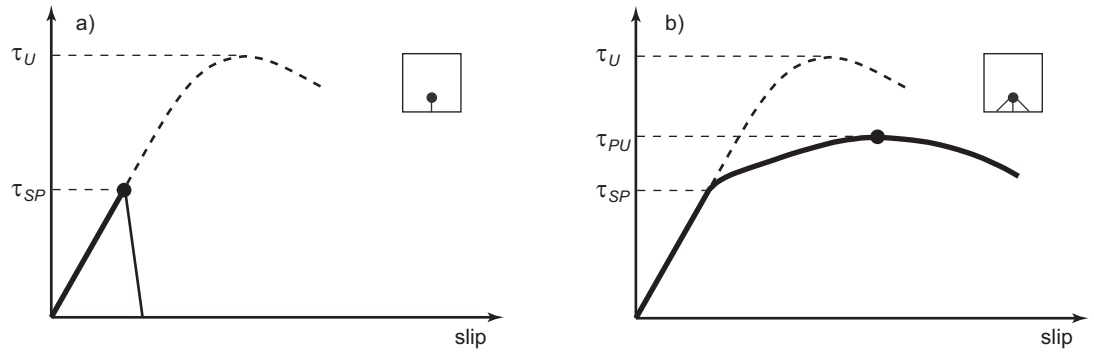

Figure 7-10: Different splitting failures: (a) Cover crack induced failure (b) Splitting off surrounding concrete

Chemical bond, surface roughness of reinforcement, concrete strength and reinforcement stiffness are the main influencing factors on bond behaviour. A comprehensive account of factors influencing bond behaviour can be found in fib Bulletin 10 (2000).

If sufficient resistance to splitting can be provided by the surrounding concrete, as for example in the case of short embedment lengths in pull-out cube tests, then the bond stress can reach the maximum average bond strength. Various mechanisms for the descending branch of the average stress strain relationships can be explained as follows.

Shearing off part of or all the surface deformations of the bar

The bond strength of FRP bars in this case is not controlled by the concrete strength, but appears to be governed either by the inter-laminar shear strength between successive layers of fibres or by the shear strength of bar surface deformations. Therefore, unlike steel bars, an increase in concrete strength will not be accompanied by a corresponding noticeable increase in the bond strength of the FRP bar. This type of bond failure can yield the highest possible bond resistance from a bar, but post peak response will be characterised by sudden loss of bond stresses as seen in curve ϕ=9.1mm of Fig. 7-9.

Concrete shear failure
With failure occurring in the concrete this mode of failure is similar to that of deformed steel bars. The concrete is crushed in front of the bar deformations and the bond strength is controlled mainly by the shear strength of concrete. In order to develop shear cracks penetrating into the concrete (micro crack), a lot of interlocking and bond need to be developed and it is unlikely that this would become a dominant mode of failure for FRP with low stiffness in the radial direction.

Squeeze through
The bar could "squeeze through" the concrete due to its low stiffness in the radial direction. Bond resistance is provided by friction through wedging of the bar surface deformations on the surrounding concrete. In this case, the bond is much more ductile and the maximum bond strength developed can be quite significant depending on the geometry of the bar deformations, the radial stiffness of the bar and the amount of concrete confinement provided.

Combined mode
Any combination of the above listed failure modes can be another possible mode of failure.

Figure 7-11, shows typical bond stress-slip characteristics obtained from pull-out tests on the following bars: 15 mm GFRP (Aslan bar-Hughes Brothers), 15 mm C-BAR, Hedlund and Rosinski (1997), 15 mm C-BAR, Karlsson (1997), 16 mm Swedish Ks400 and Ks600 steel bars, Berggren (1965), Tepfers (1973), 7 wire 12.5 mm steel strand Jokela and Tepfers (1982), CFCC (Carbon Fibre Composite Cable) 12.5 mm cable and an Arapree 2x20 mm strip, Tepfers, Molander & Thalenius (1992). The bonded lengths were in the range of 45 to 50 mm. The concrete compressive strengths for the specimens were in the range of 43-48 MPa. It can be seen from the figure, that at the beginning of loading, the GFRP bar appears to have a stiff behaviour. However, at increased loads, the GFRP bar shows considerable slip and ductility. The behaviour of the GFRP bar is similar to that of the Arapree strip at the early stages of loading. The GFRP bar specimen reached its ultimate bond strength at a slip of 4 mm. The bond strength level was similar to that of a CFCC strand. The C-BAR had the same bond stress-slip relation as the Ks600 steel bar in a pullout test with full concrete confinement, despite the fact that the steel bar had a higher relative rib area according to DIN 488 (0.13) than the C-BAR (0.08). The CFCC cable and the Arapree strip, shown in the figure as scatter bands from several tests, indicate a stiff initial response but their stiffness reduces substantially after initial slip.

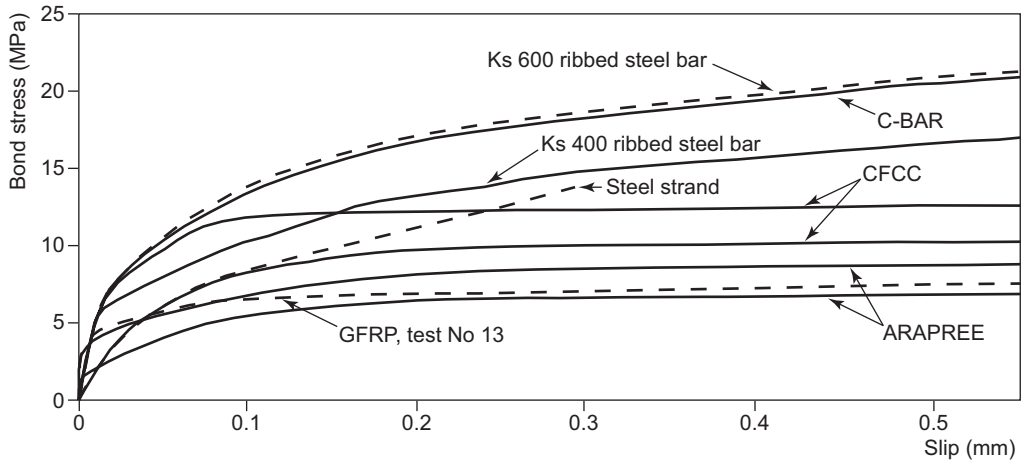

Figure 7-11: Bond stress-slip relation for different reinforcing materials

7.4 Splitting resistance of surrounding concrete

Though the bond of deformed FRP bars in confined conditions is in general good, or as good as for steel bars, concrete cover should be designed not only having durability considerations in mind, but also the splitting resistance of concrete. A full description of the theory and testing for splitting resistance is given in Annex A. The main conclusion is that the stiffness of the FRP bar may influence the splitting resistance of concrete by changing the angle "α" of the diagonal reaction force.

7.5 Analytical modelling

Analytical models of bond-slip are essential for the determination of structural performance of FRP reinforced concrete structures by means of numerical analysis. Although many experimental programs have been carried out examining the bond characteristics of FRP bars, very little work has been published on analytical modelling. In the following, a review of these works is reported.

7.5.1 Local bond modelling

Malvar (1994) proposed a refined model of the overall bond behaviour depending on two empirical constants. These constants are to be determined by curve-fitting experimental τ-s curves. Malvar's model is represented by the following relationship:

$$\frac{\tau}{\tau_m} = \frac{F \cdot (s / s_m) + (G-1) \cdot (s / s_m)^2}{1 + (F-2) \cdot (s / s_m) + G \cdot (s / s_m)^2} \tag{7-1}$$

where: τ_m and s_m are the peak bond stress and relative slip at peak bond stress;
F and G are the empirical constants depending on the type of FRP bars.

For Type 'A' bars (with an external helicoidal tow providing both a protruding deformation and a small indentation of the bar surface) constants F and G should take values of 11 and 1.2, respectively.

For Type 'D' bars (with surface deformations given by over moulding) constants F and G should take values of 13 and 0.5, respectively.

Rosetti, Galeota & Giammatteo (1995) and Cosenza, Manfredi & Realfonzo (1995) have successfully applied the well-known model for deformed steel rebars by Eligehausen, Popov & Bertero (1983) (B.P.E. model) to FRP rebars. The ascending branch of this bond-slip ($s \le s_m$) relationship is given by:

$$\frac{\tau}{\tau_m} = \left(\frac{s}{s_m} \right)^{\alpha} \tag{7-2}$$

where α is an experimental parameter less than 1 (α = 0.40 in case of steel reinforcements).

Furthermore, Eligehausen et al. (1983) proposed a model defined by the following:

- a second branch of constant bond ($\tau = \tau_m$) up to a slip $s = s_2$

- linearly descending branch from (s_2, τ_m) to (s_3, τ_3)
- a horizontal branch for $s > s_3$, with a value of τ due to the development of friction ($\tau = \tau_3$).

Values of s_2, s_3 and τ_3 have to be calibrated on the basis of experimental results. Cosenza, Manfredi and Realfonzo (1995) proposed a modified version of this model (called "double branch model") in order to model FRP-concrete bond (Fig. 7-12). In fact, by comparing experimental and analytical curves using the original B.P.E. model the authors found there was no second branch ($s_m<s<s_u$) in case of FRP rebars. The ascending branch is the same as in the original model, while the softening branch is defined by the following equation:

$$\frac{\tau}{\tau_m} = 1 - \frac{p(s - s_m)}{s_m} \tag{7-3}$$

where τ_m and s_m are shown in Fig. 7-12
α and p are parameters based on available experimental data.

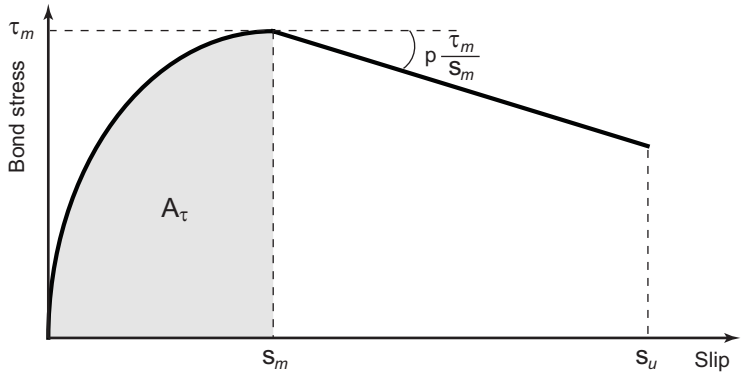

Figure 7-12: Modified B.E.P. constitutive law [Cosenza, Manfredi & Realfonzo (1995)]

The value of the parameter α, which determines the ascending branch, is derived by equating the area A_τ under the ascending branch of the experimental curve equal to the area corresponding to the analytical curve:

$$A_\tau = \frac{\tau_m s_m}{(1+\alpha)} \tag{7-4}$$

The value 'p', which determines the descending branch, is evaluated by a similar philosophy for the area underneath the experimental and analytical curves within the softening range. Cosenza, Manfredi & Realfonzo (1995**)** proposed a constitutive law to model the first branch of the τ-s curve (C.M.R. model):

$$\frac{\tau}{\tau_m} = \left(1 - e^{-s/s_r}\right)^\beta \tag{7-5}$$

in which s_r and β are parameters based on curve-fitting of experimental data.

In an investigation conducted by Cosenza, Manfredi and Realfonzo (1995, 1996a, 1996b), the Malvar model, the modified B.P.E. model and the C.M.R. model were compared against experimental results gathered from various research projects.

The analysis of the experimental data has shown that:

- The bond performance of FRP bars depends on the characteristics of the outer surface and, for the same type of surface, depends on the manufacturing process;

- It is generally possible to obtain bond strengths for FRP bars of similar or greater magnitude than for steel;

- Indented and grain covered bars seem to provide the best results in terms of bond strength.

7.6 Design rules and existing recommendations

For bond of FRP reinforcement in concrete elements some code proposals have been recently formulated in several national codes of practice:

7.6.1 Canadian Standards Association Recommendation, CSA

CAN/CSA-S806-02 (May 2002).

This standard covers requirements for the determination of engineering properties and design of building components reinforced with FRP bars, tendons, etc.

Definitions

Development length: length of embedded reinforcement required for developing the design strength of reinforcement.

Embedment length: length of embedded reinforcement provided beyond a critical section.

Only CFRP and AFRP reinforcing bars and grids are covered by this code. GFRP reinforcement is permitted as reinforcement in non-structural components only (partition walls, claddings, slabs-on-ground, and linings of floors and walls).

7.6.2 Canadian Highway Bridge Design Code, CHBDC

CAN/CSA-S6-00, Section 16, Fibre Reinforced Structures, (December 2000).

CFRP and AFRP are permitted as pre-tensioned, post-tensioned and primary reinforcement.

GFRP is permitted as post-tensioned reinforcement, when the grout is non-alkaline nor cement based.

For FRP bars and grids, the minimum concrete cover shall be 25 mm.

For an FRP tendon, the clear concrete cover shall be 40 mm, but not less than the equivalent diameter of the tendon.

Anchors for aramid fibre ropes and FRP tendons in concrete shall be of suitably durable materials, such as stainless steel and certain FRPs.

The maximum stress in FRP bars under loads at SLS shall not exceed $F_{SLS}\, f_{fu}$, where f_{fu} is the tensile strength of the FRP bar. The factor 'F_{SLS}' is given in Table 7-1.

Table 7-1: Values of factor 'FSLS'

AFRP	0.35
CFRP	0.65
GFRP	0.25

Development length l_d of FRP bars in tension shall be:

$$l_d = 0.45 \frac{k_1 k_4}{d_{cs} + K_{tr} \dfrac{E_f}{E_s}} \frac{f_{fu}}{f_{cr}} A \qquad (7\text{-}6)$$

where:

k_1 is the bar location factor;

k_4 is the bar surface factor, being the ratio of the bond strength of the FRP bar to that of an equivalent ordinary steel deformed bar, but not greater than 1;

d_{cs} is the smallest of the distance from the closest concrete surface to the centre of the bar being developed, or two-thirds of the centre-to-centre spacing of the bars being developed, in mm;

K_{tr} is the transverse reinforcement index (specified in Clause 8.15.2.2), in mm;

For FRP grids in which the intersecting orthogonal bars are fully anchored, the development length shall be such as to include at least two transverse bars of the grid lying perpendicular to the direction of the force under consideration.

Capacity of anchors shall be designed such that the FRP tendon can develop 90% of its specified tensile strength.

The end zones of pre-tensioned concrete components shall be reinforced against splitting, unless it can be demonstrated that such reinforcement is not necessary.

7.6.3 Japan Society for Civil Engineering (JSCE recommendation)

The JSCE code on concrete structures with continuous fibre reinforcement which was published in September 1997 deals with bond in the following manner.

Basic development length

As a rule, basic development length of continuous fibre tension reinforcement is to be obtained by appropriate experiment.

The basic development length of an FRP bar may be calculated from equation 7-7 when reinforcement with bond splitting type of failure is expected, but it can not be less than 20d, d being the diameter of the bar.

$$l_d = \alpha_1 \left[f_{fd} / \left(4 f_{bod} \right) \right] d > 20d \qquad (7\text{-}7)$$

where:

α_1 1.0 (for $k_c \leq 1.0$);
0.9 (for $1.0 < k_c \leq 1.5$);
0.8 (for $1.5 < k_c \leq 2.0$);
0.7 (for $2.0 < k_c \leq 2.5$);
0.6 (for $2.5 < k_c$);

$k_c = c / d + (15 \times A_t) / [(s \times d) \times (E_t/E_o)]$;

The design bond strength of concrete is given by:

$$f_{bod} = \alpha_2 \left(0.28 f_{ck}^{2/3} / \gamma_c\right) < 3.2\ N/mm^2 \quad (7\text{-}8)$$

where

γ_c =1.3 when f_{ck} <50 N/mm^2 and γ_c =1.5 in all other cases;

α_2 is:

- equal to 1 when the bond strength of FRP bars is equivalent or greater than the bond strength of deformed steel bars;
- less than 1 when the bond strength is lower than the bond strength of steel bars.

When reinforcement is placed within the top 30 cm of concreting and in a direction with an angle less than 45^o to the horizontal direction, the basic development length shall be 1.3 times l_d obtained by equation 7-7.

The basic development length for compression FRP reinforcement may be taken as 0.8 times l_d obtained following all the previous provisions.

General considerations

Development length for continuous fibre reinforcement depends on the kind of reinforcement, concrete strength, concrete cover and transverse reinforcement. Experiments need to be conducted considering this fact. In order to obtain the development length experimentally, it is preferable to adopt tests with which the actual bond characteristics in members is reflected such as the tests with beam specimens or lap splices.

"Test Method for Bond Strength of Continuous Fibre Reinforcing Materials by Pull-Out Testing (JSCE-E 53)" does not reflect bond characteristics in actual members, and thus overestimates bond strength. It should be avoided to calculate the basic development length by using the bond strength f_{bod} obtained by this method.

Based on mechanics – equilibrium of forces, the embedded length for a straight bar can be written as in equation 7-9 and the bond stress as in equation 7-10.

$$l_o \pi d f_{bod} = \frac{\pi d^2}{4} f_y \quad (7\text{-}9)$$

$$f_{bod} = \frac{d}{4} \frac{f_y}{l_0} \quad (7\text{-}10)$$

The development length for steel reinforcement with transverse reinforcement is recommended by JSCE (1997) to be (equation 7-11):

$$l_0 = \frac{\left(\frac{f_y}{1.25\sqrt{f'_{cd}}} - 13.3\right)d}{0.318 + 0.795\left(\frac{c}{d} + \frac{15A_t}{sd}\right)} \tag{7-11}$$

The bond stress of an FRP straight bar can be then calculated by substituting equation 7-11 in equation 7-10, allowing for the modular ratio E_t/E_o (E_t=E_f and E_o=E_s) (equation 7-12):

$$f_{bod} = \frac{0.318 + 0.795\left(\frac{c}{d} + \frac{15A_t}{sd}\frac{E_t}{E_o}\right)}{\frac{1}{3.2\sqrt{f'_{cd}}} - \frac{53.2}{f_y}} \tag{7-12}$$

For continuous fibre reinforcement with deformation on its surface which fails by bond splitting, the experimental bond strength is compared with that calculated by equation 7-12 in Figure 7-13.

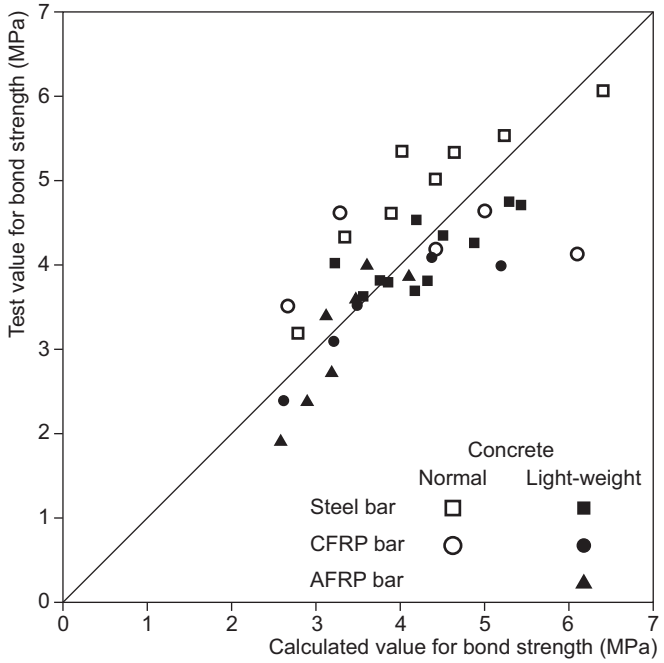

Figure 7-13: Comparison of bond strength (eq. 7-12) with test results, JSCE (1997)

Fig 7-13 indicates that equation 7-12 may be used for the cases of continuous fibre reinforcement with bond splitting failure. However, continuous fibre reinforcement with deformations which cause bond splitting failure may possess bond strength less than that of a steel deformed bar. For this type of reinforcement the modification factor α_2 ($\leq$ 1.0) needs to be multiplied for calculating bond strength by equation 7-8. The value of α_2 is generally obtained by experiment since there is not sufficient data at present.

For the reinforcement whose bond failure is of the 'pull-out' type, basic development length needs to be obtained and verified experimentally.

The term of $15\times A_t/(s\times d)$ represents the effect of transverse reinforcement. The smaller the Young's modulus is, the less effect on the bond splitting strength is.

7.6.4 American Concrete Institute design recommendations

(ACI Committee 440 - 2006)

The design of structural concrete utilising Fibre Reinforced Plastic (FRP) bars is presented as an extension of the current ACI code requirements for steel reinforced structures (ACI 318-05). Thus the proposed code requirements are analogous to current provisions but appropriate changes to accommodate the differences in the algorithms and the structural behaviour between the FRP and the steel reinforced elements are presented.

Development and splices of (non-prestressing) reinforcement

The basic development length l_d for FRP bars in tension can be obtained by:

$$l_d = \frac{\alpha \dfrac{\tau}{0.083\sqrt{f_c}} - 340}{13.6 + \dfrac{c}{d}} d \qquad \text{(SI)} \qquad (7\text{-}13)$$

where:
τ – bond stress to be developed
c - spacing or cover dimension
α – top bar modification factor
$\alpha = 1.4$ horizontal reinforcement so placed that more than 300mm of fresh concrete is cast in the member below the development length or splice
$\alpha = 1.0$ other reinforcement

Comments

The factor α accounts for the position of the reinforcement in freshly placed concrete. The value of 1.4 is based on research results.

The concrete cover has a significant effect on the type of the failure mechanisms. If the cover c is less or equal to the diameter d, a splitting failure may occur. If c is larger than d, a pull-out failure may occur.

Experimental tests have indicated that the value of the ratio of the evaluated bond strength in the specimens with concrete cover of between d and 2d varied between 1.2 and 1.5 (1.5 is a more conservative value).

8 Design philosophy

8.1 Introduction

The successful replacement of conventional steel with FRP as concrete reinforcement requires the examination of many design aspects and likely modes of failure. The previous sections deal with the various modes of failure or fracture expected from the elements made of FRP RC and present predictive models. However, it is also necessary to assess if the conventional approach to RC design is still fully valid. This chapter is an outline of Annex B, which investigates the design philosophy of existing design guidelines and deals with a new design philosophy framework.

8.2 Examination of philosophy of existing guidelines

Design guidelines and state-of-the-art reports for FRP RC structures have been published in Japan [JMC (1995), JSCE (1997)], Canada [CAN/CSA (1996), ISIS (2001), CSA-S806 (2002)], USA [ACI 440-96 (1996), ACI 440-98 (1998), ACI440.1R-01 (2001), ACI440.1R-03 (2003), ACI440.1R-06 (2006)], and Europe [Clarke et al. (1996), Thorenfeldt (1998)]. The design recommendations in these documents are mainly provided in the form of modifications to existing steel RC codes of practice, which are predominantly using the limit state design approach. The modifications consist of basic principles, which are heavily influenced by the unconventional mechanical properties of FRP reinforcement, and empirical equations that are based on experimental work on FRP RC elements. The brittle linear-elastic behaviour of FRP reinforcement is an influencing factor behind all of the existing design guidelines.

An approach for developing design guidelines such as the one described above, may seem reasonable, but may not be entirely appropriate. The rationale behind this statement is that steel RC codes of practice assume that the predominant failure mode is always ductile due to yielding of the flexural reinforcement. However, this is not the case for the above FRP RC design guidelines, which assume that brittle flexural failure would be sustained due to either concrete crushing or rupture of the FRP reinforcement. In addition, existing codes of practice have fundamental structural safety uncertainties (see Annex B), which in conjunction with the change in the type of failure and other design issues relevant to FRP RC, have major implications for the structural design and safety of FRP RC elements [Neocleous et al. (2005)].

One of the structural safety uncertainties of steel RC codes of practice is the lack of published records about the methods and data used by code committees to calculate the material partial safety factors [Neocleous et al. (2004)]. It is also not known whether the application of the partial safety factors would lead to notional structural reliability levels (P_f) that attain the target level adopted by codes of practice. Another uncertainty arises if the actual resistance-capacity of the predominant failure mode is higher than the unfactored value, as codes of practice do not provide any information about the failure mode that will actually occur first (i.e. flexural yielding, flexural concrete crushing or shear) and at which load level. One possible way of tackling this problem is through the concept of resistance-capacity margins (RCMs), which determines the capacity margin between any two failure modes. RCM may be represented as the ratio of the mean resistance-capacities predicted for each failure mode (equation 8-1).

$$RCM_{failure\ (ii)-failure\ (i)} = \frac{\mu_{failure\text{-mode}\ (ii)}}{\mu_{failure\text{-mode}\ (i)}} \tag{8-1}$$

In addition to the above uncertainties, there are design and safety philosophy issues that are directly related to FRP RC elements (see Annex B). Examination of the design and safety philosophy of the IStructE (1999) guideline led to the following findings [Neocleous (1999), Pilakoutas et al. (2002)].

- Concrete crushing is the most probable type of flexural failure because the ultimate tensile strength of FRP reinforcement is rarely attained in normal-strength concrete sections.
- The use of partial safety factors for longitudinal reinforcement ($\gamma_{f,L}$) may not be essential for the flexural design of FRP RC beams, if the type of flexural failure intended at design is concrete crushing.
- The assumption that the application of a specific value of $\gamma_{f,L}$ would always lead to the desired type of flexural failure is not valid for all design configurations. This is especially true for large values of $\gamma_{f,L}$.
- The notional structural reliability of FRP RC elements is variable due to the effect of design parameters, such as the ratio of permanent to variable load, concrete compressive strength and ratio of longitudinal reinforcement.
- The effect of the above parameters on the notional structural reliability is influenced by the type of failure for which the flexural design is performed.
- The ratio of permanent to variable load has the greatest effect on the notional structural reliability.
- Capacity margins between the flexural and shear failure mode are not uniform.

Additional design issues that require further investigation, arise when considering the long-term behaviour of FRP RC elements. The application of multiple strength-reduction factors that are indented to account for the long-term effects of FRP reinforcement may not lead to the mode of failure aimed at the short-term design or may lead to uneconomical designs. It is therefore essential to develop appropriate design provisions that take into account the long-term behaviour of FRP reinforcement. One possible solution is to use the short-term properties for the limit state design and, subsequently, to verify that (at specific time intervals), the applied stress is less than the design strength of FRP that is available at the specific time interval.

8.3 Design philosophy: background to a refined approach

In view of the above findings, the design of FRP RC elements is based on the level 1 approach of structural reliability theory with the main aims being the attainment of a desired failure-mode-hierarchy and the satisfaction of the target reliability levels [Neocleous et al. (2005)]. This design philosophy is implemented through a framework (Figure 8-1), which may form part of the overall code development process presented by Nowak and Lind (1995). The design philosophy discussed here is elaborated in Annex B; and its application is demonstrated for FRP RC beams.

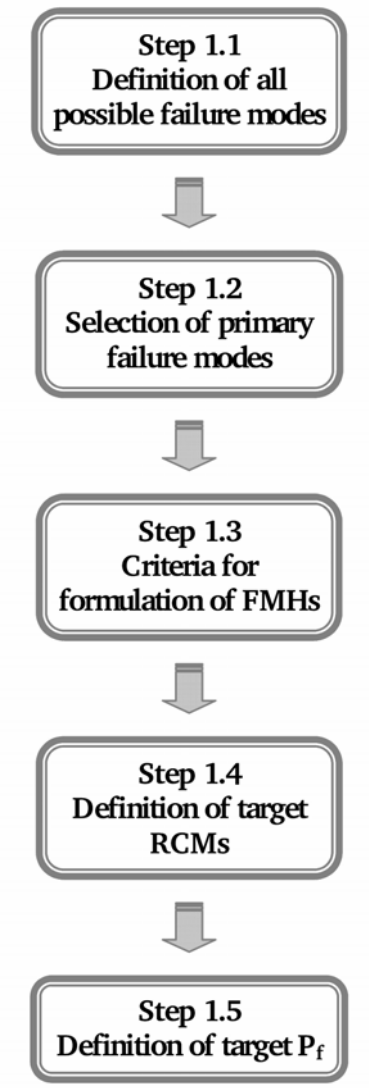

Figure 8-1: Application of possible philosophy for FRP RC [Neocleous et al. (2005]

The elaborated framework, if adopted by codes of practice, could enable the determination of appropriate partial safety factors for FRP reinforcement, as illustrated in Figure 8-2 [Neocleous et al. (2005)].

The validity of this framework is demonstrated in Annex B for concrete beams reinforced with carbon and glass FRP reinforcement (both longitudinal and transverse). Possible failure modes for FPR RC beams were initially defined and the primary failure modes (i.e. flexural concrete crushing and shear) were then identified and classified according to their seriousness in order to formulate the desired failure-mode-hierarchy. The flexural concrete crushing was selected as the predominant failure mode for design purposes. Appropriate partial safety factors were then determined by carrying out structural reliability analyses and cost optimisation. Although, the value of partial safety factor for longitudinal reinforcement does not influence the P_f for flexural concrete crushing, to be conservative, it was decided to select the lowest partial safety factors examined (1.15 and 1.3 for carbon and glass FRP, respectively). The partial safety factors for the transverse FRP reinforcement were selected on the basis of the cost optimisation (see Annex B). The selected partial factors were used for the limit state design and structural reliability of two FPR RC beams that were tested experimentally and failed due to concrete crushing.

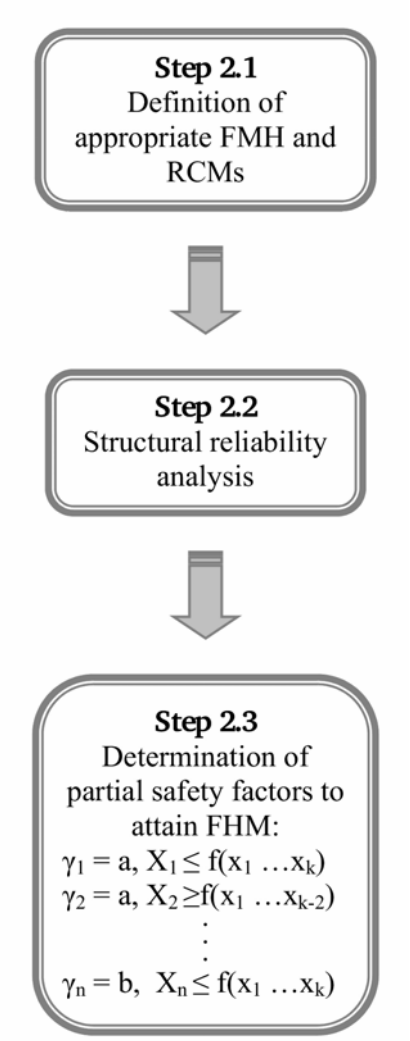

Figure 8-2: Application of possible design philosophy for FRP RC [Neocleous et al. (2005)]

The implications of the design philosophy introduced here for code developers and manufacturers are quite significant. A comprehensive application of this design philosophy would require the analysis of a greater amount of failure modes and, hence, it is necessary that reliable resistance-capacity prediction models are developed for each failure mode under consideration. Furthermore, the concept of the failure-mode-hierarchy would minimise the necessity of developing additional design guidelines and codes of practice each time a construction innovation becomes available.

Since innovation in the field of FRP reinforcement is expected to continue, it is believed that the values of the partial safety factor of FRP reinforcement (adopted for each failure-mode-hierarchy) should be provided by the FRP manufacturers according to the framework discussed above and be subjected to appropriate independent verification. The manufacturers should provide the code developers with material characteristics and any information that is essential for the development of any failure-mode-hierarchy.

A Splitting resistance of concrete

A.1 Introduction

This annex deals with the description of the theory and testing for splitting resistance of the surrounding concrete and is related to bond modelling as discussed in Chapter 7.

A.2 General

In most structures bars have limited confinement by concrete side covers of about 20 to 50mm. For these bars bond failure happens as a splitting of the concrete cover. The less confined bars are surrounded by two concrete covers c_x and c_y in the corners of a cross-section, Fig.A-1. These corner bars should form the basis for estimating values for splitting of concrete. Splitting of concrete around the FRP is mainly due to redial stresses induced by bond action exceeding the tensile strength of concrete as other micro crack generating mechanisms are less pronounced in FRP reinforced concrete. Avoiding splitting failure is essential for continuation of structural performance of the member.

In order to predict the capacity of a short anchorage, and to describe the pattern of the splitting cracks and the hoop action in the concrete cover, the so called "hydraulic-pressure analogy" (Fig. A-1) has been introduced since mid seventies by Tepfers (1973 and 1979).

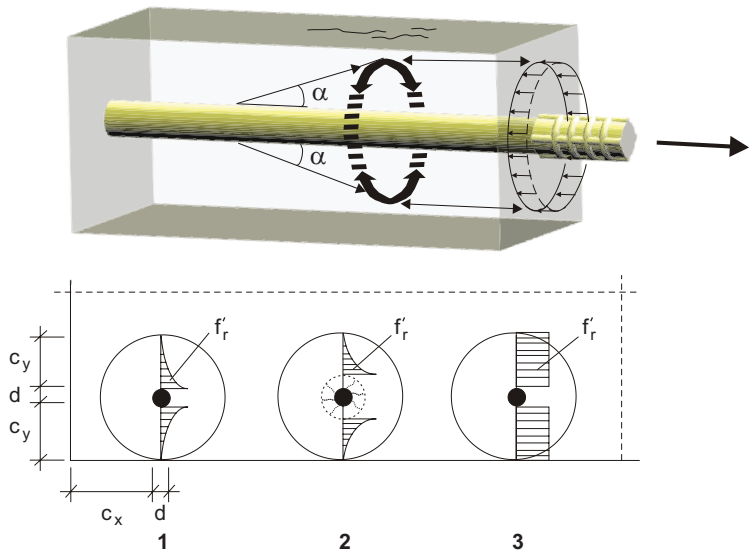

Figure A-1: Tensile stress distributions in 1 elastic, 2 partly cracked elastic and 3 plastic stage

Figure A-2 shows the relation between bond stress, τ, at cover cracking along the bar, and concrete tensile stress, f_{ct}, as a function of concrete cover thickness, c_y, normalised with respect to the bar diameter, d. Tepfers (1973, 1979) developed predictive equations for τ at the elastic stage, partly cracked elastic stage and plastic stage for the reaction force at an angle $\alpha = 45^o$, as illustrated in Figure A-2. Results from tests with Swedish Ks600 steel bars and C-BARs, fall between the partly cracked elastic and plastic stages, Karlsson (1997). However, the C-BAR results are closer to the plastic stage. Results from tests by Hedlund and Rosinski (1997) on the GFRP bar are grouped above the line that corresponds to the plastic stage. However, good agreement is achieved if, for the plastic stage, the angle α is reduced to 30^o, as shown by the dotted line. Therefore, it may be concluded that these particular GFRP bars with

a sand coated surface exert a lower lateral splitting pressure against the surrounding concrete than the bars with large surface deformations.

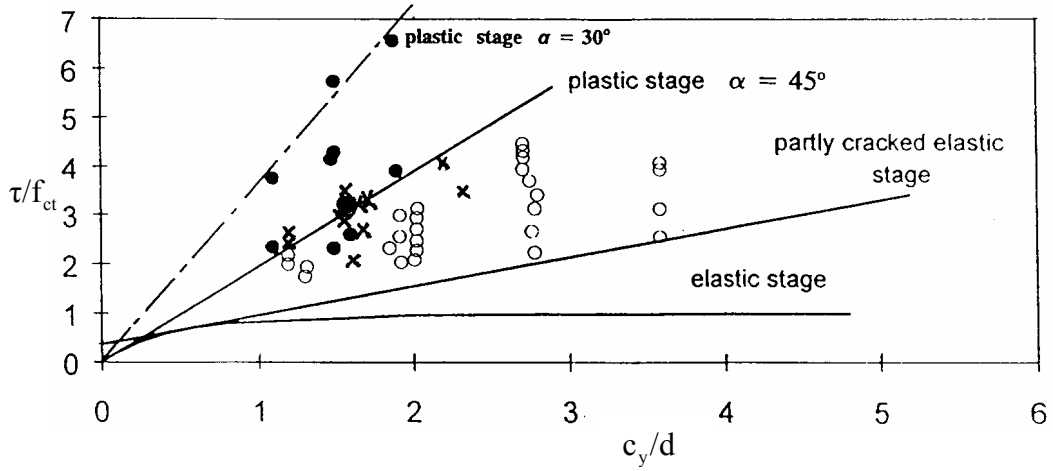

Figure A-2: Effect of thickness of concrete cover upon bond capacity of pull-out specimens on occurrence of concrete cover cracking along the bar. Open circles Ks600 steel reinforcing bars, closed circles GFRP bars (Hughes Brothers) and cross marks C-BARs,Tepfers (1997)

In elastic stage:

$$\frac{\tau}{f_{ct}} = \frac{1}{\tan\alpha}\frac{\left[\left(c_y+\frac{d}{2}\right)^2-\left(\frac{d}{2}\right)^2\right]}{\left[\left(c_y+\frac{d}{2}\right)^2+\left(\frac{d}{2}\right)^2\right]}; \qquad \text{(A-1)}$$

In partly cracked elastic stage:

$$\frac{\tau}{f_{ct}} = \frac{\left[\left(c_y+\frac{d}{2}\right)\right]}{\left[1.664\, d\ \tan\alpha\right]}; \qquad \text{(A-2)}$$

In plastic stage:

$$\frac{\tau}{f_{ct}} = \frac{2c_y}{d\ \tan\alpha}; \qquad \text{(A-3)}$$

A.3 Tests on splitting resistance of concrete

Eccentric pull out tests, ring pull out tests or splice tests can be used to investigate the splitting resistance of concrete.

A.3.1 Pull out test with eccentrically placed bars

The concrete cover splitting resistance along the bar can be studied in a pull-out test with eccentric placement of bar. Figure A-3 shows bond stress-free bar end slip relations for the

specimens. Strain gauges should be used to monitor the appearance of the cover crack. In very strong concretes the non-linearity of stress in the cover is not so pronounced and the elastic stress configuration results in earlier cover cracking. If the bar is very hard compared to concrete, stresses from concrete shrinkage may add to the bond ring stresses. Also differences in thermal elongation between concrete and FRP bar in its radial direction may give rise to extra stresses. This test is not so well fitted to study the final splitting off of the surrounding concrete, because the support friction doesn't produce the ideal combination of stresses for splitting concrete in a practical situation. Benchmark results obtained from pull-out tests with ordinary deformed steel reinforcing bar of corresponding diameter should be used for comparison.

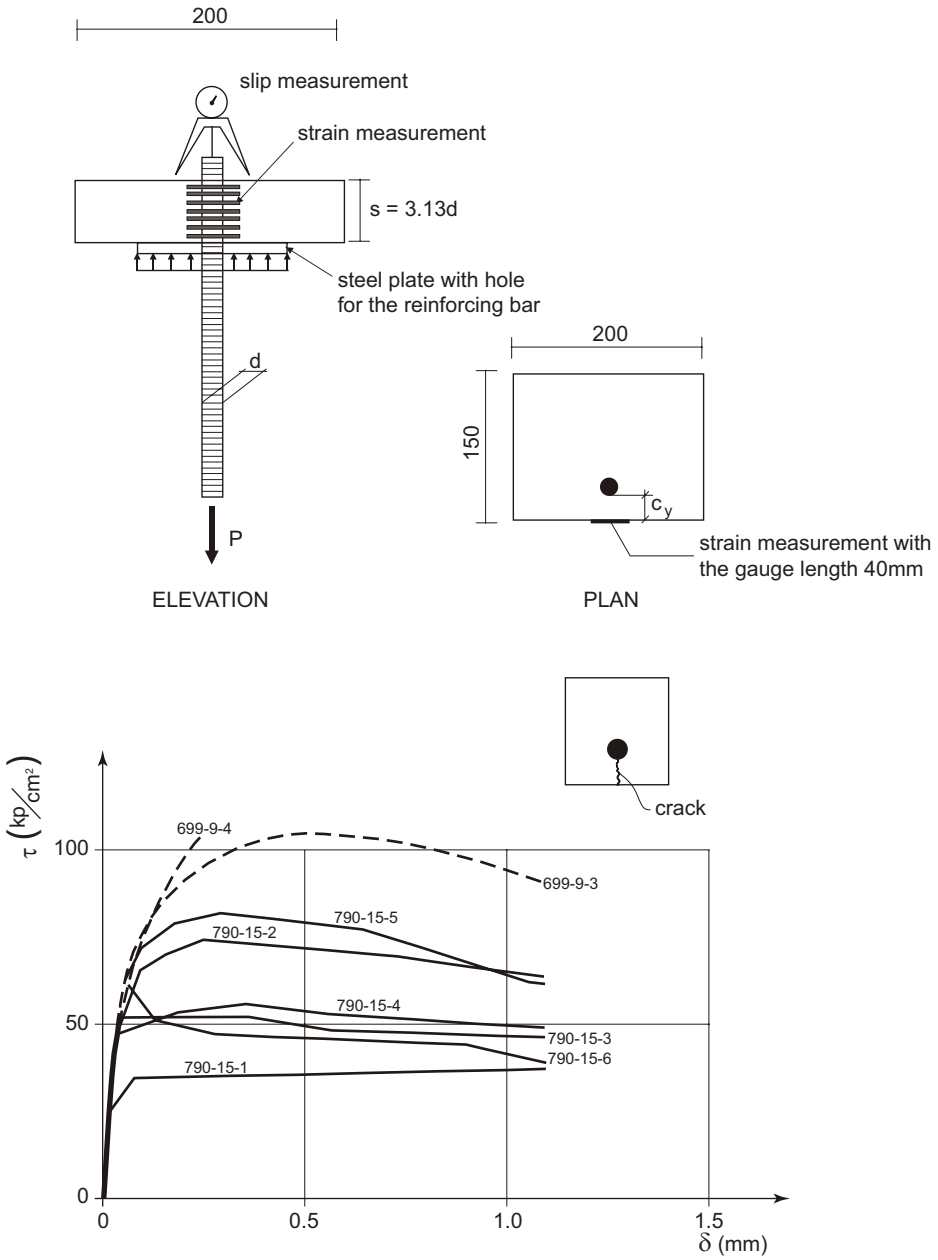

Figure A-3: Bond stress-free bar end slip for pullout specimens with eccentric bar placement. The bond stress levels for cracking of the concrete cover along the bar are marked in the diagram for the specimens, Tepfers (1993).

A.3.2 Ring pull out test

The Ring pull-out test in Fig.A-4, is a more sophisticated test, which enables to determine the splitting tendency of a bar in a direct way. With the "Ring pull-out test", Tepfers & Olsson (1992), the angle α of the bond forces in different stages of load can be estimated. The splitting tendency of the bar/rod increases, when the angle α increases. The ring pull-out test is a small cylindrical concrete body with axially placed bar. The bond length is 3 bar diameters and the height of the concrete cylinder is equal to the bond length. A thin steel cylindrical shell surrounds the concrete cylinder. At loading the radial and longitudinal bond force components are separated by a ring support with several teflon sheet layers, which prevents radial forces to be taken by the support. The circumferential strain of the steel cylinder caused by the radial bond stress components is measured with strain gauges. The bond stress component relation determines the angle α, which may change and increase when load increases. The measured free bar end slip and ring strains are shown in Fig. A-5.

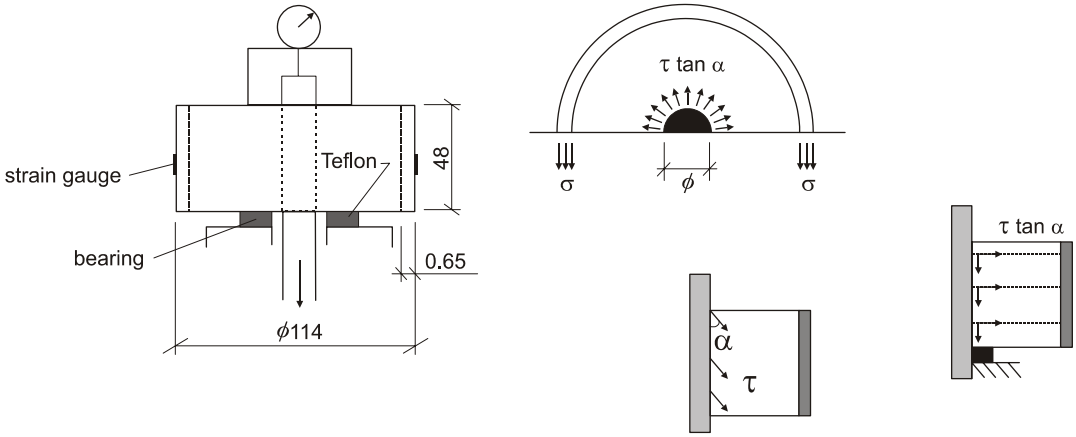

Figure A-4: Ring test for estimation of splitting tendency of reinforcing bars.

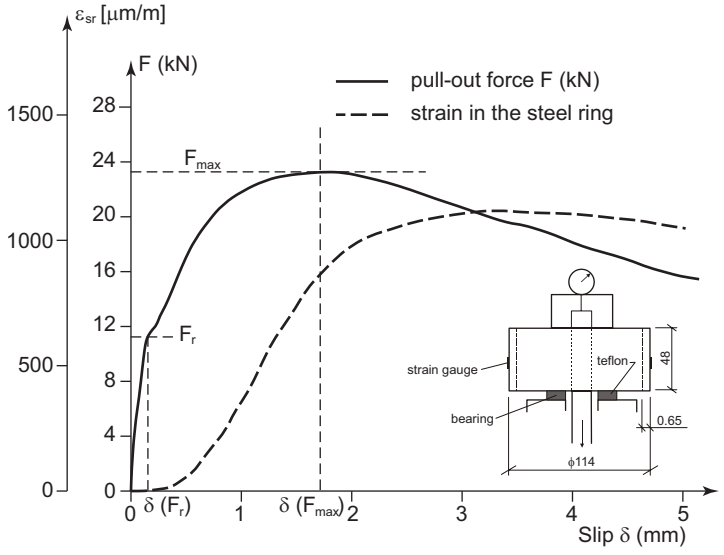

Figure A-5: Bond stress – free bar end slip and steel ring strain – slip relations for Ring test.

A.3.3 Overlap splice test

For basic information on splitting resistance of the surrounding concrete, confining reinforcement and influence of uneven bond stress distribution along the bars, the investigation of the overlap strength of spliced reinforcement is an adequate test procedure, Fig. A-6. Several splice lengths, different concrete strengths, different cover confinement and confinement by stirrups should be tested. It is questionable if the bond resistance in an overlap splice is the same or lower than that of a single anchored bar with the same concrete covers.

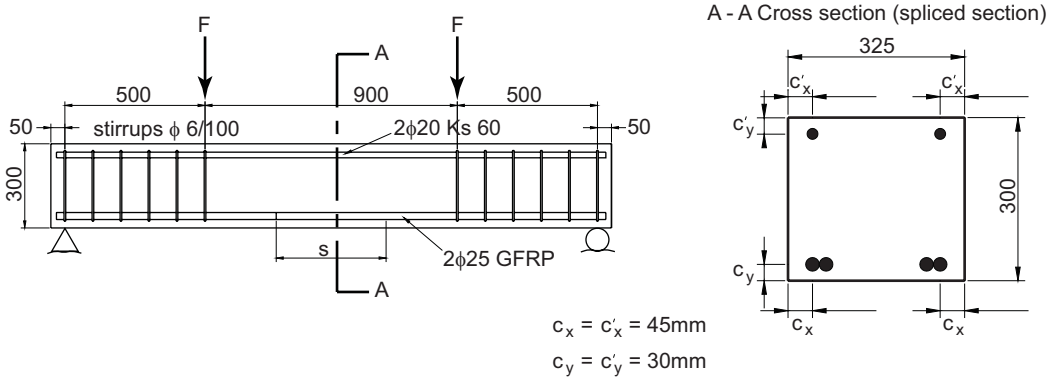

Figure A-6: Example of beam lay out for testing the strength of tensile reinforcement overlap splices.

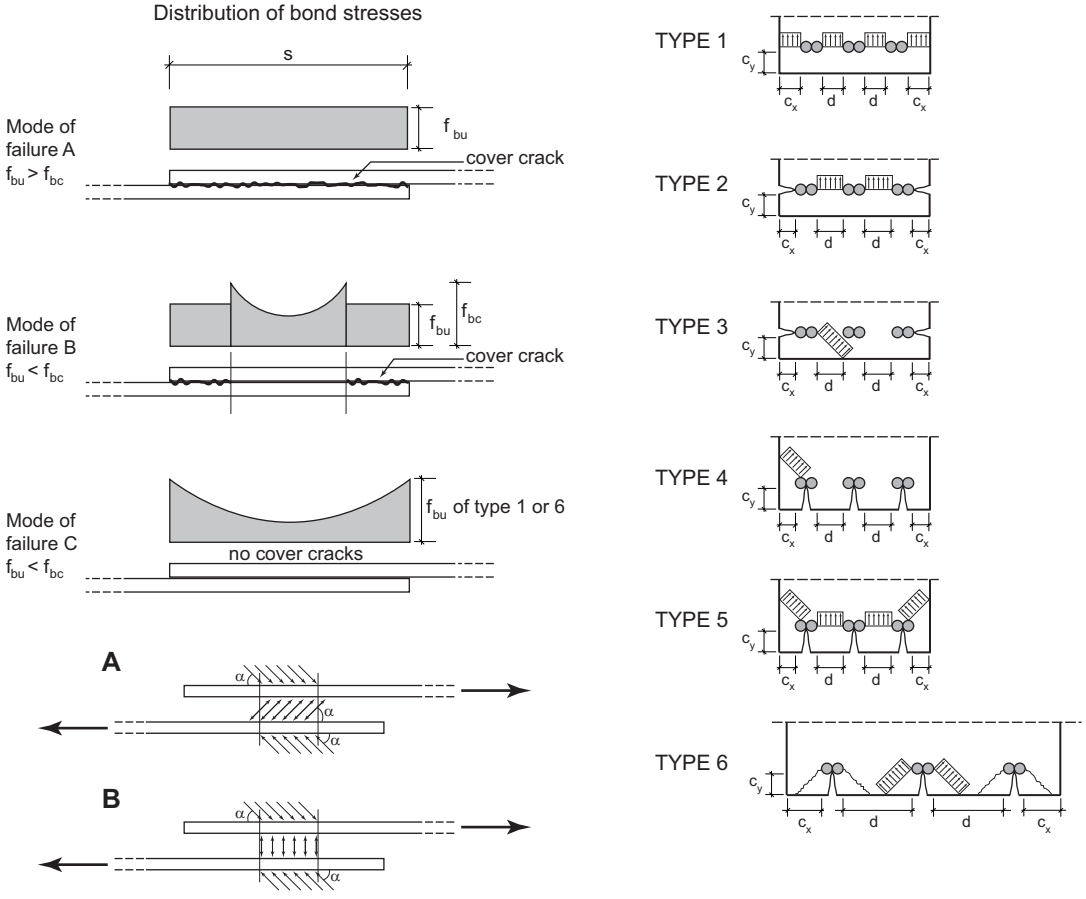

Figure A-7: Distribution of bond stresses for the failure modes A, B and C. (Tepfers, 1973)

- f_{bu} equal to the smallest ultimate failure pattern bond stress of appropriate type
- f_{bc} equal to bond stress which initates the cover crack.

When the bond reaches failure, for two side by side overlapped reinforcing bars, the bond stress distribution along the bars can be as in the three modes according to Fig. A-7.

Mode A shows bond evenly distributed when the cover along the overlapping length is cracked. The bond stress resistance f_{bu} of the cover cracked surrounding concrete is higher than the bond stress at cracking of concrete cover f_{bc}.

Mode B shows an uneven bond stress distribution with cover cracks at the ends of the overlap splice. The bond stress resistance f_{bu} of the cover cracked surrounding concrete is lower than the bond stress at cracking of concrete cover f_{bc}. The cover cracked and uncovered parts of splice determine the maximum bond resistance. In cover cracked parts the ability to slip of the bar increases and the bond stress becomes evenly distributed.

Mode C shows an uneven bond stress distribution. When the bond stress f_{bu} is reached, which cracks the cover, it immediately results in pressing off the surrounding concrete. The failure has zipper character and gives no warning of visible cracking before failure.

Evaluation of bond requires the analysis of possible resistance mechanisms by checking geometry, cracking sequences and stress distributions. There is also the question of single or double pressure developed in lapped bars, Fig. A-7. It is not possible to compare directly the results from single bar pull-out versus spliced bar types since the cracking sequence and stress distributions may be very different. For certain FRP bars the bond force angle α may be less than 45°, which means that these bars have less splitting tendency and give good anchorage, when concrete cover determines the resistance. However these bars may give less resistance, when confinement is excellent because of a weak surface layer. FRP bars with glossy surface and ribs give pronounced splitting forces and early failure by pressing off concrete cover, but may give high pull-out resistance when confinement is good, because of strong FRP bar surface layer.

B Background to a new design philosophy

B.1 Introduction

This annex deals with the design philosophy issues and initially examines the approach taken by the existing guidelines as it assesses the level of safety offered and proposes a new design philosophy framework. The new framework is evaluated by applying it to a specific FRP product.

B.2 Examination of philosophy of existing guidelines

The widespread application of any new type of reinforcement, as such as FRP, requires the development of product specifications, testing standards and design guidelines, a process that can take many years to be completed. This section deals with design philosophy and safety of the existing design guidelines for FRP. It then discusses the main issues of structural safety uncertainty.

B.2.1 Existing design guidelines

The design guideline published by the Japan Society of Civil Engineers [JSCE (1997)] is based on modifications of the Japanese steel RC code of practice [JSCE (1996)], and it can be applied for the design of concrete reinforced or prestressed with FRP reinforcement. The guideline provides a set of partial safety factors for the ultimate, serviceability and fatigue limit states (Table B-1). It is noted that the partial safety factors adopted for the ultimate and fatigue limit states are slightly higher than the ones used for steel reinforcement. The design model adopted for the ultimate limit state of bending covers both types of flexural failure; however, there is no information about the predominant mode of flexural failure that would result from the application of the proposed partial safety factors. The guideline may also be utilised as a reference document, since it includes general information about different types of FRP reinforcement, quality specifications, and characterisation tests for FRP materials.

Table B-1: Partial safety factors, γ_f, proposed for FRP reinforcement by JSCE (1997)

Limit state	Aramid FRP (AFRP)	Carbon FRP (CFRP)	Glass FRP (GFRP)
Ultimate	1.15	1.15	1.3
Serviceability	1.0	1.0	1.0
Fatigue	1.15	1.15	1.3

CSA-S806 is the most recent Canadian guideline on the design and construction of building components with FRP. In addition to the design of concrete elements reinforced or prestressed with FRP, the guideline covers a range of structural elements: FRP elements, fibre-reinforced-concrete and FRP cladding as well as concrete and masonry elements strengthened externally with FRP. The guideline also includes information about characterisation tests for FRP internal reinforcement. The guideline was approved, in 2004, as a national standard of Canada, and is intended to be used in conjunction with the national building code of Canada [CAN/CSA A23.3 (2004)]. Regarding the ultimate limit state design of FRP RC elements, there is limited information about the design philosophy of the guideline, especially for the preferred type of flexural failure; a strength reduction factor (ϕ) of 0.75 is adopted for all types of FRP reinforcement.

The Canadian Network of Centres of Excellence on Intelligent Sensing for Innovative Structures has also published a design manual that contains design provisions for FRP RC structures [ISIS (2001)]. The guideline also provides information about the mechanical characteristics of commercially available FRP reinforcement. This guideline is based on modifications to the Canadian steel RC code of practice [CAN/CSA A23.3-94 (1994)].

The American Concrete Institute published a guideline on the design and construction of concrete reinforced with FRP bars [ACI440.1R-06 (2006)], which is primarily based on modifications of the ACI-318 steel RC code of practice [ACI-318 (2005)].

Both the ISIS and ACI440.1R-06 guidelines seem to assume that the predominant mode of failure would be flexural, which would be sustained due to either concrete crushing (compressive failure) or rupture of the most outer layer of FRP reinforcement (tensile failure). To distinguish between the two types of flexural failure, the reinforcement ratio of balanced failure (ρ_{fb}) is checked in the design procedure. If the actual reinforcement ratio (ρ_f) is less than ρ_{fb}, it is assumed that flexural failure occurs due to rupture of FRP reinforcement. However, if ρ_f is greater than ρ_{fb}, then it is assumed that the element will fail due to concrete crushing. In the ideal situation where ρ_f is equal to ρ_{fb}, the concrete element is balanced and hence, flexural failure would occur due to simultaneous concrete crushing and rupture of the FRP reinforcement. It should be noted that, for FRP RC elements, the concept of balanced failure is not the same as in steel RC construction, since FRP reinforcement does not yield and, hence, a balanced FRP RC element will still fail in a sudden, brittle manner.

Table B-2 shows the values of ϕ adopted for the ultimate limit state design by the ISIS and ACI440.1R-06 guidelines The ISIS guideline adopts the same values of ϕ for both the flexural and shear design, however, different values of ϕ are used for each type of FRP reinforcement. The ACI440.1R-06 guideline uses different values of ϕ for each type of flexural failure, while - for the shear design - it adopts the value of ϕ used by ACI-318. It is also noted that, for the flexural design, the ISIS guideline applies ϕ on the internal forces, while the ACI440.01R-06 applies ϕ on the moment capacity. ACI440.01R-06 also applies environmental reduction factors on the FRP tensile strength to account for the long-term behaviour of FRPs.

Table B-2: Ultimate strength reduction factors ϕ, adopted by ACI440.1R-06 and ISIS guidelines

	ACI440.1R-06 ϕ	ISIS ϕ
Flexure: Concrete crushing	$0.3 + 0.25\frac{\rho_f}{\rho_{fb}}$ for $\rho_{fb} < \rho_f < 1.4\rho_{fb}$ or 0.65 for $\rho_f \geq 1.4\rho_{fb}$	0.6[a], 0.8[b], 0.4[c]
Flexure: FRP rupture	0.55	[a] AFRP, [b] CFRP, [c] GFRP
Shear	0.75	

The European design guideline published by Clarke et *al.* (1996) is based on modifications to European RC codes of practice [BS810 (1997), CEN (1992)]. This guideline was also published as an interim guidance on the design of FRP RC structures by the Institution of Structural Engineers [IStructE (1999)]. The guideline includes a set of partial safety factors for the material strength and stiffness, shown in Table B-3, that take into consideration both the short and long term structural behaviour of FRP reinforcement. Hence, the adopted values are relatively high when compared with the values adopted by other guidelines. The guideline does not make any distinction between the two types of flexural

failure and, in addition, does not provide clear indications about the predominant failure mode, which would result from the application of these partial safety factors.

Table B-3: Partial safety factors, γ_f, proposed for FRP RC structures by Clarke et al (1996)

	AFRP	CFRP	GFRP (E-Glass)
Strength	2.2	1.8	3.6
Stiffness	1.1	1.1	1.8

B.2.2 Structural safety uncertainties

One of the structural safety uncertainties of steel RC codes of practice is the lack of published records about the methods and data used by code committees to calculate the material partial safety factors [Neocleous et al. (2004)]. It appears that the majority of the material partial safety factors have been calibrated with pre-existing practice and experience by accounting for the variability of material strength. Over the years, these factors have been progressively reduced to account for improvements in manufacturing processes, design models and quality control procedures used in the construction industry. Modern codes of practice, such as Eurocode-2 [CEN (2004)], have adopted partial safety factors that have been primarily calibrated with pre-existing design methods, but have been further amended by safety level-2 probabilistic methods [CEN (2002)].

It is also not known whether the application of the partial safety factors would lead to notional structural reliability levels (P_f) that attain the target level adopted by codes of practice. In the case of Eurocodes, it is considered that the application of the partial safety factors will generally attain the target value of $7x10^{-05}$ (or safety index, β, of 3.8), adopted for the design working life of structural elements [CEN (2002)]. However, the Eurocodes do not provide any information about the range of P_f, expected for various types of concrete elements and failure modes (i.e. limit states). Various structural reliability assessments suggest that the structural reliability of steel RC elements, designed according to the 1992-version of Eurocode-2, varies enormously [Neuenhofer and Zilch (1993), Duprat et al (1995), Neocleous et al. (2004)]. This is mainly due to the effect of various design parameters, as demonstrated in Figure B-1 for steel RC beams designed according to the 1992 version of Eurocode-2. It is worth noticing that the ratio of the permanent to variable load (termed in Figure B-1 as "Load ratio") has the greatest effect on the structural reliability for both flexure and shear limit states. As different load ratios are implicitly used in different types of structures (due to their geometry and intended application), it is evident that there is no uniformity in structural reliability amongst different types of concrete structures [Neocleous (1999), Neocleous et al. (2004)].

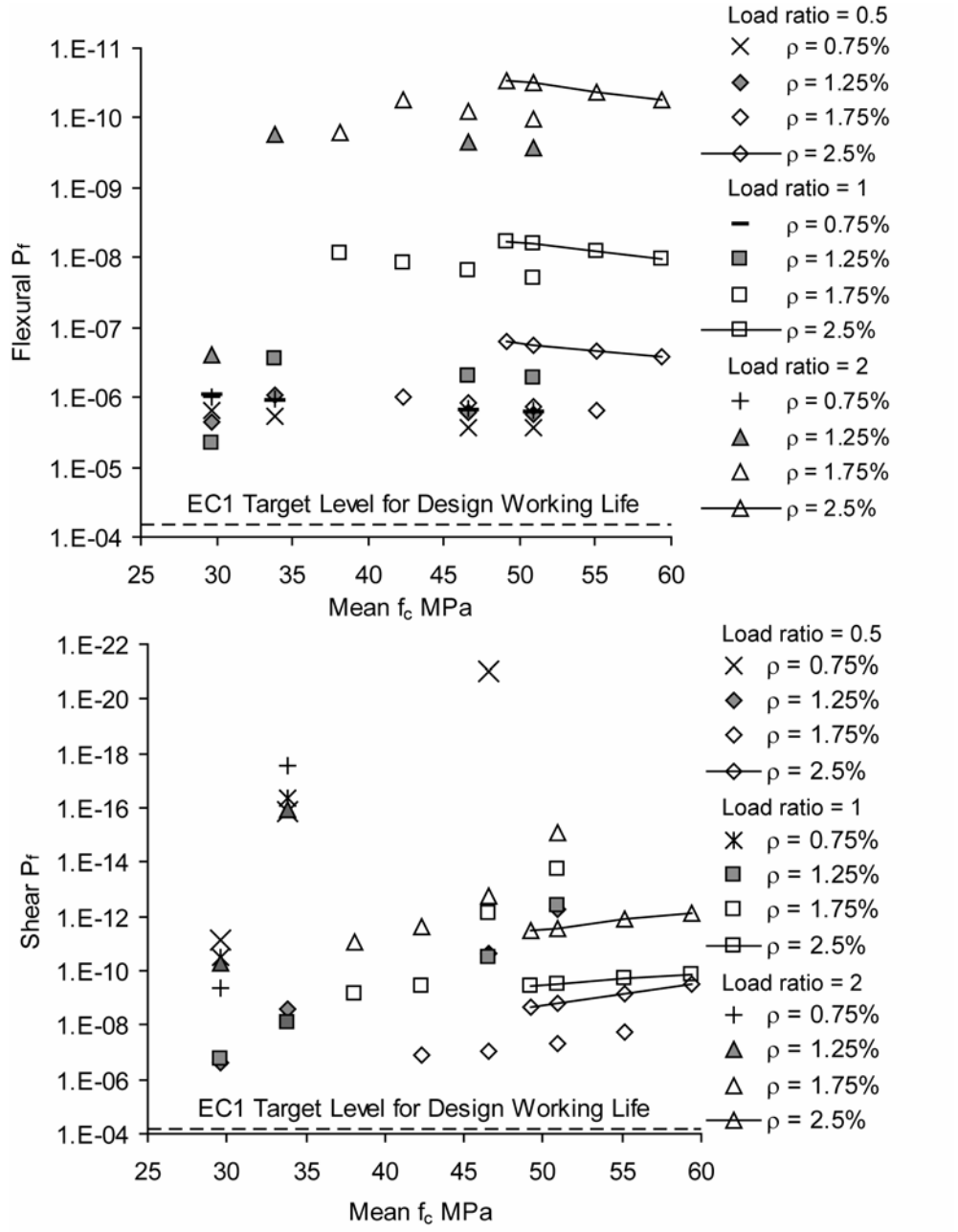

ρ ratio of longitudinal steel reinforcement, fc concrete cylinder compressive strength

Figure B-1: Effect of design parameters on flexural and shear structural reliability [Neocleous et al. (2004)]

Another uncertainty arises from the fact that the actual resistance-capacity (R_{actual}) of RC is often different from the un-factored value (R_U) predicted at the design stage. This variation exists because the actual mechanical and geometrical properties of steel reinforcement and concrete are different from those used for the prediction of R_U; model uncertainties also account for this variation. The resistance-capacity variation could be modelled by probability density functions, as exemplified in Figure B-2 for the flexural yielding, flexural concrete crushing, and shear failure modes.

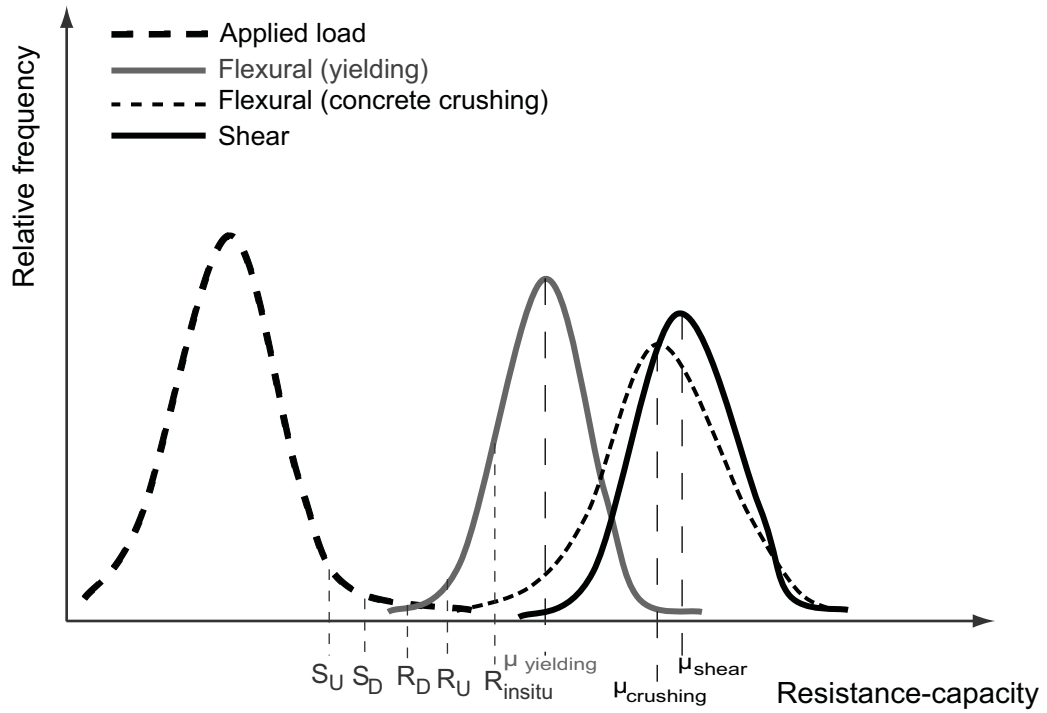

Figure B-2: Example of resistance-capacity margin between flexural and shear failure modes, after [Neocleous et al. (2005)]

The value of R_U is predicted by using the characteristic values of the main parameters (such as the strength of concrete and steel reinforcement) and, as shown in Figure B-2 for the predominant mode of failure, R_U corresponds to a value at the lower tip of the probability density function of the failure mode and it is normally expected to be lower than R_{actual}. However, if R_{actual} of the predominant failure mode is much higher than R_U, steel RC codes of practice do not provide any information about the failure mode that will actually occur first (i.e. flexural yielding, flexural concrete crushing or shear) and at which load level.

One possible way of tackling this problem is through the concept of resistance-capacity margins (RCMs), which determines the capacity margin between failure modes. RCM, between any two failure modes, may be represented as the ratio of the mean resistance-capacities predicted for each failure mode (equation B-1) [Neocleous (1999), Neocleous et al. (2004)]. In addition, RCMs can be correlated to the probability of occurrence of specific failure as demonstrated in Figure B-3 for the flexural yielding and shear failure modes [Neocleous (1999)]. It is noted that Figure B-3 shows that the RCM between the shear and flexural (yielding) failure mode of rectangular steel RC beams ranged from 0.9 to 2.1 and 1.1 to 2.8 for BS8110 and Eurocode 2 (1992-version, [CEN (1992)]).

$$RCM_{\text{failure (ii)}-\text{failure (i)}} = \frac{\mu_{\text{failure-mode (ii)}}}{\mu_{\text{failure-mode (i)}}} \qquad \text{(B-1)}$$

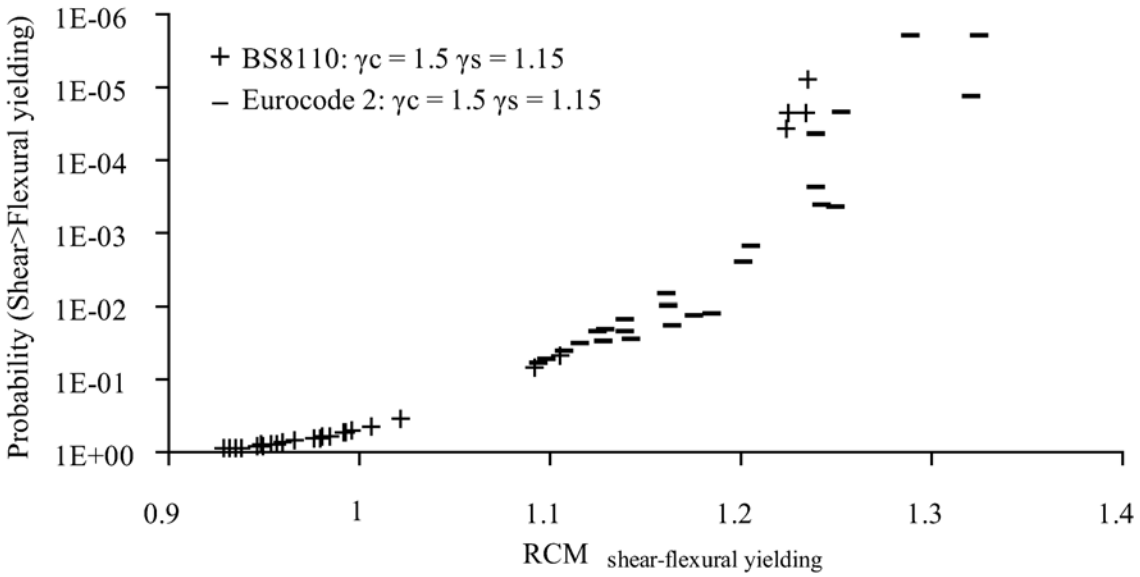

Figure B-3: Correlation of RCM and probability of occurrence of shear failure mode prior to flexural yielding

In addition to the above uncertainties, there are design and safety philosophy issues that are directly related to FRP RC elements. These issues - discussed below - were investigated through a probabilistic structural reliability assessment of forty-eight singly-reinforced FRP RC beams [Neocleous (1999), Pilakoutas et al. (2002)]. The IStructE (1999) guideline was used to design the beams. The characteristic f_c (f_{ck}) of these beams ranged from 21 to 43 MPa, whilst ρ_f ranged from 0.75% to 2.5%. Two types of FRP longitudinal and transverse reinforcement were considered: CFRP with a characteristic tensile strength (f_{fk}) of 1272 MPa and characteristic Young's modulus (E_{fk}) of 106 GPa, and GFRP with f_{fk} equal to 747 MPa and E_{fk} equal to 41.5 GPa.

Concrete crushing is the most probable type of flexural failure because the ultimate tensile strength of FRP reinforcement is rarely attained in normal-strength concrete sections [Neocleous (1999), Pilakoutas et al. (2002)]. This is exemplified in Figure B-4 for the CFRP RC beams examined in the probabilistic analysis. The strain values, calculated at the design stage for concrete in compression and CFRP rebars in tension, indicate that only six of the beams attained the design limit for the ultimate tensile strain of CFRP (i.e. 0.0067). These six beams were expected to fail due to rupture of the CFRP rebars, while the remaining beams were expected to fail due to concrete crushing.

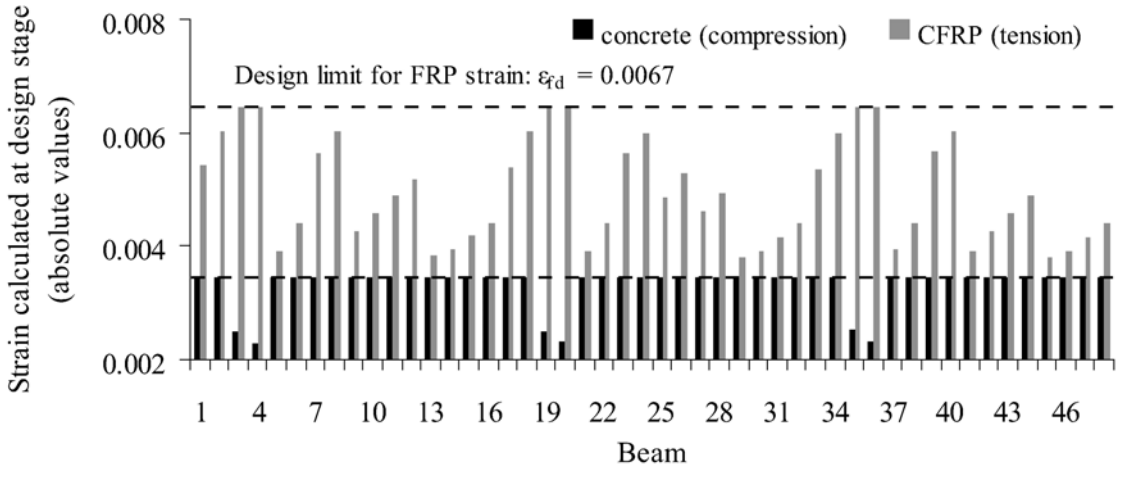

Figure B-4: Strain calculated at design stage for concrete (compression) and CFRP rebars (tension), ($\gamma_{f,L}$ = 1.8)

Furthermore, the use of partial safety factors for longitudinal reinforcement ($\gamma_{f,L}$) may not be essential for the design of FRP RC beams, if the type of flexural failure intended at design is concrete crushing [Neocleous (1999), Pilakoutas et al. (2002)]. This is because the tensile strain developed in FRP reinforcement does not change with the value of $\gamma_{f\text{-}L}$ (Figure B-5) and, consequently, the flexural R_D (Figure B-6) and notional structural reliability (Figure B-7) will not change with the value of $\gamma_{f,L}$. For example, when a $\gamma_{f,L}$ of 1.8 is used, beams 3, 4, 19, 20, 34 and 35 are expected to fail due to FRP rupture. When a $\gamma_{f,L}$ of either 1.3 or 1.15 is used, all beams are expected to fail due to concrete crushing; however, their flexural capacity and P_f do not change for the value of $\gamma_{f,L}$. It is noted that $\gamma_{f,L}$ becomes relevant for elements designed to fail in flexure due to rupture of the FRP rebars, since the $\gamma_{f,L}$ will affect the strain developed in concrete and FRP reinforcement as well as the design capacity and structural reliability of the element. It is clear that other design provisions will be required to account for the variation in the mechanical properties of FRPs, if $\gamma_{f,L}$ is not used at the design stage. It is possible that these uncertainties could be accounted for by the partial safety factor adopted for concrete strength. It is noted the partial safety factor used for the transverse reinforcement ($\gamma_{f,T}$) affects the shear capacity and, consequently, the structural reliability of FRP RC beams. Thus, this factor is essential for the shear design of FRP RC elements [Neocleous (1999)].

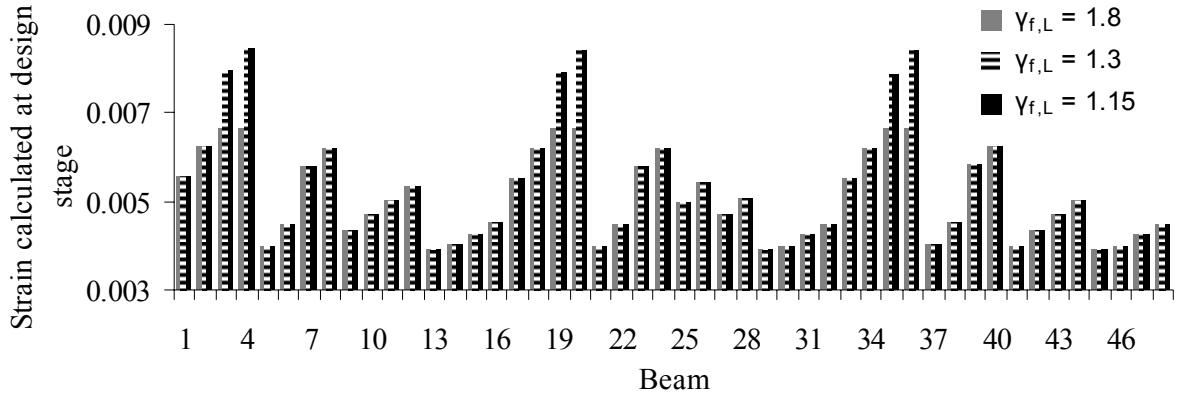

Figure B-5: Effect of $\gamma_{f,L}$ on tensile strain in CFRP reinforcement, calculated during the flexural design of CFRP RC beams [Neocleous (1999)]

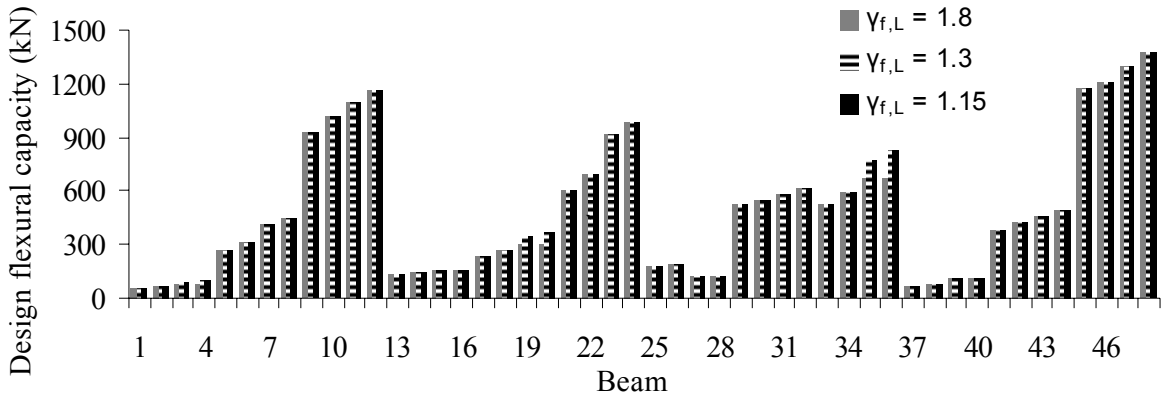

Figure B-6: Effect of $\gamma_{f,L}$ on design flexural capacity of CFRP RC beams [Neocleous (1999)]

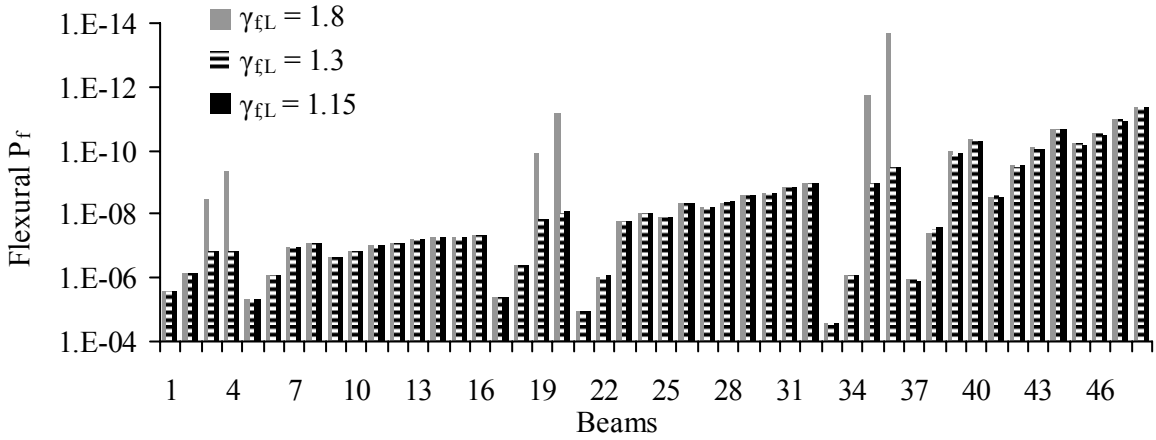

Figure B-7: Effect of $\gamma_{f,L}$ on flexural structural reliability of CFRP RC beams [Neocleous (1999)]

Another design and safety philosophy issue rises from the assumption that the application of $\gamma_{f,L}$ would always lead to the desired type of flexural failure. This assumption is not always valid, especially for the large values of $\gamma_{f,L}$. Although the application of large $\gamma_{f,L}$ is normally expected to lead to failure due to FRP rupture, the actual failure would occur due to concrete crushing [Neocleous (1999), Pilakoutas et al. (2002)]. For instance, when a $\gamma_{f,L}$ of 3.6 was used for the design of the GFRP RC beams, the failure intended at the design stage was flexure due to FRP rupture. However, it was calculated that, for most beams, there was a very high probability that the actual failure will occur due to concrete crushing. Similar probabilities of occurrence were calculated when a $\gamma_{f,L}$ of 1.3 was used.

Similarly to steel RC codes of practice, existing guidelines for FRP RC do not provide enough information about the structural reliability of FRP RC elements. Neocleous (1999) evaluated that the flexural structural reliability of FRP RC beams is not uniform across the range of beams examined (Figure B-8). This is due to the effect of the ratio of permanent to variable load (G/Q ratio), f_c and ρ_f. These parameters also affect the shear structural reliability of FRP RC beams (Figure B-9). It is noted that the effect of these parameters on structural reliability is influenced by the type of flexural failure assumed at the design stage (Neocleous (1999). Figures B-8 and B-9 also indicate that the G/Q ratio has the greatest effect on structural reliability and it may be more appropriate to use different partial safety factors (or load factors) for each G/Q ratio and different types of structures.

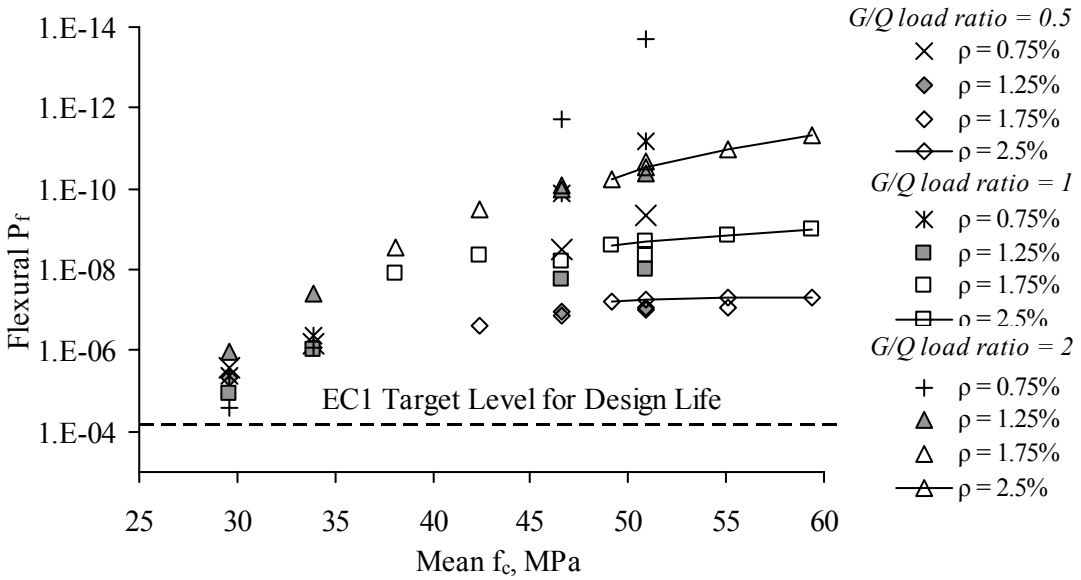

Figure B-8: Flexural structural reliability for CFRP RC beams designed with a $\gamma_{f,L}$ of 1.8 [Neocleous (1999)]

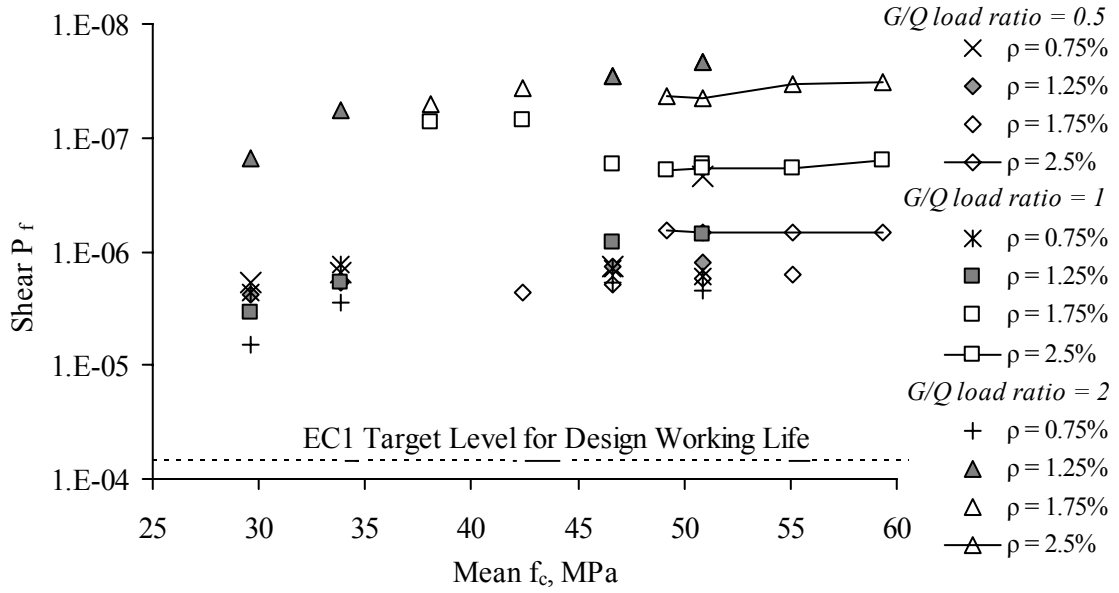

Figure B-9: Shear notional structural reliability for CFRP RC beams designed with a $\gamma_{f,T}$ of 1.8 [Neocleous (1999)]

Furthermore, the FRP RC design guidelines do not provide any information about the RCMs between the shear and flexural capacity of FRP RC elements. The structural reliability analysis performed for the 48 FRP RC beams showed that the shear-flexural RCMs are not uniform across the range of beams considered in the analysis. In addition, parameters such as ρ, f_c and γ_f affect the RCMs between the two failure modes and it is therefore possible to attain a desired failure mode hierarchy by applying appropriate limits on these parameters [Neocleous et al. (2005)].

Additional design issues that require further investigation, arise when considering the long-term behaviour of FRP RC elements. The application of multiple strength-reduction factors that are intended to account for the long-term effects of FRP reinforcement may not lead to the mode of failure aimed at the short-term design or may lead to uneconomical designs. It is therefore essential to develop appropriate design provisions that take into account the long-term behaviour of FRP reinforcement. One possible solution is to use the short-term properties for the limit state design and, subsequently, to verify that (at various time intervals), the applied stress is less than the design strength of FRP that is available at each time interval.

B.3 A new design philosophy

In view of the above findings, the design of FRP RC elements is based on the level 1 approach of structural reliability theory with the main aims being the attainment of a desired failure-mode-hierarchy and the satisfaction of the target reliability levels [Neocleous et al. (2005)]. This design philosophy is implemented through a framework (see Chapter 8, Figure 8-1), which may form part of the overall code development process presented by Nowak and Lind (1995).

B.3.1 Design framework based on a new philosophy

The first step (1.1) in the framework of the design philosophy discussed here is carried out as part of the general definition of the scope and data space of the code of practice [Neocleous

et al. (2005), Nowak and Lind (1995)]. It involves the definition of all possible failure modes that can be predicted for each type of FRP RC element (i.e. configuration) covered by the code of practice.

In the second step (1.2), the primary failure modes are selected for each type of FRP RC element. This involves classification of the each failure mode in terms of the type of failure it represents and the seriousness of the damage caused by each failure mode [Neocleous et al. (2005)].

The third step (1.3) comprises the definition of criteria for formulating failure-mode-hierarchies for each type of FRP RC element. A failure-mode-hierarchy account for all primary failure modes, and their sequence should follow the degree of undesirability of each mode of failure. The most favourable failure mode is placed on top of the hierarchy whilst the least favourable one is placed at the bottom of the hierarchy. In the example of Figure B-10 the most favourable mode of failure for FRP RC beams is flexural concrete crushing, whilst the least favourable is bond failure [Neocleous et al. (2005)].

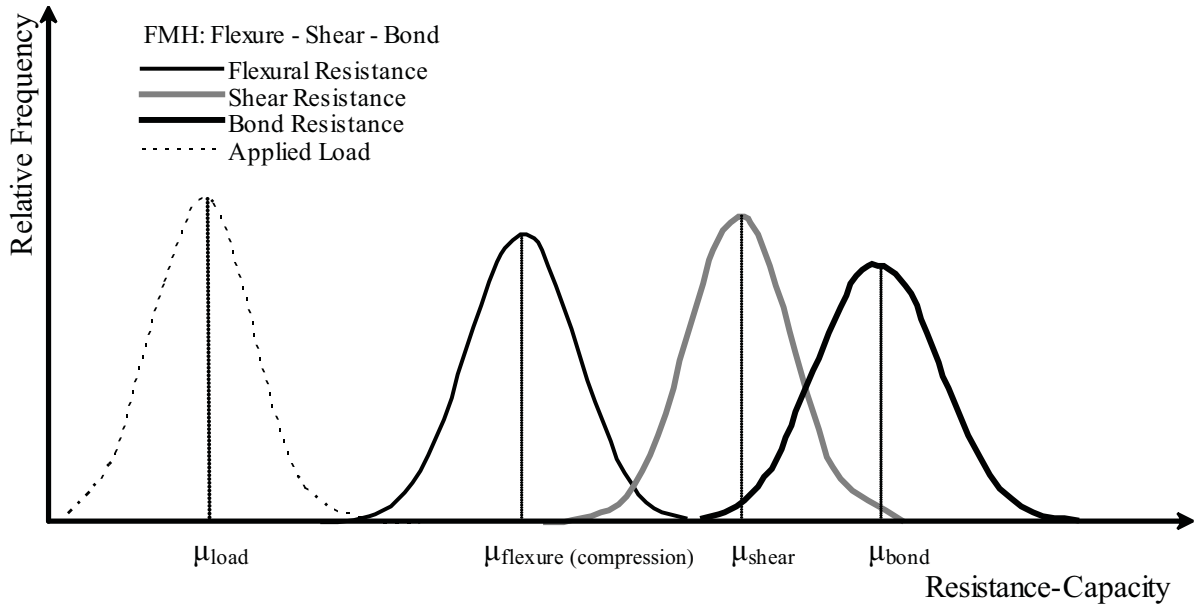

Figure B-10: Concept of failure mode hierarchy for FRP RC beams [Neocleous et al. (2005)]

The fourth step (1.4) in the process involves the definition of rules for establishing appropriate RMCs between each primary failure mode. The selection of RCMs is expected to be influenced by the relative cost of the excess resistance-capacity; however, it is logical to assume that a substantial margin will be required between the most and least favourable modes in the hierarchy. In the example of Figure B-10, a lower RCM is chosen between shear and bond failure, whilst a higher margin is used between flexure and bond.

In the fifth step (1.5), the target reliability level of the code is defined. Appropriate target reliability levels can be generally derived from calibration to existing design practices and experience, provided that the application of these practices does not result into highly non-uniform notional reliability levels [Ditlevsen (1997)]. In the case of FRP RC elements, this approach cannot be applied due to the lack of comprehensive design practices and experience. Target levels can also be determined by considering social, economic or socio-economic constrains that are relevant to structures [CEB Bulletin D' Information No 191 (1988)]. These constraints vary with the type of structure, use of structures and the social and economic conditions that exist in the country that the structures are to be built [CIRIA Report 63

(1977)]. It must be noted that the successful application of these techniques requires extensive economic data. In the current case, it is expected that the Eurocodes will form the basis of the new design guideline and therefore, it is reasonable to adopt the lifetime target level of $7x10^{-05}$ that is currently adopted by the Eurocodes [CEN (2002)].

B.3.2 Application of a new design philosophy for FRP RC

The framework introduced in the previous section, if adopted by codes of practice, could enable (through the following procedure) the determination of appropriate partial safety factors for FRP reinforcement, as illustrated in Figure 8-2 [Neocleous et al. (2005)].

The first step (2.1) in the procedure involves the definition of appropriate FMHs and RCMs for each type of structural elements using the specific reinforcing materials. At this step, appropriate models are developed to predict the elements' resistance-capacity for each failure-mode (contained in the selected FMHs).

In step 2.2, different design configurations are chosen for each type of element from the entire data space of the code, and their structural reliability is probabilistically assessed for the failure modes contained in each FMH. This is performed for different partial safety factors. Each design configuration is checked to establish whether it satisfies the target RCMs and P_f.

Based on the above, a set of partial safety factors is determined for each FMH (step 2.3) by utilising the concept of average measure of closeness between the code and the target P_f, as presented by Nowak and Lind (1995). The objective of this concept is to optimise the structural design by comparing the structural reliability with the corresponding expected total cost of construction.

It must be emphasised that, to attain the desired RCMs, it may be necessary to impose limits on the design parameters considered by each limit-state prediction model. This would result in the attainment of the chosen FMH and the satisfaction of the target P_f. Since the new philosophy aims at the differentiation of structural reliability for various types of structures, individual partial safety factors should be specified for each type of structure (e.g. buildings, bridges) covered by the code of practice.

B.4 Application of framework for CFRP RC and GFRP RC

The validity of the framework discussed here needs to be demonstrated for a number of structural elements (e.g. beams and slabs) and FRP reinforcement. For simplicity, the framework is demonstrated only for the case of concrete beams, reinforced with either CFRP or GFRP FRP reinforcement (both longitudinal and transverse). As in the previous section, the first stage involves the establishment of the design framework. The second stage deals with the determination of partial safety factors for the selected reinforcing materials.

B.4.1 Establishment of design framework

The first step (1.1) in this procedure involves the definition of all possible failure modes for each type of element covered by the code of practice. The following failure modes are defined as possible for the ultimate limit-state design of CFRP and GFRP RC beams.

1.A Flexure due to concrete crushing.
1.B Flexure due to fracture of longitudinal FRP reinforcement.
2.A Shear due to fracture (or lack) of transverse FRP reinforcement.
2.B Shear due to concrete failure.

3.A Torsion
4.A Bond due to splitting.
4.B Bond due to splicing.
4.C Bond due to anchorage.

The definition of the possible failure modes is followed by the identification of the primary modes and classification according to their seriousness (step 1.2). Flexural failure due to reinforcement fracture is unlikely due to the unrealistically low ρ needed to achieve it. The most likely type of flexural failure to be sustained by FRP RC beams is concrete crushing. Shear failure due to concrete failure is only likely in un-reinforced or over-reinforced in shear RC beams. Both situations are normally covered by using lower and upper limits for transverse reinforcement. Hence, the most likely shear failure mode is failure due to fracture of the transverse reinforcement. Since torsional stresses are normally small in RC beams, this mode is not considered in this study. Bond failure may be desirable, if a pseudo-ductile bond behaviour can be ensured, however this is not the case for the reinforcing bars under examination. Though the bond characteristics of FRP re-bars are generally good [Achillides and Pilakoutas (2002)], the models for design are still being developed and as a result, this mode of failure is not considered in the present study. Flexural failure due to concrete crushing and shear failure due to fracture of transverse reinforcement are therefore selected as the primary modes of failure.

The establishment of criteria for the formulation of the desired FMHs is the next step (1.3) in the procedure. Both primary modes of failure selected are brittle in nature, even though the flexural mode dissipates some inelastic energy through concrete non-linearity in compression. From the two modes, the flexural mode has the most reliable prediction models and as result, is selected as the predominant mode of failure for design purposes.

The formulation of the FMH is followed by the definition of target values for the RCMs (step 1.4). It must be emphasised that such targets have never been discussed by code developers, standardisation committees and researchers. Therefore, the RCMs, evaluated for steel RC beams in previous studies [Neocleous et al. (2004), Neocleous (1999)] are presumed to be sufficient. Similarly, the value of 7x 10^{-5} (set as a target P_f by Eurocode-1) is considered to be appropriate.

B.4.2 Determination of appropriate γ_f

The establishment of the design framework is followed by the determination of appropriate short-term partial safety factors for the chosen materials. Table B-4 summarises the tensile strength and Young's Modulus of the CFRP and GFRP reinforcement used in this study, which was developed during the Eurocrete project (Duranovic et al. (1997, 1997a)].

Table B-4: Mechanical properties of CFRP and GFRP reinforcement

	Tensile Strength (N/mm^2)		Elastic Modulus (N/mm^2)	
	GFRP	CFRP	GFRP	CFRP
Mean μ	810	1380	45000	115000
Standard Deviation σ	40.5	69	2250	5750
Characteristic k	747	1272	41500	106000

Tensile strain of CFRP and GFRP reinforcement: 1.2% and 1.8%, respectively

The first step (2.1) in this procedure, which has to be followed for any new material, involves the definition of appropriate FMHs and RCMs for the FRP RC beams. A single FMH is adopted here, since only two primary failure modes are considered, one of which has already been selected as the most desirable mode of failure. Hence, flexural failure due to concrete crushing is located at the top of the hierarchy and is followed by shear failure due to fracture of the transverse FRP reinforcement. In the general code development stage, it was decided to adopt target RCMs that reflect the current steel RC practice and hence, the average value of 1.4 is adopted as target for the flexure-shear RCM. In addition, the resistance-capacity prediction models [Pilakoutas et al. (2002), Guadagnini et al. (2003)], developed as part of the ConFibreCrete (1998) research network are used.

The next step (2.2) is to perform structural reliability analyses to determine the flexural P_f, shear P_f and flexural-shear RCMs for the values of γ_f tabulated in Table B-5. The values for the $\gamma_{f,L}$ and partial safety factor for transverse reinforcement ($\gamma_{f,T}$) were selected by considering the findings of previous investigations [Neocleous (1999)]. The assessment was carried out for 48 different design configurations. The analyses were performed by utilising the Monte-Carlo Simulation method [Ayyub B. M. and McCuen (1995)] in conjunction with the Latin-Hypercube and Conditional-Expectation variance reduction techniques [Avramidis and Wilson (1996)].

Table B-5: γ_f examined in the structural reliability assessment

	CFRP reinforcement	GFRP reinforcement
$\gamma_{f,L}$	1.15	1.3
$\gamma_{f,T}$	1.15, 1.5, 1.8	1.5, 1.75, 2

Results obtained for the flexural P_f indicated that, for the selected $\gamma_{f,L}$, the target P_f was attained by all design configurations. Whereas in the case of shear P_f, the target P_f was achieved by all design configurations, only if the value of $\gamma_{CFRP,T}$ and $\gamma_{GFRP,T}$ was 1.8 and 2 respectively.

Regarding the RCM, the target value of 1.4 was attained by all design configurations only if the values of $\gamma_{CFRP,T}$ and $\gamma_{GFRP,T}$ were 1.8 and 2, respectively. It is noted that the value chosen for $\gamma_{f,L}$ does not affect the flexure-shear RCMs, as the design aimed to achieve flexural failure due to concrete crushing.

The use of $\gamma_{f,L}$ also does not influence the flexural P_f (provided that flexural failure occurs due to concrete crushing). Therefore, it may be possible to eliminate the use of $\gamma_{f,L}$ and incorporate the uncertainties relevant to the longitudinal FRP reinforcement in the partial safety factor (γ_c) adopted for f_c. However, this will require the modification of γ_c used currently in flexural limit state design. To be conservative, it is decided to use the values of $\gamma_{f,L}$ currently examined (1.15 and 1.3 for CFRP and GFRP reinforcement respectively) for short-term loading conditions, since they reflect uncertainties in material characterisation. A limit is also imposed on ρ (equation B-2) to eliminate the possibility of flexural failure occurring due to reinforcement fracture.

$$\rho_{\min} = \frac{0.81\,(f_{ck}+8)\,\varepsilon_c}{f_{fk}\left(\frac{f_{fk}}{E_{fk}}+\varepsilon_c\right)} \qquad \text{(B-2)}$$

The concept of average measure of closeness [Nowak and Lind (1995)], (expressed in terms of structural utility), T (equation B-3), is utilised to select appropriate values for $\gamma_{FRP\text{-}T}$. The selection criteria comprise the attainment of the target RCMs and P_f and minimisation of the resulting cost of construction. To perform such an assessment, it is necessary to estimate the demand function, D_{fj}, for each configuration. D_{fj} is expressed as the product of the frequency of occurrence estimated for each of the main design parameters, considered by each configuration (equation B-4). The main design parameters are ρ, f_c and PVL-ratio. The values of the frequency of occurrence, estimated for each of these variables, are summarised in Table B-6.

$$T = \int MD_f d_s \tag{B-3}$$

$$D_{fj} = f_{fc}\ f_{\frac{G_k}{Q_k}}\ f_{\rho} \tag{B-4}$$

Table B-6: Frequency of occurrence (f) for ρ, fc *and* PVL-ratio

ρ %	f_ρ	f_c N/mm^2	f_{fc}	PVL-ratio$\left(\frac{G_k}{Q_k}\right)$	$f_{\frac{G_k}{Q_k}}$
0.5 - 1.0	0.25	20 - 30	0.25	0.01 - 0.8	0.3
1.0 - 1.5	0.25	30 - 40	0.25	0.8 - 1.5	0.5
1.5 - 2.0	0.25	40 - 50	0.25	1.5 - 2.5	0.2
2.0 - 3.0	0.25	50 - 60	0.25	-	-

The metric function, M_j, for each design configuration is taken as the total cost of construction, C_{Tj} (equation B-5). The C_{Tj} and initial cost of construction for each design configuration, C_{Ij}, are determined by equations B-6 and B-7, respectively. The cost of failure for each design configuration, $C_{Fj,}$ (such as the cost of loss of use and cost of fatalities) is determined by considering a number of scenarios as indicated in Table B-7. Table B-8 shows the unit prices adopted for the cost of concrete and cost of CFRP and GFRP reinforcement. It is noted that the same prices are used for longitudinal and transverse reinforcement.

$$M_j = C_{Tj} \tag{B-5}$$

$$C_{Tj} = C_{Ij} + C_{Fj} P_{fj} \tag{B-6}$$

$$C_{Ij} = C_{C_j} + C_{R_j} \tag{B-7}$$

Table B-7: Scenarios considered for cost of failure

Scenario	1	2	3	4	5	6
C_{Fj}	C_{Ij}	3 C_{Ij}	10 C_{Ij}	100 C_{Ij}	1000 C_{Ij}	10000 C_{Ij}

Table B-8 Indicative unit price for ready mix concrete and FRP reinforcement

Ready Mix Concrete £/m^3	CFRP Reinforcing Bars £/m per ϕ13.5mm (per10x4mmlink)	GFRP Reinforcing Bars £/m per ϕ13.5mm (per 10x4mm link)
55	1.95	0.82

The values of T obtained for the shear failure mode (Tables B-9 and B-10) indicated that T increases slightly with the value of $\gamma_{f,T}$. This is due to the increase in the C_{Rj} for transverse reinforcement; more transverse reinforcement is required as $\gamma_{f,T}$ increases. Furthermore, the results of the cost-optimisation indicate that, for the small values of $\gamma_{f,T}$, the average measure of closeness increases significantly, as C_{Fj} becomes relatively large. This is due to the increased influence of P_f on C_{Tj}. It is also observed that the shear average measure of closeness is significantly higher for PVL-ratio equal to 1. This is due to the relatively longer beam spans used for this particular PVL-ratio.

Table B-9: Cost-optimisation results for CFRP RC beams (shear failure)

Load Ratio	γ_{CFRP-T}	Average P_f	Average Measure of Closeness for each Scenario, £ 1	2	3	4	5	6
0.5	1.15	1.7E-05	29.76	29.77	29.79	30.08	32.94	61.59
	1.5	2.3E-06	30.34	30.34	30.34	30.37	30.71	34.03
	1.8	4.4E-07	30.84	30.84	30.84	30.84	30.89	31.39
1	1.15	4.1E-05	58.68	58.70	58.76	59.57	67.64	148.31
	1.5	3.7E-06	59.70	59.70	59.71	59.77	60.45	67.24
	1.8	4.0E-07	60.62	60.62	60.62	60.63	60.70	61.39
2	1.15	3.5E-05	33.46	33.48	33.54	34.37	42.66	125.54
	1.5	2.1E-06	34.06	34.06	34.07	34.12	34.62	39.67
	1.8	1.5E-07	34.62	34.62	34.62	34.63	34.66	35.03

Table B-10: Cost-optimisation results for GFRP RC beams (shear failure)

Load Ratio	γ_{GFRP-T}	Average P_f	Average Measure of Closeness for each Scenario, £ 1	2	3	4	5	6
0.5	1.5	5.2E-06	29.97	29.97	29.97	30.05	30.85	38.78
	1.75	1.1E-06	30.35	30.35	30.35	30.36	30.50	31.92
	2	2.3E-07	30.73	30.73	30.73	30.73	30.75	31.00
1	1.5	1.4E-05	58.98	58.99	59.01	59.28	61.99	89.02
	1.75	2.0E-06	59.66	59.66	59.67	59.70	60.08	63.84
	2	2.9E-07	60.34	60.34	60.34	60.35	60.40	60.88
2	1.5	1.6E-05	33.69	33.69	33.72	34.11	37.97	76.57
	1.75	2.1E-06	34.09	34.09	34.10	34.15	34.66	39.78
	2	2.1E-07	34.50	34.50	34.50	34.51	34.56	35.08

It was decided to select the highest value of $\gamma_{f,T}$ considered in the assessment (Table B-11), as the application of these values seemed to be the most economical (for scenarios 5 and 6) and it also satisfied both the target RCMs and P_f.

Table B-11: γ_f selected for the shear failure mode

PVL-ratio	γ_{CFRP}	γ_{GFRP}
0.5	1.8	2
1	1.75	2
2	1.75	2

B.4.3 Design example

The γ_f, recommended for load ratio equal to 0.5, are used for the limit state design and structural reliability assessment of two FRP RC beams that were tested during the Eurocrete project [Duranovic et al. (1997), (1997a)] and failed in flexure due to concrete crushing. This is to verify that the application of the chosen γ_f leads to the desired FMH and satisfies the target P_f and RCMs.

Table B-12 summarises the results obtained from the design and the structural reliability assessment of the two beams. It is clear that the application of the proposed γ_f leads to the desired FMH, since the shear resistance-capacity is higher than the flexural resistance-capacity. In addition, it is observed that the target RCMs are satisfied. It must be noted that there is a good correlation, in particular for beam CB17, between the flexural resistance-capacity and the experimental resistance-capacity. The values obtained for the flexural and shear P_f indicate that the P_{ft} of $7x10^{-05}$ is satisfied for both failure modes.

Table B-12: Design results for beams GB9 and CB17

	GB9	CB17
Experimental Load, kN	103.6	127.6
Design Load Fd, kN	63.3	72.5
Flexural P_f	2.7E-07	1.0E-06
Flexural resistance-capacity		
Mean value, $\mu_{flexure}$, kN	100.6	127.2
Design value, kN	63.3	72.5
Shear P_f	1.7E-17	7.3E-16
Shear resistance-capacity		
Mean value, μ_{shear}, kN	164.5	175.4
Design value, kN	65.0	72.9
RCM	1.6	1.4

References

Achillides, Z. (1998), *Bond behaviour of FRP bars in concrete*, PhD thesis, Centre of Civil and Structural Engineering, Department of Civil and Structural Engineering, The University of Sheffield, Sheffield.

Achillides, Z. and Pilakoutas, K. (2002), Analytical approach to the bond behaviour of FRP bars in concrete, *Proceedings of Third International Symposium on Bond in Concrete: from Research to Standards*, Budapest Hungary, 700-707.

ACI (2001), *ACI 224R-01 - Control of Cracking in Concrete Structures,* ACI Committee 224, American Concrete Institute, Farmington Hills, MI, USA.

ACI (2002), *ACI 318-02 - Building Code Requirements for Structural Concrete*, American Concrete Institute, Farmington Hills, MI.

ACI (2005), *ACI 318-05 - Building code requirements for structural concrete (ACI 318-05) and commentary (318R-05)*, American Concrete Institute, Farmington Hills, MI.

ACI (1995), *ACI 318-95 - Building Code Requirements for Structural Concrete*, ACI Committee 318, American Concrete Institute, Farmington Hills, MI, USA.

ACI (2001), *ACI 440.1R-01 - Guide for the design and construction of concrete reinforced with FRP bars,* ACI Committee 440, American Concrete Institute (ACI), Farmington Hills.

ACI (2003), ACI 440.1R-03 - *Guide for the Design and Construction of Concrete Reinforced with FRP Bars*, ACI Committee 440, American Concrete Institute, Farmington Hills, MI, USA.

ACI (2006), *ACI 440.1R-06 - Guide for the design and construction of concrete reinforced with FRP bars*, ACI Committee 440, American Concrete Institute (ACI).

ACI (2002), *ACI 440.2R-02 - Guide for the Design and Construction of Externally Bonded FRP Systems for Strengthening Concrete Structures*, ACI Report, Farmington Hills.

ACI (2004), *ACI 440.3R-04 - Guide Test Methods for Fiber-Reinforced Polymers (FRPs) for Reinforcing or Strengthening Concrete Structures*, Comitteee 440.

ACI (1996), ACI 440-96 - *State-of-the-Art Report on fiber reinforced plastic reinforcement for concrete structures,* ACI Committee 440, American Concrete Institute (ACI), Detroit.

ACI (1998), *ACI 440-98 - Provisional design recommendations for concrete reinforced with FRP bars*, ACI Committee 440 - FRP Reinforcement, American Concrete Institute (ACI).

Adimi, R., Rahman, H. A., and Benmokrane, B. (1998), Durability of FRP Reinforcements under Tension-Tension Axial Cyclic Loading, *Proceedings of the 1st International Conference on Durability of Fiber Reinforced Polymer (FRP) Composites for Construction*, Sherbrooke, Canada.

Agarwal, B.D. and Broutman, L.J. (1990), *Analysis and Performance of Fibre Composites,* Second edition. Willey-Interscience, New-York.

Almusallam, T. H. and Al-Salloum, Y. A. (2005), Durability of GFRP Rebars in Concrete Beams under Sustained Loads at Severe Environments, *Journal of Composite Materials.*

Alsayed, S. and Alhozaimy, A. (1998), Durability of FRP Reinforcements under Tension-Tension Axial Loading Cyclical Loading, *Proceedings of 1st International Conference on Durability of Fiber Reinforced Polymer (FRP) Composites for Construction*, Sherbrooke, 635-647.

Alsayed, S. H., Al-Salloum, Y. A., Almusallam, T. H., and Amjad, M. A. (1996), Evaluation of Shear Stresses in Concrete Beams Reinforced by FRP Bars, Advanced *Composite Materials in Bridges and Structures*, Montreal, Quebec, 173-179.

Alwis, K. and Burgoyne, C. J. (2006), Time-Temperature Superposition to Determine the Stress-Rupture of Aramid Fibres, *Applied Composite Materials*, 13(4), 249-264.

Ando, N., Matsukawa, H., Hattori, A. and Mashima, A. (1997), Experimental Studies on the Long-term Tensile properties of FRP Tendons, *Proceedings of the Third International Symposium on Non-Metallic (FRP) Reinforcement for Concrete Structures* (FRPRCS-3), Sapporo, Japan, Vol. 2, 203-210.

Arduini, M., Corba Colombo, A. and Vago, G. (2005), Non-metallic reinforcement technique for temporary R/C walls, *In Proceedings of 3rd International Conference on Composites in Construction (CCC),* Lyon, France, Vol. 2, 839-846.

ASTM D4475 (2002), *Standard Test Method for Apparent Horizontal Shear Strength of Pultruded Reinforced Plastic Rods by the Short-Beam Method*, ASTM International.

Avramidis, N. A. and Wilson, J. R. (1996), *Integrated variance reduction for simulation*, Operations Research, 44(2), 327-346.

Ayyub, B. M. and McCuen, R. H. (1995), *Probabilistic structural mechanics handbook-theory and industrial applications*: Chapter 4 - simulation-based reliability method (1st edn), Chapman and Hall, New York.

Bakis, C.E., Freimanis, A.J., Gremel, D. and Nanni, A. (1998), Effect of resin material on bond and tensile properties of unconditioned and conditioned FRP reinforced rods, *Proceedings of 1st Intl. Conf. on durability of fiber reinforced polymer (FRP) composites for construction,* Sherbrooke, August, 525-535.

Balàzs, G. L. and Borosnyoi, A., (2001), Long-term Behaviour of FRP, *Proceedings of the International Workshop Composites in Construction: A Reality,* Cosenza, E., Manfredi, G., and Nanni, A., eds., American Society of Civil Engineers, Reston, 84-91.

Bank, L.C. and Gentry, T.R. (1995), Accelerated Test Methods to Determine the Long-Term Behaviour of FRP Composite Structures: Environmental Effects, *Journal of Reinforced Plastic and Composites*, Vol. 14, 558-587.

Bank, L.C., Gentry, T.R., Barkatt, A., Prian, L., Wang, F. and Mangala, S.R. (1998), Accelerated ageing of pultruded glass/vinyl ester rods, *Proceedings of 2nd International Conference on Fibre Composites in Infrastructure*, Vol. 2, 423-437.

Bank, L.C., Puterman, M. and Katz, A. (1998), The effect of material degradation on bond properties of fiber reinforced plastic reinforcing bars in concrete, *ACI Materials Journal*, 95(3), 232-243.

Barbero, E.J., (1999), *Introduction to Composite Materials Design*, Taylor & Francis, Philadelphia.

Benmokrane, B. and Masmoudi, R. (1996), FRP C-Bars as Reinforcing Rod for Concrete, *Proceedings of 2nd International Conference: Advanced Composite Materials in Bridges and Structures*, Canadian Society for Civil Engineering, Montreal, Quebec, Canada, 181-185.

Benmokrane, B., Chaallal, O. and Masmoudi, R. (1996), Flexural Response of Concrete Beams Reinforced with FRP Reinforcing Bars, *ACI Structural Journal*, 91(2), 46-55.

Benmokrane, B., Debaiky, A., Nkurunziza, G. and Cousin, P. (2005), Residual Tensile Properties of GFRP Reinforcing Bars after Loading in Severe Environments, *ASCE Journal of Composites for Construction*, 10(5), 370-380.

Benmokrane, B., Wang, P., Gentry, T.R., and Faza, S. (2001), Test Methods to Determine Properties of FRP Rods for Concrete Structures, *Proceedings of the International Workshop "Composites in Construction: A Reality"*, Cosenza, E., Manfredi, G., and Nanni, A., eds., American Society of Civil Engineers, Reston 75-83.

Bischoff, P.H. (2005), A Rational Proposal for Predicting Beam Deflection, *33rd Annual Conference of the Canadian Society for Civil Engineering*, Toronto, Ontario, June 2-4, 2005, GC-299-1/10.

Bischoff, P.H. (2005), Re-evaluation of Deflection Prediction for Concrete Beams Reinforced with Steel and FRP bars, *Journal of Structural Engineering*, ASCE, 131(5), 752-767.

Bischoff, P.H. and Scanlon, A. (2007), Effective Moment of Inertia for Calculating Concrete Members Containing Steel Reinforcement Fiber-Reinforced Polymer Reinforcement, *ACI Structural Journal*, 104(1), 68-76.

Bischoff, P.H. (2007), Deflection Calculation of FRP Reinforced Concrete Beams Based on Modifications to the Existing Branson Equation, *Journal of Composites for Construction*, 11(1), 4-14.

Blontrock, H. (1999), Properties of Fiber Reinforced Plastics at Elevated Temperatures with Regard to Fire resistance of Reinforced Concrete Members, *Proceedings of the Fourth international Symposium, Fiber Reinforced Polymer Reinforcement for Reinforced concrete Structures*, ACI Ed. Dolan C. W., Rizkalla S. H. and Nanni A., Baltimore, 43-54.

Bootle, J., Burzesi, F., and Fiorini, L. (2001), Design Guidelines, In *ASM Handbook Volume 21 Composites*, ASM International, Material Park, Ohio, 388-395.

Boyle, M. M., Martin, C. J. and Neuner, J. D. (2001), Epoxy resins, In *ASM Handbook Volume 21 Composites*, ASM International, Material Park, Ohio, 78-89.

Branson, D. E. (1966), *Deflections of Reinforced Concrete Flexural Members*, ACI Committee Report, ACI-435.2R-66 (re-approved 1989), Detroit, 29.

Branson, D. E. (1977), *Deformation of Concrete Structures*, McGraw-Hill, New York, 537.

Brown, V. L. and Bartholomew, C. L. (1996), Long-term Deflection of GFRP-reinforced Concrete Beams, *Fiber Composites in Infrastructure: Proceedingsof the 1st International Conference on Composites in Infrastructures, ICCI'96,* H. Saadatmanesh and M. R. Ehsani, eds., 389-400

BSI (1990), *BS 5400-4:1990 - Steel, concrete and composite bridges,* Code of practice for design of concrete, Part 4, British Standard Institution, London.

BSI (1997), *BS 8110-1:1997-Structural Use of Concrete.* Code of Practice for Design and Construction, Part 1, British Standard Institution, London.

Budelman, H., and Rostasy, F. S. (1993), Creep Rupture Behaviour of FRP Elements for Prestressed Concrete-Phenomenon, Results and Forecast Models, *Proceedings of ACI International Symposium on FRP Reinforcement for Concrete Structures*, Vancouver, 87-100.

BÜV-Empfehlung (2002), *Tragende Kunststoffbauteile im Bauwesen [TKB] Entwurf, Bemessung und Konstruktion: Recommendation*, Load supporting plasticmembers in construction Bau-Überwachungsverein, Germany.

Byars, E.A., Dejke, V. and Demis, S. (2001), *Development drafts of a model European durability specification for FRP concrete*, Riga, Venice and Cambridge meetings of fib Task Group 9.3.

Byars, E.A., Waldron, P.W., Dejke, V. and Demis, S. (2001), Durability of FRP in Concrete, Current Specifications and a New Approach, *Proceedings of FRP Composites in Civil Engineering,* Vol. II, Elsevier, Hong Kong, December, 1497-1507.

Byars, E.A., Waldron, P.W., Dejke, V. and Demis, S. (2001), Durability of FRP in Concrete, Deterioration Mechanisms, *Proceedings of FRP Composites in Civil Engineering*, Vol. II, Elsevier, Hong Kong, December, 1517-1525.

Byars, E.A., Waldron, P.W., Dejke, V., Demis, S. and Heddadin, S. (2003), Durability of FRP in Concrete-Current Specifications and a New Approach, *International Journal of Materials and Product Technology*, 19(1/2), 40-52.

CAN/CSA (1994), *Design of Concrete Structures for Buildings (CAN3-A23.3-M94)*, Canadian Standards Association, Rexdale, Ontario, Canada.

CAN/CSA (1996), *Canadian Highway Bridge Design Code*, Section 16, Fiber Reinforced Structures," Canadian Standard Association.

CAN/CSA (2000), *Section 16 - Fiber Reinforced Structures,* Canadian Standards Association, Canadian Highways Bridge Design Code.

CAN/CSA (2006) - *Canadian Highway Bridge Design Code*, Final Draft.

CAN/CSA A23.3 (2004), *Design of concrete structures*, Canadian Standards Association, Toronto, Ontario, Canada.

CAN/CSA-S6-00 (2000), *Canadian Highway Bridge Design Code*, Canadian Standards Association, Toronto, Ontario, Canada.

CAN/CSA-S806-02 (2002), *Design and Construction of Building Components with Fibre Reinforced Polymers*, Canadian Standards Association, Toronto, Ontario, Canada.

CEB (1988), Bulletin D'Information No 191, *General principles on reliability for structures: A commentary on ISO 2394*, Comite Euro-International du Beton (CEB), 51.

CEB (1992), *Bond action and bond behaviour of reinforcement - 151,* State-of-the-Art Report, Comitee Euro-international du Beton Bulletin 151

CEB-FIP (1993), Model Code 1990, *Design Code*, Comité Euro-International du Béton. Thomas Telford Services Ltd, London.

CEN (1992), *Eurocode 2 - Design of concrete structures, Part 1 - 6: General rules and rules for buildings*, ENV 1992-1-1, European Prestandard, European Committee for Standardization (CEN), Brussels.

CEN (2002), *Eurocode 2- Basis of structural design*, EN 1990, European Committee for Standardisation, Brussels.

CEN (2004), *Eurocode 2 - Design of concrete structures - Part 1-1: General rules and rules for buildings*, EN 1992-1-1, European Committee for Standardisation, Brussels.

Chang, K. K. (2001), Aramid Fibers*, ASM Handbook*, Volume 21 Composites, ASM International, Material Park, Ohio, 41-45.

Chin, J.W., Nguyen, T. and Aouadi, K. (1998), Effects of Environmental Exposure on Fiber-Reinforced Plastic (FRP) Materials Used in Construction, *Journal of Composites Technology and Research*, 19(4), 205-213.

CIRIA Report 63 (1977), *Rationalisation of safety and serviceability factors in structural codes*, Construction Industry Research and Information Association.

Clarke J. L., O'Regan D. P. and Thirugnanenedran C. (1996), *EUROCRETE project, Modification of design rules to incorporate non-ferrous reinforcement*, EUROCRETE Project, Sir William Halcrow & Partners, London.

Clarke, J.L. (1993), *Alternative Materials for the Reinforcement and Prestressing Concrete*, Special Structures Department, Sir William Halcrow and Partners.

Clarke, J.L. and Sheard, P. (1998), Designing Durable FRP Reinforced Concrete Structures, Durability of Fibre Reinforced Polymer (FRP), Proceedings of the *1st International Conference on Composites for Construction (CDCC' 98)*, Sherbrooke, 3-24.

CNR (2006), *Istruzioni per la Progettazione, l'Esecuzione ed il Controllo di Strutture di Calcestruzzo Armato con Barre di Materiale Composito Fibrorinforzato (CNR-DT 206/2006)*, National Research Council, Rome, Italy.

ConFibreCrete (1998), *European Union TMR research network ConFibreCrete*, Internet Site: http://www.shef.ac.uk/uni/projects/tmrnet, Network Contract N° ERBF MRX - CT97 - 0135.

Cosenza E., Greco C., Manfredi G., and Pecce M. (1997), Flexural Behaviour of Concrete Beams Reinforced with Fibre Reinforced Plastic (FRP) Bars, *Proceedings of the Third International Symposium on Non-Metallic (FRP) Reinforcement for Concrete Structures*, Sapporo-Japan, Oct. 1997, Vol. 2, 463-470.

Cosenza, E., Manfredi, G., Pecce, M. and Realfonzo, R. (1999), Bond between GFRP Rebars and Concrete: an Experimental Analysis, *Proceedings of the 4th International Symposium on Fiber Reinforced Polymer for Reinforced Concrete Structures*, American Concrete Institute, Detroit, 347-358.

Cox, J. V. and Guo, J. (1999), Modeling Stress State Dependency of Bond Behaviour of Fiber Reinforced Polymer Tendons, *Fourth FRPRCS International Syompsium*, Baltimore, ACI International SP-188-68, Editors Dolan C. W., Rizkalla S.H., Nanni A., 791-805.

Creazza, G. and Di Marco, R. (1993), *Bending Moment-Mean Curvature Relationship with Constant Axial Load in the Presence of Tension Stiffening*, RILEM 26 (157), Materials and Structures, Vol. 26, 196-206.

CUR Recommendation 96 (2003), *Fibre reinforced plastics in civil engineering structures*, Gouda NL.

Curtis, P. T. (1989), The Fatigue Behavior of Fibrous Composite Materials, *Journal of Strain Analysis*, 24(4), 235-244.

Daniel, I. and Ishai, O. (1994), *Engineering Mechanics of Composite Materials*, Oxford University Press, Oxford.

De Lorenzis, L. and Tepfers, R. (2002), Bond of FRP Reinforcement in Concrete - a Challenge, Contribution to *Conference on Mechanics of Composite Materials - MCM*, June 9-13, Riga, Latvia.

De Lorenzis, L., and Nanni, A. (2002), Bond between Near-Surface Mounted Fiber-Reinforced Polymer Rods and Concrete in Structural Strengthening, *ACI Structural Journal*, Vol.99, No.2, March-April, 123-132.

Dejke, V. (2001), *Durability of FRP Reinforcement in Concrete*, Literature and Experiments, PhD Thesis at Dept of Building Materials, Chalmers University of Technology, Goteborg, Sweden.

Dejke, V. and Tepfers, R. (1997), Durability and service life prediction of GFRP for concrete reinforcement, *Proceedings of FRPRCS-5*, Edited by Ch. Burgoyne, University of Cambridge, Volume 1, Thomas Telford, London, ISBN 0 7277 3029 0, 505-514.

Dejke, V. and Tepfers, R. (2002), *Beständighet och livslängd hosfiberkompositarmerad betong*, Durability and service life of concrete reinforced with fiber composites, Bygg & teknik, 94th edition, ISSN 0281-658X, Stockholm October No. 7, 16-22.

Demis, S., Pilakoutas, K. and Byars, E. (2007), Durability of Fibre Reinforced Polymers in Concrete – Procedures for Reduced Alkalinity Exposures, *Proceedings of the* 8th *International Symposium on Fiber-Reinforced Polymer Reinforcement for Concrete Structures (FRPRCS-8)*, T. C. Triantafillou Ed., Patras, Greece, 534-535.

Desayi, P. and Ganesan, N. (1985), An Investigation on Spacing of Cracks and Maximum Crack Width in Reinforced Concrete Flexural Members, *Journal of Materials and Structures*, March April, 123 -133.

DIN 53768 (1990), *Extrapolationsverfahren für die Bestimmung des Langzeitversagensverhaltens von glasfaserverstärkten Kunststoffen* (GFK) (Extrapolation method for the prediction of the long term behaviour) Beuth Verlag Berlin.

Ditlevsen, O. (1997), Structural reliability codes for probabilistic design-A debate paper based on elementary reliability and decision analysis concepts", *Journal of Structural Safety*, 19(3), 253-270.

Duprat, F., Pinglot, M. and Lorrain, M. (1995), Reliability of reinforced concrete frame columns: Comparison Eurocode 2-BAEL 91, in Applications of statistics and probability: Civil engineering reliability and risk analysis, *Proceedings of the ICASP 7 Conference*, Paris France, Vol. 1, 10-13 July 1995, 481-488.

Duranovic, N., Pilakoutas, K. and Waldron, P. (1997), Tests on concrete beams reinforced with glass fibre reinforced plastic bars, *Proceedings of the Third International Symposium on Non-metallic (FRP) Reinforcement for Concrete Structures (FRPRCS-3)*, Sapporo Japan, Vol. 2, 479-486.

Duranovic, N., Pilakoutas, K. and Waldron, P. (1997a), FRP reinforcement for concrete structures: Design Considerations, *Proceedings of Third International Symposium on Non-metallic (FRP) Reinforcement for Concrete Structures*, Japan Concrete Institute, Sapporo, Japan, Vol. 2, 527-534.

Duranovic, N., Pilakoutas, K. and Waldron, P. (1997b), Tests on concrete beams reinforced with glass fibre reinforced plastic bars, *Proceedings of Third International Symposium on Non-metallic (FRP) Reinforcement for Concrete Structures*, Japan Concrete Institute, Vol. 2, 479-485.

El-Gamal, S., El-Salakawy, E. and Benmokrane, B. (2005), Behavior of Concrete Bridge Deck Slabs Reinforced with Fiber-Reinforced Polymer Bars Under Concentrated Loads, *ACI Structural Journal*, 102(5), 727-735.

El-Ghandour, A. (1999), *Behaviour and Design of FRP RC Slabs* PhD Thesis, The University of Sheffield, Dept. of Civil & Structural Engineering, Sheffield, UK.

El-Ghandour, A.W., Pilakoutas, K., and Waldron, P. (2003), Punching Shear Behavior of Fiber Reinforced Polymers Reinforced Concrete Flat Slabs: Experimental Study, *ASCE Journal of Composites for Construction*, 7(3), 258-265.

EN 13706 (2002), *Reinforced plastics composites - Specifications for pultruded profiles*, European Committee for Standardization.

EN 1992-1-1 (1992), *Eurocode 2 - Design of Concrete Structures, Part 1 - 6: General Rules and Rules for Buildings*, European Prestandard, European Committee for Standardization.

Epaarachi, J. A. and Clausen, P. D. (2003), An Empirical Model for Fatigue Behaviour Prediction of Glass-fibre Reinforced Plastic Composites for Various Stress Ratios and Test Frequencies, *Composites Part A: Applied science and manufacturing*, 34 (4), 313-326.

Eshani, M. R., Saadatmanesh, H., and Tao, S. (1995), Bond of Hooked Glass Fiber Reinorced Plastic (GFRP) Reinforcing Bars to Concrete, *Materials Journal*, 122(3), 247-257.

Euro-Projects (LTTC) (1997), *The development of non-ferrous reinforcement for concrete structures,* Eurocrete Project Final Report, Loughborough, UK.

Fantilli, A., Fantilli, D., Iori, I. and Vallini, P. (1998), Flexural Deformability of Reinforced Concrete Beams, *Journal of Structural Engineering*, 124(9), 1041-1049.

Faza S.S. and GangaRao, H.V.S. (1993). *Glass FRP Reinforcing Bars for Concrete*, Fiber Reinforced Plastic (FRP) Reinforcement for Concrete Structures: Properties and Applications, Developments in Civil Engineering, Vol. 42, Nanni, A. ed., Elsevier, Amsterdam, 167-188.

Faza, S. S. and GangaRao, H. V. S. (1992), *Bending and Bond Behavior of Concrete Beams Reinforced with Fiber Reinforced Plastic Rebars*, WVDOH-RP-83 Phase I Report, West Virginia University, Morgantown, 128-173.

Faza, S. S. and GangaRao, H. V. S. (1993) *Theoretical and Experimental Correlation of Behaviour of Concrete Beams Reinforced with Fibre Reinforced Plastic Rebars,* Fibre-Reinforced-Plastic Reinforcement for Concrete Structures (SP-138), A. Nanni and C. W. Dolan, eds, American Concrete Institute, Farmington Hills, MI, 599-614.

Ferry, J. D. (1980), *Viscoelastic Properties of Polymers*, 3rd edition, Willey, New York.

fib (2000), *Bond of Reinforcement in Concrete*, State-of-art Report, Bulletin 10, *fib* - International Federation for Structural Concrete, Lausanne.

fib (2001), *Design and use of externally bonded FRP reinforcement for RC structures,* Bulletin 14, *fib* - International Federation for Structural Concrete, Lausanne.

Frosch, R.J. (1999), Another Look at Cracking and Crack Control in Reinforced Concrete, *ACI Structural Journal*, 96(3), 437-442.

Gangarao, H.V.S. and Vijay, P.V. (1997), Aging of Structural Composites Under Varying Environmental Conditions, *Proceedings of the 3rd International Symposium on Non-Metallic (FRP) Reinforcement for Concrete Structures*, Vol 2, 91-98.

Gardner, N. J. (1990), Relationship of the Punching Shear Capacity of Reinforced Concrete Slabs with Concrete Strength, *ACI Structural Journal*, 87(1), 66–71.

Gay, D., Hoa, S.V. and Tsai, S. W. (2003). *Composite Materials. Design and Applications,* CRC Press, Boca Raton.

Gergely, P. and Lutz, L.A. (1968), *Maximum Crack Width in Reinforced Concrete Flexural Members,* Causes, Mechanism and control of Cracking in Concrete, SP-20, ACI, Detroit, 87-117.

Gibson, R. F. (1994), *Principles of Composite Material Mechanics,* McGraw-Hill, New York.

Greenwood, M. (2001), Pultruded Composites Durability: A Key Value. *Proceedings of Composites 2001 CFA,* Tampa F.

Guadagnini, M. (2002), *Shear Behaviour and Design of FRP RC Beams*, PhD Thesis, Department of Civil and Structural Engineering, The University of Sheffield, Sheffield, UK.

Guadagnini, M., Pilakoutas, K. and Waldron, P. (2003), Shear Performance of FRP Reinforced Concrete Beams, *Journal of Reinforced Plastics and Composites*, 22(15), 1389-1408.

Guadagnini, M., Pilakoutas, K. and Waldron, P. (2006), Shear Resistance of FRP RC Beams: An Experimental Study, *Journal of Composites for Construction (ASCE)*, 10(6), 464-473.

Hayes, M.D., Garcia, K., Verghese, N. and Lesko, J.J. (1998), The Effects of Moisture on the Fatigue Behavior of a Glass/Vinyl Ester Composite, *Proceedings of the 2nd International Conference on Fibre Composites in Infrastructure ICCI'98*, Vol. 1, 1-13.

Hollaway, L. (1993), *Polymer Composites for Civil and structural Engineering*, Blackie Academic & Professional, Glasgow.

Hsu, T.T.C., Mau, S.T., and Chen, B. (1987), A Theory on Shear Transfer Strength of Reinforced Concrete, *Structural Journal of the American Concrete Institute*, 84(2), 149-160.

Hull, D. and Clyne, T. W. (1996), *An Introduction to Composite Materials,* 2nd edition, Cambridge University Press, Cambridge.

ISIS (2001), *Reinforcing concrete structures with fibre reinforced polymers*, Design Manual No. 3, Canadian Network of Centres of Excellence on Intelligent Sensing for Innovative Structures, Winnipeg, CANADA.

ISO TC 71/SC 6 N (2003) Secretariat: *JCI Non-conventional reinforcement of concrete* - Test methods, Part 1: Fiber reinforced polymer (FRP) bars and grids.

IStructE (1999), Institution of Structural Engineers, *Interim guidance on the design of reinforced concrete structures using fibre composite reinforcement*, Published by SETO Ltd, London, UK.

JMC (1995), *Guidelines for structural design of reinforced concrete buildings structures,* Ed. by Building Research Institute, Japanese Ministry of Construction, 52.

Jones, R.M. (1999), *Mechanics of composite materials*, Taylor & Francis, Philadelphia, USA.

JSCE (1996), *Standard specification for design and construction of concrete structures, Part 1 design,* Japan Society of Civil Engineers, Tokyo, Japan.

JSCE (1997), *Recommendation for design and construction of concrete structures using continuous fibre reinforcing materials*, Research Committee on Continuous Fiber Reinforcing Materials, Japan Society of Civil Engineers, Tokyo, Japan.

JSCE-E 531 (1995), *Test Method for Tensile Properties of Continuous Fiber Reinforcing Materials,* Japan Society of Civil Engineers, Tokyo, Japan.

JSCE-E 533 (1995), *Test Method for Creep Failure of Continuous Fiber Reinforcing Materials,* Japan Society of Civil Engineers, Tokyo, Japan.

JSCE-E 534 (1995), *Test Method for Long-term Relaxation of Continuous Fiber Reinforcing Materials,* Japan Society of Civil Engineers, Tokyo, Japan.

JSCE-E 535 (1995), *Test Method for Tensile Fatigue of Continuous Fiber Reinforcing Materials,* Japan Society of Civil Engineers, Tokyo, Japan.

JSCE-E 536 (1995), *Test Method for Coefficient of Thermal Expansion of Continuous Fiber Reinforcing Material by Thermo-mechanical Analysis,* Japan Society of Civil Engineers, Tokyo, Japan.

JSCE-E 540 (1995), *Test Method for Shear Properties of Continuous Fiber Reinforcing Materials by Double Plane Shear,* Japan Society of Civil Engineers, Tokyo, Japan.

Kanakubo, T., and Shindo, M. (1997), Shear Behaviour of Fiber-Mesh Reinforced Plates, *Third International Symposium on Non-Metallic (FRP) Reinforcement for Concrete Structures*, Sapporo, Japan, 317-324.

Karbhari, V.M., Chin, J.W., Dunston, D., Benmokrane, B., Juska, T., Morgan,R., Lesko, J. J., Sorathia, U. and Reynaud D. (2003), Durability Gap Analysis for Fiber-Reinforced Polymer Composites in Civil Infrastructure, *Journal of Composites for Construction*, 7(3), 238-247.

Kato, Y., Yamaguchi, T., Nishimura, T. and Uomoto, T. (1997), Computational model for deterioration of aramid fibre by ultraviolet rays, *Proceedings of the 3rd International Symposium Non-Metallic (FRP) Reinforcement for Concrete Structures,* Vol. 2, 163-170.

Katz, A., Berman, N. and Bank, L.C. (1999), Effect of high temperature on bond strength of FRP rebars, *Journal of Composites for Construction*, 3(2), 73-81.

Kollar, L.P. and Springer, G.S. (2003), *Mechanics of Composite Structures*, Cambridge University Press, New York, USA.

Kotsovos, M. D., and Pavlovic, M. N. (1999), *Ultimate Limit State Design of Concrete Structures - A New Approach*, Thomas Telford, Ltd., London, UK.

Kumahara, S., Masuda, Y. and Tanano, Y. (1993), Tensile Strength of Continuous Fiber Bar under High Temperature, *International Symposium on Fiber-Reinforcement-Plastic Reinforcement for Concrete Structures*, SP-138, Nanni, A. and C. W. Dolan, C. W. eds., American Concrete Institute, Farmington Hills, 731-742.

Lees, J. M. and Burgoyne, Ch. J. (1997), Rigid body analysis of concrete beams pre-tensioned with partly-bonded AFRP tendons, Non-Metallic (FRP) Reinforcement for Concrete Structures, *Proceedings of the Third International Symposium,* Vol. 2, Sapporo October, 759-766.

Leonhardt, F. (1977), *Crack Control in Concrete Structures,* IABSE Surveys N. S4/77, International Association for Bridge and Structural Engineering, Zurich, Switzerland.

Lesko, J.J., Sorantia, U. and Reynaud, D. (2003), Durability Gap Analysis for Fiber-Reinforced Polymer Composites in Civil Infrastructure, *ASCE Journal of Composites in Construction*, 7(3), 238-247.

Machida, A. (1993), *State-of-the-Art Report on Continuous Fiber Reinforcing Materials*, Society of Civil Engineers (JSCE), Tokyo, Japan.

Machida, A. (1996), Designing Concrete structures with continuous fiber reinforcing materials, *Proceedings of the First International Conference on Composites in Infrastructure- ICCI'96*, Tucson Arizona, USA.

Machida, A. (1997), *Recommendation for design and construction of concrete structures using continuous fiber reinforcing materials*, Concrete Engineering Series 23, Japan Society of Civil Engineers, Tokyo, Japan.

Magnusson, J. (1997), *Bond and Anchorage of Deformed Bars in High-Strength Concrete*, Chalmers University of Technology, Division of Concrete Structures, Licentiate thesis, Work No. 1113, Publication 97:1, Göteborg, Sweden.

Mallick, P. K. (1988), *Fiber Reinforced Composites, Materials, Manufacturing and Design*, Marcel Dekker Inc., New York, USA.

Mandell, J. F. (1982), *Fatigue Behavior of Fiber-Resin Composites. Developments in Reinforced Plastics*, Applied Science Publishers, London, Vol.2, 67-107.

Maruyama, K., and Zhao, W. (1994), *Flexural and Shear Behaviour of Concrete Beams Reinforced with FRP Rods,* Corrosion and Corrosion Protection of Steel in Concrete, University of Sheffield, UK, 1330-1339.

Maruyama, K., and Zhao, W. (1996), *Size Effect in Shear Behavior of FRP Reinforced Concrete Beam*, Advanced Composite Materials in Bridges and Structures, Montreal, Quebec, 227-234.

Maruyama, T., Honma, M., and Okamura, H. (1989), *Experimental Study on the Diagonal Tensile Characteristics of Various Fiber Reinforced Plastic Rods*, Transactions of the Japan Concrete Institute, 11, 193-198.

Masmoudi, R., Thériault, M., and Benmokrane, B. (1998), Flexural Behavior of Concrete Beams Reinforced with Deformed Fiber Reinforced Plastic Reinforcing Rods, *ACI Structural Journal*, 95(6), 665-676.

Matthys, S., and Taerwe, L. (2000), Concrete Slabs Reinforced with FRP Grids. II: Punching Resistance, *ASCE Journal of Composites for Construction*, 4(3), 154-161.

Maxwell, A.S., Broughton, W.R., Dean, G. and Sims, G. D. (2005), *Review of accelerated ageing methods and lifetime prediction techniques for polymeric materials,* NPL Report DEPC MPR 016, National Physical Laboratory

Micelli, F., Myers, J. and Nanni, A. (2001), *Characterization of a new FRP Bar for Reinforcement of Concrete* , Report, Center for Infrastructure Studies, Missouri Rolla, MO, USA.

McKague, L. (2001), *Thermoplastic Resins*. In: ASM Handbook Volume 21 Composites, ASM International, Material Park, Ohio, 133-140.

Mikani, H., Katoh, M., Takeuchi, H., and Tamura, T. (1989), *Flexural and Shear Behaviour of RC Beams Reinforced with Braided FRP Rods in Spiral Shape*, Transactions of the Japan Concrete Institute, 11(1), 119-206.

Mil Handbook 17 (1999), *The Composite Materials Handbook*-Mil -17, Vol.2, Materials Properties, US Dept. of Defense, Technomic Publication, Lancaster, USA.

Mitchell, D., and Collins, M. P. (1974), Diagonal Compression Field Theory - A Rational Model for Structural Concrete in Pure Torsion, *ACI Journal*, 71, 396-408.

Mochizuki, S., Matsuzaki, Y., and Sugita, M. (1989), *Evaluation Items and Methods of FRP Reinforcement as Structural Elements*, Transactions of the Japan Concrete Institute, 11, 117-131.

Morphy, R., Sheata, E., and Rizkalla, S. (1997), Bent Effect on Strength of CFRP Stirrups, *Proceedings of the Third International Symposium on Non-Metallic (FRP) Reinforcement for Concrete Structures*, Sapporo, Japan, 19-26.

Morsh, E. (1909), *Concrete-Steel Construction*, E. P. Goodrich, translator, McGraw-Hill, New York, USA.

Mosley, W. H. and Bungey, J. H. (1990), *Reinforced Concrete Design*, 4th edition, Macmillan.

Mufti, A.A., Onofrei, M., Benmokrane, B. Banthia N., Boulfiza M., Newhook J. P., Bakht B., Tadros G. and Brett P. (2005), Report On The Studies Of GFRP Durability In Concrete From Field Demonstration Structures, *Proceedings of the Conference on Composites in Construction,* July 11-13, Hamelin P. Ed., Lyon, France.

Mufti, A.A., Banthia N., Benmokrane, B., Boulfiza M. and Newhook J. P. (2007). Durability of GFRP Composite Rods, Concrete International. 37-42

Nagasaka, T., Fukuyama, H., and Tanigaki, M. (1989), *Shear Performance of Concrete Beams Reinforced with FRP Stirrups*, Transactions of the Japan Concrete Institute, 11.

Nagasaka, T., Fukuyama, H., and Tanigaki, M. (1995), Shear Perfomance of Concrete Beams Reinforced with FRP Stirrups, *Proceedings of the International Symposium on Fibre Reinforced-Plastic Reinforcement for Concrete Structures*, 789-811.

Nakano, K., Matsuzaki, M., Fukuyama, H., Teshigawara, M. (1993), Flexural Performance of Concrete Beams Reinforced with Continuous Fibre Bars, *ACI Symposium FRPRCS-1*, 743- 766.

Nanni, A. (2001), Guide and Specifications for the Use of Composites in Concrete and Masonry Construction in North America, *Proceedings of the International Workshop Composites in Construction: A Reality*, Cosenza, E., Manfredi, G., and Nanni, A., eds. American Society of Civil Engineers, Reston, 9-18.

Nawy, E. G. (1968), Crack Control in Reinforced Concrete Structures, *ACI Journal,* October 1968, 825-836.

Nawy, E. G. (1992), *Macrocracking and Crack Control in Concrete Structures-A State of the Art*, ACI SP-133, Nawy E. G., Scanlon A. (eds), Designing Concrete Structures for Serviceability and Safety, Detroid, USA.

Neocleous, K. (1999), *Design and safety philosophy for concrete structures reinforced with fibre reinforced polymers (FRP),* Ph.D. Thesis, The University of Sheffield, Department of Civil and Structural Engineering, UK.

Neocleous, K., Pilakoutas, K. and Guadagnini, M. (2005), Failure-mode-hierarchy-based design for reinforced concrete structures, *Structural Concrete*, 6 (1), 23-32.

Neocleous, K., Pilakoutas, K. and Waldron, P. (2004), Structural safety uncertainties in codes of practice for reinforced concrete, *The Structural Engineer*, 82 (8), 28-33.

Neuenhofer, A. and Zilch, K. (1993), Probabilistic validation of EC2 partial safety factors using full distribution reliability methods, *Proceedings of IFIP WG7.5 5th Working Conference on Reliability and Optimization of Structural Systems*, Takamatsu Japan, Eds. Thoft-Christensen P. and Ishikawa H., Elsevier Science, 24-26 March, Vol. 12, 197-204.

Neville, A.M. (1996), *Properties of Concrete*, Fourth edition, Addison Wesley Longman Limited, Harlow, UK.

Newhook, J., Ghali, A. and Tadros, G. (2002), Cracking and Deformability of Concrete Flexural Sections with Fiber Reinforced Polymer, *Journal of Structural Engineering*, V. 128, No. 9, September, 1195-1201.

Nielsen, L.E. (1974), *Mechanical Properties of Polymers and Composites*, Vol. 2, Marcel Dekker, New York, USA.

Nielsen, M. P. (1984), *Limit Analysis and Concrete Plastici*ty, Prentice-Hall Inc., Englewood Cliffs, N.J., USA.

Nowak, A. S. and Lind, N. C. (1995), Chapter 15: Probability-based design codes, in *Probabilistic structural mechanics handbook-Theory and industrials applications*, 1st Edition, Chapman and Hall, New York, USA, 331-351.

Odagiri, T., Matsumoto, K., Nakai, H., (1997), Fatigue and Relaxation Characteristics of Continuous Aramid Fibre Reinforced Plastic Rods*, Proceedings of the Third International Symposium on Non-Metallic (FRP) Reinforcement for Concrete Structures (FRPRCS-3)* Sapporo, Japan, Vol.2, 227-234.

Okamoto, T., Matsubara, S., Tanigaki, M. and Jasuao, K. (1993), Practical Application and Performance ofC Beams Reinforced with Braided FRP Bars, *Proceedings of the International Symposium on Fiber-Reinforcement-Plastic Reinforcement for Concrete Structures*, SP-138, Nanni, A., and C. W. Dolan, C. W., eds. American Concrete Institute, Farmington Hills, 875-894.

Ospina, C.E. and Gross, S.P. (2005), Rationale for the ACI 440.1R-06 Indirect Deflection Control Design Provisions, *Proceedings of 7th International Symposium on FRP Reinforcement for Concrete Structures*, Kansas City, USA, 651-670.

Ospina, C.E., (2005), Alternative Model for Concentric Punching Capacity Evaluation of Reinforced Concrete Two-Way Slabs, *Concrete International*, 27(9), 53-57.

Ospina, C.E., Alexander, S. and Cheng, J.J. (2001), *Behaviour of Concrete Slabs with Fibre-Reinforced Polymer Reinforcement*, Structural Engineering Report No. 242, Department of Civil and Environmental Engineering, University of Alberta.

Ospina, C.E., Alexander, S.D.B., and Cheng, J.J.R. (2003), Punching of Two-way Concrete Slabs with Fiber-Reinforced Polymer Reinforcing Bars or Grids, *ACI Structural Journal*, 100(5), 589-598.

Pantuso, A., Spadea, G. and Swamy, R.N. (1998), An experimental study on the durability of GFRP bars, *Proceedings of the 2nd International Conference on fiber composites in infrastructure*, ICCI'98, Vol. 2, Tuscon, 476-487.

Pecce, M., Manfredi, G. and Cosenza, E. (2001), A Probabilistic Assessment of Deflections in FRP RC Beams, *Proceedings of 5th International Conference on Non-metallic Reinforcement for Concrete Structures - FRPRCS-5*, Cambridge, 16-18 July, Thomas Telford Publishing, Vol. 2, 887-896.

Pecce, M., Manfredi, G., and Cosenza, E. (2000), Experimental Response and Code Models of GFRP RC Beams in Bendino, *ASCE Journal of Composites for Construction*, Vol. 4, No. 4, November, 182-190.

Pepper, T. (2001), *Polyester Resins,* In: ASM Handbook Volume 21 Composites, ASM International, Material Park, Ohio, 90-96.

Pilakoutas, K. (2000), *Composites in Concrete Construction* in Gdoutos A., Pilakoutas K. and Rodopoulos C. (Eds), Failure Analysis of Industrial Composite Materials, McGraw-Hill, Professional Engineering, 449-497.

Pilakoutas, K. and Guadagnini, M. (2001), Shear of FRP RC: a Review of the State-of the-Art". In E. Cosenza, G. Manfredi and A. Nanni (Eds.), *Proceedings of the International Workshop Composites in Construction: A reality*, Capri Italy, ASCE Special Publication, Virginia, 173-182.

Pilakoutas, K., Neocleous, K. and Guadagnini, M. (2002), Design philosophy issues of fibres reinforced polymer reinforced concrete structures, *Journal of Composites for Construction*, 6 (3), 154-161.

Polak, M. and Blackwell, G. (1998), Modelling Tension in Reinforced Concrete Members Subjected to Bending and Axial Load*, Journal of Structural En*gineering, 124(9), 1018-1024.

Porter, M.L., Mehus, J., Young, K., Barnes, B. and O'Neil, E.F. (1997), Aging Degradation of fibre composite reinforcement for concrete structures, *Proceedings of the 2nd International Conference Advanced Composite Materials in Bridges and Structures*, Canada, 641-648.

Porter, M.L., Mehus, J., Young, K.A., O'Neil, E.F. and Barnes, B.A. (1997), Aging for fibre reinforcement in concrete, *Proceedings of the 3rd International Symposium on Non-Metallic (FRP) Reinforcement for Concrete Structures*, Vol. 2, 59-66.

Rahman, A.H., Kingsley, C., Richard, J. and Crimi, J. (1998), Experimental Investigation of the Mechanism of Deterioration of FRP Reinforcement for Concrete, *Proceedings of the 2nd International Conference on Fibre Composites in Infrastructure ICCI'98*, Vol. 2, 501-511.

Renaud, C. and Greenwood, M. (2005), Effect of Glass fibres and Environments on Long-Term Durability of GFRP Composites, Proceedings of 9 EFUC Meeting, Wroclaw, Poland.

Rizkalla, S. and Mufti, A. (2001), *Reinforcing Concrete with Fibre Reinforced Polymers*, ISIS Design Manual No 3, ISIS Canada, Manitoba.

Saadatmanesh, H. and Tannous, F. E. (1999a), Relaxation, Creep and Fatigue Behavior of Carbon Fiber Reinforced Plastic Tendons, *ACI Materials Journal*, 96(2), 143-153.

Saadatmanesh, H. and Tannous, F. E. (1999b), *Long-term Behavior of Aramid Fiber Reinforced Plastic (AFRP) Tendons, ACI Materials Journal*, 96 (3) 297-305.

Saadatmanesh, H., and Tannous, F. (1997), Durability of FRP rebars and tendons, *Proceedings of the 3rd International Symposium on Non-Metallic (FRP) Reinforcement for Concrete Structures*, Vol 2, 147-154.

Sakashita, M., Masuda, Y., Nakamura, K., Tanano, H., Nishida, I. and Hashimoto, T. (1997), Deflection of Continuous Fiber Reinforced Concrete Beams Subjected to Loaded Heating, *Proceedings of the Third International Symposium on Non-Metallic (FRP) Reinforcement for Concrete Structures (FRPRCS-3)* Sapporo, Japan, Vol.2, 51-58.

Sasaki, I., Nishizaki, I., Sakamoto, H., Katawaki, K. and Kawamoto, Y. (1997), Durability Evaluation of FRP Cables by Exposure Tests, *Proceedings of the 3rd International Symposium on Non-Metallic (FRP) Reinforcement for Concrete Structures*, Vol. 2, 131-137.

Schaff, J. R. (2001), *Fatigue and Life Prediction,* ASM Handbook Vol. 21 Composites, ASM International, Material Park, Ohio, 252-258.

Schapery, R.A. (1968), Thermal Expansion Coefficients of Composite Materials Based on Energy Principles, *Journal of Composite Materials*, 2(3), 380-404.

Scheibe, M. and Rostasy, F. S. (1995), Stress-rupture of AFRP subjected to alkaline and elevated temperatures, *Proceeding of the Second International Symposium Non-Metallic (FRP) Reinforcement for Concrete Structures*, L. Taerwe Ed., 67-73.

Schwartz, M.M. (1992), *Composite Materials Handbook,* Second Edition, McGraw-Hill, New York.

Seki, H., Sekijima, K. and Konno, T. (1997), Test Method on Creep of Continuous Fiber Reinforcing Materials, *Proceedings of the Third International Symposium on Non-Metallic (FRP) Reinforcement for Concrete Structures (FRPRCS-3)* Sapporo, Japan, Vol.2, 195-202.

Sen, R., Mullins, G. and Salem, T. (2002), Durability of E-Glass/Vinylester Reinforcement in Alkaline Solution, *ACI Structural Journal*, 99(3), 369-375.

Sen, R., Shahawy, M., Rosas, J. and Sukumar, S. (1997), Durability of AFRP & CFRP pretensioned piles in a marine environment, *Proceedings of the 3rd International Symposium on Non-Metallic (FRP) Reinforcement for Concrete Structures*, Vol 2, 123-130.

Sen, R., Shahawy, M., Sukumar, S. and Rosas, J. (1998), Effects of Tidal Exposure on Bond of CFRP Rods, *Proceedings of the 2nd International Conference on Fibre Composites in Infrastructure ICCI'98*, Vol. 2, 512-523.

Sen, R., Shahawy, M., Sukumar, S. and Rosas, J. (1999), Durability of Carbon Fibre Reinforced Polymer (AFRP) pretensioned elements under Tidal/Thermal Cycles, *ACI Structural Journal*, 96(3), 450-457.

Sheard, P., Clarke, J.L., Dill, M., Hammersley, G. and Richardson, D. (1997), EUROCRETE-Taking Account of Durability for Design of FRP Reinforced Concrete Structures, *Proceedings of the 3rd International Symposium on Non-Metallic (FRP) Reinforcement for Concrete Structures*, Vol. 2, 75-82.

Shehata E, Morphy R, Rizkalla S. (2000), Fibre Reinforced Polymer Shear Reinforcement for Concrete Members: Beaviour and Design Guidelines, *Canadian Journal of Civil Engineering*, 27(5), 859–872

Sooriyaarachchi, H. (2005), *Tension stiffening behaviour of FRP bars in concrete,* Ph D thesis, Centre of Civil and Structural Engineering, Department of Civil and Structural Engineering, The University of Sheffield, Sheffield, UK.

Sooriyaarachchi, H., Pilakoutas, K. and Byars, E. (2005), Tension Stiffening Behaviour of GRP-Reinforced Concrete, *Proceedings of 7th International Symposium for Fibre-Reinforced Polymer (FRP) Reinforcement for Concrete Structures, FRPRCS7*, American Concrete Institute SP-230, 975-989.

Steckel, G.L., Hawkins, G.F. and Bauer, J.L. (1998), Environmental Durability of Composites for Seismic Retrofit of Bridge Columns, *Proceedings of the 2nd International Conference on Fibre Composites in Infrastructure ICCI'98*, Vol. 2, 460-475.

Stone, D., Prota, A. and Nanni, A. (2002), *Deflection Assessment of an FRP-Reinforced Concrete Bridge*, Deflection Control for the Future, ACI Spring Convention, Detroit, MI, USA.

Stratford, T. and Burgoyne, C. (2003), Shear Analysis of Concrete with Brittle Reinforcement, *Journal of Composites for Construction*, 7(4), 323-330

Taerwe, L. (1993), FRP Developments and Applications in Europe, *Fiber-Reinforced-Plastic Reinforcement for Concrete Structures: Properties and Applications*, Ed. A. Nanni, Elsevier Science Publisher

Tamuzs, V., Apinis, R., Modniks, J. and Tepfers, R. (2001), The performance of bond of FRP reinforcement in concrete, *SAMPE (Society for the Advancement of Material and Process Engineering) Symposium*, Long Beach, California, 1738-1748.

Tannous, F.E. and Saadatmanesh, H. (1998), Durability and long-term behavior of carbon and aramid FRP tendons, *Proceedings of the 2nd International Conference on fiber composites in infrastructure, ICCI'98*, Vol. 2, Tuscon, 524-538.

Taranu, N. and Isopescu, D. (1996), *Structures Made of Composite Materials*, Vesper, Iasi, Romania.

Taylor, H. P. J. (1970), *Investigation of the Forces Carried Across Cracks in Reinforced Concrete Beams in Shear by Interlock of Aggregate*, 42.447, Cement and Concrete Association, London, UK.

Tepfers R., Molander I., Thalenius K., (1992), Experience from testing of concrete reinforced with

carbon fiber and aramid fiber strands, *XIV - Nordic Concrete Congress & Nordic Concrete Industry Meeting*, 6.-8 August, Icelandic Concrete Association, Reykjavik, 337-347.

Tepfers, R. (1973), *A Theory of Bond Applied to Overlapped Tensile Reinforcement Splices for Deformed Bars,* Phd thesis. Work No 723, Publication No: 73:2. Division of Concrete Structures, Chalmers University of Technology, Göteborg, Sweden.

Tepfers, R. (2002), Test system for evaluation of bond properties of FRP reinforcement in concrete, *Proceedings of the Third International Symposium on Bond in Concrete-from research to standards*, 657-666.

Tepfers, R. and Karlsson, M. (1997), Pull-out and tensile reinforcement splice tests using FRP C-BARs, Chalmers University of Technology, Division of Building Technology. Work No: 13. Publication No: 97:2, Göteborg, Sweden.

Tepfers, R. and Olsson, P.A. (1992), Ring Test for Evaluation of Bond Properties of Reinforcing Bars, *Proceedings of the International Conference Bond in Concrete -From Research to Practice*, Riga, Latvia, Vol. 1, 89-99.

Tepfers, R., Hedlund, G. and Rosinski, B. (1998), Pull-out and tensile reinforcement splice tests with GFRP bars, *Proceedings of the ICCI'98, Second International Conference on Composites in Infrastructure*, Vol. II, 37-51.

Thorenfeldt, E. (1998), *Modifications to NS3473 when using fibre reinforced plastic (FRP) reinforcement*, SINTEF Report STF22 A98741, Sweden.

Tomosawa, F. and Nakatsuji, T. (1997), Evaluation of ACM Reinforcement Durability By Exposure Test, *Proceedings of the 3rd International Symposium on Non-Metallic (FRP) Reinforcement for Concrete Structures*, Vol. 2, 139-146.

Tottori, S., and Wakui, H. (1993), Shear Capacity of RC and PC Beams Using FRP Reinforcement, *Proceedings of the International Symposium on Fiber Reinforced Plastic Reinforcement for Concrete Structures*, 615-632.

Toutanji, H. and Deng, Y. (2003), Deflection and Crack-width Prediction of Concrete Beams Reinforced with Glass FRP Rods, *Journal of Construction and Building Materials*, Vol. 17, 69-74.

Toutanji, H. and El-Korchi, T. (1998), Tensile Durability Performance of Cementitious Composites Externally Wrapped with FRP Sheets, *Proceedings of the 2nd International Conference on Fibre Composites in Infrastructure ICCI'98*, Vol. 2, 410-421.

Toutanji, H.A., and Saafi, M. (2000), Flexural Behavior of Concrete Beams Reinforced with Glass Fiber-Reinforced Polymer (GFRP) Bars, *ACI Structural Journal*, 97(5), 712-719.

Tsai, S. W. and Hahn, H. T. (1980), *Introduction to Composite Materials*, Technomic, Lancaster.

Tureyen, A. K. and Frosh, R. J. (2003), Concrete Shear Strength: Another Perspective, *ACI Structural Journal*, 100(5), 609-615.

Tureyen, A. K., and Frosch, R. J. (2002), Shear Tests of FRP Reinforced Concrete Beams without Stirrups, *ACI Structural Journal*, 99(4), 427-434.

Uomoto, T. and Nishimura, T. (1997), Development of new alkali resistant hybrid AGFRP rod, *Proceedings of the 3rd International Symposium on. Non-Metallic (FRP) Reinforcement for Concrete Structures*, Vol 2, 67-74.

Vecchio, F. J., and Collins, M. P. (1986), The Modified Compression Field Theory for Reinforced Concrete Elements Subjected to Shear, *ACI Journal*, 83, 219-231.

Verghese, N.E., Hayes, M., Garcia, K., Carrier, C., Wood, J. and Lesko, J.J. (1998), Temperature Sequencing During Hygrothermal Aging of Polymers and Polymer Matrix Composites: The Reverse

Thermal Effect, *Proceedings of the 2nd International Conference on Fibre Composites in Infrastructure ICCI'98,* Vol. 2, 720-739.

Wallenberger, F. T., Watson, J. C. and Hong, L. (2001), *Glass Fibers*. In: ASM Handbook Volume 21 Composites, ASM International, Material Park, Ohio, 27-34.

Walraven, J. C. (1981), Fundamental Analysis of Aggregate Interlock, Journal of the Structural Division, *Proceedings of the American Society of Civil Engineering*, 107 (No. ST11), 2245-2269.

Walsh, P. J. (2001) *Carbon Fibres,* ASM Handbook Volume 21-Composites, ASM International, Material Park, Ohio, 35-40.

Wang, N. and Evans, J.T. (1995), Collapse of Continuous Fiber Composite Beam at Elevated Temperatures, *Journal of Composites* 26 (1), 56-61.

Weber, A. (2004), Bewehrungsstäbe aus GFK - Materialverhalten und Anwendungsgebiete, *Proceedings of the SKZ IBK Symposium,* Leipzig, Germany.

Weber, A. (2005), *GFK-Bewehrung - Bemessung und Anwendung*, in Faserverbundwerkstoffe Innovation im Bauwesen Bauwerk Verlag, Berlin, Germany.

Weber, A. (2006), Advanced reinforcement technology with GFRP Rebar, *Proceedings of the 2nd International fib Congress,* Naples, Italy.

Weber, A. (2006a), Durability approach for GFRP Rebars, *Proceedings of the Third International Conference on FRP Composites in Civil Engineering (CICE 2006)*, Miami, Florida, USA.

Wegian, F.M. and Abdalla H.A. (2005), Shear capacity of concrete beams reinforced with fiber reinforced polymers, *Composite Structures*, 71(1), Elsevier, 130-138.

Yamaguchi, T., Kato, Y., Nishimura, T. and Uomoto, I. (1997), Creep Rupture of FRP Rods Made of Aramid, Carbon and Glass Fibers, *Proceedings of the Third International Symposium on Non-Metallic (FRP) reinforcement for Concrete Structures (FRPRCS-3),* Japan Concrete Institute, Sapporo, Japan, Vol. 2, 179-186.

Yost, J. R., Gross, S. P. and Dinehart, D. W. (2001), Shear Strength of Concrete Beams Reinforced with Deformed GFRP Bars, *Journal of Composites for Co*nstruction, 5 (4), 268-275.

Yost, J. R., Gross, S. P. and Dinehart, D. W. (2003), Effective Moment of Inertia for Glass Fiber-reinforced Polymer-reinforced Concrete Beams, *ACI Structural Journal*, 100 (6), 732-739.

Zhao, W. (1999), *Crack and Deformation Behaviour of FRP Reinforced Concrete Structures,* PhD Thesis, Department of Civil & Structural Engineering, The University of Sheffield, Sheffield, UK.

Zhao, W., Maruyama, K., and Suzuki, H. (1995), Shear Behavior of Concrete Beams Reinforced by FRP Rods as Longitudinal and Shear Reinforcement, *International Symposium on Non Metallic (FRP) Reinforcement for Concrete Structures*, 352-259.

Zhao, W., Pilakoutas, K. and Waldron, P. (1997a), FRP Reinforced Concrete: Calculations for Deflections, *Proceedings of the 3rd Symposium on Non-metallic (FRP) reinforcement for concrete structures (FRPRCS-3)*, Japan Concrete Institute, Vol., 2, 511-518.

Zhao, W., Pilakoutas, K. and Waldron, P. (1997b), FRP Reinforced Concrete: Cracking Behaviour and Determination, *Proceedings of the 3rd Symposium on Non-metallic (FRP) reinforcement for concrete structures (FRPRCS-3)*, Japan Concrete Institute, Vol., 2, 439-446.

Zia, P., Ahmad, S., and Leming, M. (1997), *High-Performance Concretes: A State-of-Art Report (1989-1994)*, United States Department of Transportation - Federal Highway Administration, Report No. FHWA-RD-97-030, Virginia, USA